



European
Consortium of
Earthquake
Shaking
Tables

Innovative
Seismic Design
Concepts for New
and Existing
Structures

ECOEST2 and ICONS were supported by the European Commission under its TMR - Training and Mobility of Researchers Programme

SEISMIC BEHAVIOUR AND DESIGN OF COMPOSITE STEEL CONCRETE STRUCTURES



Editors - André PLUMIER and Catherine DONEUX

General Editors - Roy T. Severn and Rogério Bairrão

Report No. 4 May 2001

INFORMATION TO THE READER

This report is part of a set of 9 reports presenting the results of two companion research projects: ECOEST2 - European Consortium of Earthquake Shaking Tables and ICONS - Innovative Seismic Design Concepts for New and Existing Structures. These projects were carried out from 1996 to 1999, with funding by the Training and Mobility of Researchers Programme of the European Commission.

The publication of this set of 9 reports is intended to increase the dissemination of the results achieved in both projects. The printing costs were provided through a Concerted Actions Contract of the European Commission.

List of Reports

General Editors: Roy T. Severn and Rogério Bazzurro

1. Seismic Actions
Editors: Ezio Faccioli and Roberto Paolucci
2. Seismic Assessment, Strengthening and Repair of Structures
Editor: Eduardo C. Carvalho
3. Innovative Design Concepts
Editors: Michael N. Fardis and G. Michele Calvi
4. Seismic Behaviour and Design of Composite Steel Concrete Structures
Editors: André Plumier and Catherine Doneux
5. Shear Walls Structures
Editors: Jean-Marie Reynouard and Michael N. Fardis
6. Soil Dynamics and Foundation Structures
Editors: Colin A. Taylor and Didier Combescure
7. Experimental Investigations on Semi-Active and Passive Systems for Seismic Risk Mitigation
Editor: Giorgio Franchioni
8. Cable-Stayed Bridges, Irregular Bridges and Asymmetrical Structures
Editors: Roy T. Severn and Colin A. Taylor
9. Developments in the Automatic Control of Experimental Facilities
Editors: David Stoten and Georges Magonette

Published by:

LNEC - Laboratório Nacional de Engenharia Civil
Avenida do Brasil 101, 1700-066 Lisboa, Portugal
Tel. (351) 21844 30 00, Fax (351) 21844 3011

ISBN 972-49-1890-4

EXECUTIVE SUMMARY

The report presents research activities on the seismic behaviour of composite steel concrete moment frames co-ordinated in Europe within the ICONS project. Research has been focused on problems of ductility and resistance in the case where the connections of the steel parts are full strength "rigid".

Tests have been realised on subassemblages, on elements, on a plane frame and on a 3-D frame. Some tests were run quasi statically, others on shaking tables. Numerical modelling was done in parallel. Summary reports of these activities are presented.

Based on that research and on literature data, for the structural types and elements other than those of typical European composite moment frames, design rules have been developed. These rules, which are now under implementation within the 2001 EN version of Eurocode 8 are presented with comments and reference to background.

European Commission- "Training and Mobility of Researchers" Programme
INNOVATIVE CONCEPTS IN SEISMIC DESIGN "ICONS" PROJECT

SEISMIC BEHAVIOUR AND DESIGN OF COMPOSITE STEEL CONCRETE STRUCTURES

Editors: André PLUMIER and Catherine DONEUX

Contributing organisations and individuals

ICONS contractors

University of Liege, Belgium

A. Plumier (Scientific responsible,
Coordinator of ICONS Topic 4)
C. Doneux, L. Sanchez, R. Agatino

Joint Research Center at Ispra, Italy

A. Pinto (Scientific responsible)
I. Papadopoulos, C. Plumier

Imperial College London, United Kingdom

A. Elnashai (Scientific responsible)
M. Tsujii, R. Pinho

Technical University of Darmstadt, Germany

J. Bouwkamp (Scientific responsible)
H. Parung

Polytechnical University of Madrid, Spain

E. Alarcon (Scientific responsible)
R. Perera

Invited Experts

Trinity College Dublin, Ireland

B. Broderick

Imperial College London, United Kingdom

A. Elghazouli

INSA de Rennes, France

J.-M. Aribert, A. Lachal

University of Trento, Italy

O. Bursi, R. Zandonini

University Federico II of Napoli, Italy

E. Cosenza, G. Manfredi, G. Fabbrochino

Reviewer : C. Castiglioni, **Politecnico di Milano**, Italy

May 2001

TABLE OF CONTENT

1. INTRODUCTION	7
2. DESIGN RULES FOR EUROCODE 8 AND THEIR BACKGROUND ICONS PROJECT OF A SECTION 7 OF EUROCODE 8-EN1998 (2001). SPECIFIC RULES FOR STEEL – CONCRETE COMPOSITE BULDINGS.	9
3. REPORTS ON EXPERIMENTAL ACTIVITY AND NUMERICAL MODELLING	63
<u>3.1. ISMES TESTS: Dynamic tests on the ductility of composite steel-concrete beams</u>	63
3.1.1. Introduction	
3.1.2. Ductility	
3.1.3. Experimental results	
3.1.4. Processed data	
3.1.5. Conclusion	
<u>3.2. SACLAY TEST: Cyclic test on a composite moment frame</u>	68
3.2.1. Context and aims of the research	
3.2.2. Description of the tested structure	
3.2.3. Test set up	
3.2.4. Test procedure	
3.2.5. Instrumentation	
3.2.6. Description of the test	
3.2.7. Analyses and interpretation	
3.2.8. Conclusion	
<u>3.3. ISPRA TESTS: Slab design in connection zone of composite frames Bi-directional cyclic response study of 3-D composite frame</u>	80
3.3.1. Introduction	
3.3.2. Layout of the tested structure	
3.3.3. Test program	
3.3.4. Test results – global behaviour of the frame	
3.3.5. Test results –Analysis of the moment rotation behaviour at each node	
3.3.6. Conclusions	
<u>3.4. DARMSTADT TESTS: A study on composite sub-assemblages</u>	96
3.4.1. Introduction	
3.4.2. Description of the specimens	
3.4.3. Test Setup	
3.4.4. Instrumentation	
3.4.5. Test Procedure	
3.4.6. Experimental results	
3.4.7. Conclusion	
<u>3.5. MOMENT TRANSFER</u>	107
3.5.1. Eurocode 4	
3.5.2. Slab to column force transfer. Plumier ‘s approach	
3.5.3. The concept of tension flange in reinforced concrete joints. Paulay ‘s approach.	

<u>3.6. MODELLING: Influence of a transverse beam in a typical composite steel concrete beam to column joint</u>	116
3.6.1. Description of the model	
3.6.2. Calibration of the basic model.	
3.6.3. Partial parametric study	
3.6.4. Conclusions and future research	
<u>3.7. BEHAVIOUR FACTORS. Particularities raised by the evaluation of load reduction factors for seismic design of composite steel-concrete structures</u>	128
3.7.1. Introduction	
3.7.2. Force reduction in EC8.	
3.7.3. Estimation of reduction factor using MDOF analysis.	
3.7.4. Behaviour factor for composite structures.	
3.7.5. Conclusions.	
<u>3.8. Evaluation of behaviour factor for moment resisting composite frames on the basis of the Ispra Test</u>	132
3.8.1. General	
3.8.2. Evaluation of the behaviour factor	
3.8.3. Behaviour factor of composite frames	
<u>3.9. Analytical investigation of the behaviour of composite beams with shear connectors</u>	138
3.9.1. Significance of the Problem	
3.9.2. Proposed Modelling of Composite Beams	
3.9.3. Parametric Study on Composite Beams	
3.9.4. Comparison of Conventional and Partially Encased Composite Beams	
3.9.5. Analysis of Two Span Composite Beams	
3.9.6. Summary of Analytical Observations	
<u>3.10. BRISTOL TESTS. Experimental evaluation of behaviour factors</u>	160
3.10.1 Testing objectives	
3.10.2 The Bristol shaking table	
3.10.3 Model Characteristics and Dynamic Similitude	
3.10.4 Design of frame models	
3.10.5 Limit State Criteria	
3.10.6 Execution of the shaking table tests	
3.10.7 Results of shaking table tests	
3.10.8 Summary and Conclusions	
<u>3.11. ATHENS TESTS. Behaviour of a moment connection of a beam with slab under dynamic loading</u>	181
3.11.1 Introduction	
3.11.2 Test Specimens and Test Setup	
3.11.3 Test Program	
3.11.4 Test Results	
3.11.5 Test Interpretation	
3.11.6 Conclusions	
<u>3.12. REFERENCES of the technical reports</u>	193
4. DATA BANK OF LITERATURE REFERENCES ON COMPOSITE STRUCTURES	197
5. CONCLUSIONS AND RESEARCH NEEDS	198

1. INTRODUCTION : CONTEXT AND OBJECTIVES OF THE ICONS TOPIC 4 COMPOSITE STEEL CONCRETE RESEARCH PROJECT.

In 1994, during the preparation of the Eurocode 8 on seismic design of structures, composite steel concrete structures were the only type for which it was considered that the available background was so weak that no design rules could be provided. Only an informative annex was given, reflecting the mentioned weakness by presenting guidance which was questionable in several aspects.

This situation was due to the fact that experimental research on composite structures had, until then, essentially considered the case of vertical loading. Under horizontal loading like earthquakes, the response of structures is very different of what it is under gravity loads. In moment frames, for instance, significant positive bending moments can appear at the beam ends.

It also appeared in recent earthquakes (Northridge 1994, Kobe 1995) that the behaviour of composite moment frames could be bad. Reasons were partly to be found on the steel material and welding side, but specific aspects of the behaviour of composite elements and structures, like the influence of the unsymmetrical aspect of sections in beams with slab, contributed.

This situation was the incentive to prepare research proposals.

The definition of the research proposals took into consideration the following elements. Composite constructions can correspond to many different structural typologies or systems, as long as concrete and steel are combined, and the complete understanding of all aspect of the seismic behaviour of all types of composite structure requires years of research efforts. As research developments in the U.S. were bearing on composite moment frames with partial strength connections and on composite systems combining concrete walls or columns with steel or composite beams, it was considered that the research work in Europe should focus on moment frame structures with rigid connections.

Two main design options exist for such frames.

Either the composite behaviour of beams at their connections to the columns is neglected; then, the design can be based on the properties of the beams steel sections only; however, this requires a proper disconnection of the slab from the steel sections, because the capacity design of columns requires a safe (over)estimation of the plastic moments of beams.

Or it is taken advantage of the stiffness and plastic resistance of the composite beams; then, design data must be provided: effective widths of beams (under positive and negative bending, for the elastic as well as the plastic parts of the local behaviour), adequate sections and layout of the re-bars in the slab, proportions of steel sections and slab which realise a ductile behaviour of the plastic hinges(classes of sections), structural behaviour factors corresponding to these classes, requirements on the type and number of connectors between steel and concrete, stability checks for columns...

Following these considerations, research proposals were prepared.

An essential one was presented as Topic 4 in the ICONS project, a research network submitted to the Training and Mobility of Researchers programme of the European Commission.

The approval of the project by DG XII gave the opportunity to organise a coordinated set of activities, by funding a network of Institutions, researchers and their participation to meetings and experimental activities. The project also gave the possibility to invite experts from outside of the contract network. This activity was especially developed within the ICONS Topic 4 group dealing with composite steel concrete structures by organising what was called the "ICONS Topic 4 Extended Group". This group worked essentially on the development of rules for the design of steel concrete structure, contributing to what is reflected in the Section 2 of this Report "Design Rules for Eurocode 8 and their Background". As the title express it, this Section 2 provides the design guidance needed for Eurocode 8, up to the point that the rules given in this Report and in the Project Nr 2 of final version of Eurocode 8 (prEN 1998-2) are similar.

As mentioned, the ICONS Topic 4 activity was one among several research projects.

Other activities, out of which many were promoted by the European Commission, contributed to the development of background and concepts for the seismic behaviour of composite steel concrete structures.

Several experimental activities were realised in large European testing installations, with the support of the ECOEST1 and ECOEST2 programmes of the DG XII of the European Commission. These are programmes for the "Access to Large Scale Facilities for the Training and Mobility of researchers". In that context, tests have been made on the shaking tables at BRISTOL (UK), ATHENS (GREECE) and BERGAMO (ITALY). One plane frame was tested cyclically at SACLAY (FRANCE).

An important test of a full scale 3 D structures, 3 storey high and 3 bays by 3 bays in plan took place at the Elsa reaction wall facility of the European Joint Research Centre JRC at ISPRA (ITALY). It was supported by funds from DG III of the European Commission.

All these testing and the parallel numerical modelling and analysis, which are presented in Section 3 of this Report, contributed to clarify a number of issues in seismic design of composite steel concrete structures and provided background for the design rules in development.

Besides of these contributions, other research activities contributed to background knowledge. The RECOS project of Prof. MAZZOLANI included developments of testing on connectors realised in France by ARIBERT and LACHAL. RECOS was part of the COPERNICUS programme supported by DG XII of the European Commission.

National projects, like the one of BURSI in Italy, also brought useful data.

All this information, through the channel of the ICONS Topic 4 Extended Group, contributed to the developments of the design rules presented in Section 2.

Part of the work presented in this Report came in parallel and sometimes a step ahead of developments within the Eurocode 4, which is devoted to the design of composite structures under static loading. In order to homogenise the approaches for static and seismic design, an official liaison was organised. Professor ARIBERT was appointed by the Eurocode 4 drafting Committee to check that the seismic design guidelines developed within the ICONS Topic 4 Extended Group were a logical extension of Eurocode 4.

2. DESIGN RULES FOR EUROCODE 8 AND THEIR BACKGROUND.

ICONS PROJECT OF A SECTION 7 OF EUROCODE 8-EN1998 (2001). SPECIFIC RULES FOR STEEL – CONCRETE COMPOSITE BUILDINGS.

*A. Plumier, C. Doneux
Department of Civil Engineering, University of Liege, Belgium*

FOREWORD.

The document presented hereafter is structured like the the 2nd draft to the EN-EuroNorm version of Eurocode 8, prEN 1998, delivered in May 2001. The Sections and paragraphs are numbered like those of Section 7 Composite Steel Concrete Structures of that document.

The content of the document is not developed with essential consideration of displacement based design, which will be the future step, for the next generation of seismic codes.

To a large extent, this Section 2 can be considered as the background document to the definitive EN-1998 version of Eurocode 8 available in December 2001.

This document has been prepared by the ICONS Extended Group, which included ICONS contractors and the invited experts listed on the cover page.

The contributions to the drafting activity took different forms: documents, which are listed in the references to this Section, comments, remarks and active participation to 6 meetings dedicated to the preparation of this Section of the Report.

TABLE OF CONTENT

OF THE ICONS PROJECT OF A SECTION 7 OF EUROCODE 8 - EN1998 (2001).

7.1. GENERAL

7.1.1. Scope

7.1.2. Design concepts

7.1.3. Rules for the design of non-dissipative structures

7.2. MATERIALS

7.2.1. Concrete

7.2.2. Reinforcing steel

7.2.3. Steel sections

7.3. STRUCTURAL TYPES AND BEHAVIOUR FACTORS

7.3.1. Structural types

7.3.2. Behaviour factors

7.4. STRUCTURAL ANALYSIS

7.4.1. Scope

7.4.2. Stiffness of sections

7.4.3. Diaphragms

7.5. DESIGN CRITERIA AND DETAILING RULES COMMON TO ALL STRUCTURAL TYPES FOR DISSIPATIVE STRUCTURAL BEHAVIOUR

7.5.1. General

7.5.2. Specific criteria for dissipative structures

7.5.3. Plastic resistance of dissipative zones

7.5.4. Detailing rules for composite connections in dissipative zones

7.5.5. Detailing rules for foundations

7.6. DETAILING RULES FOR MEMBERS

- 7.6.1. General
- 7.6.2. Steel beams composite with slab
- 7.6.3. Effective width of slab
- 7.6.4. Fully encased composite columns
- 7.6.5. Partially encased members
- 7.6.6. Filled composite columns

7.7. DESIGN AND DETAILING RULES FOR MOMENT FRAMES

- 7.7.1. Specific criteria
- 7.7.2. Analysis
- 7.7.3. Detailing rules for beams and columns
- 7.7.4. Beam to column connections
- 7.7.5. Conditions for disregarding the composite character of beams with slab

7.8. DESIGN AND DETAILING RULES FOR COMPOSITE CONCENTRICALLY BRACED FRAMES

- 7.8.1. Specific criteria
- 7.8.2. Analysis
- 7.8.3. Diagonal members
- 7.8.4. Beams and columns

7.9. DESIGN AND DETAILING RULES FOR COMPOSITE ECCENTRICALLY BRACED FRAMES

- 7.9.1. Specific criteria
- 7.9.2. Analysis
- 7.9.3. Links
- 7.9.4. Members not containing the seismic links

7.10. DESIGN AND DETAILING RULES FOR STRUCTURAL SYSTEMS MADE OF REINFORCED CONCRETE SHEAR WALLS COMPOSITE WITH STRUCTURAL STEEL ELEMENTS

- 7.10.1. Specific criteria
- 7.10.2. Analysis
- 7.10.3. Detailing rules for Ductility Class I composite walls
- 7.10.4. Detailing rules for Ductility Class I coupling beams
- 7.10.5. Additional detailing rules for Ductility Class S

7.11. DESIGN AND DETAILING RULES FOR COMPOSITE STEEL PLATES SHEAR WALLS

- 7.11.1. Specific criteria
- 7.11.2. Analysis
- 7.11.3. Detailing rules

7.12. CONTROL OF DESIGN AND CONSTRUCTION

ANNEX J.

SEISMIC DESIGN OF THE SLAB REINFORCEMENTS OF COMPOSITE BEAMS IN MOMENT FRAMES

7. SPECIFIC RULES FOR STEEL – CONCRETE COMPOSITE BUILDINGS

7.1 General

7.1.1 Scope

(1) P For the design of composite steel concrete buildings, Eurocode 4 applies. The following rules are additional to those given in Eurocode 4.

(2) Except where modified by the provisions of this Section, the provisions of Sections 5 (*C. Reinforced concrete*) and 6 (*C. Steel structures*) apply.

7.1.2 Design concepts

(1) P Earthquake resistant composite buildings shall be designed according to one of the following concepts:

Concept a Dissipative structural behaviour with composite dissipative zones.

Concept b Dissipative structural behaviour with steel dissipative zones.

Concept c Non-dissipative structural behaviour.

(2) In concepts a and b, the capability of parts of the structure (dissipative zones) to resist earthquake actions beyond their elastic range is taken into account. When using the design spectrum defined in 3.2.2.4, the behaviour factor q is taken greater than 1,5 (see 7.3.2.).

(3) In concept b, structures are not meant to take any advantage of composite behaviour in dissipative zones; the application of concept b is conditioned by a strict compliance to measures that prevent involvement of the concrete in the resistance of dissipative zones; then the composite structure is designed to Eurocode 4 under non seismic loads and to section 6 of this Part 1 to resist earthquake action; the measures preventing involvement of the concrete are defined in paragraph 7.7.5.

(4) In non dissipative structures (concept c), the action effects are calculated on the basis of an elastic analysis without taking into account non-linear material behaviour but considering the reduction in moment of inertia due to the cracking of concrete in part of the beam spans, according to general structural analysis data defined in paragraph 7.4. and specific ones related to each structural type in paragraphs 7.7. to 7.11. When using the design spectrum defined in clause 3.2.2.4, the behaviour factor q is taken equal to 1,5. The resistance of the members and of the connections should be evaluated in accordance with Eurocode 3 and 4.

(5) The design rules for dissipative composite structures (concept a), aim at the development in the structure of reliable local plastic mechanisms (dissipative zones) and of a reliable global plastic mechanism dissipating as much energy as possible under the design earthquake action. For each structural element or each structural type considered in this Section, rules allowing this general objective to be reached are given at paragraphs 7.5. to 7.11. with reference to what is called the specific criteria. These criteria aim at the development of a design objective that is a global mechanical behaviour for which design indications can be given at present

C. Implicitly, this last sentence means that there may be other reasonable design objectives, but that the present state of the art is not such that design guidance can be provided.

(6) For design to concept a, dissipative composite structural behaviour, two structural ductility classes, I (Intermediate) and S (Special) are defined. They correspond to an increased ability of the structure to dissipate energy through plastic mechanisms. A structure belonging to a given ductility class has to meet specific requirements in one or more of the following aspects: structural type, class of steel sections, rotational capacity of connections, and detailings.

(7) For design to concept b, dissipative steel structure, Section 6 applies.

(8) Globally, the design options are those of Table 7.1

Table 7.1. Design concepts, behaviour factors and structures ductility classes

Design concept	Behaviour factor q	Ductility class
Concept c) Non dissipative structure	$1 \leq q \leq 1,5$	O for Ordinary
Concept a) or b) Dissipative structure	$1,5 < q < 4$	I for Intermediate
Concept a) or b) Dissipative structure	$q \geq 4$	S for Special

C. There is no direct relationship between the ductility class of a structure and a target global drift which this structure should be able to achieve. There is a precise requirement on the available local plastic rotations, as defined in testing procedures like ECCS NT-45 or ATC-24, for a given ductility class. However, on average, global drifts and local plastic rotations are of the same order of magnitude, so that Ductility class I corresponds approximately to a target global drift of the structure equal to 25mrad and Ductility class S to a target global drift of 35mrad.

7.1.3 Rules for the design of non dissipative structures.

(1)P Seismic design of non dissipative structures (concept b) is made according to EN 1993-1 and EN 1994-1, without any additional requirements than those of (2), 6.2(1) and 6.2 (2). It may be applied only in low seismicity regions.

C. Clause 6.2(1) and (2) are as follows:

(1)P *Structural steel should conform to standards referred to in EN 1993-1-1 and comply with the requirements of clause 3.2.3(1) of the same document*

(2)P *In bolted connections high strength bolts in category 8.8 or 10.9 should be used.*

(2)P K bracings (see fig. 6.1), in which the diagonals intersection lies on a column, may not be used in seismic zones.

C. fig. 6.1 is reproduced hereunder.

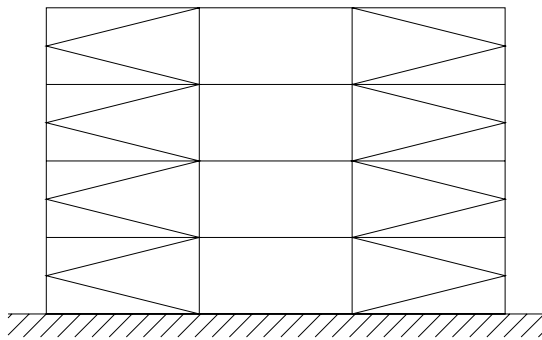


Figure 6.1. Frame with K bracings

7.2 MATERIALS

7.2.1 Concrete

(1) In dissipative zones, the use of concrete class lower than C20/25 or higher than C40/50 is not allowed.

7.2.2 Reinforcing steel

(1) Reinforcing steel considered in the plastic resistance of dissipative zones should satisfy the requirements of tables 5.2 and 5.3 of Section 5. Steel of ductility class E (table 5.3) is required for dissipative structures and for highly stressed regions of non dissipative structures. This requirement applies to both bars and welded meshes.

(2) Except for closed stirrups or cross ties, only ribbed bars are allowed as reinforcing steel in regions with high stresses.

(3) Welded meshes not complying with the ductility requirements of (1) may be used in dissipative zones. In that case, ductile reinforcements duplicating the mesh must be placed.

C. The problem behind the above statement is that in moment frames a reliable negative plastic moment in the connection zone can only be based on the presence of reinforcements guaranteed ductile, while the beam plastic moment considered in the capacity design of column must include all possible contributions of the reinforcements, non ductile welded mesh included for instance. When duplication of non ductile reinforcement by means of ductile reinforcements is realised, the capacity design of columns comes to an over design of these columns. In practice, the more economical solution will be obtained without continuity of non ductile reinforcements in dissipative zones.

7.2.3 Steel sections

(1)P Structural steel should conform to standards referred to in EN 1993-1-1 and comply with the requirements of clause 3.2.3(1) of the same document

(2)P In bolted connections high strength bolts in category 8.8 or 10.9 should be used.

(3)P The value of the yield strength $f_{y\max}$ which cannot be exceeded by the actual material used in the fabrication of the structure shall be specified and noted on the drawings.

(4) $f_{y\max}$ should not be more than 35% higher than the yield stress defining the steel grade (e.g. 235 for S235).

C. The value 35% corresponds to the following background: practice indicates that the actual value of the yield strength of steel is of the order of $1,25 \times f_y$; a 10% margin on 1,25 gives approximately 1,35; an additional 10% margin is accepted at the control stage (see 6.12)

(5)P The required fracture toughness of steel and welds and the lowest service temperature adopted in combination with earthquake action should be defined in the project specification

(6)P The control of material properties shall be made according to 6.12.

C. Clause 6.12 is as follows:

6.12. Control of design and construction

(1)P In addition to the provisions given in Part 1-1 of Eurocode 3, the following specific requirements shall be met :

a) The drawings made for fabrication and erection shall indicate the details of connections, sizes and qualities of bolts and welds as well as the steel grades of the members, noting the maximum permissible yield stress $f_{y\max}$ of the steel to be used by the fabricator in the dissipative zones.

b) 6.2(1) to 6.2(5) shall be fulfilled.

c) The control of the tightening of the bolts and of the quality of the welds shall follow the rules laid down in EN 1090.

d) During construction it shall be ensured that no structural changes involving a variation in the stiffness or in the strength of more than 10 % of the values assumed in the design occur.

(2)P *Whenever one of the above conditions is not satisfied, appropriate corrections or justifications shall be provided in order to meet the requirements of this Code and assure the safety of the structure.*

7.3 Structural types and behaviour factors

7.3.1 Structural Types

(1)P Composite steel concrete structures shall be assigned to one of the following structural types according to their behaviour under seismic actions. See Table 6.2a for moment frames, concentrically braced frames, frames with eccentric bracings and inverted pendulum structures. See Table 7.2 for composite structural systems behaving like walls and for composite steel plate shear walls.

a) Moment resisting frames, in which the horizontal forces are mainly resisted by members acting in an essentially flexural manner. In these structures, the dissipative zones are mainly located in plastic hinges in the beam or in the beam-column joints and energy is dissipated by means of cyclic bending. Beams and columns can be either steel or composite.

b) Composite concentrically braced frames consist of concentrically connected members designed so that the dissipative action will occur primarily through tension yielding and buckling of the braces. All other truss members should not yield or buckle and connections should not fail. Columns and beams shall be either structural steel or composite structural steel; braces shall be structural steel. The bracings may belong to one of the following two categories:

-Active tension diagonal bracings, in which the horizontal forces can be resisted by the tension diagonals only, neglecting the compression diagonals

-V bracings, in which the horizontal forces can be resisted by considering both tension and compression diagonals. The intersection point of these diagonals lies on a horizontal member which must be continuous.

K bracings, in which the diagonals intersection lies on a column (see fig. 6.1) are not allowed.

c) Composite eccentrically braced frames consist of braced systems for which each brace intersects a beam either at an eccentricity from the intersection of the centreline of the beam and the column or at an eccentricity from the intersection of the centreline of the beam and an adjacent brace. The beam portions between the points of intersection of either a brace and the adjacent column or two adjacent braces are called links. Members not containing the links may be either structural steel or composite structural steel. Other than for the slab, the links shall be structural steel. The dissipative action occur only through yielding in shear of these links. Configurations that ensures that all links will be active, like those of Table 7.2, should be used.

d) Inverted pendulum structures, as defined in 6.3, and in which dissipative zones are mainly located in the columns. This type of structure can be considered a moment resisting frame provided that the

earthquake resistant structures possess more than one column in each resisting plane and that the limitation of axial force $N_{Sd} < 0,3 N_{pl, Rd}$ is satisfied.

e) Composite structural systems which behave essentially as reinforced concrete walls. Table 7.2. The composite systems may belong to one of the following types:

In Type 1, the walls are made of steel or composite frames working together with infill panels.

In Type 2, encased steel sections are used as vertical edge reinforcement of concrete walls.

In Type 3, steel or composite beams are used to couple two or more reinforced concrete or composite walls.

f) Composite steel plate shear walls consist of a vertical steel plates with reinforced concrete encasement on one or both sides of the plate and structural steel or composite boundary members.

7.3.2 Behaviour factors

(1) P The behaviour factor q , introduced in 3.2.2.4, accounts for the energy dissipation capacity of the structure. Unless demonstrated according to (4) below, q takes the values given in Table 6.2a or in Table 7.2, provided that the regularity requirements of Section 4 and the rules in 7.5 to 7.11 are met

C. These values are similar to those of the chapter on steel and reinforced concrete structures. It has been shown [9] that the values of q does not differ significantly from one material type to another, as long as a correct evaluation of the "first yield" in the structure is made. It should correspond to the loading for which the first plastic hinge starts rotation. However, some factors could influence these values of q :

-the concentration of plastic rotations in the first hinges formed, because of the difference between

M_{Rd}^+ and M_{Rd}^- of composite section

-the effect of reduced low cycle fatigue resistance of T sections, in comparison to symmetrical sections

-the effect of increased damping, in comparison to steel structures, due to cracking and to friction at steel concrete interface.

(2) If the building is non-regular in elevation (see clause 4.2.9.3) the q -values of Table 6.2a and Table 7.2 should be reduced by 20 %

(3) When calculations are not performed in order to evaluate the multiplier α_u/α_1 , the approximate values of the ratio α_u/α_1 presented in Table 6.2a and Table 7.2 may be used. The parameters α_1 and α_u are defined as in 6.3.2 (3)

(4) Values of q factors higher than those given in Table 6.2a or in Table 7.2 are allowed, provided that they are justified by calculating α_u/α_1 from a geometric first order global inelastic analysis.

(5) The maximum value of α_u/α_1 to be used in design is equal to 1.6, even if the analysis mentioned in (4) above indicates higher potential values.

Table 7.2. Structural types and maximum associated behaviour factors

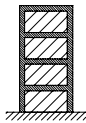
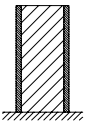
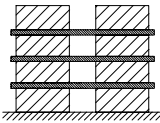
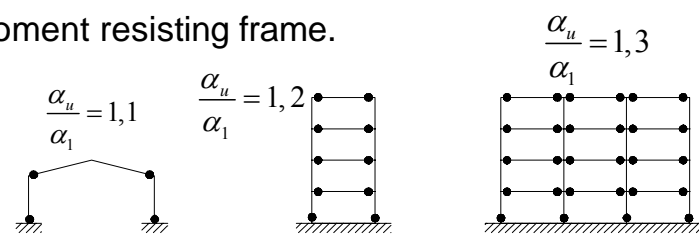
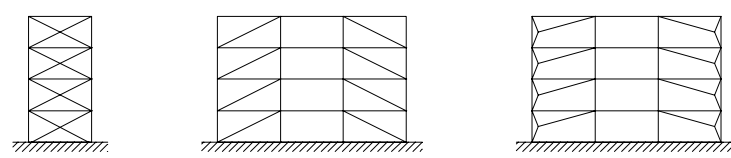
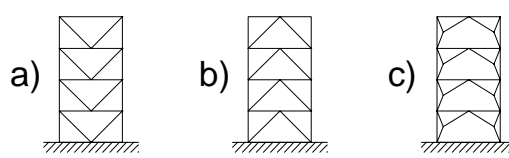
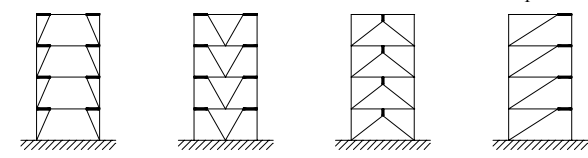

		Ductility Class	
		S	I
<p>e) Reinforced concrete shear wall elements. $\frac{\alpha_u}{\alpha_1} \approx 1.1$</p> <div style="display: flex; justify-content: space-around; align-items: flex-start;"> <div style="text-align: center;">  <p>TYPE 1</p> <p>Steel or composite moment frame with concrete infill panels.</p> </div> <div style="text-align: center;">  <p>TYPE 2</p> <p>Concrete walls reinforced by encased vertical steel sections.</p> </div> <div style="text-align: center;">  <p>TYPE 3</p> <p>Concrete shear walls coupled by steel or composite beams.</p> </div> </div>		$4 \frac{\alpha_u}{\alpha_1}$	$2.5 \frac{\alpha_u}{\alpha_1}$
<p>f) Composite steel plate shear walls with RC elements. $\frac{\alpha_u}{\alpha_1} \approx 1.2$</p>		$4 \frac{\alpha_u}{\alpha_1}$	$2.5 \frac{\alpha_u}{\alpha_1}$

Table 6.2.a. Structural types and maximum associated behaviour factors

		Ductility Class	
		S	I
<p>a) Moment resisting frame.</p>  <p>• Dissipative zones in the beams and bottom of columns</p>		$5 \frac{\alpha_u}{\alpha_1}$	4
<p>b) Frame with concentric bracings.</p> <p>Diagonal bracings.</p>  <p>Dissipative zones -tension diagonals only-</p>		4	4
<p>V - bracings.</p>  <p>Dissipative zones (tension & compression diagonals).</p>		2,5	2
<p>c) Frame with eccentric bracings.</p>  <p>- Dissipative zones (bending or shear links).</p>		$5 \frac{\alpha_u}{\alpha_1}$	4
<p>d) Inverted pendulum.</p>  <p>- Dissipative zones at the column base.</p> <p>$N_{Sd} / N_{Pl,Rd} > 0,3$</p>		$2 \frac{\alpha_u}{\alpha_1}$	2

7.4 Structural analysis

7.4.1 Scope

The following rules apply for a static equivalent dynamic elastic analysis of the structure under earthquake action.

7.4.2 Stiffness of sections

(1) The stiffness of composite sections in which the concrete is in compression is computed considering a modular ratio n

$$n = E_a / E_c = 7$$

(2) For composite beams with slab in compression, the moment of inertia of the section, referred to as I_1 , is computed considering the effective width of slab defined in 7.6.3.

C. In EC4 wording, I_1 is the second moment of area of the effective equivalent steel section calculated assuming that concrete in compression is uncracked. It is usually used for the second moment of area under sagging bending.

(3) The stiffness of composite sections in which the concrete is in tension is computed considering that the concrete is cracked and that only the steel parts of the section are active.

(4) For composite beams with slab in tension, the moment of inertia of the section, referred to as I_2 , is computed considering the effective width of slab defined in 7.6.3.

C. In EC4 wording, I_2 is the second moment of area of the effective equivalent steel section calculated neglecting concrete in tension but including reinforcement. It is usually used for the second moment of area under hogging bending.

(5) The structure is analysed considering the presence of concrete in compression in some zones and concrete in tension in other zones; the distribution of the zones is given in Sections 7.7 to 7.11 for the various structural types.

7.4.3 Diaphragms

(1) Design of floor diaphragms should comply with 4.5.2.5

(2) The analysis of the structure is made considering that all the members of the seismic resisting structure are active.

7.5 Design criteria and detailing rules for dissipative structural behaviour common to all structural types.

7.5.1 General.

(1) The design criteria given in 7.5.2. apply for earthquake-resistant parts of structures, designed according to the concept of dissipative structural behaviour.

(2) The design criteria given in 7.5.2 are deemed to be satisfied, if the detailing rules given in par. 7.5.3 - 7.5.5 and in par. 7.6 to 7.11 are observed.

7.5.2 Design criteria for dissipative structures

(1) P Structures with dissipative zones shall be designed such that these zones develop in those parts of the structure where yielding or local buckling or other phenomena due to hysteretic behaviour do not affect the overall stability of the structure.

(2) P Structural parts of dissipative zones shall have adequate ductility and resistance. The resistance shall be verified according to Eurocode 3 (concept b) and to Eurocode 4 (concept a). Ductility is obtained by compliance to detailing rules.

(3) P Dissipative zones may be located in the members or in the connections, if the effects of such connections on the behaviour of the structure are assessed.

(4) P When dissipative zones are located in the members, the non-dissipative parts and the connections of the dissipative parts to the rest of the structure shall have sufficient overstrength to allow the development of cyclic yielding in the dissipative parts.

(5) P When dissipative zones are located in the connections, the members shall have sufficient overstrength to allow the development of cyclic yielding in the connections.

7.5.3 Plastic resistance of dissipative zones

(1) Two plastic resistances of dissipative zones are considered in the design of composite steel concrete structures: a lower bound plastic resistance (index p , R_d) and an upper bound plastic resistance (index U , R_d).

(2) The lower bound plastic resistance of dissipative zones is the one considered in design checks concerning sections of dissipative elements; e.g. The lower bound plastic resistance of dissipative

zones is computed considering the concrete component of the section and only the steel components of the section which are certified ductile.

(3) The upper bound plastic resistance of dissipative zones is the one considered in the capacity design of elements adjacent to the dissipative zone; e.g. in the capacity design verification of 4.5.2.3(4), the design values of the resisting moments of beams are the upper bound plastic resistances, $M_{U,Rd,b}$ whereas those of the columns are the lower bound ones, $M_{pl,Rd,c}$.

(4) The upper bound plastic resistance is established considering the concrete component of the section and all the steel components present in the section, including those that are not certified ductile.

(5) Action effects, which are directly related to the resistance of dissipative zones, must be determined on the basis of the resistance of the upper bound resistance of composite dissipative sections; e.g. the design shear force at the end of a dissipative composite beam must be determined on the basis of the upper bound plastic moment of the composite section.

7.5.4 Detailing rules for composite connections in dissipative zones

(1) Non dissipative composite connections in dissipative zones should have an adequate design and sufficient overstrength to allow for yielding of the connected members.

C. f_{yd} should be an appropriate estimation of the actual value of the yield strength of the parts which the designer intends to be dissipative, so that neighbour parts really have an overstrength to the dissipative parts. A previous comment about 7.2.3 (4) gives indication on that matter.

(2) The overstrength condition for connections need not apply if the connections are designed to contribute significantly to the energy dissipation capability inherent to the chosen q-factor.

(3) The adequacy of design should limit localization of plastic strains and high residual stresses and prevent fabrication defects. The adequacy of design should be supported by experimental evidence.

(4) The integrity of the concrete in compression should be maintained during the seismic event, yielding taking place essentially in the steel sections.

(5) Yielding of the reinforcing bars in a slab should be allowed only if beams are designed to comply with clause 7.6.2.(8)

(6) For the design of welds and bolts, 6.5.5 (4), 6.5.5 (5), 6.5.5 (6) and 6.5.5 (7) applies.

C1. These clauses are as follows.

6.5.5(4) Non dissipative connections of dissipative members made by means of full penetration butt welds are deemed to satisfy the overstrength criterion

6.5.5(5) For fillet weld or bolted non dissipative connections, the following requirement should be met:

$$R_d \geq 1,5 \times R_{fy} \quad (6.1)$$

R_d resistance of the connection according to clause 6 of Part 1-1 of Eurocode 3 and R_{fy} plastic resistance of the connected dissipative member.

C2. In the ENV and in prEN-1, the requirement was $R_d \geq 1,2 \times R_{fy}$. The present requirement is in fact not different, because previously R_{fy} had to be computed considering an "appropriate estimation f_{yd} of the actual value of the yield strength of the connected members", which is of the order of $1,25 f_y$ (e.g. 300 N/mm^2 for an S235 steel). For clarity, the present draft considers that the designer should not be left in front of problems like the definition of "appropriate estimation f_{yd} ..." . All design is now done with the classical design values of f_y and an increased coefficient for overstrength covers the "estimation" problem.

The present coefficient is thus 1,2 (the old one) \times 1,25 = 1,5

6.5.5 (6) Only categories B and C of bolted joints in shear and category E of bolted joints in tension should be used, with controlled tightening of the bolts in accordance with EN 1993-1-1.

6.5.5 (7) Shear joints with fitted bolts are also allowed. For bolted shear connections, the shear resistance of the bolts should be higher than 1,2 times the bearing resistance.

(7) Local design of the reinforcing bars needed in the concrete of the joint region will be justified by models that satisfy equilibrium (e.g. Annex J of this section for slabs).

(8) The stiffness, strength and ductility of connections under cyclic loading should be supported by experimental evidence, in order to comply with specific requirements defined for each structural

type and structural ductility classes. This applies to all types of connections in dissipative zones. The requirements on ductility are expressed for various structural types in par.7.6. to 7.11. When expressed in term of plastic rotation capacity, the parameter used is θ_p defined in 6.5.5 (8).

C1. The definition in 6.5.5(8) is as follows.

the parameter used is θ_p defined as $\theta_p = \delta / 0,5L$ (6.2)

where δ and L are respectively the beam deflection at midspan and the beam span. See fig. 6.2.

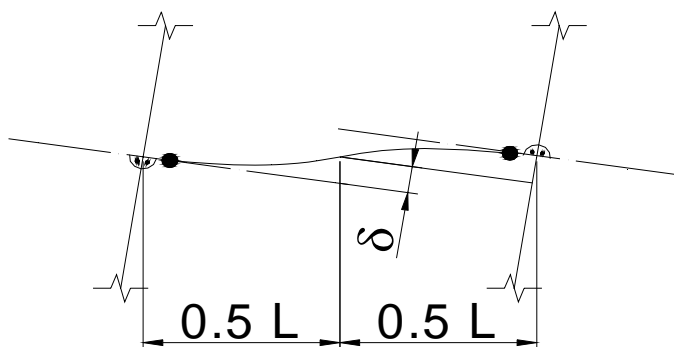


Figure 6.2. Calculation of the plastic rotation angle.

C2. In moment frames under static loading, the rotations may be calculated using prEN 1994-1-1 and its Annex J. The rotation capacity should not be less than 35 mrad for negative bending and 20 mrad for positive bending. Currently, it is not possible to quantify in a general approach the effect of hysteresis on stiffness degradation. None the less, it is estimated that the calculation according to Annex J of EN 1994 is adequate to account for strength degradation. For the steel components, both the stiffness and the strength of joints are not so sensitive to hysteretic effects. The requirements on rotation capacity derive from [10] [11].

(9) In fully encased framed web panels of beam/column connections, the panel zone resistance can be computed as the sum of contributions from the concrete and steel shear panel, if the following conditions are checked:

- a) the aspect ratio h_b/b_p of the panel zone is such that: $0,6 < h_b/b_p < 1,$
- b) $V_{wp,Sd} < 0,8 V_{wp,Rd}$

where

$V_{wp,Sd}$ design shear force in the web panel due to the action effects, taking into account the plastic resistance of the adjacent dissipative zones in beams or connections

$V_{wp,Rd}$ shear resistance of the composite steel concrete web panel according to Eurocode 4.

h_b , b_p as defined at fig. 7.1a)

(10) In partially encased stiffened web panels, an assessment similar to (9) is permitted if, in addition to the requirements of (9), one of the following conditions is fulfilled:

reinforcements complying with 7.6.2 (3) and (5) are present

no reinforcements are present, provided that both $h_b/b_b < 1,2$ and $b_c/b_p < 1,2$

where h_b , b_b , b_c and b_p are defined at fig. 7.1a).

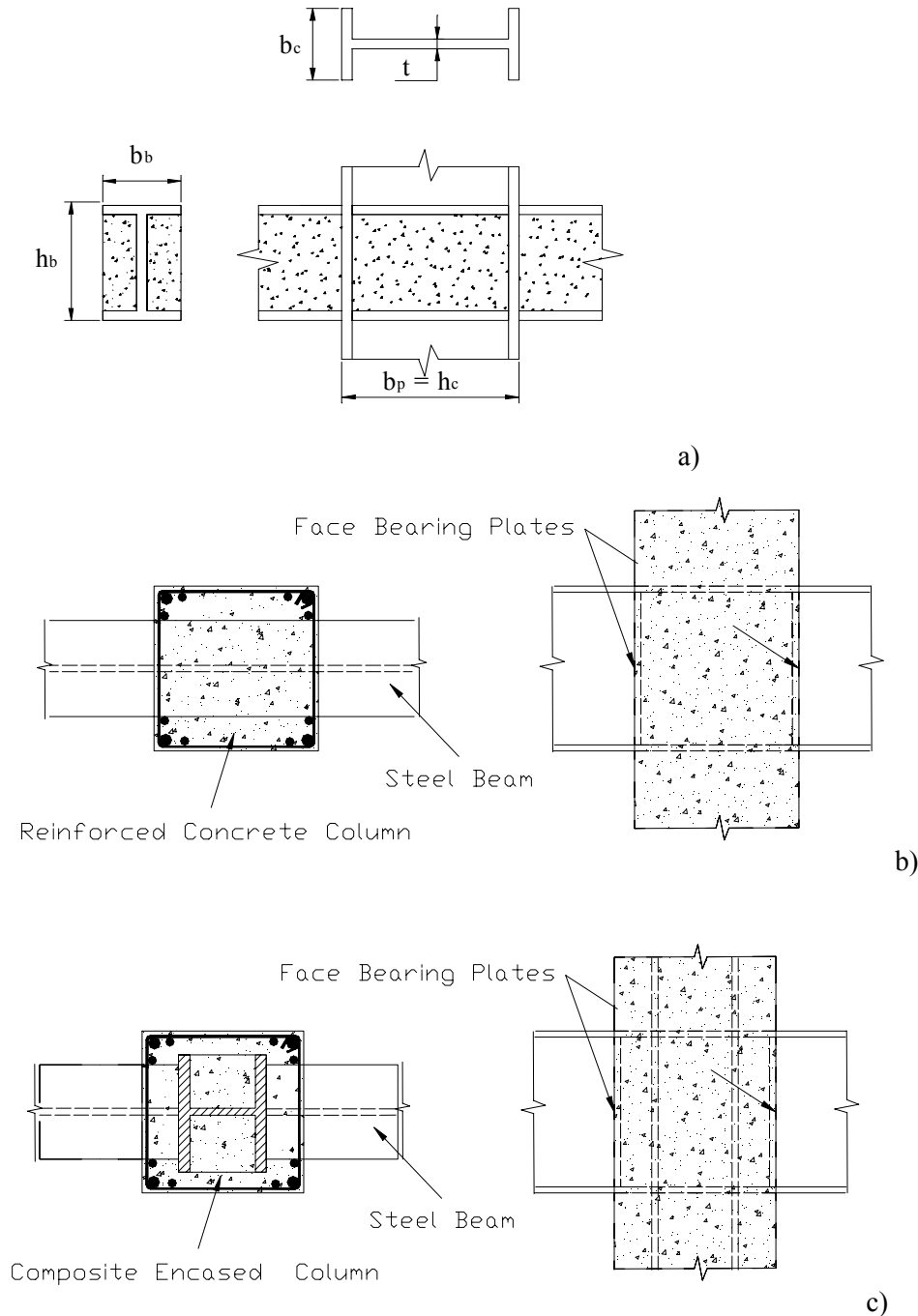


Figure 7.1. Web panel framed by flanges and stiffeners.

a) Partially encased steel beam to steel column connection. b) Steel beam to reinforced concrete column connection. c) Steel beam to fully encased column connection

(11) When a dissipative steel or composite beam is framing into a reinforced concrete column as shown in fig. 7.1 b), vertical column reinforcements with design axial strength equal to the shear strength of the coupling beam shall be placed close to the stiffener or face bearing plate adjacent to the dissipative zone. It is permitted to use vertical reinforcements placed for other purposes as part of the required vertical reinforcement. The presence of face bearing plates is required; they will be full depth stiffeners of a combined width not less than $(b_b - 2 t)$; their thickness will not be less than $0,75 t$ or 8 mm; b_b and t are respectively the beam flange width and the panel web thickness. Figure 7.1.

(12) When a dissipative steel or composite beam is framing into a fully encased composite column as shown at fig. 7.1 c), the beam column connection can be designed either as a beam/steel column connection or a beam/composite column connection. In the latter case, vertical column reinforcements

can be calculated either as in (11) above or by considering a distribution of the shear strength of the beam between the column steel section and the column reinforcements. In both instances, the presence of face bearing plates as defined in (11) is required.

C. Face bearing plates considerably increase the resistance of the joint by increasing stiffness, by delaying localised cracking and crushing of concrete and by confining the concrete. They act as shear connectors for concrete contributing to the shear strength of the panel zone (see 10) and (11)).

(13) The vertical column reinforcement specified in (11) and (12) above shall be confined by transverse reinforcement that meets the requirements for members defined in 7.6.

C1. The rules (11), (12), (13) have been defined by the ASCE task Committee on Design Criteria for Composite Structures in Steel and Concrete, with a restriction: because of the limited experimental background: these rules are acceptable for seismic regions with design Peak Ground Acceleration are less than 0,29g (EPA < 0,20 g). As this approximately covers the expected PGA in Europe, the restriction is not mentioned in the Eurocode 8 rules.

C2. For construction reasons, the steel beam flanges should not exceed half the column width (see Fig. 7.1)

7.6 Rules for members

7.6.1 General

(1) Composite members, which are part of the earthquake resistant structures, must comply with the rules of Part 1-1 of Eurocode 4 and with additional rules defined in this Section of Eurocode 8.

C. Fully encased beams are at present out of the scope of Eurocode 4; partially encased beams are considered. The same option is chosen here.

(2) The earthquake resistant structure is designed with reference to a global plastic mechanism involving local dissipative zones; there are members part of the earthquake resistant structure in which dissipative zones are located and other members without dissipative zones.

(3) For tension members or parts of members in tension, the ductility requirement of clause 5.4.3.(4) of Eurocode 3 should be met.

(4) Sufficient local ductility of members which dissipate energy under compression and/or bending should be ensured by restricting the width-to-thickness ratios of their walls. Steel dissipative zones and the unencased steel parts of composite sections should meet the requirements of 6.5.3(1) and Table 6.3. Dissipative zones of encased composite members should meet the requirements of Table 7.3. The limits given for flange outstands of partially encased members may be relaxed if special details are provided as described in 7.6.5.

C. Clause 6.5.3(1) and Table 6.3 are as follows.

(1).Sufficient local ductility of members which dissipate energy by their work in compression or bending should be ensured by restricting the width-thickness ratio b/t according to the cross sectional classes specified in EN 1993-1-1. The relationship between the global ability of the structure to dissipate energy, or ductility class, expressed by the behaviour factor q, and the local ductility provided by steel elements of various cross sectional classes is expressed in Table 6.3.

Table 6.3: Requirements on cross sectional class related to a structure q-factor

Ductility class	Behaviour factor q	Cross sectional class
S	$q > 4$	class 1
I	$2 < q \leq 4$	class 2
I	$1,5 < q \leq 2$	class 3

Table 7.3. Relation between behaviour factor and limits of wall slenderness.

Ductility Class of Structure	S	I	O
Behaviour Factor (q)	$q \geq 4$	$1.5 < q < 4$	$1 \leq q \leq 1.5$
Partially Encased H or I Section (flange outstand limits c/t)	10 ϵ	15 ϵ	21 ϵ
Filled Rectangular Section (h/t limits)	24 ϵ	38 ϵ	52 ϵ
Filled Circular Section (d/t limits)	80 ϵ^2	85 ϵ^2	90 ϵ^2

$$\epsilon = (f_y/235)^{0.5}$$

C1. Table 7.3 has been developed by BRODERICK and ELGHAZOULI [25]. It is the outcome of a thorough analysis of the existing literature in 2000. The limits given in Table 7.3 are based on available experimental and analytical investigations on the rotation capacity of composite members. These limits are selected to provide cyclic rotation capacity over 35 and 25 mrad for Ductility Classes S and I, respectively, under a maximum axial load representing 30% of the plastic section capacity. The slenderness limits of partially encased sections for the three ductility classes correspond to the limits of Class 1, 2 and 3, respectively, in EC4. Also, the limits given for Ductility Class O of filled sections are the same as the corresponding Class 3 values in EC4.

C2. Table 6.3 and 7.3 make explicit a fact which was implicit in Part 1.3 of the ENV version of Eurocode 8 (ENV 1998, 1994): for steel structures, ductility classes were already defined through the relationship between local behaviour (classes of sections of the members) and global behaviour (behaviour factors q).

C3. For moment frames, the Seismic Provisions for Steel and Composite Buildings drafted by AISC [1] distinguish similarly between ordinary, intermediate and special moment frames, with increasing ability to dissipate energy in plastic mechanisms.

C4. For partially-encased members, the values given in Table 7.3 are related to the conventional configuration for which static design rules are available in EC4. Nevertheless, these limits may be relaxed considerably if additional links are welded to the inside of the flanges within the entire expected length of dissipative zones. The restraining effects of these links has been set forward in several studies, including the recent thesis by ABED [26].

Special rules for these additional links are given in 7.6.5 .

C5. For columns, the code should provide provisions for four different design situations: a) the column is a dissipative member with composite dissipative zones

b) the column is a dissipative member, but only the resistance of the steel part is considered in the dissipative zones

c) the column is a non-dissipative composite member

d) the column is a non-dissipative steel member

Situation (a) requires most design guidance and the content of this Section 7 relates mainly to this case.

However, the majority of column members are non-dissipative and only their elastic cyclic response needs to be assured. Non-dissipative columns may be designed as composite if it is assured that their cyclic elastic response is adequate. Situation (d) may often provide a simple workable solution requiring only a few simple earthquake-resistant rules.

Only dissipative columns (the minority) need to be detailed to ensure an adequate inelastic cyclic response before they can be designed as composite members.

Three cross-section types are considered for columns: fully-encased(7.6.4), partially-encased(7.6.5) and filled(7.6.6).

(5) More specific detailing rules for composite members are given in 7.6.2., 7.6.4., 7.6.5 and 7.6.6.

(6) A behaviour factor $q > 6$ may be used if the design compressive axial force N_{sd} in the columns and the non-dimensional slenderness considered in the most unfavourable buckling plane of these elements (obtained on the basis of a buckling length equal to the distance between axis intersections) satisfy the following requirement:

$N_{sd}/N_{pIRd} < 0.15$ and $\bar{\lambda} < 1.1$ if the column is in bending with double curvature

$N_{sd}/N_{pIRd} < 0.15$ and $\bar{\lambda} < 0.65$ if the column is in bending with single curvature

(7) In the design of all types of composite columns, the resistance of the steel section alone or the combined resistances of the steel section and the concrete encasement or infill may be considered.

(8) The design of columns in which the member resistance is considered to be provided only by the steel section may be carried out according to the provisions of Section 6. In case of dissipative columns, the capacity design provisions of 7.5.2 and 7.5.3 must be considered.

C. This clause ensures that the design shear force of columns and the column base moment, for instance, are determined on the basis of the moment of resistance of the full composite section.

(9) For fully encased columns with composite behaviour, the minimum cross sectional dimensions shall not be less than 250 mm.

C. This restriction need only apply to fully-encased members as it is similar to clause on reinforced

concrete structures.

(10) The shear resistance of non-dissipative composite columns shall be determined according to the rules given in Eurocode 4.

(11) In columns, when the concrete encasement or infill are assumed to contribute to the axial and/or flexural resistance of the member, the design rules given in 7.6.4 to 7.6.6 apply. These rules ensure full shear transfer between the concrete and the steel parts in a section and protect the dissipative zones against premature inelastic failure.

C. In EC4, the interaction of the steel and concrete parts of columns can be achieved through the use of bond alone. Allowable design bond stresses are specified for this purpose. The same approach is employed in Japanese design practice, but not in the ACI and AISC codes [13], in which all shear transfer between the steel and concrete is based entirely on direct bearing. However, the AISC code does allow bond stress alone to be employed in fully-encased beams.

These EC4 design bond stresses may not be reliable in cyclic response conditions. Wherever the bond stress is inadequate, it is necessary to provide shear connectors. In braced frames, a small number of such connectors may be required close to the beam-column connection. For filled columns, Japanese practice achieves shear transfer through the connection detail in the interior of the column.

In non-dissipative columns, it may be valid to assume that composite action can be achieved through bond alone. However, to allow for cyclic response effects, the allowable design values of the bond stress should be lower than in EC4. Tests by Roeder on embedded steel sections [13] suggest that only one-third of the static bond capacity should be allowed. This is reflected in provision (12). Such a code provision may allow a column without shear connectors to be designed as composite whenever the seismic action effects are not too high.

(12) For earthquake-resistant design, the design shear strengths due to bond and friction given in Table 6.6 of Eurocode 4 must be reduced by a factor of 0.3.

(13) When for capacity design purposes, the full composite resistance of a column is employed, complete shear transfer between the steel and reinforced concrete parts must be ensured. If insufficient shear transfer is achieved through bond and friction, shear connectors shall be provided to ensure full composite action.

C1. In the columns of braced frames, axial forces are more significant than bending moments and the response will normally be elastic. It must be assured that the axial force is shared between the concrete and steel parts. There will be a high bond demand wherever the column axial force increases. This will occur at floor levels where bracing members and beams are connected to the column [14].

C2. For fully-encased composite columns under vertical loading, sufficient transfer of forces is normally provided through bond and friction. It is not certain that this approach remains valid under cyclic loading conditions. Statement (12) allows this practice to be applied to non-dissipative columns of frames subjected to seismic action. Statement(13) is relevant for columns in moment resisting frames and is similar to the NEHRP Recommended Provisions and should be conservative.

C3. For partially encased columns, the provisions are the same as those proposed for fully-encased columns. Most test data on beams and beam-columns refer to the case where mechanical connection using welded reinforcement is present. In most cases, full shear connection was achieved. In some tests at Liege, the reinforcement spacing was too great and full shear connection was not achieved. It is possible that sufficient shear transfer could be achieved through bond alone, but the cases where this applies are not known for cyclic inelastic response.

C4. Hajjar [15] has shown that the global response of moment-resisting frames with filled columns, as displayed in push-over analyses, does not vary significantly with the stiffness or strength of the shear connection achieved through bond and friction. That is, the same response is displayed with and without composite action.

However, the provisions of the NEHRP Recommended Provisions stipulate that shear connectors must be provided in composite columns subjected primarily to flexure. A conservative approach, in the absence of better information, would be to adopt this provision in EC8.

(14) Wherever a composite column is subjected to predominately axial forces, sufficient shear transfer must be provided to ensure that the steel and concrete parts share the loads applied to the column at connections to beams and bracing members.

(15) Except at their base in some specific structural types, columns are generally not designed to be

dissipative. However, to match uncertainties of design, specific reinforcements of the concrete encasement are defined for regions which may yield. These regions are called “critical regions”. Their specific reinforcements are defined in 7.6.4.

C. Dissipative zones in columns normally only occur at their base. However, the EC8 detailing rules for RC columns consider critical zones at the upper and lower ends of all column lengths. It is proposed that the same principle be applied to fully encased columns, in which the protection of concrete is critical for safety.

(16) Provisions 5.6.2.1 and 5.6.3 concerning anchorages and splices in the design of reinforced concrete columns apply also to the reinforcements of composite columns.

C. These are the relevant EC8 rules for RC columns. The NEHRP stipulates the ACI rules for longitudinal reinforcement.

7.6.2 Steel beams composite with slab

(1) The design objective of the rules in this section is to maintain the integrity of the concrete slab during the seismic event, while yielding takes place in the bottom part of the steel section and/or in the rebars of the slab.

(2) If it is not intended to take advantage of the composite character of the beam section for energy dissipation, paragraph 7.7.5. has to be considered.

(3) Beams conceived to behave as composite elements in dissipative zones of the earthquake resistant structure shall be designed for full or partial shear connection according to 6.3.1.3. of Eurocode 4 (prEN 1994-1-1), provided that the minimum connection degree is not less than 0,8 and the total resistance of the shear connectors within any hogging moment region is not less than the plastic resistance of the reinforcement

C. The indication 0,8 comes out from research works [2] and [3], but other authors[22] oppose to this opening to partial shear connections. Dynamic experimental testing under ECOEST funding in Athens(see Section 3.11 of the Report) demonstrated that specimens with a stud spacing corresponding to a partial degree of shear connection of 70 % had a good low cycle fatigue behaviour, much better than those with a degree of connection of 45% : they showed a life expectancy under maximum, yield introducing, forcing conditions, which was over 3 times higher, with number of cycles far above what may be expected in an earthquake. It must also be pointed out that the following rule (4) means in a certain way that the real degree of shear connection is about 1.

(4) The design resistance of connectors in dissipative zones is obtained from the design resistance provided in 6.7.3. of Eurocode 4 applying a reduction factor equal to 0.75

C. Recent experimental evidences indicate such a value [4][22]. In the absence of more accurate design rules, the design resistance of shear connectors should be determined from push-type tests in accordance with the procedures established in 10.2 of Eurocode 4. In detail, the testing equipment should provide symmetric boundary conditions when testing specimens subjected to cyclic loading. The cyclic slip capacity δu can be obtained from the aforementioned tests. For headed stud shear connectors, the cyclic slip capacity can be derived from the one relevant to a monotonic push-type test applying a reduction factor equal to 0.5.

(5) The design resistance of shear connectors related to the failure of the steel devices should be greater than the design resistance of shear connectors related to the concrete failure.

C. This is justified by the fact that the brittle failure of the steel devices used as connector must be avoided in order to achieve high values of slip ductility of shear connectors[16]. This condition results in imposing an upper bound to f_c . This condition might be necessary only when partial shear connectors are used.

(6) Full shear connection is required when non ductile connectors are used

(7) When a profiled steel sheeting with ribs transverse to the supporting beams is used, the reduction factor k_t of the design shear resistance of connectors given by the relation 6.16 of Eurocode 4 should be further reduced by applying the rib shape efficiency factor k_r given at fig.7.2.

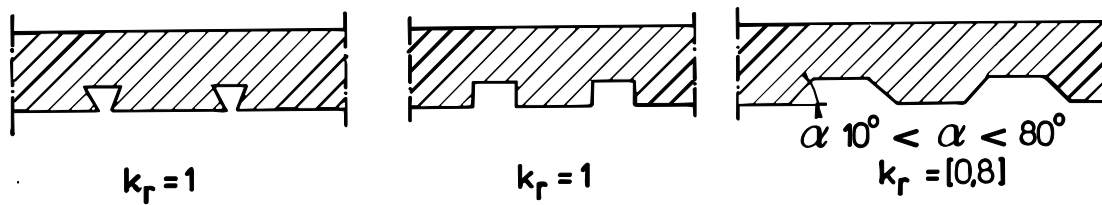


Figure 7.2. Values of the rib shape efficiency factor.

C1. Recent experimental evidences[18] have shown that steeldeck with trapezoidal shapes having positive slopes α induce uplift forces in the slab which can generate a concrete cone failure at the connector; the problem is not yet calibrated and the above k_r are only suggested.

C2. Furthermore, the additional reduction factor k_r might also be influenced by other parameters as the number of shear connectors per rib and the procedure of welding (either through the steel sheeting or directly on the steel flange for sheeting with holes).

C3. Preferably, the re-bars of the slab should be positioned under the level of the head of the connectors. This has 2 positive effects :

- it equalises the required displacement of the connectors, contributing to a better correspondence between the design hypothesis of equal values of resistance provided by connectors
- it contributes to prevent uplift of the slab by improving the resistance of the slab under the level of connectors heads.

(8)P To achieve ductility in plastic hinges, the ratio x/d of the distance x between the top concrete compression fibre and the plastic neutral axis to the depth d of the composite section should comply with:

$$x/d < \varepsilon_{cu} / (\varepsilon_{cu} + \varepsilon_a)$$

Where ε_{cu} is the crushing strain of concrete in cyclic conditions
 ε_a is the total strain in steel at Ultimate Limit State

(9) Using for usual reinforced concrete $\varepsilon_{cu} = 2,5 \cdot 10^{-3}$ and considering that for regular structures $\varepsilon_a = q \varepsilon_y = q f_y / E$, the x/d upper limit values of Table 7.4 are derived.

Table 7.4. Limit values of x/d for ductility of beams with slab

Ductility class	q	f_y (N/mm ²)	x/d upper limit
S	$q \geq 4$	355	0,19
S	$q \geq 4$	235	0,26
I	$1,5 < q < 4$	355	0,26
I	$1,5 < q < 4$	235	0,35

C1. The value to consider for ε_{cu} is the critical point. At the beam column joint, the concrete is reinforced and confined laterally by the slab. Experiments like [18] does not consider the confinement. ε_{cu} has to be defined by calibration of cyclic testing of joints where the slab faces a column to succeed in providing realistic approaches. Then, the values given above are more on the safe side than it seems when one refers to purely uniaxial failure strains.

C2. Other formulations are possible. In the AISC draft, a complete formula is given. The distance from the maximum concrete compression fibre to the plastic neutral axis shall not exceed:

$$\frac{Y_{con} + d_b}{1 + \left(\frac{1,700 F_y}{E_s} \right)}$$

where Y_{con} = the distance from the top of the steel beam to the top of concrete, in.

d_b = the depth of the steel beam, in.

F_y = the specified minimum yield strength of the steel beam, ksi.

E_s = the elastic modulus of the steel beam, ksi.

It corresponds to $\varepsilon_a > 5 f_y / E$ and a concrete deformation $\varepsilon_{cu} = 3 \text{ ‰}$

(10) In dissipative zones of beams, specific ductile reinforcements of the slab called “seismic rebars” (see fig. 7.3) should be present in the connection zone of the beam to the column. Their design is defined in Annex J to this Section 7.

C. For beams with slab in which dissipative zones are located, specific reinforcements of the slab called "seismic rebars" must be present in the zones of connections of the beams to the columns. Their sections A_s and their lay out must be designed to reach ductility. It has been established that there cannot be one simple single rule which would guarantee that this goal is achieved. In fact, the design is different for exterior and interior columns; it is also different when beams transverse to those primarily bent by the earthquake action are, or not, present, that is when beams are present, or not, on two orthogonal axis directions at their connections to the columns. This has led to the definition of an “Annex J” on slab design in the connection zones.

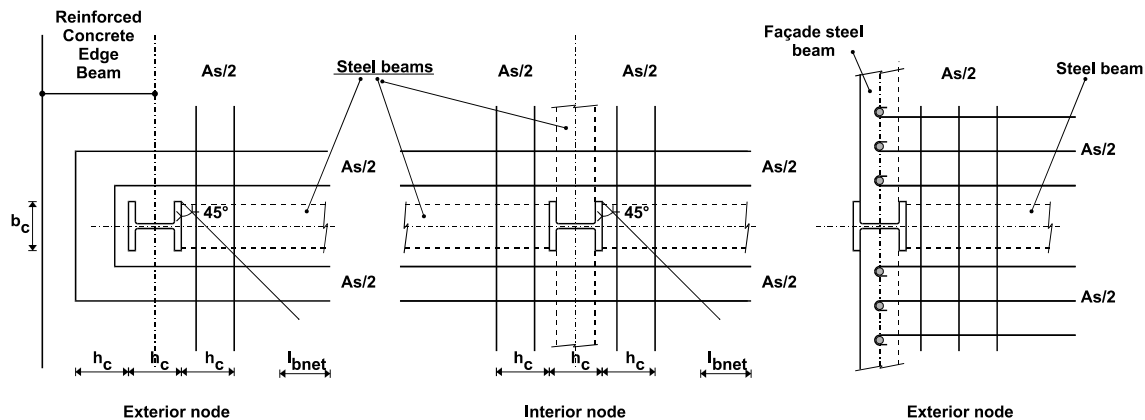


Figure 7.3: Layout of “Seismic Rebars”

7.6.3 Effective width of slab.

C1. This paragraph has to tackle several problems, because its content should provide design data bringing fair estimate of:

- the periods of the structure, which are a matter of elastic stiffnesses, having implications on the design forces (action effects) in the standard design method using design spectra
- the plastic resistances of dissipative zones and of the structure as a whole, for which reliable lower bound estimates are needed
- the capacity design of non dissipative elements, which should be based on upper bounds resistances of the dissipative zones.

The matter as such is vast, especially if one considers the many various possible design of "composite steel concrete" structures and the possible variety of design concepts for dissipative zones. As a first step, and in order to come out with a design tool in a short time, the code proposal can only exist if its scope is restricted to one definite option concerning the local plastic mechanism in dissipative zones and the global plastic scheme of the whole structure, as it expressed in 7.6.2. (1).

C2. The following text only deals with effective width of slab in composite T beams

(1) The total effective width b_{eff} of concrete flange associated with each steel web should be taken as the sum of effective widths b_e of the portion of the flange on each side of the centreline of the steel web (Figure 7.4). The effective width of each portion should be taken as b_e given in Table 7.4, but not greater than b defined hereunder in (2).

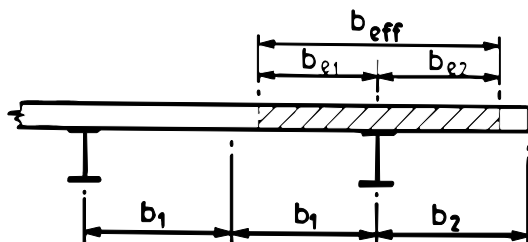


Figure 7.4. Definition of effective width b_e and b_{eff} .

- (2) The actual width b of each portion should be taken as half the distance from the web to the adjacent web, except that at a free edge the actual width is the distance from the web to the free edge.
- (3) The portion b_e of effective width of slab to be used in the determination of the elastic and plastic properties of the composite T sections made of a steel section connected to a slab are defined in Table 7.5 and Figure 7.5. These values are valid when the seismic re-bars defined in 7.6.2 (10) are present.

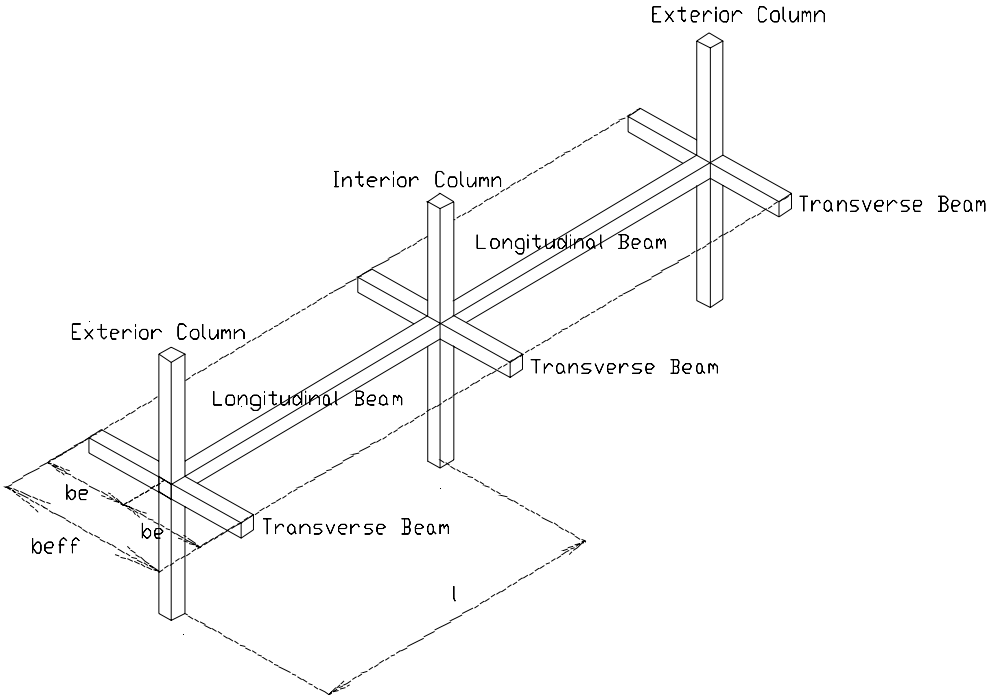


Figure 7.5. : Definition of Elements in Moment Frame Structures.

Table 7.5. Effective width b_e of slab

b_e	Transverse beam	b_e for M_{Rd} (PLASTIC)	b_e for I (ELASTIC)
At interior column	Present or not present	For M^- : 0,1 l For M^+ : 0,075 l	0,05 l 0,0375 l
At exterior column	Present as an edge beam fixed to the column, either in the plane of the columns, with connectors for full shear and specific detailing for anchorage of re-bars or exterior to the column plane, with re-bars of the hair pin type	For M^- : 0,1 l For M^+ : 0,075 l	0,05 l 0,0375 l
At exterior column	Not present or no re-bars anchored	For M^- : 0 For M^+ : $b_c/2$ or $h_c/2$	0 0,025 l

C1. At present, the values given here in Table 7.5 have been established by DONEUX and PLUMIER on the basis of ARBED-ECSC research in the 80's[19], the Ispra 3D test[17], the Darmstadt tests[20], respectively Sections 3.3 and 3.4 of the Report, and the Saclay test (section 3.2 of the Report). The analysis of the test results indicated quite repetitive values for what concerns the evaluation of the plastic moment M_{Rd} in all the test performed, in spite of the differences existing in dimensions, type of formwork, layout of re-bars... On the contrary, the effective widths deduced from the elastic part of the tests were quite variable from test to test or from X to Y direction in the Ispra-3D test. This may be the result of the influence of several factors, which is more important on the elastic stiffness than on the plastic resistance. These factors are, for instance:

the existence of an initial cracked state of the slab induced by the shrinkage; this cracked state can be different with permanent metal decking formwork from what it is with classical temporary formwork ; it is for sure different when different conditions are realised during the drying period of the concrete
different influences of metal deck in X and Y direction depending on the direction of waves
different densities of re-bars in the slab, by their influence of the effects of shrinkage
the 2D or 3D character of the slab in tests.

Considering this variability of b_e 's deduced from tests, the option taken by the drafting committee has been to keep in Table 1 rather lower estimates of the effective width to be used in the evaluation of the elastic stiffness rather than averages of test results.

C2. In Eurocode 4, the effective width b_e of the portion of the flange on each side of the centreline of the steel web is linked with the bending moment diagram and should be taken as $b_e = \frac{\ell_o}{8} \dots (\leq b)$. The length ℓ_o is the approximate distance between points of zero bending moment. For simply-supported beams it is equal to the span. For typical continuous beams, ℓ_o may be assumed to be as shown in Figure C1, in which values at supports are shown above the beam, and midspan values below the beam.

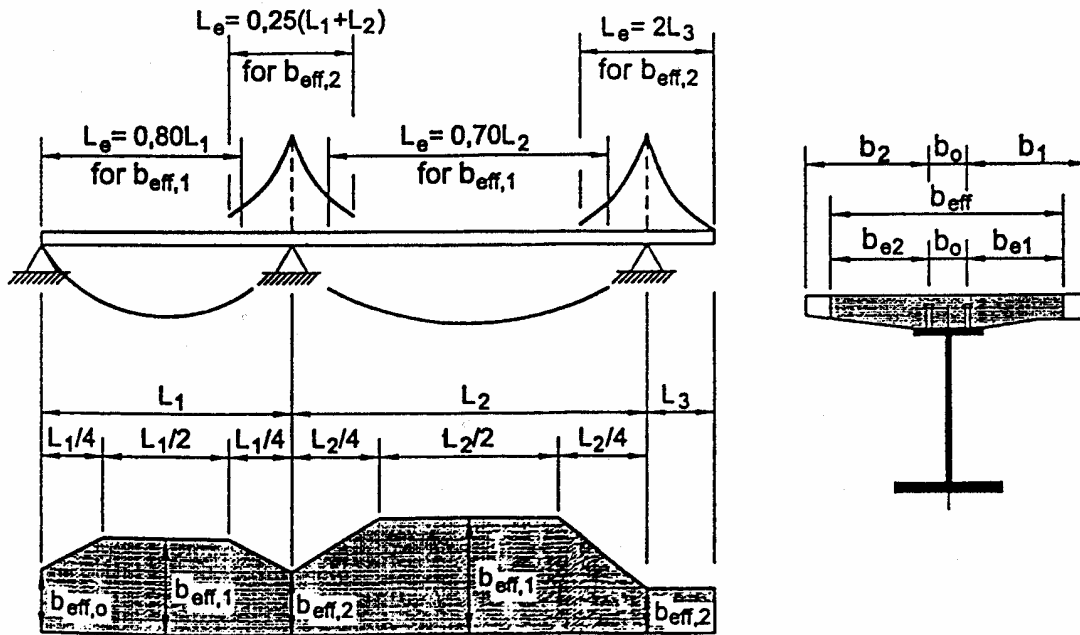


Figure C1 Equivalent spans, for effective width of concrete flange. The same definition can be used for earthquake loading while remaining consistent with the experimental results, if appropriate lengths ℓ_o are defined for horizontal loading situation. Figure C2 presents the equivalent of Figure C1 for earthquake loading. The partial effective widths deduced from Figure C2 are consistent with the experimental values:

$$b_e^+ = \frac{\ell_o^+}{8} = 0,075 L \qquad b_e^- = \frac{\ell_o^-}{8} = 0,1 L$$

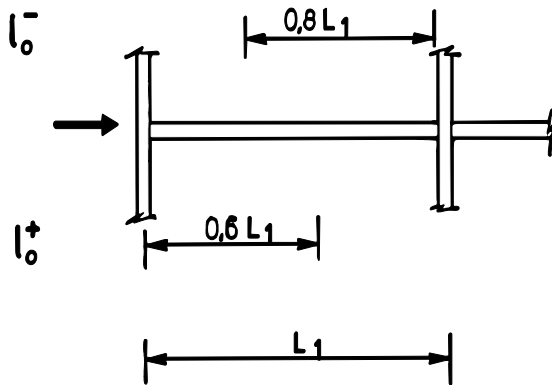


Figure C2 : Equivalent spans for effective width of concrete flange – C3. The effective width defined for the evaluation of plastic moments are explains the values given at Table 6.6.3. much larger than the width of the columns flanges, though recent evaluations[21] indicate that most of the resistance is activated on the column width. As mentioned previously, the real resistance of the concrete in that zone is higher than f_c because the slab realises a confinement in the direction transverse to the beam

7.6.4 Fully Encased Composite Columns

C1. This Section has been essentially developed by BRODERICK and ELGHAZOULI [25]. It is the outcome of a thorough analysis of the existing literature in 2000.

C2. The following relates to the design condition where the reinforced concrete part of the section is assumed to contribute to the resistance of the member and the member is designed to be dissipative with composite dissipative zones. The proposals are largely based on the ENV 1998 RC detailing rules for DC'M'. Where relevant, comparisons are made with the corresponding guidance given by the AISC and NEHRP for fully-encased composite columns.

(1) In dissipative structures, critical regions are present at both ends of all column lengths in moment frames and in the portion of columns adjacent to links in eccentrically braced frames. The lengths l_{cr} of these critical regions are defined as

$$l_{cr} = \max(h_c, l_{cl}/6, 450\text{mm}) \quad \text{for structural ductility class I,}$$

$$l_{cr} = \max(1.5h_c, l_{cl}/6, 450\text{mm}) \quad \text{for structural ductility class S.}$$

h_c is the height of the composite section and l_{cl} is the clear length of the column

C. The rule for DC'H' is: $\max(1.5d_c, l_{cl}/5, 600\text{mm})$. The rule for DC'L' is: $(d_c, l_{cl}/6, 450\text{ mm})$. In comparison, the AISC and NEHRP rules for fully-encased composite columns both stipulate that l_{cl} be taken as the maximum of $(d_c, l_{cl}/6, 457\text{ mm})$, i.e. a similar distance to that proposed above. This applies to columns in the higher Seismic Performance Categories (NEHRP) and to Intermediate and Special Moment Frames (AISC).

(2) To satisfy plastic rotation demands and to compensate for loss of resistance due to spalling of cover concrete, the following shall be satisfied within the critical regions defined above:

$$\alpha\omega_d = k_o \mu_\phi v_d \varepsilon_{sy,d} (0,35A_c/A_o + 0,15) - 10\varepsilon_{cu}$$

in which the variables are as defined in 5.4.3.2.3(8), but with

$$k_o = 65 \text{ and } \mu_\phi = 5 \quad \text{for ductility class I,}$$

$$k_o = 60 \text{ and } \mu_\phi = 9 \quad \text{for ductility class S}$$

and with the normalised design axial force v_d defined as

$$v_d = N_{Sd}/N_{pl,Rd} = N_{Sd}/(A_a f_{yd} + \alpha A_c f_{cd} + A_s f_{sd})$$

C. In ENV 1998, for DC'H', $k_o = 55$ and $\mu_\phi > 13$, while for DC'L', $k_o = 65$ and $\mu_\phi > 5$. The above modification of the expression of the normalised axial force allows for the contribution of the steel section. The original ENV 1998 expression for RC columns is:

$$v_d = N_{sd}/(A_c f_{cd}).$$

Similar modifications are included in the AISC and NEHRP codes. In both of these codes, the ACI rule for minimum areas of confining reinforcement is adopted [for 'special systems' (AISC) and 'performance categories D and E' (NEHRP)], but with the required area being reduced by the factor $(1 - A_a f_y/N_{sd})$. The provision above is a more conservative modification of the existing RC rule, as it assumes that axial load is shared equally between the steel and concrete.

(3) The spacing s of the confining hoops in critical regions shall not exceed

$$s \leq \min(b_o/2, 200\text{mm}, 9d_{bL}) \quad \text{in structural ductility class I.}$$

$$s \leq \min(b_o/3 \text{ or } 150\text{mm} \text{ or } 7d_{bL}) \quad \text{in structural ductility class S}$$

in which b_o is the minimum dimension of the concrete core and d_{bL} is the diameter of the longitudinal bars

(4) The diameter of the hoops, d_{bw} , shall be at least

$$d_{bw} \geq 6 \text{ mm} \quad \text{in structural ductility class I}$$

$$d_{bw} \geq \max(0,35 d_{bl,max} [f_{ydL}/f_{ydw}]^{0.5}, 6\text{mm}) \quad \text{in structural ductility class S}$$

C. Rules (2) to (4) ensure protection of the concrete at the top and bottom of each column length. The values given are the same as those specified for RC columns in DC'M' frames.

The 6mm minimum applies for all ductility classes. The rules for minimum hoop spacing adopted in the US guidance for composite columns is similar to the EC8 RC column detailing rules and the values given in the AISC Provisions are identical to those given in the NEHRP Recommendations. The minimum spacing specified for columns of 'special frames' is similar to that proposed above, namely $s \leq \min(b_c/4, 102\text{mm}, 24d_{bw})$ in the critical regions and $s \leq \min(6d_{bL}, 152\text{mm})$ throughout the column. (b_c is the least dimension of the column cross-section). The requirements for 'intermediate frames' (AISC) and frames in the middle Seismic Performance Category (NEHRP) are similar to those for EC8 DC'L'.

In this context, the most useful test data available relates to a series of 8 two-thirds scale tests conducted by Ricles and Paboojian [12]. These indicated that a maximum hoop spacing of $s_{max} = 6.9d_{bl}$ should be used if a rotation ductility of at least 6.0 is required.

The minimum diameter of hoop reinforcement required by both the NEHRP and AISC is either $b_c/50$ or 10mm, whichever is the smaller.

(5) In critical regions, the distance between consecutive longitudinal bars restrained by hoop bends or cross-ties should not exceed 250mm in structural ductility class I or 200 mm in structural ductility class S.

(6) In the lower two stories of a building, hoops according to (3), (4) and (5) shall be provided beyond the critical regions for an additional length equal to half the length of the critical regions.

(7) In dissipative columns, the shear resistance shall be determined on the basis of the structural steel section alone.

C. This rule is a conservative proposal in the absence of better research. Eurocode 4 allows the shear to be divided between the steel and concrete, and both the AISC and NEHRP codes determine shear strength on the basis of the steel section and the tie reinforcement. In the test series described above, however, the contribution of the concrete was seen to reduce drastically at even moderate displacements, while the contribution of the tie-reinforcement was not fully mobilised. As a result, the authors recommend the proposal (7) above. This topic requires additional consideration.

7.6.5 Partially-encased members

C1. This Section has been essentially developed by BRODERICK and ELGHAZOULI [25]. It is the outcome of a thorough analysis of the existing literature in 2000.

C2. Unlike fully-encased columns, there is no need to consider critical regions in partially-encased members. Partially-encased columns are treated here in the same manner as steel columns in which the implications of accidental overload may not be as significant as in fully-encased columns. Furthermore, the capacity design overstrength factor of 1.2 should limit column overloading effects considerably. On the other hand, detailing rules for intended dissipative zones must be satisfied.

(1) In dissipative zones where energy is dissipated by plastic bending of a composite section, the longitudinal spacing of the transverse reinforcement, s , should satisfy the requirements of 7.6.4(3) over a length greater or equal to l_{cr} for dissipative zones at member end and $2l_{cr}$ for dissipative zones in the member.

C. These values reflect conditions realised in test specimens. Tests at Imperial College (152 UC) used a spacing of 40mm in the critical region and 80mm elsewhere. Tests at Liege, Milan and Darmstadt (HEB300 and HEA260) used a spacing of 150mm throughout.

(2) In dissipative members, the shear resistance shall be determined on the basis of the structural steel section alone, unless special details are provided to mobilise the shear resistance of the concrete encasement.

C. As with fully-encased columns, rule (2) is a conservative proposal in the absence of better research. It is possible to ensure that the concrete encasement can contribute to the shear resistance of the member, but there will be additional detailing requirements. While this may be worthwhile in the case of beams (especially in eccentrically braced frames), the shear force in column members is not expected to be as high. Hence the conservative approach of (2) should not be too restrictive. The contribution of tie reinforcement to the shear resistance has not been investigated in tests.

(3) The relationship between the ductility class of the structure and the allowable slenderness (c/t) of the flange outstand in dissipative zones is given in Table 7.3.



a) hoops welded to web

b) straight bars welded to flanges

Figure 7.6. Details of transverse reinforcements.

C. These values are obtained from a parametric study with extended test results. They correspond to the c/t ratios required to provide a rotation ductility capacity of 6, 4 or 2 given an allowable axial load of 30% of section capacity.

(4) The additional links welded to the inside of the flanges, as shown in Figure 7.6, may delay local buckling in the dissipative zones. The limits given in Table 7.3 for flange slenderness may be increased if these bars are provided at a longitudinal spacing (s_l) which is less than the flange outstand: $s_l/c < 1.0$.

For $s_l/c < 0.5$, the limits given in Table 7.3 may be increased by up to 50%.

For values of $0.5 < s_l/c < 1.0$, linear interpolation may be used.

The additional straight links should also comply with the requirements (5) and (6).

C. The additional straight links provide significant enhancement to the local buckling limits given in Table 7.6.1. Experimental studies indicate that these limits may be conservatively increased by at least 50% when $s_l/c = 0.5$. Values of s_l/c smaller than 0.5 have not been investigated experimentally and hence no additional relaxation on flange slenderness is proposed beyond this limit. On the other hand,

the upper limit of $s/c=1.0$ is proposed as wider spacing may be shown to provide only marginal improvement in rotation capacity. For s/c greater than 1.5, experimental evidence indicate these bars would not delay the initiation of local flange buckling.

(5) The diameter d_{bw} of the additional straight links referred to in (4) shall be at least 6mm. When transverse links are employed to prevent local flange buckling as described in (4), d_{bw} should not be less than

$$d_{bw} \geq [(b t_f/8)(f_{ydf}/f_{ydw})]^{0.5}$$

in which b and t_f are the width and thickness of the flange and f_{ydf} and f_{ydw} are the design strengths of the flange and reinforcement.

C. Rules(4) and (5) are intended to reflect minimum conditions in test specimens and may be conservative. The latter requirement seeks to prevent premature yielding of the reinforcement when acting as a tie by ensuring that the yield resistance of the reinforcement is at least 3% of that of the flange.

(6) The additional straight links referred to in (4) should be welded to the flanges at their both ends and the capacity of the welds should not be less than the tensile yield strength of the straight links. A clear concrete cover of at least 20 mm, but not exceeding 40 mm, should be provided to these links.

C. This provision is included to ensure that the capacity of the link is not reduced by the end weld, that the bars are protected by a concrete cover and that the position of the straight links is effective in restraining the buckling of the flange.

(7) The design of partially-encased composite members may consider the resistance of the steel section alone or the composite resistance of the steel section and concrete encasement.

(8) The design of partially-encased members in which only the steel section is assumed to contribute to member resistance may be carried out according to the provisions of Section 6, but the capacity design provisions of 7.5.2. and 7.5.3 must be considered.

7.6.6. Filled composite columns

C. This Section has been essentially developed by BRODERICK and ELGHAZOULI [25]. It is the outcome of a thorough analysis of the existing literature in 2000.

(1) The relationship between the ductility class of the structure and the allowable slenderness d/t or h/t , representing the ratio between the maximum external dimension and the wall thickness, is given in Table 7.3

C. The local detailing of a filled column is more straightforward than that for partially-or full-encased columns, and depends only on the d/t ratio. Rectangular cross-sections are less ductile than circular ones, so lower slenderness ratios are required for the same design behaviour factor q .

(2) In dissipative members, the shear resistance of the column shall be determined on the basis of the structural steel section alone or on the basis of the reinforced concrete section alone; in that case, the steel tube is considered only as a shear reinforcement.

C. Local detailing requires d/t (rectangular) and h/t (circular) ratios for ductility classes O, I and S. The rules for composite columns given in EC4 are adequate for frames in class O and for non-dissipative members. These EC4 limits are equivalent to a Class 3 section classification; however, because filled sections are not normally employed in beam members, no d/t or h/t values are given for Class 1 or Class 2 sections. EC3 does provide Class 1 and Class 2 limits for hollow sections. For rectangular hollow sections, the EC3 limits are 33ε , 38ε and 42ε for Class 1, 2 and 3 respectively. For circular hollow sections, the EC3 limits are $50\varepsilon^2$, $70\varepsilon^2$ and $90\varepsilon^2$ for Class 1, 2 and 3 respectively. In comparison with hollow sections, the presence of concrete in filled sections delays local buckling, suggesting that the above EC3 values could be relaxed. In EC4, such a relaxation is implied for rectangular sections ($d/t \leq 42\varepsilon$), but not for circular sections ($h/t \leq 90\varepsilon^2$). It is well established, however, that circular sections possess higher local buckling resistance and better post buckling behaviour than rectangular sections. In contrast, the rotation capacity of filled rectangular columns is significantly reduced in the presence of axial loads. The effect of axial loads is not considered in the above code slenderness limits.

The d/t and h/t limits proposed for frames in classes I and S are based on empirical formulae for rotation capacity derived in the US-Japan research programme. Separate formulae express the rotation capacity of rectangular and circular filled beam columns as a function of the d/t or h/t ratios of the section, the axial force ratio, and concrete strength. Specifically, these formulae provide the deflection rotation at which the resistance of test specimens fell below 95% of their maximum resistance. Assuming conservative values of axial force ratio (0.3) and concrete strength (40 MPa), the slenderness limits required to provide rotation capacities of 25 mrad (for Class I) and 35 mrad (for Class S) are:

DC	R_{95}	d/t	h/t
S	0.035	22.3	70.3
I	0.025	31.2	95.3

The minimum steel yield strength employed in the U.S.-Japan tests was 275 N/mm^2 , implying:

DC	R_{95}	d/t	h/t
S	0.035	24.2ε	$82.7 \varepsilon^2$
I	0.025	33.9ε	$112 \varepsilon^2$

U.S.-Japan equations:

$$\text{Rectangular: } R_{95} (\%) = (100 t/d \beta) / (0.15 + 3.79N/N_{pl})$$

$$\beta = 1.0 - (f_c - 40.3)/566 \leq 1.0$$

$$\text{Circular: } R_{95} (\%) = 8.8 - 6.7(N/N_{pl}) - 0.04(h/t) - 0.012f_c$$

The proposed values in EC8 are more strict than those given for Class 1 and 2 rectangular hollow sections in EC3, but more relaxed than the EC3 limits for circular hollow sections. The above equations indicate that filled rectangular sections meeting the Class 1 and 2 h/t ratios specified in EC3 possess sufficient rotation capacity for Class S and I frames, respectively, if the axial force ratio is only 0.15, but not if it is 0.3.

(3) In non-dissipative members, the shear resistance of the column shall be determined according to the rules given in Eurocode 4.

7.7 Design and detailing rules for moment frames

7.7.1 Specific criteria.

(1) Moment resisting frames shall be designed so that plastic hinges form in the beams and not in the columns. This requirement is waived at the base of the frame, at the top floor of multi-storey buildings and for one storey buildings.

C. As the condition :
$$\theta = \frac{P_{\text{tot}} \cdot d_r}{V_{\text{tot}} \cdot h} \leq 0,10$$

defined in 4.5.2.2 (2) has to be satisfied at every storey, only moment resisting frames with limited sway may in fact be designed. This condition means that second order (P – D) effects need not be considered and the internal forces and moments may be determined using a first order theory considering the initial geometry of the structure. When SLS (Serviceability Limit State) requirements on drift are strong, this criteria is practically always fulfilled.

(2) The composite beams shall be designed such that they have adequate ductility and that the integrity of concrete is maintained.

(3) The beam to column joints shall have adequate overstrength to allow the plastic hinges to be formed in the beams or in the connections of the beams (see 7.5.4.).

(4) The required hinge formation pattern should be achieved by observing the rules given in 7.7.3

7.7.2 Analysis

(1) The analysis of the structure is performed on the basis of the section properties defined in 7.4.

(2) In beams, two different flexural stiffness are considered : EI_1 for the part of the spans submitted to positive (sagging) bending (uncracked section) and EI_2 for the part of the span submitted to negative (hogging) bending (cracked section).

(3) The analysis can alternatively be performed considering for the entire beam an equivalent moment of inertia I_{eq} constant for the entire span :

$$I_{eq} = 0.6 I_1 + 0.4 I_2.$$

C1. This value of the equivalent moment of inertia is a proposal which needs further validation. No such explicit value has been proposed until now in Eurocode 4 for the analysis of moment frames submitted to horizontal loading. Under vertical loading the rule is I_2 over 15 % the span on each side of each internal support and I_1 elsewhere, which correspond to $E_{eq} = 0,7 I_1 + 0,3 I_2$.

In fact, there is not one single answer to the definition of I_{eq} , because it is a function of the ratio between vertical and horizontal loadings and of the ratio between I_1 and I_2 .

If vertical loading is zero, which correspond to the smallest extension of the positive bending zone and is thus on the safe side, it can be established that the I_{eq} giving the same drift as the real distribution of I_1 and I_2 is :

$$I_{eq} = \frac{I_1^2 + I_2^2}{I_1 + I_2}$$

For $I_1 = 2 I_2$ this formula give $I_{eq} = 1,66 I_2$,

while $I_{eq} = 0,6 I_1 + 0,4 I_2 = 1,60 I_2$. These two values match well.

C2. In the FEMA 267 (1997) and the AISC seismic provisions (1997), the elastic analysis is based on the properties of the bare steel frame, that is $I_{eq} = I_1$. The resulting calculation of building stiffness and period underestimates the actual properties substantially. Although this approach result in unconservative estimates of design force levels (period T being overestimated, pseudo acceleration β (T) are underestimated), it produces conservative estimates of interstorey drift demands. It is considered in the U.S. that since the design of most moment-resisting frames are controlled by considerations of drift, this approach is preferable to methods that would over-estimate building stiffness because many of the elements that provide additional stiffness may be subject to rapid degradation under severe cyclic lateral deformation, so that the bare frame stiffness would be a reasonable estimate of the effective stiffness under long duration ground shaking response.

This option can be justified by a temporary lack of experimental data. It is an approximation, even when there is a degradation of stiffness under cyclic deformations. This approximation may be acceptable for high beams (beam depth above 700 mm) for which I_1 is not too much different of I_2 ; for beams depth under 500 mm, the analysis made considering a bare frame is unrelated to the real behaviour of the structure, especially when measures are taken to achieve ductility in the connection

zone.

C3. It has been estimated by the drafting panel that three facts support the option of considering composite structures :

- the experimental basis allow this definition
- the application field, which does not include sway frames of high flexibility (see 7.7.1), provides a safety margin covering potential discrepancies between real and design elastic flexibility of structures
- the earthquake durations expected in most parts of Europe are not such that section degradation is likely to take place.

Furthermore, it does not seem a good option to underestimate the stiffness of sections to take into account potential degradation of dissipative zones ; this fatigue aspect of composite sections should rather be defined as such, by the development of a fatigue ULS which should be considered in the design as is at present the deformation ULS.

(4) For columns, the stiffness is: $(EI)_c = EI_a + 0.5 E_{cm} I_c + E I_s$

where E and E_{cm} are the modulus of elasticity for steel and concrete

and I_a , I_c and I_s are the moment of inertia of the steel section, of the concrete and of the rebars respectively.

7.7.3 Detailing rules for beams and columns

C. In Eurocode 8, design clauses common to all moment frames, independently of their constitutive material, are expressed in a general Section. They are as follows.

(3) In multi storey buildings, formation of a soft storey plastic mechanism shall be prevented, as such a mechanism may entail excessive local ductility demands in the columns of the soft storey.

(4). Unless otherwise specified in Sections 5 to 8, to satisfy the requirement of par.(3), at all beam-column joints of frame buildings, including frame-equivalent ones in the meaning of clause 5.1.2(1), with two or more storeys, the following condition should be satisfied:

$$\sum M_c \geq 1.35 \sum M_b \quad (4.17)$$

In Eq.(4.17):

$\sum M_c$ is the sum of moments at the centre of the joint corresponding to the resisting moments of the columns framing into the joint. The minimum value of column resisting moments within the range of column axial forces produced by the seismic design situation should be used in Eq.(4.17).

$\sum M_b$ is the sum of moments at the centre of the joint corresponding to the resisting moments of the beams framing into the joint.

(5) Eq.(4.17) should be satisfied within two orthogonal vertical planes of bending, which, in buildings with frames arranged in two orthogonal directions, are defined by these two directions. It should be satisfied for both directions (senses) of action of the beam moments around the joint (positive and negative), with the column moments always opposing the beam moments. If the structural system is a frame or a frame-equivalent in only one of the two main horizontal directions of the structural system, then Eq.(4.17) should be satisfied just within the vertical plane through that direction.

(6) The requirement (4) is waived at the top level of multi-storey buildings.

(7) In moment frames, redistribution of bending moments, according to 5.5 of EN1992-1, for concrete structures, according to 5.2.1.3 of EN 1993-1 for steel structures and according to 5.1.4.7 of prEN 1994-1-1 for composite steel concrete structures, is permitted.

The specific clauses for composite steel concrete structures are as follows.

(1) Composite T beams design should comply with 7.6.2. Partially encased beams design should comply with 7.6.5.

(2) Beams should be verified as having sufficient safety against lateral or lateral torsional buckling according to clause 4.6.2. of Eurocode 4, assuming the formation of a negative plastic moment at one end of the beam.

(3) For plastic hinges in the beams, it should be verified that the full plastic moment resistance and rotation capacity is not decreased by compression and shear forces. To this end, the following inequalities should be verified at the location where the formation of hinges is expected.

$$\frac{M_{Sd}}{M_{pl,Rd}} \leq 1,0 \quad \frac{N_{Sd}}{N_{pl,Rd}} \leq 0,15 \quad \frac{V_{Sd}}{V_{pl,Rd}} \leq 0,5$$

where

N_{Sd} , M_{Sd} design action effects (resulting from the structural analysis),

$N_{pl,Rd}$, $M_{pl,Rd}$, $V_{pl,Rd}$ design resistances according to 4.4. of Part 1-1 of Eurocode 4,

$V_{Sd} = V_{Sd,G} + V_{Sd,M}$ in which $V_{Sd,G}$ is the shear force due to the non-seismic actions and $V_{Sd,M}$ is the shear force due to the application of the resisting moments $M_{Rd,A}$ and $M_{Rd,B}$ with opposite signs at the extremities A and B of the beam.

(4) Composite trusses may not be used as dissipative beams. For the verification of columns the most unfavourable combination of the axial force N and the bending moments M_x and M_y shall be assumed.

(5) The transfer of the forces from the beams to the columns should comply with the design rules given in clause 4.10 of ENV 1994-1-1 (or Section 8 of pr EN 1994-1-1).

(6) The following inequality must apply for all composite columns:

$$N_{Sd} / N_{pl,Rd} < 0,30$$

C. In moment-resisting frames, column response is primarily flexural and may be dissipative. To ensure a satisfactory cyclic response, it is necessary to limit column axial force below a certain value. The rule (7) is conservative; it could be relaxed with more test data. However, it should not be too restrictive as moment capacity decreases significantly above this level of axial load. In braced frames, concrete infill is used to increase the axial resistance of the member to prevent buckling. Some bending moment may also be present, but this is taken into account using interaction curves and no explicit limit on axial load need to be imposed.

(7) The resistance verifications of the columns should be made according to 4.8. of Part 1-1 of Eurocode 4.

(8) The column shear force V_{Sd} (resulting from the structural analysis) should be limited to $V_{Sd} / V_{pl,Rd} < 0,5$

(9) When q is greater than 4 and less than 6, the cross section of the columns shall be class 1 and the following requirements shall be satisfied prior to further verifications of the element:

for a column in bending with double curvature:

$$\text{if } N_{Sd} / N_{pl,Rd} > 0.15 \quad N_{Sd} / N_{pl,Rd} + 0.8 \bar{\lambda} < 1$$

$$\text{if } N_{Sd} / N_{pl,Rd} < 0.15 \quad \bar{\lambda} < 1.6$$

for a column in bending with single curvature:

$$\text{if } N_{Sd} / N_{pl,Rd} > 0.15 \quad N_{Sd} / N_{pl,Rd} + 1.35 \bar{\lambda} < 1$$

$$\text{if } N_{Sd} / N_{pl,Rd} < 0.15 \quad \bar{\lambda} < 1.1$$

C. The origin of this requirement is to be found in the fact that numerous dynamic non linear analysis show the following: in spite of the application of the design rules presented here, some plastic hinges forms in columns (most are in beams and no storey mechanism takes place however); the restrictions above, like those of (6) and of 7.6.1(6) are introduced to prevent the overall buckling of columns where these plastic hinges can be formed.

7.7.4 Beam to column connections

(1) The connection design should be such that the plastic rotation capacity θ_p in the plastic hinge, as defined in par. 6.5.5, is not less than 35 mrad for structures of ductility class S and 25 mrad for structures of ductility class I. These values should be supported by experimental results.

(2) Connection design should comply with 7.5.4.

(3) The connections of the beams to the columns should be designed for the required degree of overstrength (see 7.5.3) taking into account the moment resistance $M_{pl,Rd}$ and the shear force ($V_{G,Sd} + V_{M,Sd}$) evaluated in 7.7.3.

7.7.5 Condition for disregarding the composite character of beams with slab.

(1) The plastic resistance of a composite section can be computed considering only the steel section if the slab is totally disconnected from the steel frame in a circular zone around a column of diameter

$2b_{\text{eff}}$, b_{eff} being the greater of the effective widths of the beams connected to that column.

(2) Totally disconnected means that no contact between slab and any vertical side of any steel element (e.g. columns, shear connectors, connecting plates, corrugated flange, steeldeck nailed to flange of steel section) exists.

(3) In partially encased beams, the contribution of concrete between the flanges of the steel section has to be taken into account.

7.8 Design and detailing rules for composite concentrically braced frames

7.8.1 Specific criteria

(1) Composite frames with concentric bracings shall be designed so that yielding of the diagonals in tension will take place before failure of the connections and before yielding or buckling of the beams or columns.

(2) Columns and beams shall be either structural steel or composite.

(3) Braces shall be structural steel.

C. As mentioned in 7.3.1(1)c), braces have to be structural steel. In principle, braces could also be composite. However, considering the complexity of the brace member design, using composite brace members in which the concrete is effective under compression only, the design is even more complex. Basically, in the initial design phase the resistance of the diagonals under compression is neglected and only the diagonals under tension are assumed to resist the lateral earthquake loads. However, in the subsequent capacity analysis the entire system needs to be considered, including the diagonals which experience compression under seismic lateral loads. In case the buckling capacity of a diagonal under compression at a certain story is more than 50% of the tensile capacity of the other diagonal at that same level, the lateral story resistance provided by the two diagonals at the moment of first buckling is larger than the design lateral load which was used initially to design the tensile-loaded diagonals. Hence, at that moment during an earthquake, the columns will experience larger axial forces than first used in the initial design phase. Of course, subsequently, the lateral force capacity will reduce to the corresponding capacity of the tension diagonal only and the columns will not be overloaded any longer. (Assuming that at each level the buckling resistance of the diagonals is 60% of the tensile capacity of the corresponding diagonals under tension, the columns would experience a load of 120%, or an overload of 20%).

In order to limit such possible overloads, it is essential to develop a design in which the compression capacity of the diagonals is low. The clause 3.5.5.2 (1) of ENV 1998 which limits for diagonal members the non-dimensional slenderness to $\bar{\lambda} < 1,5$ does not intend to reach that goal. It intends to avoid the possibility of shocks due to sudden elastic re-tensioning of the diagonal when the reversal of forces takes place and the non-dimensionless slenderness limit is there to “prevent elastic buckling” of the diagonal. The limit on λ corresponds to a design resistance in compression N_{Rd} which is about 35% of the tensile capacity, but N_{Rd} is a lower characteristic value, so that the real resistance in compression may well be 60% of the tensile capacity or more; the overloading of the columns with respect to their design resistance can then be critical. As, in order to design a dissipative system, the diagonals should buckle to allow the tensile diagonals to yield it seems more effective to put both an upper and a lower limit on $\bar{\lambda}$. The proposal is $1,3 < \bar{\lambda} < 2,0$. Under this condition, introducing a composite brace would increase the difficulties to design a slender diagonal member which would buckle early.

(4) 6.7.1 (2) applies

C. Clause 6.7.1(2) is as follows. The diagonal elements of bracings should be placed in such a way that the structure exhibits similar load deflection characteristic at each floor and in every braced direction under load reversals. To this end, the following rule should be met storey by storey:

$$\frac{|A^+ - A^-|}{A^+ + A^-} \leq 0,05$$

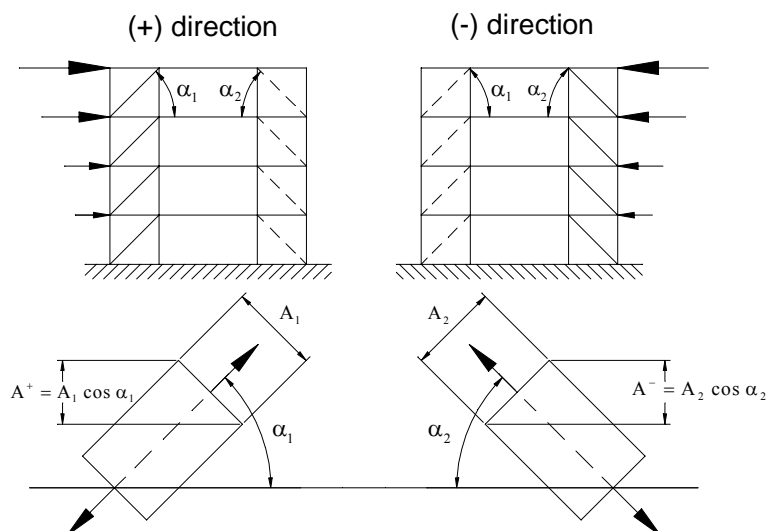


Figure 6.4. Example of application of 6.7.2.1(2) where A^+ and A^- are the areas of the horizontal projections of the cross-sections of the tension diagonals, when the horizontal seismic actions have a positive or negative direction respectively (see fig. 6.4).

7.8.2 Analysis

(1) 6.7.2 applies.

C. Clause 6.7.2 is as follows.

6.7.2. Analysis

(1) Under gravity load conditions, only beams and columns shall be considered to resist such loads, without considering the bracing members.

(2) Under seismic action, the diagonals are considered in the analysis.

(3) Under seismic action, in frames with diagonal bracings, only the tension diagonals are assumed to participate in the structural resistance.

(4) Under seismic action, in frames with V bracings, both the tension and compression diagonals are assumed to participate in the structural resistance

7.8.3 Diagonal members

(1) 6.7.3 applies.

C. Clause 6.7.3 is as follows.

(1) In frames with diagonal bracings, the non-dimensional slenderness as defined in EN 1993-1 should be limited to: $1,3 < \bar{\lambda} \leq 2,0$ The 1,3 limit is defined to avoid overloading columns above the action effects obtained from an analysis where only the tension diagonal is active.

(2) In frames with V bracings, the non-dimensional slenderness as defined in EN 1993-1 should be limited to: $\bar{\lambda} \leq 2,0$

(3) The yield resistance $N_{pl,Rd}$ of the gross cross-section of the diagonals should be such that : $N_{pl,Rd} \geq N_{Sd}$.

(4) In frames with V bracings, the compression diagonals should be designed for the compression resistance according to clause 5 of Part 1-1 of Eurocode 3.

(5) The connections of the diagonals to any member should fulfil 6.5.5 (4) In order to satisfy a homogeneous dissipative behaviour of the diagonals, it should be checked that the maximum overstrength Ω_i defined in 6.7.4(1) does not differ from the minimum value Ω by more than 20%.

7.8.4 Beams and Columns

(1) 6.7.4 applies.

C. Clause 6.7.4 is as follows.

(1) Beams and columns with axial forces should meet the following minimum resistance requirement:

$$N_{Rd}(M_{Sd}) \geq 1,20 \cdot (N_{Sd,G} + \Omega \cdot N_{DSd,E}) \quad (6.11)$$

where

$N_{Rd}(M_{Sd})$ design buckling resistance of the beam or the column according to Eurocode 3, taking into account the interaction between the bending moment M_{Sd} defined as its design value in the seismic design situation

$N_{Sd,G}$ axial force in the beam or in the column due to the non-seismic actions included in the combination of actions for the seismic design situation,

$N_{Sd,E}$ axial force in the beam or in the column due to the design seismic action multiplied by the importance factor,

Ω minimum value of $\Omega_i = N_{pl,Rdi}/N_{Sdi}$ over all the diagonals of the braced frame system, where

$N_{pl,Rdi}$ design resistance of diagonal i ,

N_{Sdi} design value of the axial force in the same diagonal i in the seismic design situation

(2) In frames with V-bracings, the beams should be designed to resist:

all non-seismic actions without considering the intermediate support given by the diagonals.

the unbalanced vertical seismic action effect applied to the beam by the braces after buckling of the compression diagonal. This force is calculated using $N_{pl,Rd}$ for the brace in tension and $0,3 N_{pl,Rd}$ for the brace in compression

(3)P In frames with diagonal bracings in which the tension and compression diagonals are not intersecting (e.g. diagonals of Fig. 6.4), the design shall consider the tensile and compression forces developing in the columns adjacent to the diagonals in compression and corresponding to the buckling load of these diagonals.

7.9 Design and detailing rules for composite eccentrically braced frames

7.9.1 Specific criteria

(1) Composite frames with eccentric bracings shall be designed so that the dissipative action will occur essentially through yielding in shear of the links. All other members should remain elastic and failure of connections should be prevented.

(2) Columns, beams and braces can be structural steel or composite

C. The above scope leaves in principle the door open to all design options for what concerns all types of members. These can be made of steel only or composite. However, there are still uncertainties, in both options. For instance, assuming that the capacity of a composite link can be assessed correctly, the braces and columns can be designed correctly to withstand the seismic action forces. However, cyclic non linear seismic exposure, which for eccentric bracings corresponds at the ultimate stage to plastic rotations more important than those met in moment frames, generates necessarily a concrete deterioration which leads to a link with reduced resistance, reflecting basically the steel section capacity only, or less. Should the composite action be underestimated, e.g. neglecting the concrete presence, the underestimated link capacity leads to an under-design of both braces and columns. In that condition, the larger than considered link capacity leads to an overload of the brace and column members and their failure.

Another problem arise when the evaluation of effective width of collaborating slab is needed, when for instance composite links active in bending would be designed; there is clearly a lack of experimental background on this topic.

The gap in knowledge is even greater for what concerns “disconnection” of the slab in order to allow a reference to pure steel as being the only resisting part of sections in bending: it is not obvious that a local disconnection allows a reference to steel resistance only; on the contrary, in the context of moment frames, there has been experimental evidence that too local disconnections had a limited effect and that a composite resistance was still operative; membrane forces in the slab might realise force transfers which are not really mastered at present.

From these considerations, it can be concluded that links working in bending in beam elements with slab always raise an evaluation problem. Beam links made of an encased steel section with possible slab and working in shear correspond to an adequately mastered situation, because the slab contribution in the shear resistance of the links is negligible. Vertical steel links also correspond to a mastered situation.

(3) The braces, columns and beam segments outside the link segments shall be designed to remain

elastic under the maximum forces that can be generated by the fully yielded and/or cyclically strain-hardened beam link.

7.9.2 Analysis.

- (1) The analysis of the structure is made on the basis of the section properties defined in 7.4.2
- (2) In beams, two different flexural stiffnesses are considered : EI_1 for the part of the spans submitted to positive (sagging) bending (uncracked section) and EI_2 for the part of the span submitted to negative (hogging) bending (cracked section).

7.9.3 Links

C. Sections 6.8.2, 6.8.3 and 6.8.4 on steel eccentric braced frames are reproduced at the end of paragraph 7.9.4.

- (1) Links shall be made of steel sections, possibly composite with slabs. They may not be encased.
- (2) Rules on seismic links and their stiffeners presented in 6.8.2. apply. Links may be long or intermediate with a maximum length e :

$$e < 2M_{p, link} / V_{p, link}$$

The definitions of $M_{p, link}$ and $V_{p, link}$ are given in 6.8.2(3). For $M_{p, link}$, only the steel components of the link section are considered in the evaluation.

- (3) When the seismic link frames into a reinforced concrete or an encased column, face bearing plates shall be provided on both sides of the link at the face of the column and in the end section of the link. These bearing plates should conform to 7.5.4.
- (4) The design of beam/column connections adjacent to dissipative links should conform to 7.5.4.
- (5) Connections should meet the requirements of steel eccentrically braced frames as in 6.8.4.

7.9.4 Members not containing seismic links.

- (1) The members not containing seismic links should comply with the rules presented in 6.8.3, considering the combined resistance of steel and concrete in case of composite elements and the relevant rules for members in 7.6 and in Eurocode 4.
- (2) Where a link is adjacent to a fully encased composite column, transverse reinforcement meeting the requirements of clause 7.6.5. shall be provided above and below the link connection.
- (3) In case of a composite brace under tension, only the cross-section of the structural steel section should be considered in the evaluation of the resistance of the brace.

C. Sections 6.8.2, 6.8.3 and 6.8.4 on steel eccentric braced frames are as follows.

6.8.2. Seismic links

- (1) *The web of a link shall be single thickness without doubler plate reinforcement and without hole or penetration.*
- (2) *Seismic links are classified into 3 categories according to their length e*
short links, which dissipate energy by yielding essentially in shear
long links, which dissipate energy by yielding essentially in bending
intermediate links, in which the plastic mechanism involves bending and shear.
- (3) *For I sections, the following parameters are used to define the plastic design resistances and limits of categories:*

$$M_{p, link} = f_y b t_f (d - t_f) \quad V_{p, link} = (f_y / \sqrt{3}) t_w (d - t_f)$$

- (4) *For I sections, the length e of the links defining the categories are :*

$$\begin{array}{ll} \text{short links} & e < 1,6 M_{p, link} / V_{p, link} \\ \text{long links} & e > 3,0 M_{p, link} / V_{p, link} \\ \text{intermediate links} & \text{in between.} \end{array}$$

- (5) *If $N_{sd} / N_{Rd} \leq 0,15$, the following inequalities should be checked*

$$\text{short links} : V_{sd} \leq 1,5 V_{p, link} \quad (6.12) \quad \text{long links, at both ends} : M_{sd} \leq 1,5 M_{p, link} \quad (6.13)$$

intermediate links, at both ends :

$$M_{sd} \leq M_{p, link} \left(1,2 + 0,3 \frac{e \frac{V_{p, link}}{M_{p, link}} - 1,6}{3 - 1,6} \right) \quad (6.14)$$

in those expression, N_{sd} , M_{sd} , V_{sd} are the design forces as defined in (6.3), (6.4), (6.5), referring to the

link and its length e .

(6) If $N_{Sd}/N_{Rd} > 0,15$, the following reduced values $V_{p,link,r}$ and $M_{p,link,r}$ have to be considered in relations (6.12), (6.13), (6.14)

$$V_{p,link,r} = V_{p,link} \left((1 - N_{Sd} / N_{pl,Rd}) \right)^{0,5} \quad M_{p,link,r} = M_{p,link} \left((1 - N_{Sd} / N_{pl,Rd}) \right)^{1,0}$$

(7) If $N_{Sd}/N_{Rd} \geq 0,15$, the link length e shall not exceed :

$$1,6 M_{p,link} / V_{p,link} \quad \text{when } R = (N_{Sd} \cdot t_w \cdot (d - 2 t_f) / V_{Sd} \cdot A) < 0,3$$

$$(1,15 - 0,5 R) 1,6 M_{p,link} / V_{p,link} \quad \text{when } R \geq 0,3.$$

(8) The link rotation angle is the inelastic angle between the link and the element outside of the link. It shall not exceed the following values :

0.08 radians for links of length $1.6 M_p/V_p$ or less

0.02 radians for links of length $3.0 M_p/V_p$ or greater

The value determined by linear interpolation between the above values for links of length between $1.6 M_p/V_p$ and $3.0 M_p/V_p$.

(9) Full-depth web stiffeners shall be provided on both sides of the link web at the diagonal brace ends of the link. These stiffeners shall have a combined width not less than $(b_f - 2 t_w)$ and a thickness not less than $0.75 t_w$ nor 10 mm, whichever is larger, where b_f and t_w are the link flange width and link web thickness, respectively.

(10) Links shall be provided with intermediate web stiffeners as follows :

a. Short links shall be provided with intermediate web stiffeners spaced at intervals not exceeding $(30 t_w - d/5)$ for a link rotation angle of 0.08 radians or $(52 t_w - d/5)$ for link rotation angles of 0.02 radians or less. Linear interpolation shall be used for values between 0.08 and 0.02 radians.

b. Long links, shall be provided with intermediate web stiffeners placed at a distance of 1.5 time b_f from each end of the link.

c. Intermediate links, shall be provided with intermediate web stiffeners meeting the requirements of 1 and 2 above.

d. Intermediate web stiffeners are not required in links of lengths greater than $5 M_p/V_p$.

e. Intermediate link web stiffeners shall be full depth. For links that are less than 600 mm in depth, stiffeners are required on only one side of the link web. The thickness of one-sided stiffeners shall not be less than t_w or 10 mm, whichever is larger, and the width shall be not less than $(b_f/2) - t_w$. For links that are 600 mm in depth or greater, similar intermediate stiffeners are required on both sides of the web.

(11) Fillet welds connecting a link stiffener to the link web shall have a design strength adequate to resist a force of $f_y A_{st}$, where A_{st} is the area of the stiffener. The design strength of fillet welds fastening the stiffener to the flanges shall be adequate to resist a force of $A_{sf} f_y/4$.

Lateral supports shall be provided at both the top and bottom link flanges at the ends of the link. End lateral supports of links shall have a design strength of 6 percent of the expected nominal axial strength of the link flange computed as $f_y b_f t_f$.

(13) In beams where a seismic link is present, the shear buckling resistance of the web panels outside of the link should be checked to comply with section 5 of Part 1-1 of Eurocode 3.

6.8.3. Members not containing seismic links

(1) The members not containing seismic links, like the columns and diagonal members, in case horizontal links in beam are used, and also the beams members, in case vertical links are used, should be verified in compression considering the most unfavourable combination of the axial force and bending moments:

$$N_{Rd} (M_{Sd}, V_{Sd}) \geq 1,20 (N_{Sd,G} + \Omega N_{Sd,E}) \quad (6.15) \quad \text{where}$$

$N_{Rd}(M_{Sd}, V_{Sd})$ axial force design resistance of the column or diagonal member according to Eurocode 3, taking into account the interaction with the bending moment M_{Sd} and the shear V_{Sd} taken at their design value in the seismic situation

$N_{Sd,G}$ compression force in the column or diagonal member due to the non-seismic actions included in the combination of actions for the seismic design situation,

$N_{Sd,E}$ compression force in the column or diagonal member due to the design seismic action multiplied by the importance factor,

Ω for short links, minimum value of $\Omega_i = 1,5 V_{p,link,i} / V_{Sdi}$ of all links; for intermediate and long

links, minimum value of $\Omega_i = 1,5 M_{p,link,i}/M_{Sdi}$ of all links; V_{Sdi} , M_{Sdi} are the design values of the shear force and of the bending moment in link i in the seismic design situation; $V_{p,link,i}$, $M_{p,link,i}$ are the shear and bending plastic design resistances of link i as in 6.8.2

(3) In order to satisfy a homogeneous dissipative behaviour of the whole set of seismic links, it should be checked that the ratios Ω_i defined above do not differ from the minimum value Ω by more than 20%.

6.8.4. Connections of the seismic links

(1) The connections of the seismic links or of the element containing the links should be designed considering the section overstrength Ω_s and the material overstrength (see 6.5.5).

(2) Semi-rigid and/or partial strength connections are permitted; then it is not the link itself which dissipate energy, but its connections. This is allowable, provided the following is satisfied: a) the connections have adequate rotation capacity consistent with global deformations; b) members framing into the connections are demonstrated to be stable at ULS; c) the effect of connections deformations on global drift is taken into account.

(3) When partial strength connections are used for the seismic links, the capacity design of the other element in the structure should be derived from the plastic capacity of the links connections.

7.10 Design and detailing rules for structural systems made of reinforced concrete shear walls composite with structural steel elements

7.10.1 Specific criteria.

(1) The provisions in this Section apply to composite structural systems belonging to three types defined in 7.3.1. Figure 7.7 and 7.8.

C. When properly designed, these systems have shear strength and stiffness comparable to those of pure reinforced concrete shear wall systems. The structural steel sections in the boundary members however increase the flexural resistance of the wall and delay plastic flexural hinging (tall walls). Like for reinforced concrete structures, two levels of ductility and two values of the behaviour factor are defined, depending on the level of requirements in the detailing rules. Most of the design guidance in this Section 7.10 refers to the U.S. research and practice [1].

(2) Structural systems Types 1 and 2 are designed to behave as shear walls and dissipate energy in the vertical steel sections and in the vertical reinforcements .

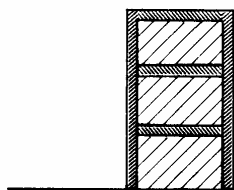
(3) In structural system Type 1, the story shear forces should not be carried primarily through diagonal compression struts in the concrete infills.

(4) Type 3 is designed to dissipate energy in the shear walls and in the coupling beams.

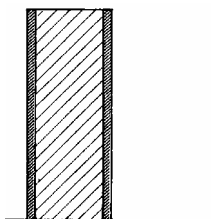
7.10.2 Analysis.

(1)P The analysis of the structure shall be made on the basis of the section properties defined in Section 5 for concrete walls and in 7.4.2. for composite beams.

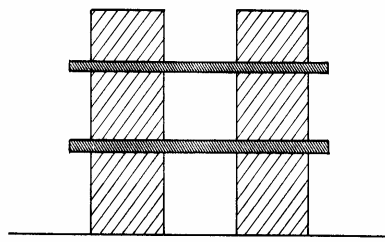
(2)P In structural system Type 1 and Type 2, when vertical encased or partially encased structural steel sections function as boundary members of reinforced concrete infill panels, the analysis shall be made considering that the earthquake action effects in these vertical boundary elements are axial forces only.



Type 1 Steel or composite frame with concrete infills



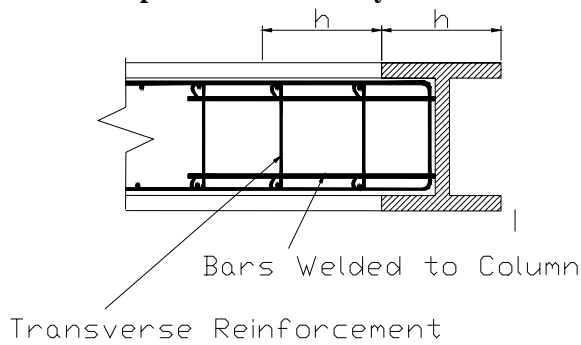
Type 2 Concrete walls reinforced by vertical steel sections.



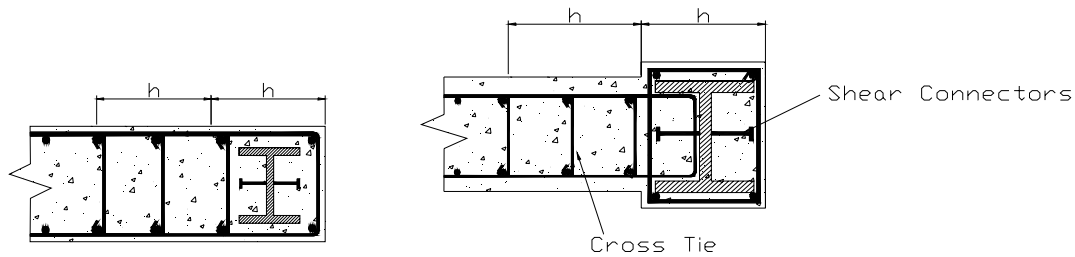
Type 3

Concrete shear wall coupled by steel or composite beams.

Figure 7.7. Composite Structural Systems with shear walls



Partially encased steel boundary element used as columns in system Type 1 and Type 2. Details of transverse steel belong to structure ductility class S

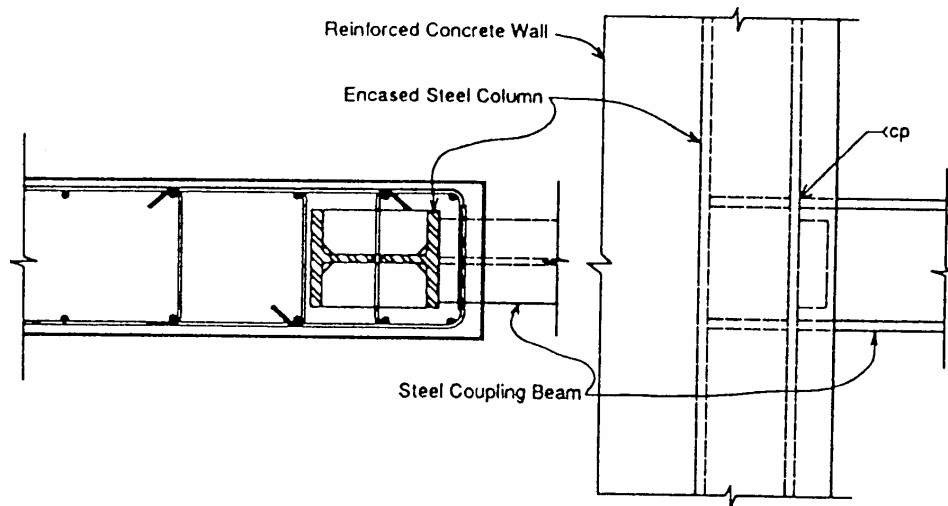


Fully encased composite boundary element used as columns in systems type 1 and Type 2. Details of transverse reinforcements for ductility class S

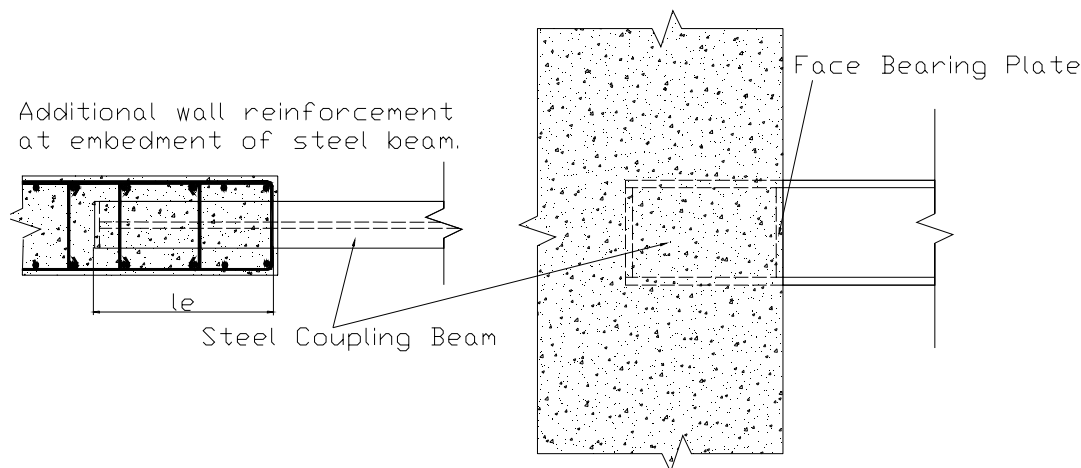
Figure 7.8. Details of partially and fully encased composite boundary elements in Structures of Ductility Class S

(3) These axial forces should be determined assuming that the shear forces are carried by the reinforced concrete wall and that the entire gravity and overturning forces are carried by the shear wall acting composedly with the vertical boundary members.

(4) In structural system Type 3, if composite coupling beams are used, 7.7.2(2) and (3) applies.



Detail of framing of a steel coupling beam into a reinforced concrete wall with composite boundary member.(from [1]).



Details of framing of a steel coupling beam into a reinforced concrete wall
Figure 7.9. Coupling beam framing into a wall with details of ductility class S

7.10.3 Detailing rules for ductility class I composite walls.

- (1)P The reinforced concrete of infill panels in Type 1 and of the wall in Types 2 and 3 shall meet the requirements of Section 5.
- (2)P Partially encased steel sections used as boundary members of reinforced concrete panels shall belong to a class of cross section related to the behaviour factor of the structure as indicated in Table 7.3.
- (3)P Fully encased structural steel sections used as boundary members in reinforced concrete panels shall be designed to 7.6.4.
- (4)P Partially encased structural steel sections used as boundary members of reinforced concrete panels shall be designed to 7.6.5.
- (5)P Headed shear studs or welded reinforcement anchors shall be provided to transfer vertical and horizontal shear forces between the structural steel of the boundary elements and the reinforced concrete.

C. Tests on concrete infill walls have shown that if shear connectors are not present, story shear forces are carried primarily through diagonal compressions struts in the wall panel (Chrysostomou, 1991). This behaviour often includes high forces in localised areas of the walls, beams, columns, and connections. The shear stud requirements will improve performance by providing a more uniform

transfer of forces between the infill panels and the boundary members.

7.10.4 Detailing rules for ductility class I coupling beams.

(1)P Coupling beams shall have an embedment length into the reinforced concrete wall sufficient to develop the maximum possible combination of moment and shear generated by the bending and shear strength of the coupling beam. The embedment length l_e shall be considered to begin inside the first layer of confining reinforcement in the wall boundary member Figure 7.9. The embedment length shall not be less than 1,5 times the height of the coupling beam.

C. Two examples of connections between steel coupling beams to concrete walls are shown in Figure 7.9 The requirements for coupling beams and their connections are based largely on recent tests of unencased steel coupling beams (Harries, et al., 1993 ; Shahrooz et al., 1993). These test data and analyses show that properly detailed coupling beams can be designed to yield at the face of the concrete wall and provide stable hysteretic behaviour under reversed cyclic loads. Under high seismic loads, the coupling beams are likely to undergo large inelastic deformations through either flexural and/or shear yielding.

(2)P The design of beam/wall connections shall conform to 7.5.4.

(3) The vertical wall reinforcements, defined in 7.5.4 (11) and (12) with design axial strength equal to the shear strength of the coupling beam, shall be placed over the embedment length of the beam with two-thirds of the steel located over the first half of the embedment length. This wall reinforcement shall extend a distance of at least one anchorage length above and below the flanges of the coupling beam. It is permitted to use vertical reinforcement placed for other purposes, such as for vertical boundary members, as part of the required vertical reinforcement. Transverse reinforcements should conform to 7.6.

7.10.5 Additional detailing rules for Ductility Class S.

(1)P Transverse reinforcements for confinement of the composite boundary members, either partially or fully encased, shall be placed; they shall extend to a distance of $2h$ into the concrete walls -fig 7.8; h is the depth of the boundary element in the plane of the wall.

(2)P The requirements to links in frames with eccentric bracings apply to coupling beams.

7.11 Design and detailing rules for composite steel plates shear walls

7.11.1 Specific criteria

(1)P Composite steel plate shear walls are designed to yield through shear of the steel plate.

(2)P The steel plate shall be stiffened by encasement and attachment to the reinforced concrete in order to prevent buckling of steel.

7.11.2 Analysis

(1) The analysis of the structure is made on the basis of the materials and section properties defined in 7.4.2 and 7.6.

7.11.3 Detailing rules

(1)P It will be checked that $V_{Sd} < V_{Rd}$ where f_{yd} is the design yield strength of the plate
 A_{pl} is the horizontal area of the plate

C. Steel plate reinforced composite shear walls can be used most effectively where story shear forces are large and the required thickness of conventionally reinforced shear walls is excessive. The provisions limit the shear strength of the wall to the yield strength of the plate because there is insufficient basis from which to develop design rules for combining the yield strength of the steel plate and the reinforced concrete panel. Moreover, since the shear strength of the steel plate usually is much greater than that of the reinforced concrete encasement, neglecting the contribution of the concrete does not have a significant practical impact.

(2)P The connections between the plate and the boundary members (columns and beams) as well as the connections between the plate and the concrete encasement shall be designed such that full yield strength of the plate can be developed.

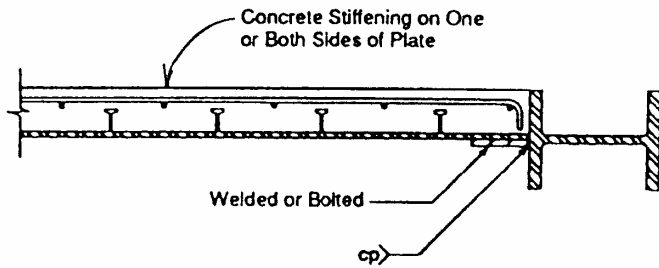
C. This rule means that local as well as overall plate buckling has to be avoided. For what concerns local buckling, this can for instance be achieved by limiting studs spacing in such a way that h/t values of unstiffened parts of the steel plate remain under limiting values of h/t . It is recommended that overall buckling of the composite panel be checked using elastic buckling theory considering the section stiffness of the composite wall.

(3)P The steel plate shall be continuously connected on all edges to structural steel framing and boundary members with welds and/or bolts to develop the yield strength of the plate in shear.

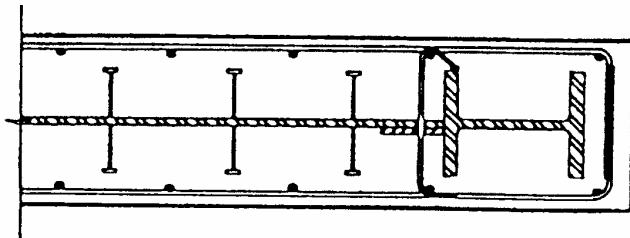
(4)P The boundary members shall be designed to meet the requirements of Section 7.10.

(5)P Concrete may be provided on one side or on both sides of the steel plate.

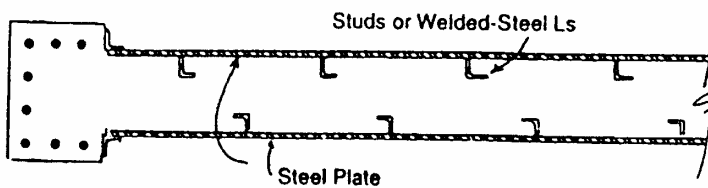
(6) The minimum concrete thickness is 200 mm when it is provided on one side and 100 mm on each side when provided on both sides.



Concrete stiffened steel shear wall with steel boundary member.



Concrete stiffened steel shear wall with composite (encased) boundary member.



Concrete filled composite shear wall with two steel plates.

Figure 7.10. Possible sections of steel shear walls (from [1])

- (7) The minimum reinforcement ratio in both direction shall not be less than 0,25%
- (8) Openings in the steel plate shall be stiffened as required by analysis.

7.12 Control of design and construction

- (1) For the control and design of construction, Section 6.12 applies.

C. Section 6.12 is reproduced under 7.1.3.

ANNEX J : SEISMIC DESIGN OF THE SLAB REINFORCEMENTS OF COMPOSITE BEAMS WITH SLAB IN MOMENT FRAMES

AJ.1. General

The plastic hinges developed in the beam ends of a composite moment frame have to be ductile. Two conditions have to be fulfilled to ensure that a high ductility in bending is obtained :

- early buckling of the steel part must be avoided
- early crushing of the concrete of the slab must be avoided

Each of these two conditions brings a limit of the section A_S of the reinforcement present in the slab of a composite T beam made of a steel section with slab.

AJ.2. Requirement on the section A of re-bars in order to avoid premature buckling of the steel section

Rule 7.6.1 (4) applies.

C. Sufficient local ductility of members, which dissipate energy by their work in compression or bending, is ensured by restricting the width-thickness ratio b/t according to the cross sectional classes specified in EN 1993-1-1. The values of the b/t ratios for a web subjected to bending and compression depend on the slenderness of its part in compression, that is, of the position of the plastic neutral axis in the section.

For a typical composite section made of a steel section with slab, the critical action for the determination of the class of the steel walls of the section is the negative bending moment. It comes down to the determination of the class of the lower flange of the steel section, which is totally in compression, and to the determination of the class of the web, which is in bending. The position of the plastic neutral axis of the composite section under negative moment determines the slenderness of the part of the web in compression and consequently its class. The position of the neutral is directly linked with the section of the reinforcement in the effective width. With an increase of reinforcement in the effective width, the neutral axis rises in the section and the slenderness of the web in compression increases. The ductility requirement on the steel web leads thus implicitly to a condition on the section of re-bars $A_S < A_{limit\ class\ i}$ in the effective width b_{eff}

The higher the required class of section is (the highest class corresponds to class 1), the more restrictive the condition on the re-bars is, that means the lower is the value of $A_{limit,}$, which enables a section to belong to a given class.

AJ.3. Requirements on the section A of re-bars in order to avoid premature crushing of the concrete

C. The EC4 approach ensures a ductile behaviour in the slab under negative moment; it doesn't take the presence of a transverse beam into account. Developments aiming at a ductile behaviour of the slab under positive moment conclude that the plastic resistance of the full composite section cannot be developed without transverse beam –see comment C3 in AJ.3.2.2. The following presentation tries to list all the possible situations and to determine the “controlled” situations, meaning by that word the situations for which design can be made, and the other situations, which require further research to be clearly under control.

AJ.3.1. Exterior column - bending of the column in direction perpendicular to façade **Applied beam bending moment is negative - $M < 0$**

C. Next figure shows the possible situations considered in this paragraph and presents the notations used in the text.

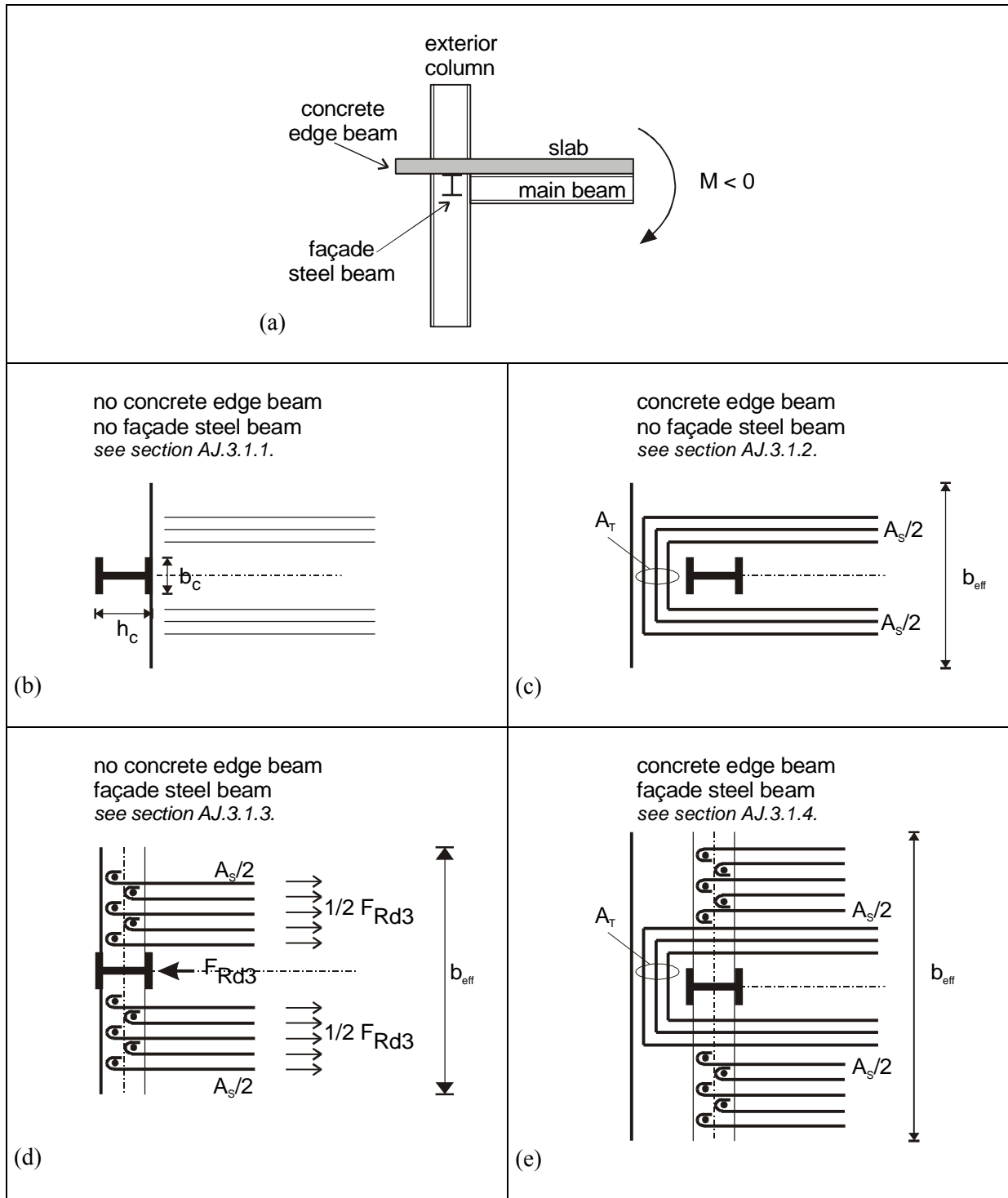


Figure AJ.1. Configurations of exterior composite beam-to-column nodes under negative bending moment in direction perpendicular to façade

AJ.3.1.1 No façade steel beam - no concrete edge beam See Figure AJ.1.(b)
 When no façade steel beam and no concrete edge beam are present, the transferable moment is the steel beam plastic moment only.

AJ.3.1.2 No façade steel beam - concrete edge beam present See Figure AJ.1.(c)
 When there is a concrete edge beam and no façade steel beam, EC4 applies.

C. For clarity of the text, some clauses of EC4 are reproduced here

$F_{Rd0} = 1.1 (0.85 f_{ck}/\gamma_c) b_c d_{eff}$ where: for a solid slab, d_{eff} is the overall depth of the slab
for a composite slab, d_{eff} is the thickness of the slab above the ribs of the profiled sheeting

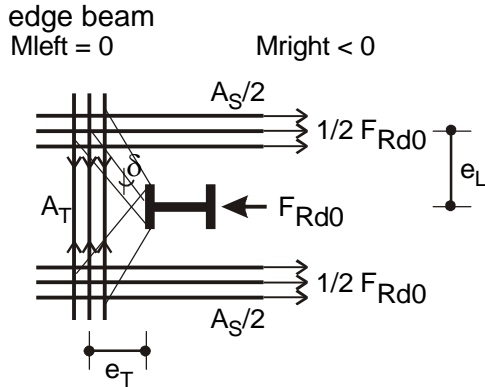


Figure C1

The ductility condition on the longitudinal re-bars, which ensures that their yielding takes place before the crushing of concrete is:

$$A_S \leq 0.94 b_c d_{eff} \frac{f_{ck}/\gamma_c}{f_{sk}/\gamma_s}$$

Longitudinal reinforcement for a composite joint shall be positioned so that the distance e_L from the axis of the column web to the centroid of the longitudinal reinforcement placed each side of the column, see Figure above, is within the following limits:

$0.7 b_c \leq e_L \leq 2.5 b_c$ where b_c is the width of the column steel section

The condition to exclude the failure of the transverse re-bars is:

$$A_T \geq \frac{A_S}{2 \tan \delta} \frac{f_{sk}/\gamma_s}{f_{sk,T}/\gamma_s} \quad \text{with } \tan \delta = 1.35 \left(\frac{e_T}{e_L} - 0.2 \right)$$

It becomes:

$$A_T \geq \frac{A_S}{2} \frac{f_{sk}/\gamma_s}{f_{sk,T}/\gamma_s} \quad \text{when the compressed struts are inclined at } 45^\circ$$

AJ.3.1.3 Façade steel beam present – no concrete edge beam See Figure AJ.1.(d)

(1) When a façade steel beam is present rather than a concrete edge beam, the only way to transfer the moment is to use the façade steel beam to anchor the slab forces.

(2) An effective anchorage of the re-bars on the shear connectors of the façade steel beam has to be realised.

(3) The façade beam has to be fixed to the column

(4) The reinforcing steel section A_S in the effective width should check:

$$A_S \leq F_{Rd3}/(f_{sk}/\gamma_s) \quad \text{where } F_{Rd3} = n \times F_{stud} \text{ on the effective width}$$

n = number of connectors in the effective width

$F_{stud} = P_{Rd}$ = design resistance of one connector

(5) The façade beam should be checked in bending, shear and torsion under the horizontal force applied at the connectors

C. The force transfer through a transverse beam (façade steel beam) is more complex than it seems

from the relationship above. It corresponds to a relatively flexible transfer of forces from the slab to the column implying

- the shear and bending of the shear connectors on the transverse beam and
- the bending, shear and torsion of the transverse beam.

An accurate calculation of these force transfers as well as the plastic resistance of the transverse beam is difficult because the stress state in the transverse beam is complex. However, for H or I section, because of their low torsion rigidity, we can estimate the stresses and F_{Rd3} if we ignore the web and consider that the torque is resisted only by non-uniform torsion. Then the only part of the section to be checked is the top flange, which is horizontally sheared and bent. A design method is described in a PhD-thesis under preparation [27].

AJ.3.1.4 Façade steel beam and concrete edge beam present See Figure AJ.1.(e)

- (1) When both a façade steel beam and a concrete edge beam are present, two mechanisms of transfer of forces are possible: the mechanism described in EC4 and the transfer through the façade steel beam.
- (2) AJ.3.1.3 (3), (4) and (5) apply to the section of re-bars anchored to the transverse beam
- (3) AJ.3.1.2 apply to the section of re-bars anchored in the concrete edge beam

C. The simple addition of the resistances F_{Rd0} (see definition in comment to AJ.3.1.2.) and F_{Rd3} is rather coarse and may be incorrect; this static equilibrium solution only holds if the most rigid force transfer mechanism is ductile enough ; it would not be the case if the concrete would crush on the flange of the column and bring resistance F_{Rd0} down to zero before a real force transmission takes place through the transverse beam.

AJ.3.2. Exterior column - bending of the column in direction perpendicular to façade **Applied beam bending moment is positive – M>0**

AJ.3.2.1. No façade steel beam – no concrete edge beam See Figure AJ.2.(b-c)

(1) When the concrete slab is limited to the interior face of the column, the transfer of moment is made by direct compression of the concrete on the column flange.

(2) The maximal force transmitted to the slab is:

$$F_{Rd1} = b_c d_{eff} (0.85 f_{ck}/\gamma_c)$$

(3) Confinement of the concrete close to the column flange by transverse re-bars is required. The section of these re-bars should comply with

$$A_T \geq 0.21 d_{eff} b_c \frac{0.15 \ell - b_c}{0.15 \ell} \frac{f_{ck}}{f_{sk}} \frac{1}{\gamma_s}$$

over a length of beam equal to b_{eff} and should be uniformly distributed over that length.

The distance of the first re-bar to the column flange should not exceed 30 mm.

(4) The section A_T of re-bars defined in (3) can be partly or totally realised by re-bars placed for other purposes, like for instance the bending resistance of the slab.

C. F_{Rd1} is a rather concentrated force, which is spread through the width of the slab and induces a transverse tension force F_{t1} . This requires transverse anti bursting reinforcements.

Early developments (see Section 3.5.) assumed that the spreading of force F_{Rd1} approximately took place on a distance equal to half the effective width b_{eff} of the slab in current sections and generate a transverse tension force F_{t1} , which can be computed explicitly if b_{eff} is defined.

$$F_{t1} = \frac{F_{Rd1}}{4} \frac{b_{eff} - b_c}{b_{eff}} = 0.21 f_{cd} \cdot b_c \cdot d_{eff} \cdot \frac{b_{eff} - b_c}{b_{eff}} = A_S f_{sk} / \gamma_s$$

If b_{eff} is assumed to be equal to 0.15ℓ , the above equation gives the present limit to A_S .

Slightly modified rules could be proposed, more linked with the confining effect of reinforcement on the concrete close to the column in a PhD-thesis under preparation [27].

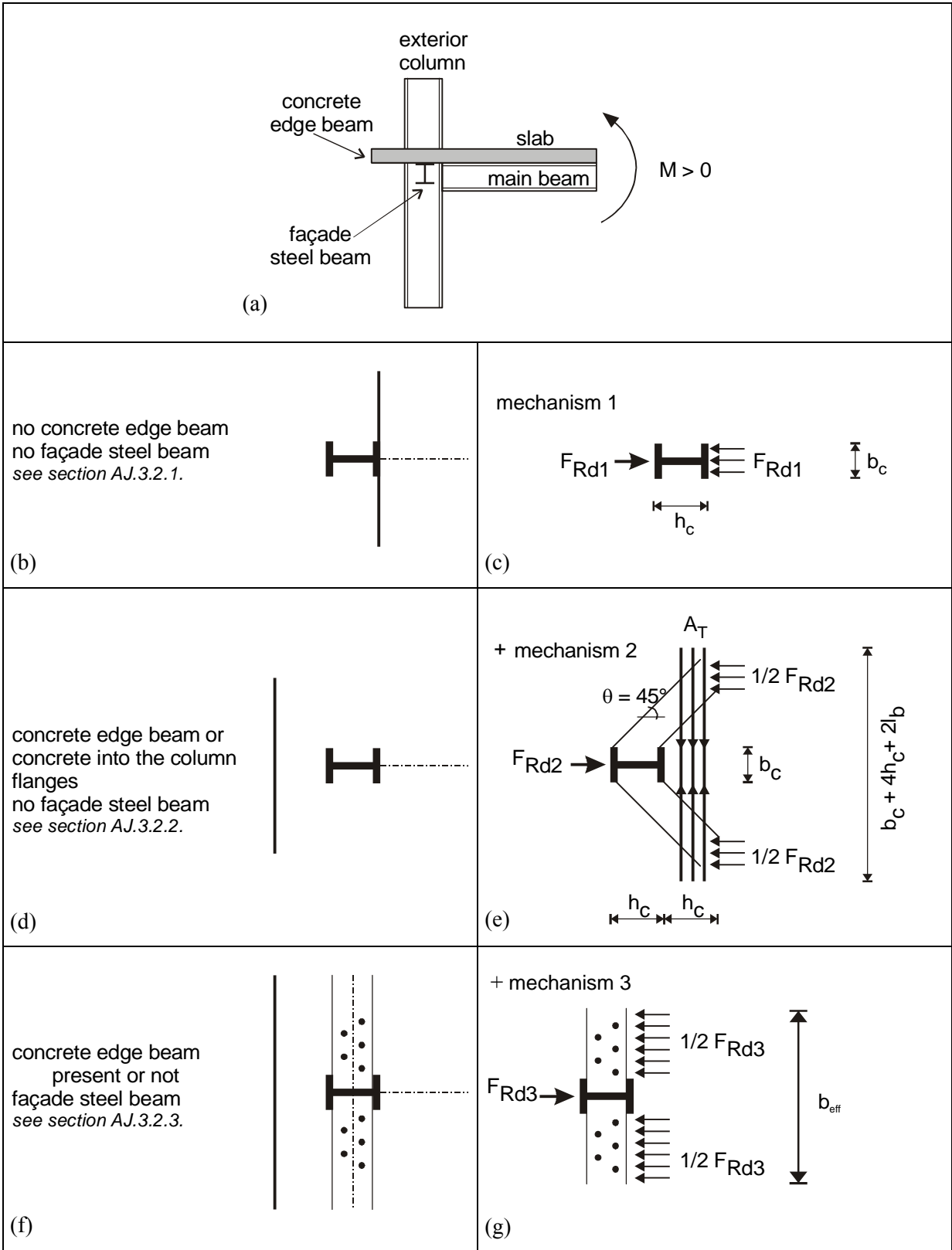


Figure AJ.2. Configurations of exterior composite beam-to-column nodes under positive bending moment in direction perpendicular to façade and possible transfer of slab forces.

AJ.3.2.2. No façade steel beam – concrete edge beam present or concrete into the column flanges

See Figure AJ.2.(c-d-e)

- (1) When no façade steel beam is present, the transferable moment is linked with two mechanisms:

Mechanism 1: direct compression on the column

$$F_{Rd1} = b_c d_{eff} (0.85 f_{ck}/\gamma_c)$$

Mechanism 2: compressed concrete struts inclined on the column sides. If incline is equal to 45°:

$$F_{Rd2} = 0.7 h_c d_{eff} (0.85 f_{ck}/\gamma_c)$$

where for a solid slab d_{eff} is the overall depth of the slab

for a composite slab d_{eff} is the thickness of the slab above the ribs of the profiled sheeting

b_c is the width of the column steel section

h_c is the height of the column steel section

- (2) The required tension tie steel section is (see Figure AJ.2.(e)):

$$A_T \geq \frac{F_{Rd2}}{f_{sk,T}/\gamma_s} = 0.3 h_c d_{eff} \frac{f_{ck}/\gamma_c}{f_{sk,T}/\gamma_s}$$

- (3) Section A_T is distributed over a width equal to h_c . It has to be fully anchored. The resulting length of re-bars is $L = b_c + 4 h_c + 2 l_b$, where l_b is the anchorage length of the re-bars according to EC2.

- (4) The maximum compression force transmitted is $F_{Rd1} + F_{Rd2} = b_{eff} d_{eff} (0.85 f_{ck}/\gamma_c)$.

It corresponds to a maximal effective width of $b_{eff\ connec}^+ = 0.7 h_c + b_c$.

$M_{pl,Rd}$ should be computed considering $b_{eff\ connec}^+$.

C1. In the experimental specimens used to develop these design formulas [17-20-23-24], both mechanisms 1 and 2 have never been dissociated. So, the transverse re-bars present in the zone of compression of the concrete close to the column face were the transverse re-bars designed to avoid splitting of the composite section and the additional transverse re-bars carrying the tension forces of the tension tie (mechanism 2). No specific re-bars were added for mechanism 1 and the behaviour of the slab was good (no early crushing). We conclude that in configurations implying mechanisms 1 and 2, the transverse re-bars necessary to develop the concrete struts in compression of mechanism 2 are sufficient to confine the concrete stressed in mechanism 1 and improve its ductility.

C2. The resistance of mechanism 2 and the corresponding condition on the tension tie are obtained on the basis of 2 assumptions: - inclined struts at 45°, and

- a concrete resistance of the struts of $f_{strut} = v f_{cd} = 0.6 f_{cd}$

If the incline θ of the compression struts is not fixed and if the resistance of the concrete struts is related with parameter v , the resistance of mechanism 2 and the required tension tie section can be expressed as function of θ and v

$$F_{Rd2} = 2 F_{cd} \cos\theta = 2 v f_{cd} \cdot d_{eff} \cdot h_c \sin\theta \cos\theta = 0.85 f_{cd} \cdot d_{eff} \cdot b_{eff}$$

$$A_T \geq v \sin^2\theta d_{eff} h_c \frac{f_{ck}/\gamma_c}{f_{sk,T}/\gamma_s}$$

Variations of the parameters θ between 45° and 30° and v between 0.6 and 1 gives the following range of variation for A_T :

<i>Incline of the struts θ</i>	<i>Concrete resistance f_{strut}</i>	<i>Transverse reinforcement $A_T >$</i>
45 °	0.6 f_{cd}	0.3 $d_{eff} h_c f_{cd}/f_{sd}$
	1. f_{cd}	0.5 $d_{eff} h_c f_{cd}/f_{sd}$
30°	0.6 f_{cd}	0.15 $d_{eff} h_c f_{cd}/f_{sd}$
	1. f_{cd}	0.25 $d_{eff} h_c f_{cd}/f_{sd}$

The choice of the incline of the struts influences greatly the section of transverse reinforcement necessary to anchor the compressive struts. Taking 30° instead of 45° reduces the section by a factor 2, which is not negligible. The specimens tested were designed with the assumption of 45° and behaved well. Exploitation of a numerical model is under way to establish the more adequate θ .

The choice of a low resistance of the compressed concrete in the inclined struts has not so many implications on the required transverse re-bars if the composite T section is designed to fail by yielding of the steel section. In composite section designed to concentrate the plastic deformations in the steel section, the plastic neutral axis is high in the section, that is, lies in the upper flange of the steel section or in the slab. At the limit, the neutral axis lies in the concrete slab and the compression in the slab is limited by the plastic resistance in tension of the whole steel section.

If the resistance of concrete is taken greater than 0.6 f_{cd} , it corresponds in the design formula to an increase of the effective width. The neutral axis rises in the section and the whole depth of the slab is not in compression anymore, or the depth in compression decreases. Considering higher resistance of the struts will not change anything to the total force transmitted by the slab because it is limited by the yielding of the steel section. If the formulas are adapted with the real depth of slab in compression, the required transverse reinforcement will be unchanged

On the other hand, if the composite section is not designed with a positive plastic neutral axis high in the section, the choice of a too small resistance of the concrete struts underestimates the real plastic moment of the section. In this field of application, some calibrations are still needed.

C3. It is interesting to compare $b_{eff\ connec}^+$ and b_{eff}^+ of a composite T beam. For the evaluation of a plastic moment, Table 7.5 indicates $b_e = 0.075 \ell$ under M^+ , which corresponds to $b_{eff}^+ = 2b_e = 0.15 \ell$. This value is identical to the one defined in EC4 for the stiffness and plastic moment.

Considering (4) above in a practical case in which $b_c \cong h_c$ and $b_c \cong 0.05 \ell$, $b_{eff\ connec}^+$ is obtained:

$$b_{eff\ connec}^+ = 0.7 h_c + b_c \cong 1.7 b_c \cong 0.085 \ell \quad \ll \quad b_{eff}^+ = 0.15 \ell$$

$$b_{eff\ connec}^+ \cong 0.5 b_{eff}^+ (EC4)$$

From that result, we can conclude that, without an additional mechanism or without considering the confining effect of the transverse re-bars, the full positive composite plastic moment can not be transferred. Only one half of the EC4 effective width can effectively be realised in the connection zone.

The assessment of the effect of confinement on the concrete resistance in function of the transverse reinforcement section is under way [27], but it does not demonstrate that a well designed transverse steel beam is not useful. The presence of a transverse steel beam can help in the transfer of a full plastic moment, if its stiffness is high enough in comparison with the stiffness of mechanism 1 and 2. The problem is to design properly a rigid enough transverse beam mechanism.

The rest of the document assumes that the mechanism of transverse beam is rigid enough to participate in the transfer of resisting forces of the composite beam.

AJ.3.2.3. Façade steel beam present – concrete edge beam present or not

See Figure AJ.2.(c-e-f-g)

(1) When a façade steel beam is present, a third force transfer F_{Rd3} implying the façade steel beam is activated in compression.

$$F_{Rd3} = n \times F_{stud} \text{ in the effective width} \quad \text{with } n = \text{number of connectors in the effective width}$$
$$F_{stud} = P_{Rd} = \text{design resistance of one connector}$$

(2) AJ.3.2.2. applies

(3) The maximum compression force transmitted is $b_{eff} d_{eff} (0.85 f_{ck}/\gamma_c)$. It is transmitted if:

$$F_{Rd1} + F_{Rd2} + F_{Rd3} > b_{eff} d_{eff} (0.85 f_{ck}/\gamma_c)$$

The "full" composite plastic moment is achieved by choosing n in order to achieve the adequate F_{Rd3} . The maximum effective width is given in Table 7.5.

C. The experimental observations in the Ispra test [17] and the Darmstadt tests [23] indicate that the plastic bending moment transferred from beam to column corresponds to this design hypothesis.

AJ.3.3. Interior column - $A_T = A_S/2$

C. The proposed "seismic" reinforcement section A_T is a transverse reinforcement ensuring the transfer of compression by strut and tie mechanism. In case of a real building resisting by moment frames in the 2 directions, it is easier to handle with identical sections in both directions. So, it has been decided that it would be better if the beam-to-column joints of the frames were designed with the same reinforcement around the column, longitudinal and transverse. And the proposed reinforcing steel section is valid for longitudinal and transverse reinforcement ($A_T = A_S/2$). But, it is clear that in the case of a building with resisting frames only in one direction, the design of transverse and longitudinal reinforcement could be totally separated.

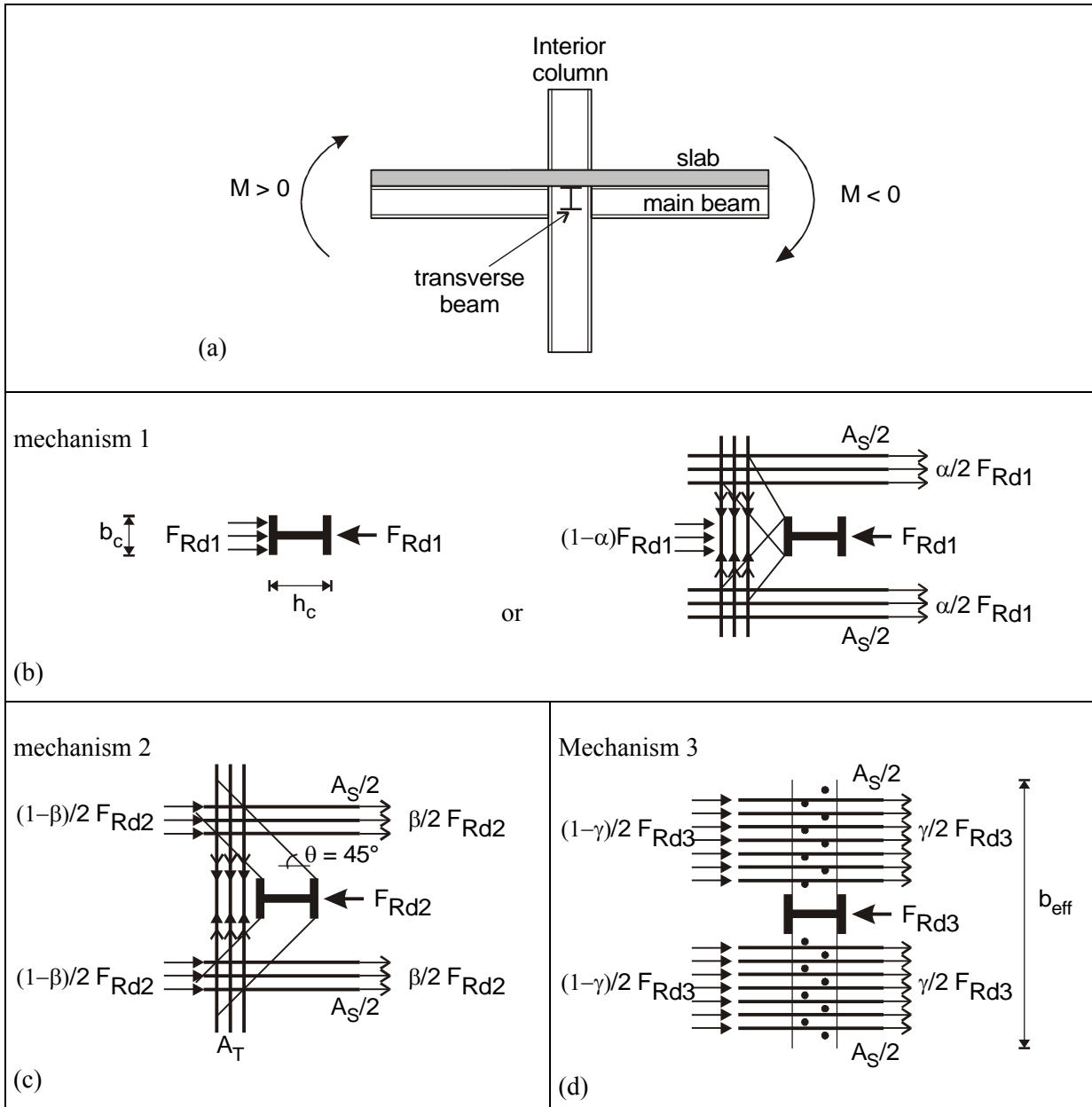


Figure AJ.3. Possible transfer of slab forces in an interior composite beam-to-column node with and without transverse beam under positive bending moment at one side and negative bending at the other side

AJ.3.3.1. No transverse beam present

- (1) When no transverse beam is present, the transferable moment is linked with the two mechanisms:

Mechanism 1: direct compression on the column

$$F_{Rd1} = b_c d_{eff} (0.85 f_{ck}/\gamma_c)$$

Mechanism 2: compressed concrete struts inclined at 45° on the column sides

$$F_{Rd2} = 0.7 h_c d_{eff} (0.85 f_{ck}/\gamma_c)$$

- (2) Required tension tie section:

$$A_T \geq \frac{F_{Rd2}}{f_{sk,T}/\gamma_s} = 0.3 h_c d_{eff} \frac{f_{ck}/\gamma_c}{f_{sk,T}/\gamma_s}$$

- (3) The same section A_T has to be placed on each side of the column.

- (4) The resistance is at the most:

$$F_{Rd1} + F_{Rd2} = (0.7 h_c + b_c) d_{eff} (0.85 f_{ck}/\gamma_c)$$

The action force is the sum of the tension coming from the re-bars at the negative moment side and the compression of the concrete at the positive moment side:

$$F_{St} + F_{Sc} = A_S (f_{sk}/\gamma_s) + b_{eff}^+ d_{eff} (0.85 f_{ck}/\gamma_c) \quad \text{with } A_S \text{ considered in effective width } b_{eff}^-$$

C. It is impossible to transfer an action that would correspond to the effective width under positive bending moment deduced from EC4 ($b_{eff}^+ = 0.15 \ell$) at one side and to the effective width under negative bending moment at the other side, because it was already not possible for an exterior node under positive moment only. Adding a negative moment still makes the situation worse. As the real effective widths for positive and negative moments are not known, this situation is not controlled.

AJ.3.3.2. Presence of transverse beam

- (1) When a transverse beam is present, a third force transfer F_{Rd3} implying the façade steel beam is activated.

$$F_{Rd3} = n \times F_{stud} \text{ in the effective width} \quad \text{with } n = \text{number of connectors in the effective width}$$

$$F_{stud} = P_{Rd} = \text{design resistance of one connector}$$

- (2) AJ.3.3.1. applies for the condition on the tension tie for mechanism 2.

- (3) The resistance is at the most:

$$F_{Rd1} + F_{Rd2} + F_{Rd3} = (0.7 h_c + b_c) d_{eff} (0.85 f_{ck}/\gamma_c) + n F_{stud} \quad \text{in } \max (b_{eff}^-, b_{eff}^+)$$

The applied force is the sum of the tension coming from the re-bars at the negative moment side and the compression of the concrete at the positive moment side:

$$F_{St} + F_{Sc} = A_S (f_{sk}/\gamma_s) + b_{eff}^+ d_{eff} (0.85 f_{ck}/\gamma_c) \quad \text{with } A_S \text{ considered in effective width } b_{eff}^-$$

- (4) In a design aiming at yielding located essentially in the bottom flange of the steel section and no crushing of concrete, the design condition is :

$$1.2 (F_{Sc} + F_{St}) \leq F_{Rd1} + F_{Rd2} + F_{Rd3}$$

C1. If it is fulfilled, the situation is controlled and the transferred forces correspond to the proposed EC8 effective widths : $b_{eff}^- = 0.2 \ell$ and $b_{eff}^+ = 0.15 \ell$.

If it is not, the situation is not controlled and the real effective widths in the positive and negative moments zones are not known.

C2. The simple addition of the resistances F_{Rd1} , F_{Rd2} and F_{Rd3} may be incorrect; this static equilibrium solution only holds if the most rigid force transfer mechanism is ductile enough ; in the case of an interior column, the modelling [27] has shown that mechanism 3 (participation of transverse beam) is always too flexible to increase significantly the plastic moment of the composite beam, if this one is an H or I steel section with high density of studs. The solution to activate the transverse beam would be to add rigid pieces directly welded to the column through the thickness of the slab, or to design additional connecting elements providing a reaction as stiff as the direct compression of concrete on the column flange.

C3. General remark. The practical problem in choosing to dissipate energy essentially in the yielding of the steel section of the composite T beam with slab is that it requires resistant concrete slabs strongly reinforced around the columns. The large section of reinforcement will lead to relatively high slenderness of the web of the steel sections and to the difficulty of achieving the required class of section. The difficulty is to realise a beam column joint with a ductile behaviour at the positive moment side simultaneously with a ductile behaviour at the negative moment side, when it is imposed to take the same section for longitudinal and transverse reinforcement ($A_T = A_S/2$).

REFERENCES

- [1] AISC – Seismic provisions for structural steel buildings.1997
- [2] Richard Yen, J.Y., Lin Y., and Lai, M.T., "Composite beams subjected to static and fatigue loads" J. of Structural Eng. June 1997, 765-771.
- [3] Bursi, O.S. and Zandonini, R., "Quasi-static Cyclic and Pseudo-dynamic Tests on Composite Substructures with Softening Behaviour" selected paper in Stability and Ductility of Steel Structures, Usami T. and Itoh Y. ed. Elsevier, 1998, 119-130.
- [4] Bursi, O.S. and Gramola, G., "Behaviour of headed stud shear connectors under low-cycle high amplitude displacements", Revised for Materials and Structures, Vol.32, May 1999, pp.290-297.
- [5] Plumier, A., Problems and options in the seismic design of composite frames, University of Liege Internal Report, 1996.
- [7] Doneux, C. Research on energy dissipation capacity of composite steel/concrete structures. Tests on 3 composite joints at Technical University of Darmstadt – Report II – April 1999.
- [8] Paulay, T. and Priestley, M.J.N. Seismic design of Reinforced Concrete and Masonry buildings, ed. John Wiley & sons, 1992.
- [9] Sanchez, L. and Plumier, A. Particularities raised by the evaluation of load reduction factors for the seismic design of composite steel concrete structures, Symposium on Stability and Ductility of Steel Structures, SDSS 1999, (Timisoara)
- [10] Design guide for partially restrained composite connections, J. of Struct. Eng. ASCE, October 1998, 1099-1114.
- [11] Astaneh-Asl, A. Seismic design of bolted steel moment-resisting frames, in Steel Tips, Structural Steel Education Council, Moraga, Calif., (1995) .
- [12] Ricles, JM and Paboojian, SD., 'Seismic performance of steel-encased composite columns', J. Struct. Engng, 120, 8, 1994, pp. 2474-2494.
- [13] Roeder C.W., Chmlelowski R. and Brown C.B. 'Shear Connector Requirements for Embedded Steel Sections', Journal of Structural Engineering, 125, 2, 1999, pp.143-151
- [14] Roeder (1999b)
- [15] Hajjar, J.F., Molodan A., Schiller P.H. (1998). A distributed plasticity model for cyclic analysis of concrete-filled steel tube beam-columns and composite frames. Engineering Structures, vol.20, nos 4-6, pp. 398-412.
- [16] Zandonini, R. and Bursi, O.S. ``Cyclic behavior of headed stud shear connectors'', Proc. of the Fourth Conference on Composite Construction in Steel and Concrete, May 28- June 2, Banff, Alberta, 2000
- [17] Plumier, A, Doneux, C, Bouwkamp, JG and Plumier, C. "Slab Design in Connection Zone of Composite Frames" Proceedings of the XIth European Conference on Earthquake Engineering, Paris, 1998
- [18] Plumier, C and Doneux, C, "Dynamic tests on the ductility of composite steel-concrete beams" Proceedings of the XIth European Conference on Earthquake Engineering, Paris, 1998

- [19] Ballio, G; Plumier, A and Thunus, B, "Influence of concrete on the cyclic behaviour of composite connections" Proceedings of the IABSE Symposium, Brussels, 1990
- [20] Plumier, A and Doneux, C, "Lastabtragung in biegesteifen Flachdecken-Verbundrahmensystemen unter Erdbebeneinwirkung", Stahlbau, 6/1999
- [21] Doneux, C , "A Three Dimensional finite element modelling of a Typical Composite Steel-Concrete Beam to Column Joint" Fifth International Conference on Computational Structure Technology, Leuven, 2000
- [22] Aribert, JM and Lachal, A, "Behaviour of steel concrete shear connectors under repeated cyclic loading for seismic design of connections"-Génie Parasismique et Réponse Dynamique des Ouvrages, 5^e Colloque National AFPS, Cachan (France), 19-21 Octobre 1999.
- [23] Doneux, C and Parung, H, (1998) "A study on composite beam-column subassemblages", Proceedings of the 11th ECEE Conference, Paris.
- [24] Bouwkamp, J., Parung, H. and Plumier, A. (1998), "Bi-directional cyclic response study of a 3-D composite frame", Proceedings of the 11th ECEE Conference, Paris.
- [25] Broderick, B and Elghazouli, A (2000), "Development of design guidance for composite encased, partially encased and filled sections", Internal Report University of Liege, 2000
- [26] Abed, A (2001), "Etude du comportement de structures en profils mixtes acier-béton partiellement enrobés soumises à l'action sismique", Thèse de Doctorat en Sciences Appliquées de l'Université de Liège.
- [27] Doneux, C. (2001), "Etude du mécanisme de transfert des flexions à la jonction poutre-poteau dans les structures en portiques mixtes", PhD Thesis under preparation - University of Liege

3. REPORTS ON EXPERIMENTAL ACTIVITY AND NUMERICAL MODELLING

3.1. ISMES TESTS: Dynamic tests on the ductility of composite steel-concrete beams

C. Plumier, C. Doneux

Department of Civil Engineering, University of Liege, Belgium

3.1.1. Introduction

The final purpose of the test program is to determine the condition to realise ductile composite steel-concrete section when these are submitted to seismic action. One important problem in this context is the value of the concrete crushing strain needed in the plastic design of ductile composite steel-concrete sections submitted to seismic action. The value $2 \cdot 10^{-3}$ is currently admitted in the design for static condition (Eurocode 4). Given the context of earthquake resistant design, the idea was to check whether this value could be admitted to be bigger or not, because of the dynamic and accidental character of the action.

The composite sections were chosen to favour a failure by concrete plastic crushing taking in account the limitations of the shaking table:

- Specimen maximum mass: $20 \cdot 10^3$ kg;
- Maximum acceleration: 50 m/s²;
- Maximum length of the specimen: 3.5 m.

The tests have been realised at ISMES, Bergamo, Italy.

3.1.2. Ductility

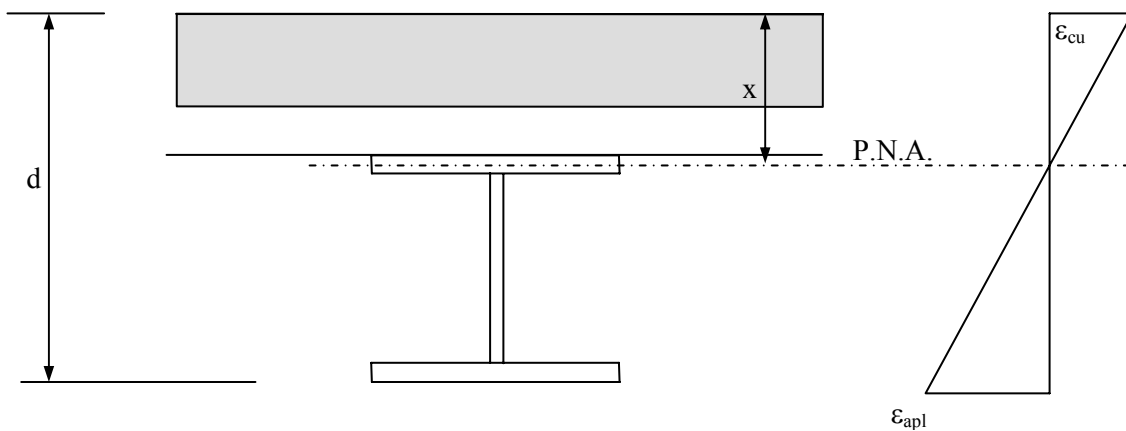


Figure 3.1.1. Composite steel-concrete section (P.N.A= Plastic Neutral Axis)

The ductility of a structure or a member of a structure is defined as its ability to deform inelastically without total fracture or substantial loss of strength. The ductility of a composite steel-concrete section can be characterised by the ratio x/d (Figure 3.1.1.) which is related to the concrete crushing strain ϵ_{cu}

by:
$$x/d \leq \frac{\epsilon_{cu}}{\epsilon_{cu} + \epsilon_{apl}}$$

where x = distance from the top of the concrete to the plastic neutral axis of the composite section; d = total height of the composite section; ϵ_{apl} = plastic strain of the steel bottom flange (Eurocode 4).

An evaluation of the composite beam ductility is the ductility ratio, calculated, in these cases, as the ratio of the maximum mid span deflection to the deflection at the first yield.

3.1.3. Experimental results

Description of the tests

The tests were conducted as shaking table tests, as shown in Figure 3.1.2. The beams were tested in pairs of two, where the load is applied at mid span at two application points.

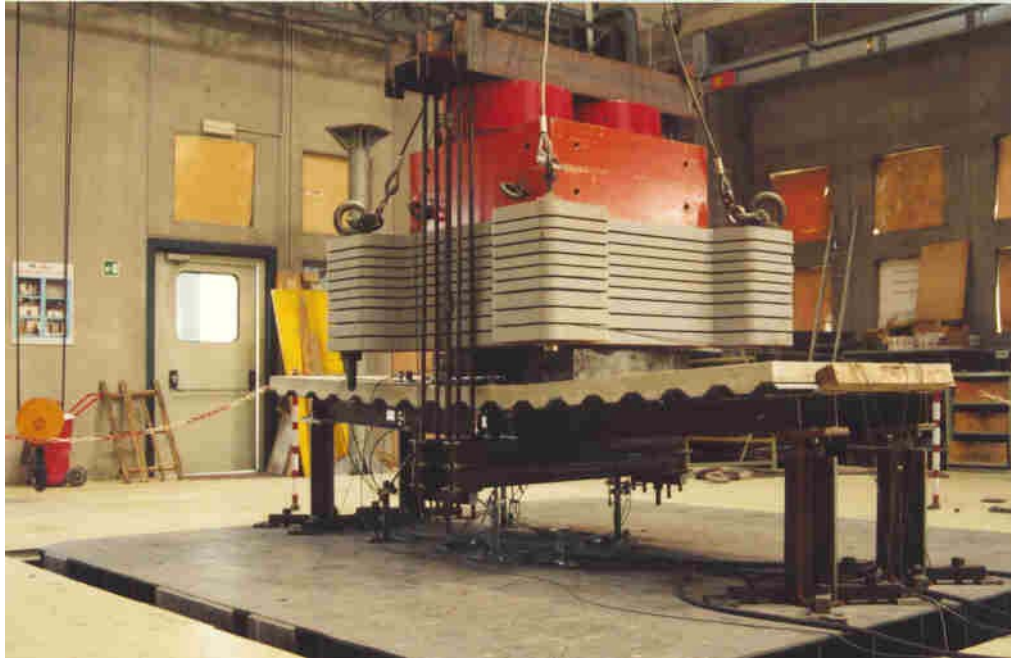


Figure 3.1.2. Photograph of the test set-up

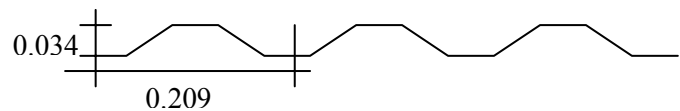
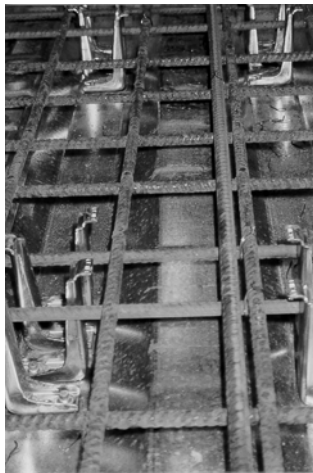


Figure 3.1.3. Steel-deck (indicative values in m)

Figure 3.1.4. Connectors and reinforcing bars configuration

Specimens description

- Two steel sections HEA 140 ($f_y = 330 \text{ N/mm}^2$): 3.330 m long.
- Concrete ($f_{ck} = 23.8 \text{ N/mm}^2$): 0.1 m thickness
- Steel-deck: Figure 3.1.3
- Steel-concrete connection: HILTI shear connectors like on Figure 3.1.4

Instrumentation

The instrumentation used in the first test on the beam HEA 140 has been:

- Strain gages on the steel beams.

On each beam were located four strain gages, two at quarter span and two at mid span. All of them

were situated under each flange.

- Horizontal displacement transducers.

There were two types of displacement transducers depending on the length of their base: 40 cm or 8 cm. The two LVDT's with a base of 40 cm length were located at mid span. Two of the LVDT's of base 8 cm were also located at mid span. Two others of 8 cm were situated at the quarter span. The distance between the concrete surface and the measure devices was 3.6 cm in all the cases.

- Vertical displacement measurements.

They were used to measure the vertical deflection of the beam at quarter and mid span. There were also two types according to the maximum displacement range: +/-50 and +/- 20mm.

- Accelerometers.

Four of them were installed on the concrete slab over the supports, one on the masses and the last one in the centre of the concrete slab.

The position of the instrumentation can be seen on the following sketch:

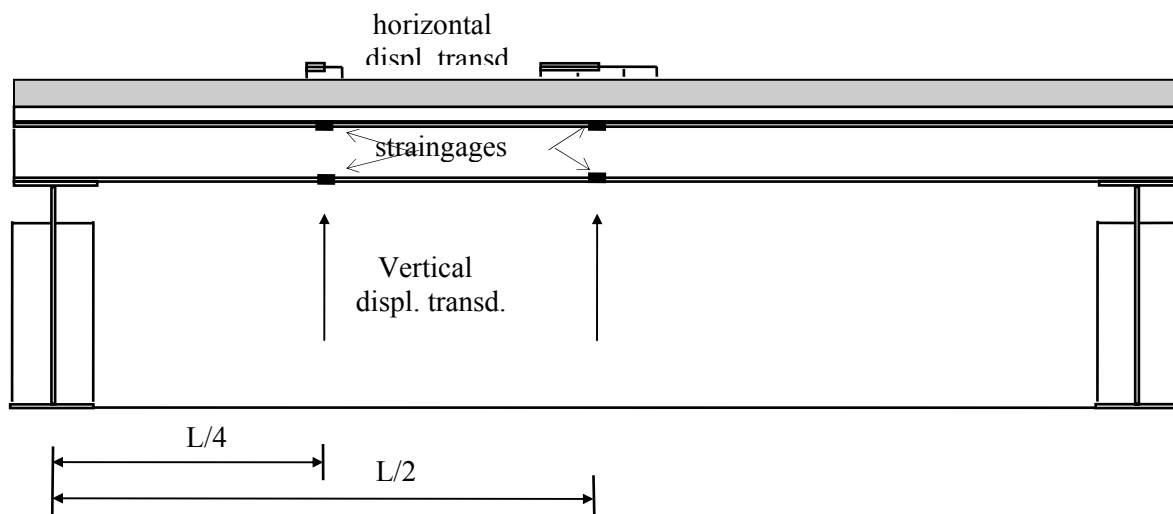


Figure 3.1.5. Side view of instrumentation

Tests Management

The sequence of testing is the same for the three tests. What changed was only the load applied to the specimens.

- Static test

The static test consist in the application of a small load and the measurement of all the deformations and displacements which will to be used as references to check the design and real material characteristics.

- Natural frequency determination

The natural frequency of the specimen is determined by some dynamic tests at low level of acceleration with diverse frequency excitation and an analysis of the amplification factor (ratio: specimen acceleration/table acceleration).

This test gives useful indication to prepare the time history for the dynamic test; in order to attain the maximum acceleration of the masses applicable to the specimen.

- Dynamic test

With the shaking table, the specimen is submitted to a vertical acceleration. The amplitude of the acceleration is increased till the ultimate state. In these cases, the visible sign of the breaking down of the beam is the concrete compression crack. The figure 3.1.6 shows the type of time history applied.

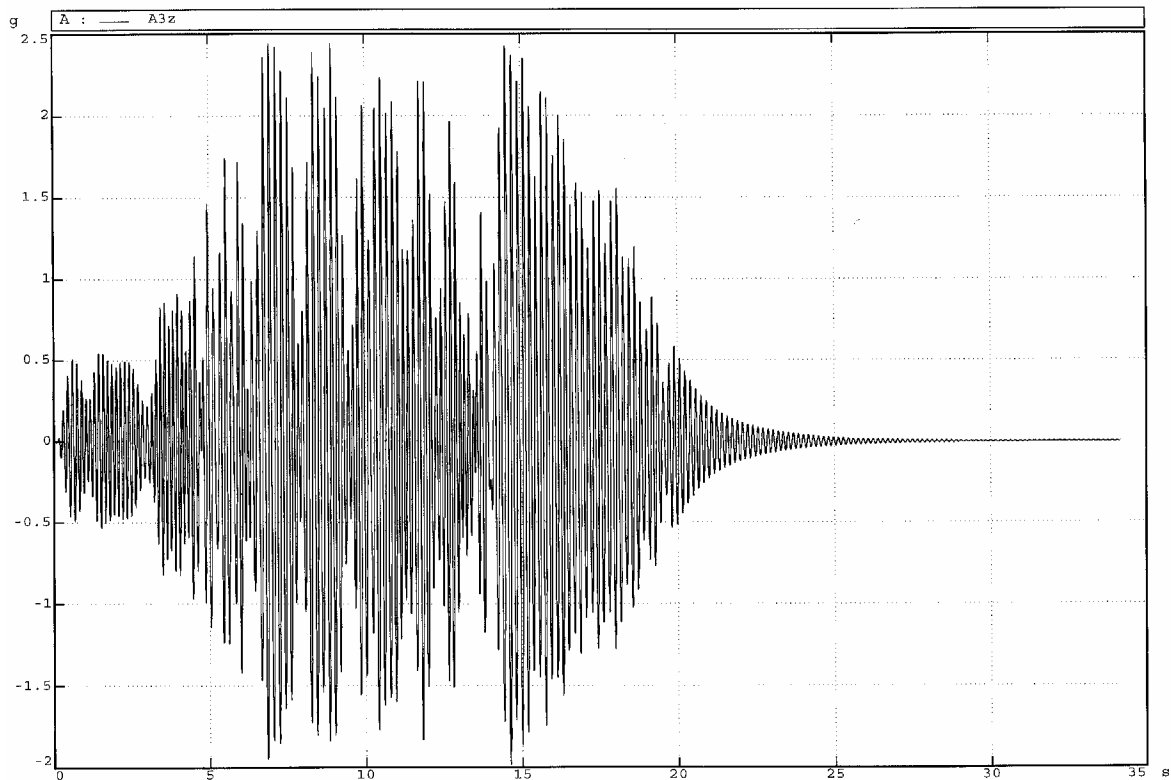


Figure 3.1.6. Time history applied to specimen number 3 for the ultimate test

3.1.4. Processed data

Ultimate concrete deformation

The static tests, on the concrete (0.15*0.30 m cylinders), give about:

$$\epsilon_{cu-static, \text{compression test}} = 2,9 \cdot 10^{-3}$$

The dynamic tests, on the composite steel-concrete beam gives about:

$$\epsilon_{cu-dynamic, \text{composite beam}} \cong 2,4 \cdot 10^{-3}$$

Ductility

The beam is resisting as a partial connection beam and there is, in the ultimate state, a considerable slide (about 10 mm), between the steel section and the concrete. This means that there are two neutral axes for the composite section, as shown in Figure 3.1.7.

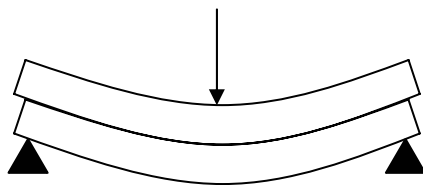


Figure 3.1.7. Exaggerated slide between the steel and the concrete

The formula of the ductility of the composite sections is not applicable.

So, the evaluation of the ductility is based on the mid-span vertical deflections, which gives the ductility ratio. In the table 3.1.1, the comparison between the ductility ratio of the composite beam, the ductility of the steel section and the concrete is given.

Table 3.1.1. Ductilities for the three tests

Test	Ductility Ratio	Steel Ductility	Concrete Ductility
I	4.3	5	2
II	3	7.8	1.9
III	4	8	2

Figure 3.1.8 of the moment at mid-span versus the deflection gives a convenient idea of the ductility.

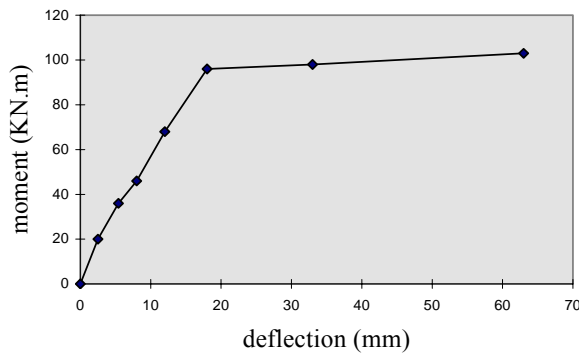


Figure 3.1.8. Comparison of deflection and moment at mid-span

Damping

As an unexpected result, the damping (given in table 3.1.2) is, in these tests, at a very high level. The Eurocode 8 gives a multiplying factor η , to take in account in the design spectrum, for values of damping higher than 5%.

The impact of this result should be moderated by the fact that the structure tested is not a building, but a beam.

Table 3.1.2. Evaluation of the damping for diverse accelerations

Damping δ	Low Acceleration	Medium Acceleration	Ultimate test
Test I	11%	13%	21%
Test II	9.7%	11.2%	15.7%
Test III	8%	11%	16%

3.1.5. Conclusion

The paper deals with the results of a shaking-table test program on composite steel-concrete beams. The first aim was to define the conditions required for designing ductile composite steel-concrete beams under positive bending moments.

One important parameter to characterise the behaviour of these beams and their ductility at the design stage is the ultimate deformation of the concrete ϵ_{cu} , in dynamic cyclic conditions. This parameter end out to be greater than the $2 \cdot 10^{-3}$, value given by Eurocode 2, for design static conditions, but is smaller than the value obtained by the static concrete test. The ductility ratio of the composite beams, based on the mid-span vertical deflections values, is greater than 3.

looking forward

The existence of relative sliding between steel and concrete brings damping. It has been evaluated and found greater than 15% at high level of acceleration ($25-30 \text{ m/s}^2$). A study on the influence of the degree of connection on the damping is needed to calibrate this effect.

The steel-deck shape can influence a lot the failure mode and the ductility of the beam. A study involving diverse steel-deck shapes is needed to evaluate this influence to eventually forbid some shapes for the application to composite beams under seismic action (Mele & Puhali 1985)

3.2. SACLAY TEST: Cyclic test on a composite moment frame

*M.R. Agatino, C. Doneux, A. Plumier
Department of Civil Engineering, University of Liege, Belgium*

3.2.1. Context and aims of the research

For construction in seismic regions, steel structures in general offer a large advantage with respect to reinforced concrete structures, due to reduced dead load, and thus reduced inertial forces. The energy dissipation approach (i.e., capacity design) for the seismic design of steel structures is based on the concept that the structures have to possess sufficient strength, ductility and energy absorption capabilities to dissipate the energy associated with earthquakes through suitable inelastic mechanisms, thus preventing failure and safeguarding human lives. Hence, selection of the dissipative mechanisms appears to be a fundamental requisite and, as a consequence, the hysteretic behaviour of the individual frame components plays a relevant role in the definition of the global response of the structure.

However, evidence of structural collapses has been reported in occasion of recent earthquake events (Northridge 1994, Kobe 1995) and a significant population of steel structures suffered extended damage, in buildings, bridges, and viaducts.

The Northridge and Kobe earthquake caused several unexpected brittle failures in connections of a large number of moment resisting frames, which were traditionally considered ductile and capable of withstanding repeated cycles of large inelastic deformation. One of the main lessons learned from the Northridge and Kobe earthquakes is related to the deficiency of beam-to-column joints in moment resisting frames of buildings that did not collapse, yet exhibited significant structural damage.

Local failures of the main steel structural elements as well as of their beam-to-column joints, or both, took place. Such failures, however, did not result in severe overall deformations, thus remaining hidden behind undamaged architectural panels. A variety of local collapses was observed, among which a recurrent case was identified in the failure of welded beam-to-column joints. Generally, failure presented full penetration weld fractures in the bottom flange, very few had this fracture at the top flange. In all cases there was little or no evidence that plastic hinges had developed in the beams prior to weld fractures. In addition to these and other experimental research programs, a number of numerical models were also developed by various authors. Most of these models are empirical, and need experimental results for the calibration of the various parameters assumed as governing the behaviour of the connection.

The earthquake has given large evidence to this phenomenon which, although not involving the frame global collapse, drastically changes the expectations. As a consequence, extensive experimental researches were carried out all over the world on members and joints aimed both to the analysis of their cyclic performance and to the understanding of the damage cumulating process.

The test described here deals with low-cycle fatigue of rigid beam-to-column joints in composite sections in order to study how the presence of the concrete slab modifies the behaviour of steel connections.

The purpose is to contribute to a deeper knowledge of the following problems: the composite section characteristics to be used in design of moment frames with composite beams; the low cycle fatigue behaviour of composite sections and the implications of early local failure in the global frame response. It is clear that the unsymmetrical shape of composite steel concrete section may be a cause for larger strains in the bottom flange of such sections in comparison to symmetrical pure steel sections, once a real collaboration between steel and concrete exists.

3.2.2. Description of the tested structure

The structure consists of:

- 1 longitudinal composite beam, divided into 3 parts,
- 4 transversal beams,
- 4 columns,
- one reinforced concrete slab,

- one longitudinal steel loading beam for distribution of external applied load to columns.

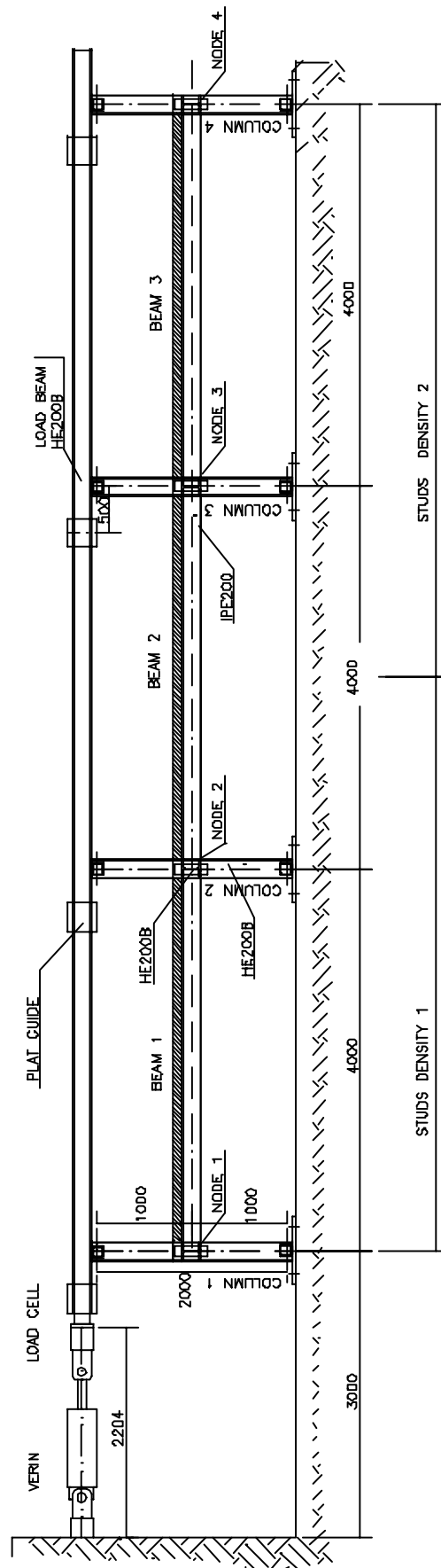


Figure 3.2.1. General view of the specimen

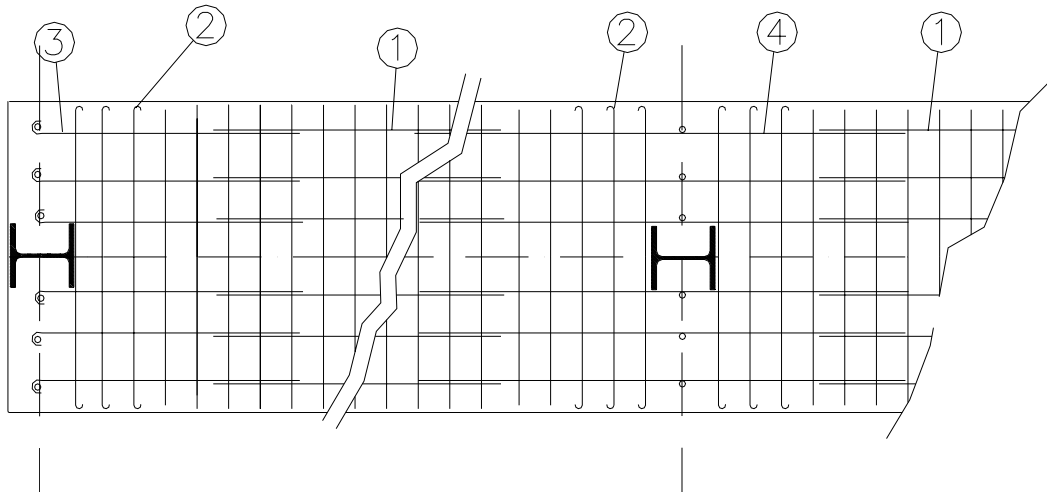


Figure 3.2.2. Reinforcement of the slab and anchoring on the transverse beam

- | | | |
|-----|---------------------------------|----------|
| (1) | wire mesh 150x150x10 | |
| (2) | $\phi 10$ – loops at both sides | L=1.30 m |
| (3) | $\phi 10$ – loops at one side | L=1.15 m |
| (4) | $\phi 10$ – no loop | L=1.70 m |

The numbering of the beams and of the nodes are given at Figure 3.2.1. which shows the steel structure in plan. Two studs densities are used in the specimen dividing the beam in one full shear connection zone ($\eta > 100\%$) and one partial shear connection zone of degree $\eta = 75\%$.

At the external columns, one original detailing for the re-bars is tested. It corresponds to anchor the longitudinal re-bars by a loop around the studs present on the transverse beam (Figure 3.2.2.).

LONGITUDINAL BEAM

The beam, divided into 3 spans of equal dimension, is an IPE200. Each span is 3800 mm in length. The steel utilised is E24-2, with real $f_y = 340.6 \text{ N/mm}^2$ and $f_u = 540.78 \text{ N/mm}^2$.

The part I of the beam (beam1) has 27 studs spaced of 136 mm ($\eta > 100\%$). The part II of the beam (beam2) has over half of its length 14 studs spaced of 136 mm and on the second half 9 studs spaced of 200mm. The part III of the beam (beam3) presents 18 studs spaced of 200 mm ($\eta = 75\%$).

The shear connection are headed studs with diameter 13 mm and height 75 mm.

TRANSVERSAL BEAMS

There are 8 transversal beams and each one is 495 mm in length and of HEB200 type. The steel is type E36-3. Each beam has 3 studs equal to the studs used on the longitudinal beam.

COLUMNS

The 4 columns HEB200 are 2100 mm in length. The steel used is E36-3. Two connecting plates are welded top and bottom of each column (100x100x5) in steel E24-2. One doubler plate is welded on the web of each column in the panel next to the longitudinal beam. These plates are 300x120x10 in steel E24-2.

SLAB IN REINFORCED CONCRETE

The concrete slab is 12 m in length, 1 m in width and 0.1 m in thickness. It has been realised in just one time, horizontally. The slab is divided into 3 parts and the reinforcement is made by:

- 3 welded mesh (150x150x10) of 980 mm in width, 3000 mm in length and with a diameter of the bars of 10 mm;
- 18 re-bars of 10 mm in diameter and 1300 mm in length, curved at the ends;
- 12 re-bars of 10 mm of diameter and 1150 in length, curved just in one end;
- 12 re-bars of 10 mm in diameter and 1700 in length.

Fig. 3.2.2. shows these curved re-bars which represent one original detailing in the exterior column

zones. The steel used for the re-bars is S400. These reinforcing elements have been placed in the middle of the thickness of the slab. No welding has been applied.

LOADING BEAM

The load has been applied to the structure through one loading beam: one HEB200 of 13.76 in length, with one end plate to which a load cell has been fixed.

3.2.3. Test set up

The test has been realised in the Iris hole of the EMSI laboratory. The structure is placed vertically in the hole and it is loaded cyclically quasi-statically by one 500kN MTS hydraulic jack placed at the bottom of the hole. The load is distributed to the columns of the structure by the loading beam (HEB200). No dead loads were applied to the specimen. The beam-to-column transfer is realised by providing the necessary hinge supports conditions at both ends of the columns.

3.2.4. Test procedure

The specimen was subjected to displacement-controlled cyclic load. The applied displacement is quasi-static triangular. The cyclic displacement history was characterised by two phases:

- Phase A, with an increasing displacement range in the elastic range in order to define the first yielding displacement v_y of the structure (3x10 mm, 3x15 mm, 1x20 mm, 1x25 mm, 1x30 mm, 1x35 mm, 1x40 mm, 1x45 mm); v_y was found equal to 33.20 mm.
- Phase B, the fatigue test, with constant displacement of 80 mm (+/- 2.5 v_y) until the total collapse of the structure.

3.2.5. Instrumentation

Only the instrumentation used to describe the global behaviour of the frame presented in the results is reported here. There are:

- one 500 kN load cell between the jack and the loading beam.
- 16 strain gages on the columns, two on each flange of the column and symmetrically at 300 mm from the axes of the longitudinal beam, to deduce the moments in the columns.
- 3 strain gages on the load beam, to evaluate a possible normal force.

3.2.6. Description of the test

The observation during the test have been the following:

- At the 5th cycle: the buckling of the lower flange of the IPE200 corresponding to the 1st node and the 4th one. Cracking of the slab near these nodes is observed;
- Between the 5th and the 15th cycle: progressive cracking in IPE200 beam in the 1st node;
- 10th cycle: the first crack is observed in the IPE200 corresponding to the 1st column;
- 15th cycle: the crack is completely passed through the web of the IPE200;
- 20th cycle: the crack is starting in the flange of the beam IPE200 near the 4th node;
- Between the 20th and 33rd cycle: progressive cracking of the flange longitudinal beam near the 4th node;
- 25th cycle: fall of one great piece of concrete. Studs are evidentes;
- 33rd cycle: the cracking of the web of the longitudinal beam 3 near the 4th node;
- 35th cycle: buckling of IPE200 near the 2nd and 3rd node starts. Under negative bending a gap of 0.5 to 1 cm between the concrete and the upper flange of the IPE200 is observed, and under positive bending the concrete against the upper flange:

- 42th cycle: buckling of the beam IPE200 in the 2nd node;
- 44th cycle: : the crack on the IPE200 the 4th node is completely open;
- From cycle 44 to 60: progressive buckling of the longitudinal beams near nodes 2 and 3;
- 102nd cycle: failure of the specimen is reached.

The behaviour of the joints corresponding to nodes 2 and 3 is not easily observable consequently to the geometrical position of the specimen in the hole.

Hereafter the scheme of the structure is reported with the number of cycles to failure for each node.

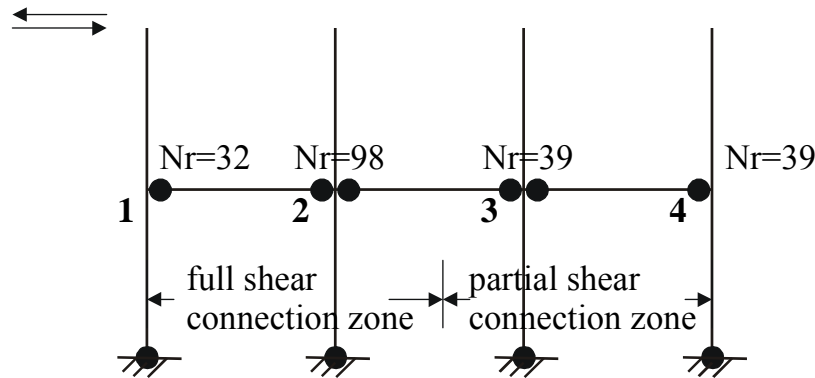


Figure 3.2.3. Position of failure zones and number of cycles to failure.

We can point out that :

- the beam at the exterior nodes has failed before the beam connected to the internal nodes
- the beam close to the node in the full shear connection zone fails before the zone of the partial shear connection

The progressive development of local failure in the structure results first from the original distribution of moments, second from the fact that the static scheme of the structure is modified progressively during the test.

The structure has an evolutionary stiffness. The first failure appearing at the external nodes should result from the fact that the internal nodes are less stressed than the external ones.

3.2.7. Analyses and interpretation

a Graphics

A first analysis has been made plotting the data recorded in function of the time applied.

We have reported the global load-displacement curve for the top of the first column for phase B (Figure 3.2.4.), where the load was applied. Then for each node we have deduced the Moment-Rotation curves and Figure 3.2.5. reports these curves in phase B from cycle 13 to 32.

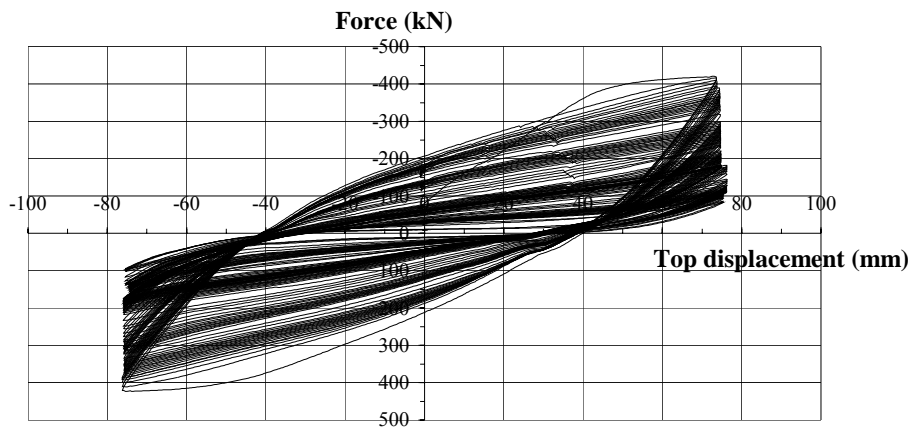
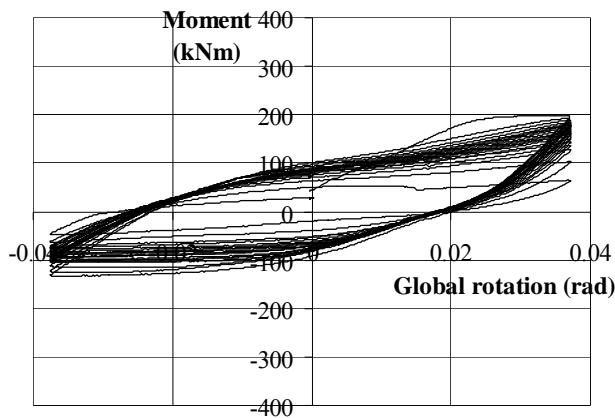
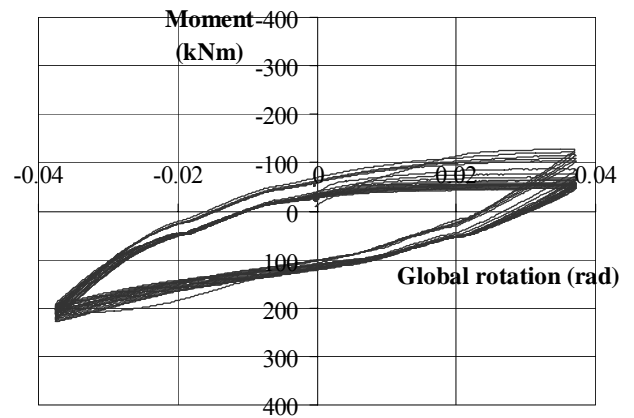


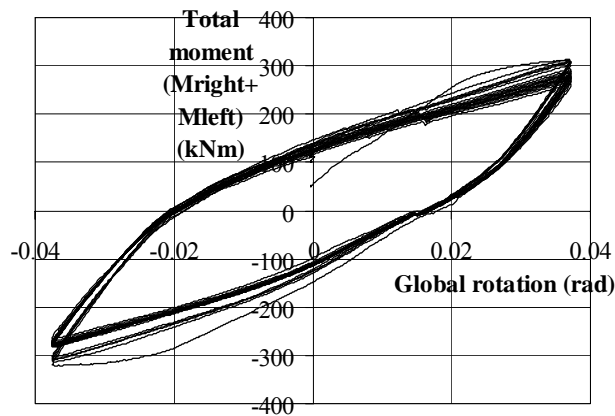
Figure 3.2.4. Force (Dverin) – Displacement at the top of column 1 during phase B



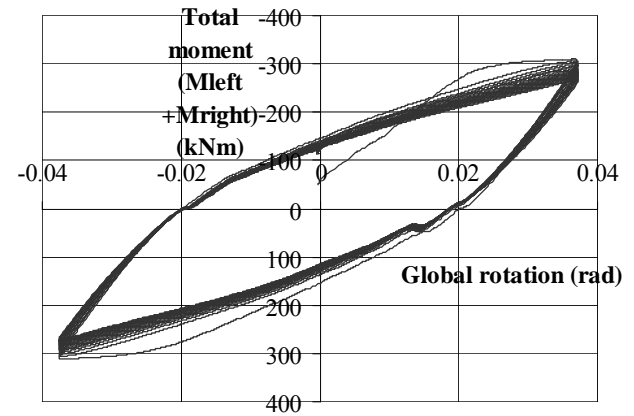
(a) Node 1 (exterior)



(b) Node 4 (exterior)



(c) Node 2 (interior)



(d) Node 3 (interior)

Figure 3.2.5. Moment rotation curves for the 4 nodes of the frame. Phase B, cycles 13 to 32.

b Low – cycle fatigue

The results have been analysed in terms of fatigue. The reference theory of our analysis is the Ballio-Castiglioni approach, which validity has been verified for steel elements and constructions.

This method consists basically in considering that the same Wohler (S-N) lines usually given in recommendations and EC-3 for high cycle fatigue can be also applied in the low cycle fatigue contest.

The low cycle fatigue is similar to the high one but involves the plastic domain of material behaviour.

This means that the nominal stress range satisfies $|E\Delta\varepsilon^+| > f_y$ and/ or $|E\Delta\varepsilon^-| > f_y$ and that the collapse occurs to a small number of cycles (generally $N < 10^4$).

The failure prediction function used by the S-N curve based approach has the form:

$$N S^m = K \quad (1)$$

Where N is the number of cycles to failure executed at the constant stress (strain) range

$$S = E(E\Delta\varepsilon^+ + E\Delta\varepsilon^-)$$

The non dimensional constant m and the dimensional parameter K depend on both the typology and mechanical properties of the considered steel element.

The fundamental hypothesis of the unified approach Ballio-Castiglioni for the design of steel structures is the validity of the following equation:

$$\frac{\Delta\varepsilon}{\varepsilon_y} = \frac{\Delta v}{v_y} = \frac{\Delta\phi}{\phi_y}$$

Where ε is the strain, v the displacement, ϕ the rotation (or the curvature), Δ represents the range and the index y identify the yielding of the material (ε_y) as well as the conventional yielding with reference to the global parameter (v_y and ϕ_y).

For a linear elastic material, the relationship between the strain ε and the load causing the displacement v can be written as :

$$E \cdot \varepsilon = \sigma(F)$$

At the yield, it becomes

$$E \cdot \varepsilon_y = \sigma(F_y)$$

So the parameter S (stress range) can be defined as:

$$S = \Delta\sigma^* = E \cdot \Delta\varepsilon = E \cdot \frac{\Delta v}{v_y} \cdot \varepsilon = \frac{\Delta v}{v_y} \cdot \sigma(F_y) = \frac{\Delta\phi}{\phi_y} \cdot \sigma(F_y)$$

the term $\Delta\sigma^*$ represents the effective stress range, associated to the real strain range

$\Delta\varepsilon = (\Delta\varepsilon^+ + \Delta\varepsilon^-)$ in an ideal member made of an indefinitely linear elastic material. It should be noted that under cycles in the elastic range $\Delta\sigma^*$ coincides with the actual stress range $\Delta\sigma$.

The equation (1) can be written:

$$N \left(\frac{\Delta v}{v_y} \cdot \sigma(F_y) \right)^m = K \quad (2)$$

$$N \left(\frac{\Delta\varepsilon}{\varepsilon} \cdot \sigma(F_y) \right)^m = K \quad (3)$$

For symmetrical steel sections and symmetrical imposed displacement, $\Delta\varepsilon^+ = \Delta\varepsilon^- = \Delta\varepsilon / 2$.

Composite sections with slabs are not symmetrical and this should bring some modifications to $\Delta\varepsilon$:

For a symmetrical steel section, the position of the neutral axis for both positive and negative bending is constant $x = h/2$.

The epsilon values of the bottom fibres due to a positive bending and a negative bending are equal in both cases :

$$\Delta \varepsilon_{\text{steel}} = \varepsilon_a^+ + \varepsilon_a^- = 2\varepsilon_a^+ = 2\varepsilon_a^-$$

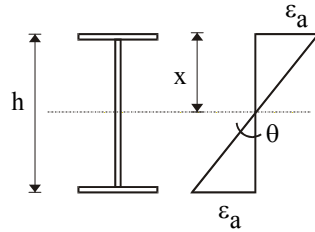


Figure 3.2.6. Distribution of strains in a steel section

For a composite section, which is unsymmetrical, the neutral axis (one under maximum positive bending moment and another one under negative bending moment) change their position from the position in the symmetrical steel section. Both for positive and negative maximum bending moment, it is approximately positioned in the upper flange of composite section, so that equal to $d = h$. For this reason the range of the strain ε of the bottom fibre of a composite section submitted to a rotation α equal to that in a steel profile described above is, with reference to symbols of figure 3.2.7:

$$\Delta \varepsilon_{a(\text{comp})} = \varepsilon_a^+ + \varepsilon_a^- = \varepsilon_{a(\text{steel})} (d^+ + d^-) / (h/2)$$

and as we have approximately $d^+ = d^- = h$

$$\Delta \varepsilon_{a(\text{comp})} = \varepsilon_{a(\text{steel})} \cdot \frac{2h}{h/2} = 4\varepsilon_{a(\text{steel})} = 2 \cdot \Delta \varepsilon_{(\text{steel})}$$

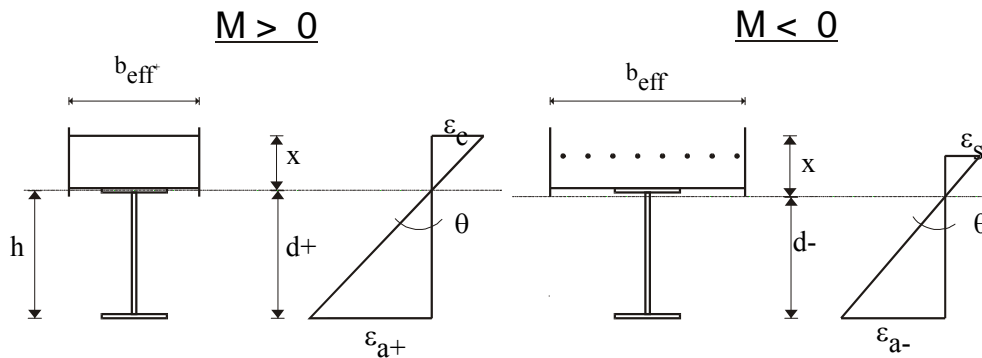


Figure 3.2.7 . Distribution of strains in a composite section

Therefore the equivalent stress range $\Delta \sigma^*$ in the bottom flange of a composite section, related to the range stress of a symmetric steel section submitted to an equal rotation θ is:

$$\Delta \sigma_{\text{comp}}^* = 2 \cdot \Delta \sigma_{\text{steel}}^*$$

So we can expect to have less cycles to failure for a composite section made of a steel section with slab than for the steel profile alone, if we submit both to equal displacement.

We have elaborated the Saclay results in terms of fatigue considering $\sigma(F_y) = f_y$, yield stress of the IPE. The reduction in fatigue life due to the composite character of the section can be established using the fatigue line of a steel element represented by equation (2)

K and v_y are the ones of the steel element, but $\Delta \varepsilon$ is multiplied by 2. Assuming $m=3$, we have

$$N_{\text{composite}} = N_{\text{steel}} / 2^m = N_{\text{steel}} / 8 .$$

Figure 3.2.8. shows the $\Delta \sigma^*$ versus the number of the cycles to failure. The points obtained using equation (2) are placed on the typical line for IPE200 section: the results of the composite section processed in that way correspond well to the fatigue curve of the IPE steel section used .

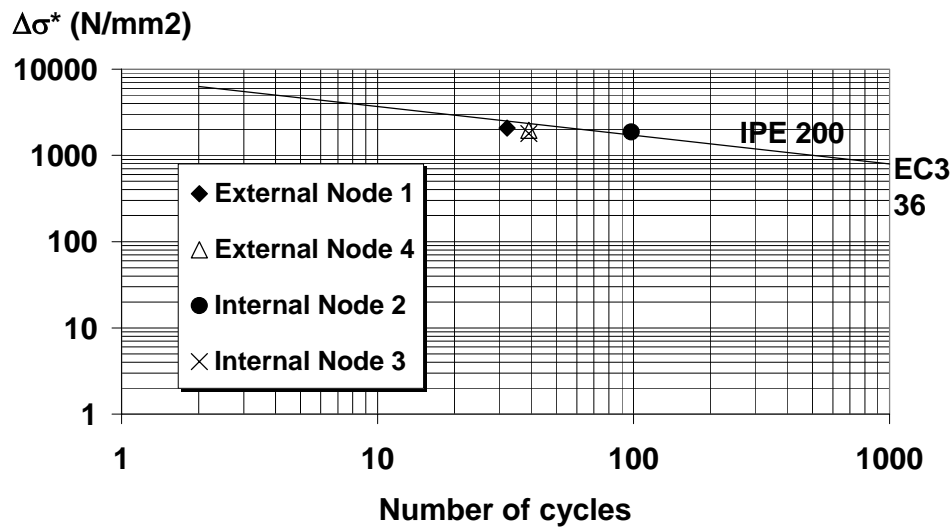


Figure 3.2.8. $\Delta\sigma^*$ versus the number of cycles to failure and the IPE200 fatigue line

c Effective widths for plastic moments

For both exterior nodes and internal ones, the plastic moments have been calculated according to the Icons Draft for composite structure as reported in EC8 and compared with the experimental ones defined according to the ECCS testing procedure. The values for the external nodes are reported in Table 3.2.1.

Table 3.2.1: Exterior nodes

	Effective width b_{eff} (m) used in computation	Calculated plastic moments (kNm)	Experimental plastic moments (kNm) Exterior node 1	Exterior node 4
Positive bending	EC8 0.15 L = 0.6 m	151.8	180	177
	Total width of slab (1 m)	165	180	177
Negative bending	EC8 0.2 L = 0.8 m	92.4	107	120
	Total width of slab (1 m)	100	107	120

For the internal node, the plastic moment is given by $M_{pl} = M^+ + M^-$ and the calculated and experimental values are reported in Table 3.2.2.

Table 3.2.2: Interior nodes

Effective width b_{eff} (m)	Calculated plastic moments (kNm)	Experimental plastic moments (kNm) Interior node 1	Interior node 4
EC8 0.15 L (M+) 0.2 L (M-)	244	297.5	288
Total width of slab (1 m)	265	297.5	288

As far as the internal node is concerned, we consider that the full width of the slab is activated. We observe for both external and internal nodes that

$$M_{pl} \text{ experimental} > M_{pl} \text{ calculated}$$

For the positive bending moment, there is a difference of 15% for Node 1 and 29.7 % for Node 4. And for positive bending moment, the difference is the 18.5 % for Node 1 and 16% for Node 4. This may be due to the properties of the material (strain hardening), to the confinement of the concrete near the column and to the way of defining the experimental plastic moment, according to the ECCS,

which for sure does not correspond to the calculated full plastic capacity of the section..

d Effective width for elastic inertia

We have tested in numerical models of the tested structure the Icons-EC8 proposal for the elastic effective width (supposing cracked concrete in tension) :

- a. $I^+ = I1$ with $b_{eff} = b_{eff\ plast} / 2 = 0.075 L$ on $0.6 L$
 $I^- = I2$ with $b_{eff} = b_{eff\ plast} / 2 = 0.1L$ on $0.4 L$
- b. $I_{equivalent} = 0.6 I^+ + 0.4 I^-$ on L

For the understanding of the problem, numerical analysis have been made using the Castem 2000 finite element program for one elastic analysis in the 4 different following cases:

1. A frame in which the studied beam is simplified as IPE200 beam with the following characteristics:
 $A_{steel} = 28.48 \text{ cm}^2$
 $I_{steel} = 1943 \text{ cm}^4$
2. A frame, in which the studied beam is simplified as a beam with Inertia equal to the Equivalent Inertia proposed by the ICONS Draft for the EC8:
 $I_{eq} = 0.6 * I^+ + 0.4 * I^- = 4558.224 \text{ cm}^4 = 2.34 I_{steel}$
3. A frame, in which the studied beam is simplified as a beam made by two different elements having two different value of Inertia:
 I^1 for one part of beam of length equal to $0.6 * L = 2.4 \text{ m}$ With $I^1 = I^+ = 6150 \text{ cm}^4$
 I^2 for the other part of the span with length equal to $0.4 * L = 1.6 \text{ m}$ With $I^2 = I^- = 2170 \text{ cm}^4$
4. An elastic analysis for a frame with an Inertia for the studied beam, in order to make a better choice of the elastic inertia representing the composite section studied:

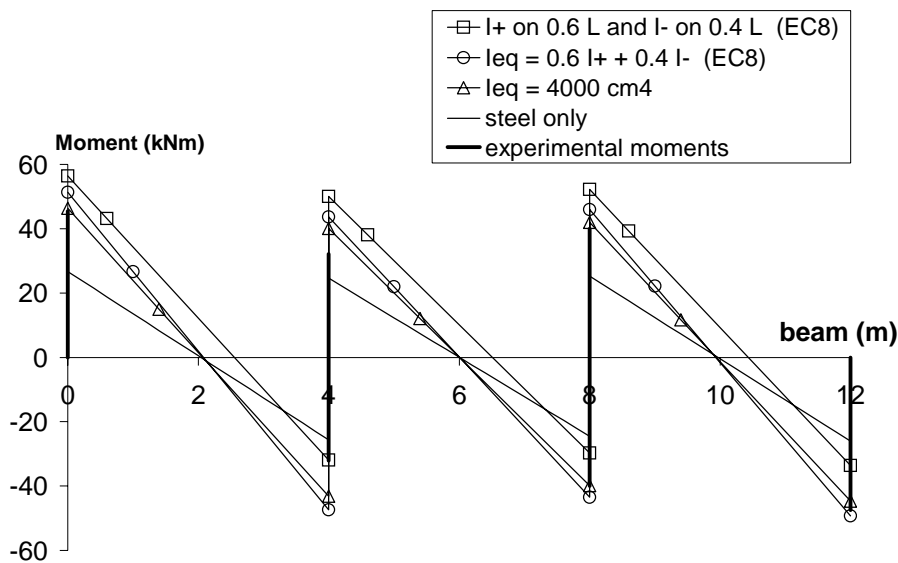


Figure 3.2.9. Distribution of the elastic experimental and computed moments in the composite beam

From the results of the analysis in the hypothesis 1,2 and 3, we can conclude concerning the value of the effective width to consider in the elastic range that :

- The composite character exists in the elastic range;
- b_{eff}^+ (EC8) overestimates the positive moments and b_{eff}^- (EC8) underestimates the negative moments
- $I_{equivalent}$, as proposed by EC8, gives the best estimate of the moment distribution along the composite beam

The analysis n°4 indicates the following:

- It is impossible to fit the experimental distribution of bending moments with only one or even two values of inertia;
- Negative inertia considering that the concrete is fully cracked are too unfavourable;
- EC8 links the positive effective width of the slab to the span of the beam. For the elastic behaviour, it seems better to link the effective width with the width of the column
- The best fitting are for $I_1=I_2=I=4000 \text{ mm}^2$ corresponding to $b_{\text{eff}}=b_{\text{column}}/2$ (see Figure 3.2.9.).

e. Effectiveness of the slab connection to transversal beam (new design)

Concerning the innovative design of slab re-bars connection to transverse beams, we can conclude:

- the anchorage of the re-bars to the studs of the transverse beam under negative bending is fully effective for plastic resistance
- the compression of the concrete on the transverse beam under positive bending is fully effective for plastic resistance

f. Non linear fibre model

A non-linear analysis of the structures has been made using fibres elements of the CASTEM 2000 code. The fibre modelling uses the simplified cinematic hypothesis of the Timoshenko beam theory. It assumes that plane sections remain plane after deformation, but not necessarily normal to the beam axial axis. This hypothesis has been considered in order to allow the development of the so called generalised fibre model, in the sense that very complex interaction between normal force, bending moment and shear can be taken into account.

For the material, an uniaxial material constitutive relationship for concrete and steel is considered.

Concrete behaviour is represented by the law given by the French code BAEL. No confinement is taken into account. Cyclic behaviour accounts for stiffness degradation and crack closing phenomena.

Steel behaviour is represented by a modified Menegotto-Pinto model with a three stage monotonic curve (linear, plateau and hardening). Baushinger effects are taken into account and buckling effects can be simulated.

The Moment-rotation curves for node 1 in the experimental case and the numerical one and the first experimental cycles elastic are presented in Figure 3.2.10.

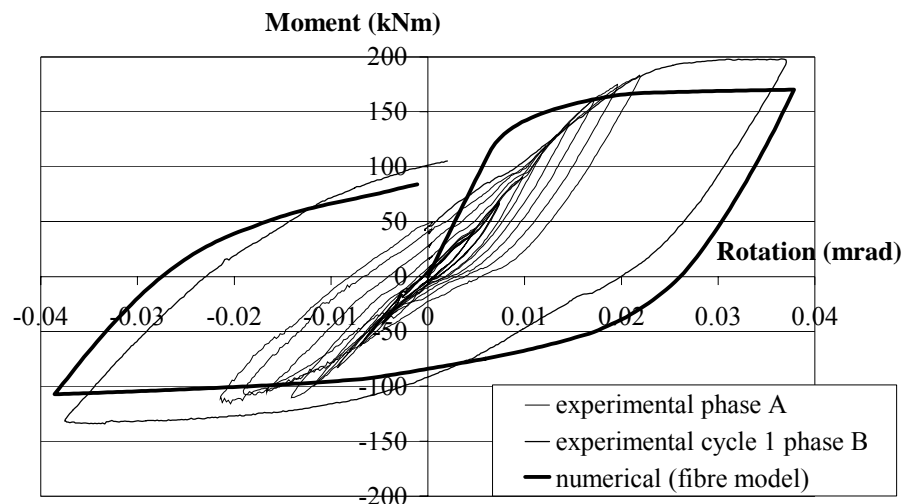


Figure 3.2.10. Comparison of the experimental and numerical moment rotation curves for node 1

The numerical negative moment under estimates the experimental one of about 20% and of about 14% the positive one. This under estimation of the resistance of the section can be explained for negative bending, by the fact that the tension resistance of the concrete is neglected. For the positive bending, the model used should be improved.

3.2.8. Conclusions

From the experimental study on a 3 bays plane composite frame under cyclic loading, we can conclude the following:

- The bottom fibres of composite section follow the same fatigue curve as the steel section used (Figure 3.2.8.);
- The test has demonstrated the effectiveness of the anchorage of the re-bars to the studs of the external transverse beam, under negative bending, and of bearing of compression of the concrete on the transverse beam under positive bending;
- As far as the inertia is concerned, the provisory b_{eff}^+ proposed in the ICONS-EC8 1998 draft version overestimates the positive moment of inertia;
- On the contrary, the b_{eff}^- proposed in the same document underestimates the negative moments of inertia;
- These two results have to be considered to improve the values of b_{eff} finally proposed; these ones should give the best possible estimate of the response of the structure, because in seismic design, lower bound values can be on the safe side for some aspects of the response and on the unsafe side for other aspects : typically safe side for resistance and unsafe side for displacements, meaning seismic forces and P-D effects.
- The $I_{\text{equivalent}}$, proposed by the ICONS-EC8 1998 document gives the best estimate of the moment distribution along the composite beam;

3.3 ISPRA TESTS: Slab design in connection zone of composite frames

Bi-directional cyclic response study of 3-D composite frame

A. Plumier, C. Doneux

Department of Civil Engineering, University of Liege, Belgium

J.G. Bouwkamp, H. Parung

Institute of Steel Construction, Darmstadt University of Technology, Germany

3.3.1. Introduction

A full scale 3 D test of a 3 storey composite steel concrete frame has been run at the ELSA facility of the European Joint Research Centre at Ispra, Italy – Figure 3.3.1. – Picture 3.3.1.

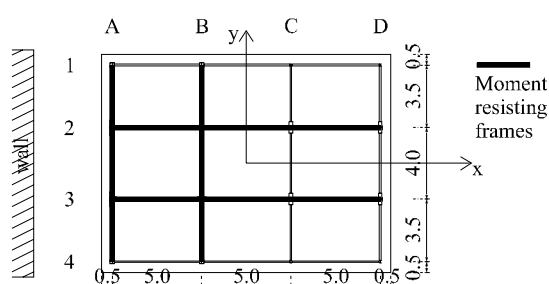


Figure 3.3.1. Plan of the 3-D Composite Frame

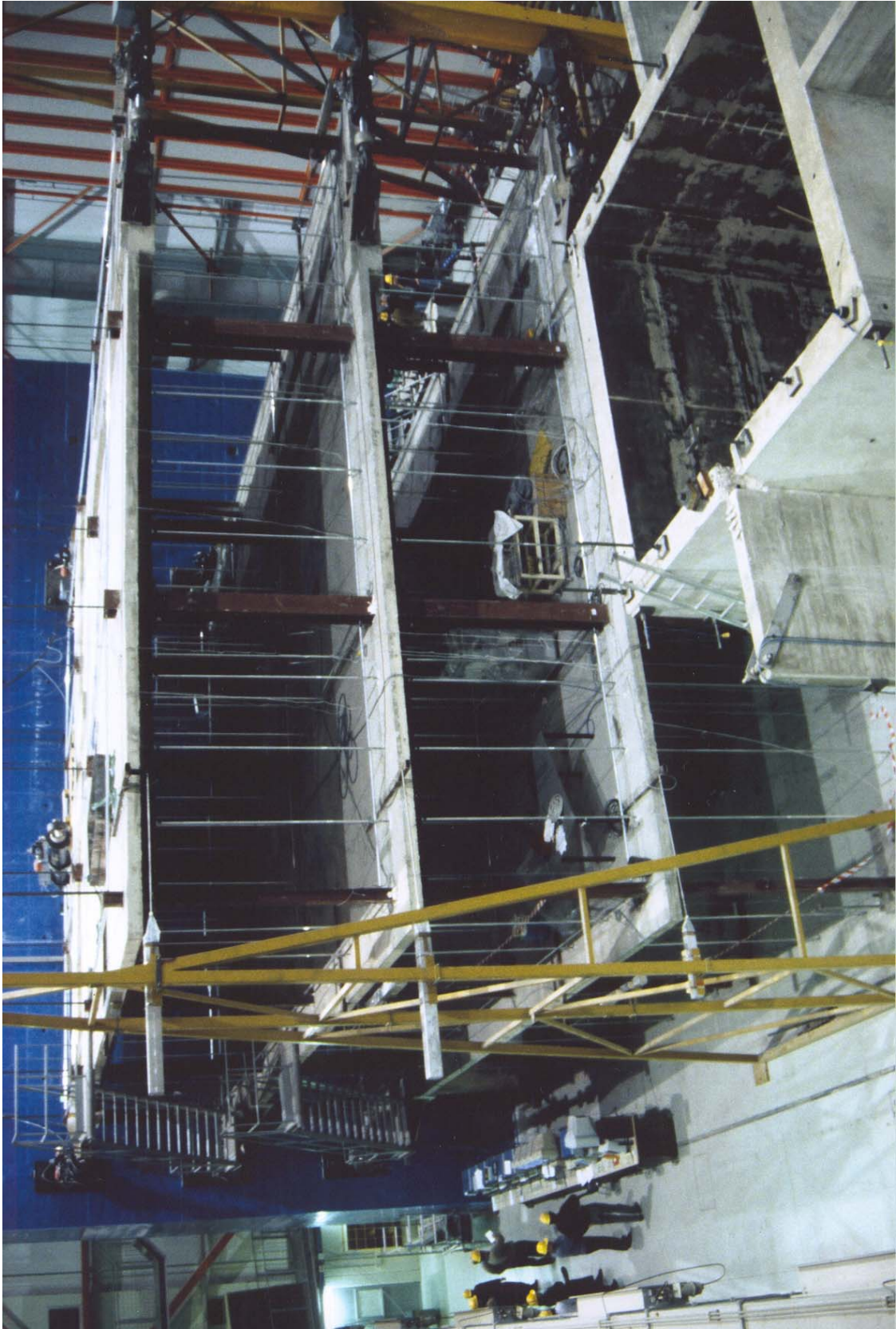
The structure was a 3-story steel composite frame with a 3-bay by 3-bay column layout and overall dimensions of 16 x 12 m in plan and 9.5 m in height. The moment frame connections were designed with end-plated beams bolted to the column flanges or, in case of intersecting moment frames, to end-plated beam stubs extending from the columns. Earlier studies by ARBED, 1990, have been focused on the cyclic moment resistance of connections of composite steel/concrete beams and columns. The present study covers in fact the behaviour of a 3-D steel frame with composite concrete slabs.

The test program focuses particularly on evaluating the design rules affecting the participation of the composite concrete slab in the beam-column moment transfer; both rigid and semi-rigid steel joints with varying slab designs were incorporated. Taking full advantage of the unique two-dimensional test capacities at the ELSA facility, the layout of the moment resisting frames along the two major axes allowed to study the bi-axial response of both interior and exterior rigid and semi-rigid beam-column connections. The steel moment-resistant connections were designed using typical European, high-strength bolted, beam end-plates. This design eliminates on site welding which has been found a source of failure during recent earthquakes in the United States and Japan.

With the aim of developing code design specifications for inclusion in EC8, different slab designs in the column regions were incorporated in the test frame to possibly enhance the cyclic moment transfer into the columns and to determine the moment resistance of the beam/slab connections. Both the influence of additional slab reinforcement around the columns and the effect of a concentration of shear studs on the transverse beams near the columns were investigated. Also, because of the different beam sizes at the various floors, the effect of the slab-thickness-to-beam-depth, could be studied. On the other hand, to assess the effect of limiting the slab participation in the beam-to-column moment transfer, certain joints were designed with styrofoam strips placed around the column section; in those cases additional slab reinforcement and shear studs in the beam-column region were deleted.

The structure has been designed such that yielding should take place in the bottom flange of the steel sections with minor involvement of yielding or cracking of the slab. To achieve this, a design method of the reinforcements of the slab and of the shear connectors needed locally around the column to transmit positive bending moments, was developed. It is explained at paragraph 2. Based on this method a standard or reference layout of reinforcements and studs in the slab has been defined and

installed in reference zones of floors 1, 2 and 3 - corresponding to lines 1 and 2 of Figure 3.3.1. In lines 3 and 4, the layout has been modified, in three different ways at Floors 1, 2 and 3, so that on the whole the tested structure is an assembly of various parts with various density of parameters.



Picture 3.3.1. General view of the structure

3.3..2. *Layout of the tested structure*

General

Giving the test capacity and space limitations of the ELSA facility, a 3-story high, 3-D composite frame with a 3 bay by 3 bay column layout and overall dimensions of 16.0 x 12.0 m in plan, and 9.5 m in height was designed. Moment resistant frames were laid out along column lines 2 and 3, and A and B (Fig. 3.3.1). The floor design was a 15 cm (total thickness) slab on corrugated metal decking. The moment resistant frames have been designed for code-specified earthquake forces. Frames positioned along other column lines were designed for gravity loads only (using standard shear tabs). Effectively, these „simple“ (non-moment) connections act, together with the concrete slab, as semi-rigid connections.

Considering the fact that the test structure represents one quarter of a 6 bay x 6 bay structure, the two moment resistant frames in each direction of the test structure represent a structure with a symmetrical layout of four frames in each direction. This symmetrical layout allows the design assumption that, in each direction, the total horizontal design load can be distributed equally over four pertinent frames. Reflecting the total structural layout, it is justified that, for each direction, the design of the two moment resistant frames of the test structure can be carried out assuming that the total horizontal load in each direction is divided equally between the two pertinent frames. The frame design followed standard design practices, using standard rolled sections of Fe360 for the steel frame, Fe510 for the beam end-plates, HV10.9 bolts, C30/37 concrete for the slab and BSt500S for the reinforcing steel. In the design, typical dead and live loads, as used in building design, combined with EC8 defined earthquake design loads (Zone 4, S=1 and q=6) have been considered using code-specified load superposition rules. For fabrication it was specified that the yield stress for the beams should not exceed 300 MPa.

Finally, the real structure is as described below. The steel sections are IPE 300 at floor 1, IPE 270 at floor 2 and IPE 240 at floor 3. The real yield stress f_y of the sections are respectively 270 Mpa, 280 Mpa and 300 Mpa. The concrete slab is realised using a metal decking with ribs 55 mm high, so that the slab being 150 mm thick offers as effective thickness 95 mm. The basic reinforcement of the slab is a welded mesh $\phi 10@ 150 \times 150$. The beams are connected to the slab by means of welded studs $\phi 16$ mm and 100 mm high. All connections of the steel sections in lines 2, 3 (direction x) are rigid ones. The steel sections of the beams of lines A and B transverse to lines 2 and 3 are rigidly connected to these ones. The steel section of the beams in lines C and D, transverse to lines 2 and 3, are only web connected by 2 bolts to the "Christmas tree" of columns.

Model Design

Following EC8 provisions, the horizontal earthquake induced mass-inertia forces have been represented by static equivalent forces at each floor level. With the beam-end moments due to earthquake forces far exceeding those due to gravity loads, the bending moment distribution along the beam has been approximated as linear (beam moment inflection near the beam mid span). Assuming composite behaviour under a positive moment only, each beam in the basic frame model was divided in two different half-span sections, namely, a composite and a steel section. The composite section was based on an EC4 defined total effective slab width of $2b_{e} = L/4$, with L = centre distance between columns, and a steel/concrete moduli ratio $n = E_a / E_c = 7$.

Frame Design

For the design of the moment resistant frames, the strong-column weak-beam design concept was adopted. Hence, the column moment capacity was based on at least 1.2 times the plastic moment capacity of the adjacent beam(s). Basically, in order to avoid column failure under actual earthquake exposure, it is essential that, in design, the positive-moment capacity of the composite beams is not undervalued; in that case an insufficient column resistance might, under seismic exposure lead to possible premature column failure. To prevent such potential failure, the plastic moment capacity of the composite beam need to be calculated assuming a realistic, sufficiently large, effective width of slab at the column junction. In fact, in the design of the test structure the same effective width of $L/4$, which was used for the composite half-span, was used also to calculate the positive-moment

composite-beam capacity at the column. In order to clarify this design assumption, different layouts of additional slab reinforcement near the column and the introduction of shear-stud concentrations on transverse beams in that area have been introduced in this study. In designing the frame members, the effect of both shear and axial forces have been taken into account in calculating the plastic moment capacities of both beams and columns. The HS bolted beam end-plates (Fe510) were designed elastically for 1.2 times the composite beam plastic moment capacity and an „allowable“ stress of $f_y/1.5$.

Following the above design procedure and assuming a steel yield stress of 240 MPa and a f_{ck} for the concrete of 30 MPa, the moment resistant frames 2/3 and A/B were designed as shown in Figure 3.3.2. Disregarding bi-axial moment superposition, the columns at the intersection of column lines 2/3 and A/B were designed as HEM 260, with the web oriented along column lines 2/3. All other columns were designed for strong-axis bending only.

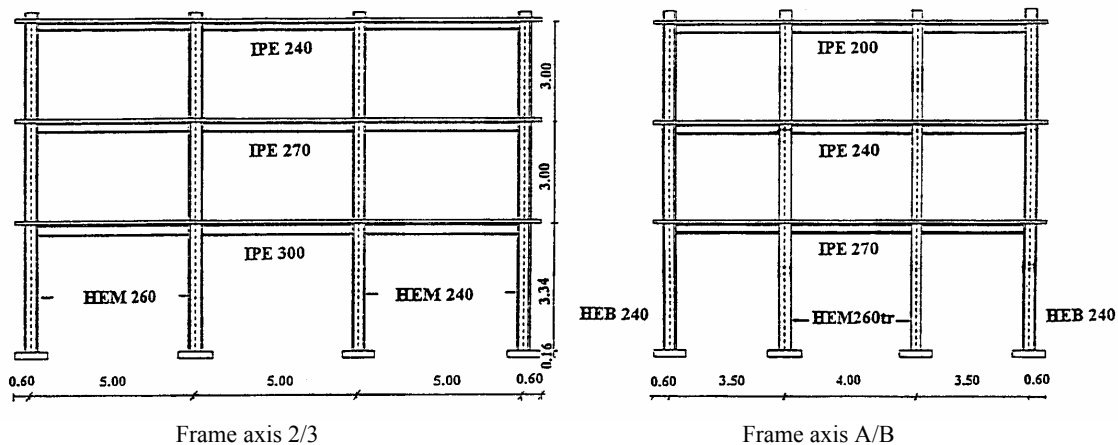


Figure 3.3.2. Moment resistant frames

In the design of the frames (columns), drift limitations governed. For the frames 2/3, with a first period of the frame calculated as 0.606 sec. and a behaviour factor $q = 6$, the total base shear was calculated as $0.105 \times 1260 \text{ kN} = 132.3 \text{ kN}$ per frame. Using equivalent static loads of 66, 44 and 22 kN at the 3rd, 2nd and 1st floor levels, respectively, the elastic inter-story drifts of 5.13 mm, 6.48 mm, and 5.97 mm for the first, second, and third floors, respectively, were smaller than the maximum allowable drift of $0.0025 \times$ inter-story height, or 7.5 mm. Drift limitations also governed the design of frames A/B. In this case, with a first period calculated as 0.758 sec., the base shear per frame was $0.09 \times 1260 = 113.4 \text{ kN}$. The equivalent static loads of 57, 38 and 19 kN at the third, second and first floor levels, respectively, resulted in elastic inter-story drifts for the first, second and third floors of 5.36 mm, 6.86 mm, and 7.16 mm, respectively. These values were smaller than the code-specified allowable maximum inter-story drift of 7.5 mm.

The design of the remaining frames, 1 and 4 and C and D, were non-moment resistant frames carrying gravity loads only. Although the shear-tab connections between beams and columns were designed for shear only, in reality these connections are semi-rigid as they have a certain moment resistance due to the horizontal force resistance of the shear-tab and composite concrete slab. In the design of the beams and columns this additional effect has not been considered.

Although the beam spans in the two types of non-moment resistant frames are different, different beam sections could have been selected. However, for simplicity, all beams have been designed as IPE 200. Also, considering the test structure as one-quarter of the total structure, the exterior column rows 1 and 4 are in fact an exterior and interior column row of the total structure. However, for structural simplicity and test purposes (symmetry and joint comparative behaviour along column lines 1 and 4), all columns have been designed as HEB 140 sections.

Beam-column connection design

Beam end-plated bolted connections were used for the moment resistant frames. While the beams were of Fe 360 grade steel and the end plates of Fe 510 grade steel, all bolts were specified as high

strength HV M20-10.9 bolts. The bolted connections for these frames were designed to resist the full plastic moment capacity of the composite beams (including an overstrength factor 1.2). In addition, a safety factor of 1.5 was used in the design of the end plates and bolts in order to prevent any possible yielding in the connection and to force the plastic zone into the beam section. Following this procedure, the design force for the bolts at the bottom flange (under a plastic, positive moment of a composite-section) would be larger than at the top flange (under a plastic, negative moment of the steel-section only). This could lead to different bolt designs at the top and bottom. However, for practical purposes, the connections have been designed with the same size and number of bolts for both the top and bottom flanges. The size and the number of bolts required for each joint is shown typically in Figure 3.3.3. Backup plates (washers) were used to strengthen the column flanges. In order to prevent column web yielding, web doubler plates were used at each floor level of the interior columns of frames 2 and 3.

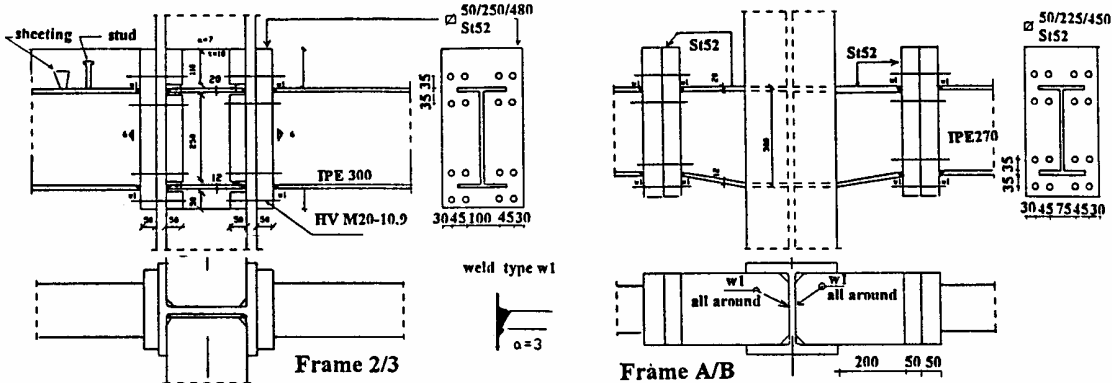


Figure 3.3.3. Beam - column moment connections

The connections between beam flanges and end plates were designed with full penetration welds and a 3 mm backup weld. The web connections were double fillet welds, each equal to at least 0.65 the beam-web thickness. The tapered beam stubs („Christmas trees“) on either side of the interior columns of frames A and B were necessary to assure the bi-axial moment transfer and to accommodate for the difference in beam height (3 cm) at the moment-frame intersections. The stubs had to withstand the typical beam plastic moments in frames A and B and provide the continuity for transmitting moments acting along axes 2 and 3. As the upper flanges of the stubs had to resist also transverse horizontal bending caused by transverse shear-stud forces (due to the slab action near the column under bending along frame axes 2 and 3), the flanges were designed with Fe510 steel and an increased thickness of typically 20 mm.

All connections of frames 1, 4, C and D were semi-rigid, with the beams connected to the columns and beam stubs by means of shear tabs and M20-10.9 bolts. Although the shear tabs were designed to transmit gravity loads only, a limited ductile behaviour can be developed under rotation if one of the following conditions would be fulfilled, namely: a) the bolt bearing resistance in the beam web or tab is smaller than the bolt shear resistance, or b) the net-section resistance of the tab or the tear-out force of the beam web under horizontal tension (due to moment force-couple) is larger than the resistance of the tab gross section. In fact, if the bolt resistance in shear is larger than the bearing resistance of the shear tab, ovalisation of the holes will take place before shear failure of the bolts. Also, if the resistance is larger than the gross-section resistance, the strap will yield before failure in tension of the net section. In both cases a certain ductility will occur. In this frame design, bearing in the beam web will govern the response and ovalisation.

Column base design

Considering the design of the columns of the moment-resistant frames at the base, it was decided to introduce 500 mm long „dogbones“ starting 250 mm above the base plate. The „dogbones“, with tapered ends of 100 mm and a centre section of 300 mm, were introduced to prevent premature failure (fracture) of the column section or the full-penetration K-welds immediately above the base plate, but also, to introduce a designated area where the column would yield. The flange reductions for the HEM

260 and 240 columns at the centre section were 2x40 mm and 2x35 mm, respectively. For the HEB 240 columns the reduction was 2x35 mm. This basic solution had been tested successfully by Rea, 1969. The 1200 mm square base plates with a thickness of 160 mm were anchored to the 1000 mm anchor-bolt grid of the ELSA research facility.

Specific features of the various zones of the tested structure

Slab reinforcement and shear connectors

In line 2 of the structure (see Figure 3.3.4.), a reference or standard seismic reinforcement, computed as defined in section 3.5. is installed. It is similar at Floor 1, 2 and 3 and consist of re-bars $\phi 12$ mm with layout RE2 for exterior columns and 2 different layout RE1A and RE1B at interior columns.

In line 2 of the structure and on transverse beams, welded studs $\phi 16$ mm and 100 mm high are installed ; their number and positions comply with the normal requirements under design vertical loads and with the design relationship for transverse beam contribution expressed in 2 above ; for this reasons studs are also present on the "Christmas tree" installed on the columns.

In line 3 of the structure, modifications are brought to the reference layout.

At floor 1, the number of specific "seismic" re-bars is increased from 2 to 3.

At floor 2, the concrete slab is disconnected from the beams and "Christmas trees" in a 1 m diameter zone around the columns. Disconnection means no studs and no contact between concrete and column, by means of styrofoam installed around the columns before pouring the concrete. This layout aims at testing a construction procedure used to realise the correspondence between the structure and design hypothesis which would consider only steel sections as effective.

At floor 3, the concrete slab is partially disconnected from the beams (no studs in a 1 m diameter, but contact between concrete and column).

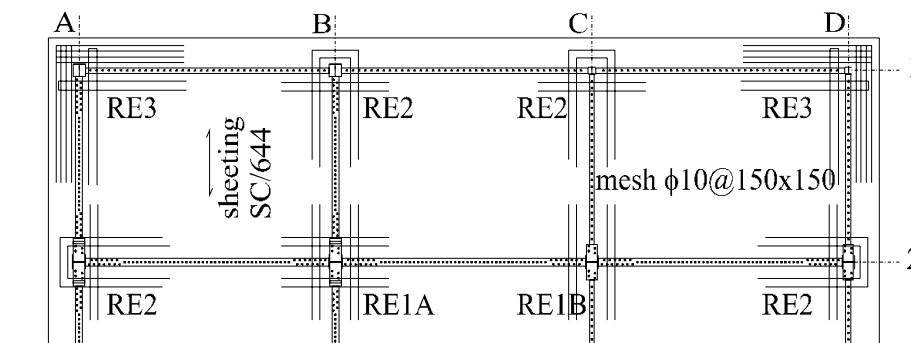


Figure 3.3.4. Layout of studs and re-bars on lines 1 and 2 of floor 1, 2 and 3

3.3.3. Test program

Test setup and actuator layout

Considering the capacities of the ELSA reaction wall and the layout of the test structure, it was decided to place the structure with column line A parallel and as close as possible to the face of the reaction wall. This permits the maximum transverse (Y-direction) test loads to be resisted directly by the reaction wall; for Y-directional loading an additional lighter reaction frame was necessary at the far end of the test structure near column line D. With the structure placed closely to the reaction wall, the actuators in the X-direction had to be placed on the outside of the structure, near column lines 1 and 4. In general, actuators are placed at the above positions at each floor level.

The connections between the actuators and the slab were designed such, that the actuators could transmit the maximum expected loads of the two 3rd floor actuators under X-direction loading and the actuator near the wall under Y-direction loading. Because pre-test analyses indicated the need of a capacity of slightly more than 500 kN , actuators with a capacity of +/- 1000 kN and a stroke +/- 50 cm were selected. All other actuators had capacities of +/- 500 kN and a stroke of +/- 50 cm.

For the load transfer into the slab, special mounting plates were used. Also, on each floor, the

thickness of the cantilever slab in the mounting area was increased to the level of the bottom flange of the local edge beam. Because of concern about the horizontal shear transfer capacity of the slab in transmitting the actuator forces from the outside of the slab to the inner moment-resistant frames, it was decided to strengthen the slab in these regions by introducing ribs on the slab which would cross the edge beam and extend over to the next frame.

Unfortunately, because of a last minute change in the selection of the mounting plates, the slab thickness was changed from 12 to 15 cm. This caused an increase in both the overall stiffness of the test structure and, more critically, the compressive resistance of the slab in the beam-column moment-connection region. This is contrary to the initial design considerations and leads to higher positive moments capacities. Fortunately, the basic overstrength design of the columns was such that the increased beam moments would not cause yielding of the columns.

Instrumentation

The instrumentation for the test structure consisted of typical LVDT displacement transducers –four on each floor - to measure the overall horizontal displacements of the test structure (floors), 12 actuator load cells, strain gages and displacement potentiometers.

Each column was instrumented with strain gages to register the M_x and M_y moments at two sections and the axial force at one section (mid-height of column). This layout provides data on the column shear forces and permits evaluating the sum of the column moments of individual columns above and below each floor; or in fact the sum of the positive and negative beam moments. Disregarding elastic deformations of the columns, the beam-moment sum can be plotted against the total column drift, thus resulting in a total-moment - rotation data output. As it was planned to develop the moment-rotation response of individual joints, the strain gage data was supplemented with data from vertical-displacement potentiometers, located at the $\frac{1}{4}$ - , mid-span and $\frac{3}{4}$ -span points along each beam and measurements of beam elongations (due to cyclic composite action). By using this total data set (552 channels), the cyclic moment-rotation response of individual beam-column connections can be determined and the effect of the different design options on the cyclic beam-column behaviour evaluated. In this data reduction process a specially developed computer program, called SIMP (Ungureanu, 1993), will be used.

Test Procedure

The testing was carried out by a set of four double-acting load cylinders at each floor (total 12 actuators). In order to evaluate the effect of the different structural parameters used in the design of the rigid and semi-rigid connections, it was decided to subject the test frame to simple one-directional cyclic loading along each of the major axes. Basically, the displacement inducing 3rd floor actuators were displacement-controlled, while the corresponding 1st and 2nd floor actuators were force-controlled with forces of 1/3 and 2/3 of the forces recorded by the pertinent test control actuators at the 3rd floor.

In addition, to the one-directional loading in the X- and Y- directions (Test Phases 1 and 2), the test structure was subjected also to a number of pre-induced Y-directional displacements followed by a series of cyclic, displacement controlled, X-direction loads (Test Phase 3). By repeating the X-direction

cyclic loads for different preset displacements in the Y-direction, the basic effect of bi-directional loading on the cyclic response in the X-direction can be evaluated.

To further assess the bi-directional response of the 3D test structure, a series of pseudo-dynamic tests (PDT) has been carried out (Test Phase 4). This phase is not only important from the point of view of the structural response, where this test phase constitutes a novum, but also from the point of view of 3-dimensional PDT test control using 12 actuators.

Finally, to evaluate the ultimate behaviour of a composite steel/concrete frame, the last phase covers the cyclic, displacement controlled, testing of the structure in the X-direction (Test Phase 5).

Considering these program objectives, the following specific test program has been executed:

- Phase 1. Quasi-static cyclic loading in X-direction;
max. top-floor displacement of +/- 180 mm (2%) ,
- Phase 2. Quasi-static cyclic loading in Y-direction as in phase 1,
- Phase 3. Quasi-static cyclic loading with following bi-directional loading:
induce and hold Y-directional displacement of 90 mm and follow with X-directional

- Phase 4. loading of 2 cycles of +/- 90 mm. Repeat procedure for Y-X displacements of 180mm. PDT Tests
- Phase 5. Quasi-static cyclic loading in X-direction as in phase 1, maximum top floor displacement 420 mm, or about 5 % of total height.

3.3.4. Test results – global behaviour of the frame

In this section, the general results, covering the basic observed behaviour of the test frame under the different displacement-controlled loading histories, other than the PDT test phase, are presented and discussed.

Test phase 1

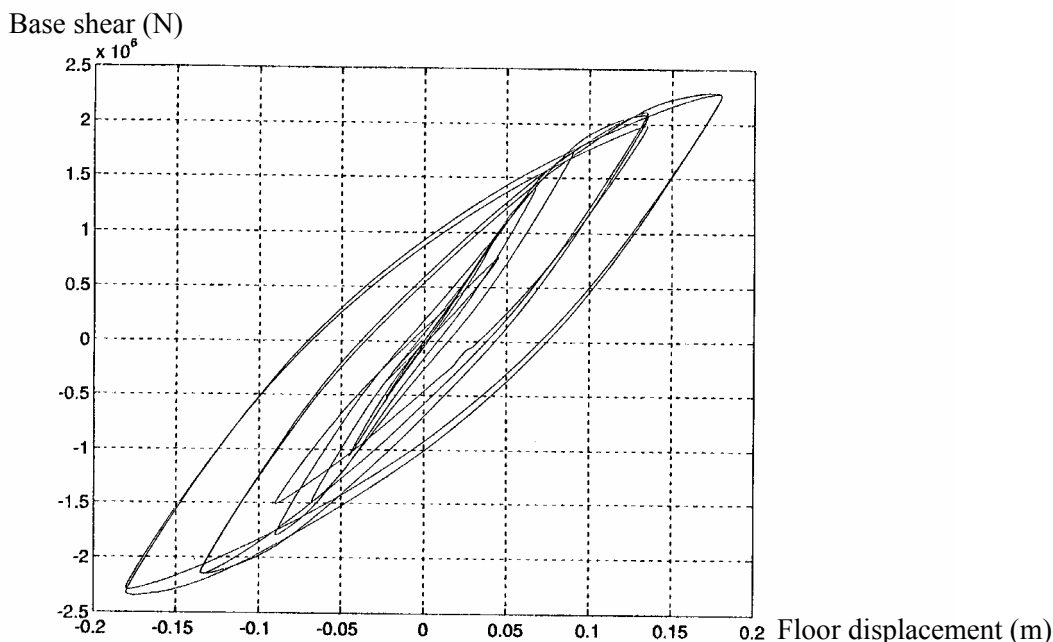


Figure 3.3.5. Base shear vs. top X-displacement

In Test Phase 1, the quasi-static load sequence was controlled by a X-directional displacement history of single cycles of +/- 22.5, 45, 67.5 and 90 mm followed by double cycles of +/- 135 and 180 mm. After having reached a displacement of - 180 mm in the last full test cycle, the frame was subjected to a diminishing displacement sequence of +135, -90, +45, -22.5 and 0 mm. Following ELSA test practice, the X-direction corresponds with the East-West direction (West being the side of the reaction wall) and the Y-direction being the North-South direction.

With a floor load distribution of 1, 2/3 and 1/3 for the three floors, the overall cyclic load-displacement history is presented in Figure 3.3.5. and shows the total test load (or base shear) versus the 3rd floor displacement. It is of interest to compare the maximum introduced load (base shear) of 2280 kN with the code design base shear of 132 kN (each) for frames 2 and 3. Whereas the Darmstadt tests showed a resistance for the semi-rigid connections of about 1/8 of the moment rigid connections, one could assume a base shear resistance for frames 1 and 4 of about 16 kN (each). This results effectively in a total design base shear of about 296 kN as compared to the maximum introduced value of 2280 kN; a ratio of almost 8.

Considering Figure 3.3.5., the hysteretic response shows an excellent energy absorbing behaviour of the test structure with only a small drop in resistance at the 2nd cycle under maximum displacement (at -0.18 m). This was caused by a weld fracture at the bottom flange of the east beam at column 2C at the 2nd floor. Failure was due to insufficient penetration welding. Not knowing the weld conditions of the

other joints, it was decided not to repair this connection as it would delay testing.

Another significant observation to be made from Figure 3.3.5. is the drop in stiffness of the test structure under the unloading cycles of +0.135, -0.090, +0.045, -0.0225 m and zero. During the last four half cycles, from - 0.090 to 0 m, the frame stiffness, here defined as the base shear or sum of the floor loads in kN per 1 cm of 3rd floor displacement, remained constant and had been reduced to 168 kN/cm, or 72% of the initial elastic stiffness of 232 kN/cm. The effective stiffness (at 0.18 m) had been reduced to 127 kN/cm (or about 55% of the initial stiffness).

Test phase 2

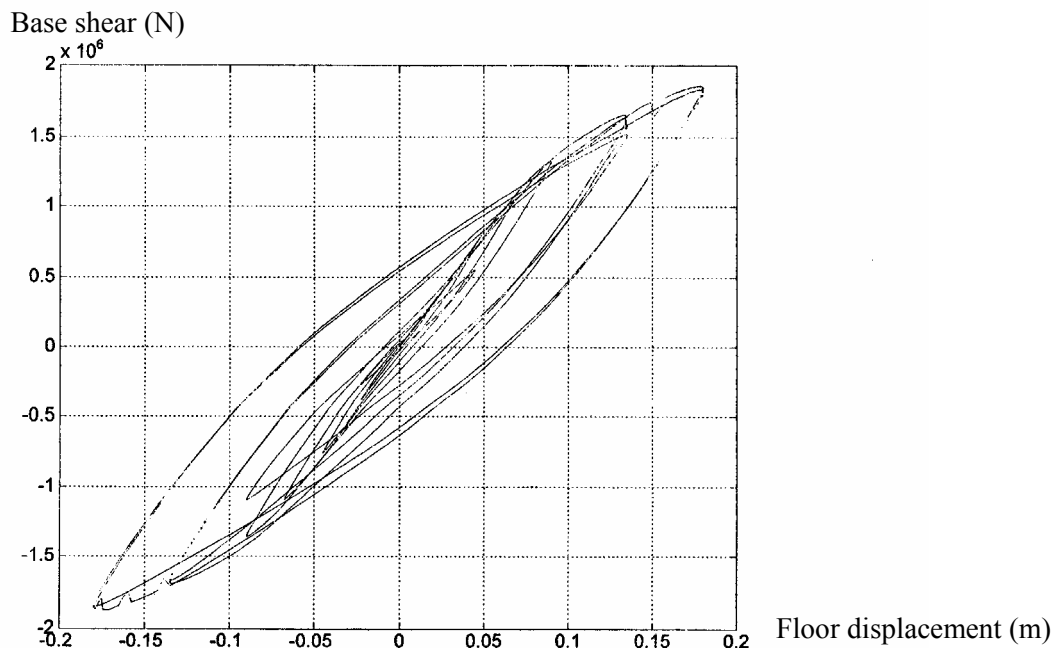


Figure 3.3.6. Base shear vs. top Y-displacement

The quasi-static load sequence of Test-phase 2 was controlled by the Y-directional, or North-South, actuators with 3rd floor single displacement-cycles of +/- 22.5, 45, 67.5 and 90 mm and double displacement-cycles of +/- 135 and 180 mm. After the last cycle, the test structure was subjected to reduced displacements of +135, -90, +45, -22.5 and 0 mm. During this test-phase, the X-directional actuators, located along the north- and south-sides of the structure, respectively, were locked at a „no-displacement“. The resulting actuator forces provided the torsional resistance necessary to counteract the torsional unbalance resulting from the eccentric frame layout in the Y-direction.

On all four sides of the structure, the 2nd and 1st floor actuators were force-controlled at ratios of 2/3 and 1/3 of the pertinent 3rd floor actuator. The cyclic load-displacement response of the structure during test-phase 2, as presented by the total test load in the Y-direction, or base shear, versus the 3rd floor displacement, is shown in Figure 3.3.6.

Considering the 3rd floor actuator forces for the second displacement cycle of +/- 180 mm, at -180 mm, the west- and east-actuators recorded values of 744 kN and 174 kN, respectively. The sum of these values, or 918 kN, compares very well with the value of 890 kN which had been derived from the non linear pre-test analysis and the resistance of the semi-rigid frames, which on the basis of the Darmstadt tests were estimated to have a resistance of 1/6 of the moment-rigid frames.

The experimental results indicate a maximum base shear of 1836 kN at a displacement of 180 mm. The code specified base shear used in the design of frames A and B was 113 kN. With the resistance of the semi-rigid frames (C and D) having been estimated each as 1/6 of the moment frame resistance, the total design base shear of the structure can be set at about 264 kN. Hence, the resistant capacity of 1830 kN at 2% drift is almost 7 times the effective design base shear.

The hysteretic behaviour shows an excellent energy absorption. The loading in later phases of the test was affected by a some force relaxation caused by the interactive behaviour of the EW and NS actuators. The unloading displacement cycles of +0.135, -0.090, +0.045, -0.0225 m and zero, show, similarly as in test-phase 1, a clear reduction in the total frame stiffness. In fact, the initial stiffness of 160 kN/cm reduced to an effective stiffness at 18 cm of 103 kN/cm, or about 64% of the initial stiffness. In the last four half cycles, from - 0.090 to 0 m, the frame stiffness was constant and had been reduced to 122 kN/cm, or 76% of the original stiffness.

Test phase 3

In this test phase the cyclic behaviour of the test structure under bi-directional loading has been studied. Specifically, the behaviour under quasi-static cyclic displacement-controlled loading in the X-direction has been investigated after the structure had been deformed first to certain predefined displacements in the Y-direction and was being held in that position. Under this test condition, it is possible to compare the response in the X-direction for different Y-deformations and assess the influence of bi-directional loading on the resistance of the test structure under X-directional cyclic loading. Considering the fact that the structure had been tested before separately in both the X- and Y-directions up to maximum 3rd floor displacements of 0.18 m, it was decided to simultaneously subject the test structure to the same maximum displacements; resulting in a deformation of almost 0.255 m (drift of 2.8%). This was considered acceptable because the columns had been designed to remain well in the elastic range. It was decided to impose only two pre-deformations in the Y-direction, namely, 0.09 and 0.18 m, respectively. This is illustrated by the data point ranges of 500- 900 and 2000-2400 of the total displacement history shown in Figure 3.3.7. With the objective to limit the number of X-directional cycles in each range, only two full cycles with the same maximum displacements as imposed in the Y-direction were introduced. In the remainder of Test Phase 3, the Y displacement was set at zero. The effect of deterioration due to bi-directional deformations, has been evaluated by subjecting the undeformed frame (y = 0), before and after each X-directional test sequence of the predeformed frame, to a typical two-cycle X-directional test sequence; thus resulting in a total of 6 test sequences.

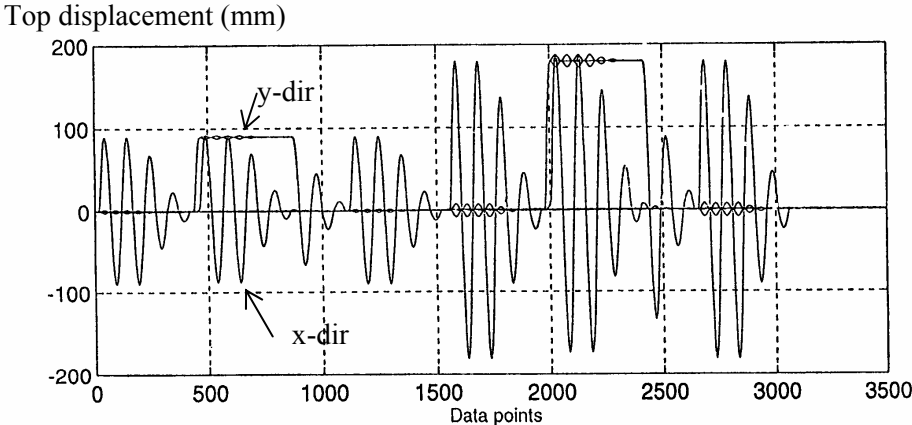


Figure 3.3.7. X-Y Displacement history for Test Phase 3.

During this 3rd Test phase, the Y-directional actuators at the 3rd floor, located at the west- and east-sides of the structure as well as the X-directional actuator at the north-side, were all displacement controlled; the other X-directional actuator (on the south-side) was forced controlled and set equal to the north-side actuator force. The actuators on the 2nd and 1st floors were again all force controlled with force ratios of 2/3 and 1/3 of the pertinent 3rd floor actuator forces.

In order to allow an assessment of the effect of Y-directional predeformation on the X-directional cyclic behaviour of the test frame, the hysteretic X-directional response for the maximum (+/- 0.18 m) amplitude for Y = 0, 0.18 and 0 m, respectively, the pertinent results are presented in the following table. Specifically, values of the initial stiffness K_i , being the shear load in kN per cm of 3rd floor displacement at the start of each X-direction test cycle, the maximum positive and negative base shear

loads for the first and second test cycle, the effective test stiffness K_t (max. load versus max. displacement) and the end stiffness K_e of the cyclic response for the last 3 half-cycles, have been tabulated.

The test data of the final three tests show that the average effective stiffness K_t of 127 kN/cm in the first test cycle is equal to the effective stiffness recorded in Test Phase 1. A significant loss of resistance (10%) in the 2nd and 3rd sequences as compared with test sequence 1 can be noted. Also, the end stiffness K_e , showed a similar reduction after completing the last two test cycles, namely from 151 to 135 kN/m. In line with the above observations, the energy dissipation during the last three sequences, dropped from 100% to subsequently 97 and 87%, respectively.

An inspection of the test structure after completion of the six test sequences showed that, other than the earlier failed 2nd floor connection 2C - East, the bottom flange welds of six additional rigid beam-column connections in the moment resistant frames 2 and 3 (X-direction) had failed, namely: at the 1st floor, connections 2A - East, 3A - East and 3B - West, and at the 2nd floor, connections 2B - East, 3B - East and 3D - West. Considering the loss of resistance noted in the 2nd and 3rd cycle it is fair to state that the weld failures occurred during the last two sequences.

Table 3.3.1. Comparison of the global stiffness of the structure during testing

Ki (kN/cm)	max. cyclic loads (kN)		Kt (kN/cm)	Ke (kN/cm)
	positive	negative		
163	2327	2263	127	151
	2270	2224	125	
164	2106	2134	118	147
	2161	2091	118	
148	2060	2036	114	135
	2060	2005	113	

Detailed inspection showed that these connections had all failed because of improper welding of the beam bottom flanges to the beam end-plates. The welds were undersized double-fillet welds, rather than full-penetration flange welds, as specified. With 7 connections out of a possible 36 (in the X-direction) having failed, or 20%, it was assumed that the beam bottom-flange welds would be faulty in general. Considering the remaining test program, with ultimate testing to failure in the X-direction, it was decided to have all flange welds in frames 2 and 3 repaired and strengthened with oversized double-fillet welds. On the other hand, as substantiated by the performance of the test structure after repair (showing a resistance equal to the 1st test sequence) the test structure in Phase 3 would have performed without failure if all welds had been executed as specified.

Test Phase 5

In test-phase 5, a cyclic, quasi-static, X-directional load sequence until failure was performed using the same actuator control and load distribution as before. Because of stroke limitations only a maximum displacement of +/- 42 cm, or a drift of about 4.7% could be introduced. Accordingly, 2 cycles of +/- 180 mm followed by 3 cycles each of +/- 270, 360 and 420 mm were introduced. After the final cyclic, the displacement was reduced to about +125 mm and subsequently to 0 mm.

The cyclic relationship between the total (base) shear force versus the X-directional 3rd floor displacement is shown in Figure 3.3.8. The results indicate, that the maximum cyclic loads at +/- 180 mm are on average 2165 kN in the first cycle and 2100 kN in the second cycle, and compare well with the corresponding average values of 2050 and 2030 kN, respectively, recorded at the end of Test Phase 3; thus indicating that the repair of the earlier failed joints had been successful.

The overall test results show, that a maximum base shear resistance of the test structure of 2400 kN was reached at a top-floor displacement of 27 cm or 3% drift; corresponding with a set of floor loads of 1200, 800 and 400 kN, respectively. Increasing the 3rd -floor displacements to 36 and 42 cm, respectively, the total resistance reduced to 2030 and 1990 kN, respectively. After repeating the last cycle (+/- 42 cm) three times, the test was terminated after the resistance (base shear) had dropped to 1700 kN or 71% of the maximum. At that stage, the bottom flanges and webs of all joints on the first floor along column lines 2 and 3, and all joints on the second floor along column line 2 had fractured. Also, the columns 2A and 2D (frame 2) at the first floor had fractured at the dog bone cut-out. The

latter failures were triggered by the high stress concentration at the cut-out edge surface (which had been flame cut).

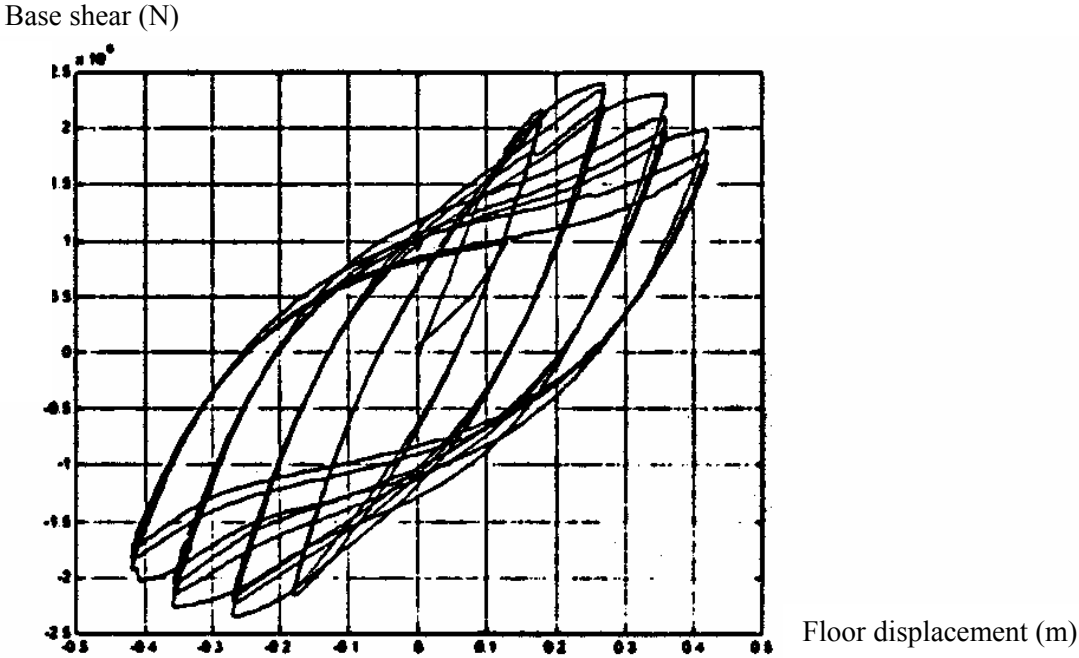


Figure 3.3.8. Total base shear vs. top-floor X-displacement - Phase 5



Picture 3.3.2. Buckling and fracture of the bottom flange



Picture 3.3.3. Fracture of the dog bone after phase 5.

Overstrength of the structure α_u/α_1

A global overstrength factor for the structure is assessed on the basis of the global base shear – top displacement curves of test phase 1 and test phase 5. On Figure 3.3.5., the curve begins significantly to diverge from the elastic slope for a top displacement of 0.05 m and a total base shear of 1100 kN. The ultimate base shear can be taken as the maximal base shear and the overstrength is then

$$\alpha_{\max} / \alpha_1 = 2400 / 1100 = 2.2$$

However, it is usual to consider that the failure is reached after a drop of 20 % of the maximal load. So the overstrength becomes:

$$\alpha_u / \alpha_1 = 0.8 \cdot 2400 / 1100 = 1.75$$

3.3.5. Test results –Analysis of the moment rotation behaviour at each node

The following analysis concentrates on the plastic behaviour of the rigid connections.

Moment rotation curves

In order to conclude about the moment-rotation behaviour of individual joints under cyclic loading the strain gage data in the columns have been used to determine the moments along the length of each column. Equilibrium then provides the sum of the beam moments at each joint. An overall rotation is used to characterise the deformation of the connection zones. It is defined as the 3rd floor displacement divided by the height of the structure. Diagrams giving the sum of the beams moments at every connection versus the overall rotation provide a basis for comparison accurate enough for the discussion on absolute values of plastic moments presented hereafter. They are used to determine the positive and negative plastic moments M_{xp}^+ , found at the intersection between the line of elastic behaviour and a tangent line to the plastic branch having a slope of 1/10 of the elastic one.

The maximum recorded positive and negative moments during a particular test phase without reaching an ultimate rotation (failure) are also determined.

Besides the experimentally derived values, the following theoretical bending moments have been defined and computed with actual yield stress (f_y):

$M_{\text{ref steel}}$, plastic moment of steel section, $M_{\text{ref.comp}}^+$ or $M_{\text{ref.comp}}^-$, positive or negative plastic moment of a composite section with effective width, and $M_{\text{ref.comp}}^{+-}$ sum of these two last values, which is the sum of the composite left and right beam moments at an "interior" column.

Definitions of effective widths

The definition of the plastic moment resistance of composite beam raises the question of the definition of "effective widths".

In codes, effective width are at present defined to allow a global elastic analysis of structures under vertical loads. The problem studied here is the plastic resistance of beams in a frame submitted to horizontal loading, in which the diagrams of moments are totally different. There is thus no code reference to compute $M_{\text{ref comp}}$. However, a proposal of definition of effective width for structural concrete frames has been made by Paulay & Priestley (1992).

The following definition of effective width have been considered to compute $M_{\text{ref comp}}$. In the Eurocode 4 context, for negative moments M^- , the diagrams of moments in a part of the span 0.4ℓ of beam in the frame is similar to the one in a cantilever; so, for a beam in symmetrical situation (see Figure 3.3.9.):

$$b_{\text{eff}} = 2 b_e = 2 (2 \ell_c) / 8 = 2 (0.8 \ell) / 8 = 0.2 \ell = 1.25 \text{ m}$$

For positive moments M^+ , no situation similar to the one of the tested frame does exist in Eurocode 4. It can only be referred to the general definition stating that the span to consider is the one between to points of contraflexure in the beam, that is 0.6ℓ and to the general definition of b_{eff} for positive moments, that is for a symmetric beam:

$$b_{\text{eff}} = 2 b_e = 2(0.6 \ell) / 8 = 0.15 \ell = 0.75 \text{ m}$$

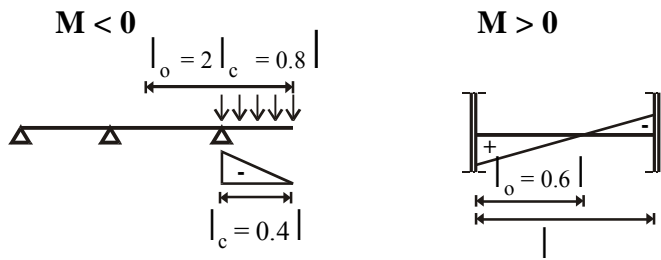


Figure 3.3.9. Effective width in seismic context deduced from Eurocode 4

Plumier's developments on the transfer of slab compression force in the absence of transverse beams propose 2 mechanisms of transfer linked with their corresponding effective width as seen at Figure 3.3.10. For more detail, see section 3.5.

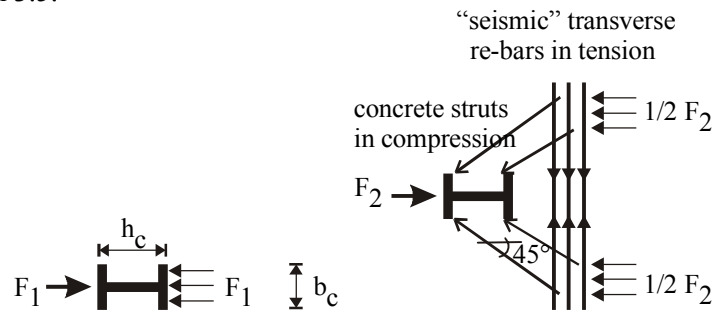


Figure 3.3.10. Transfer of compression from slab to column from Plumier (1998)

-mechanism 1: direct compression of the concrete on the flange of the column;

$$b_{\text{eff}} = b_{\text{column}} = 0.268 \text{ m for the HEM260 or } 0.248 \text{ m for the HEM240}$$

-mechanism 2: mobilisation of inclined concrete struts on the sides of the columns, made possible by specific reinforcing bars ("seismic re-bars")

$$b_{\text{eff}} \cong 0.6 h_{\text{column}} = 0.174 \text{ m for the HEM260 or } 0.162 \text{ m for the HEM240}$$

Paulay's developments on effective width of slab in T concrete beams of frames refer to the very context of seismic loading. The effective width is the smallest of the following quantities :

1. One-fourth of the span of the beam under consideration, extending each side from the center of the beam section, where a flange exists ; this means for instance $b_{\text{eff}} = 2 \times 0.25 \ell = 0.5 \ell = 2.5 \text{ m}$ in lines 2 and 3 of the tested structure.
2. One-half of the span of a slab, transverse to the beam under consideration, extending each side from the centre of the beam section, where a flange exists ; this means for instance $b_{\text{eff}} = 0.5 \times (3.5 + 4) = 3.75 \text{ m}$ in lines 2 and 3 of the tested structure.
3. One-fourth of the span length of a transverse edge beam, extending each side of the center of the section of that beam which frames into an exterior column and is thus perpendicular to the edge of the floor ; this means for instance $b_{\text{eff}} : 0.25 \times (3.5 + 4) = 1.75 \text{ m}$ in lines 2 and 3 of the tested structures and $b_{\text{eff}} = 0.5 + 0.25 \times 5 = 1.75 \text{ m}$ in line A.
4. In the case no edge beam is present, two times the width of the column.

In lines 2 and 3 of the test frame, Paulay's definition for M' means $b_{\text{eff}} = 0.35 \ell = 1.75 \text{ m}$, value which is significantly higher than the ones derived from Eurocode 4 (0.2ℓ). However, it must be noticed that the contribution of an effective width of slab to the plastic moment of a beam is not proportional to b_{eff} . The diagram of Figure 3.3.11., established for an IPE composite beam of the tested structure, shows that additional width above $b_{\text{eff}} = 1 \text{ m}$ brings relatively small increase in M_p . For a ratio on the effective widths of 1.75, the ratio on the negative plastic moments lies between 1.10 and 1.21.

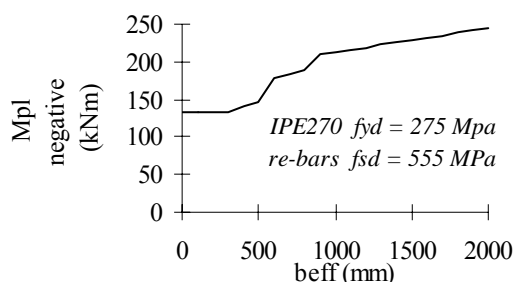


Figure 3.3.11. Influence of the effective width on the negative plastic moment of a composite section

Similarly, the high difference between the tested effective widths under positive moment does not lead to a proportional difference between the corresponding plastic moments. The increase in effective widths between mechanisms 1 and 2 and mechanism 1 alone corresponds to a ratio $b_{\text{eff}(2+1)}/b_{\text{eff}(2)}$ of 1.65, and the corresponding increase in plastic moment lies between 17 and 21 %. For the comparison of the effective width deduced from EC4 and the effective width of mechanisms 1 and 2, the increase in effective width lies between 70 and 83 % and the increase of the positive plastic moment is of maximum 18 %.

Theoretical evaluation of negative plastic moments of composite beams

Even when an effective width of slab is well defined, there are several definitions of the plastic moments of beams.

In a beam submitted to vertical loading and designed with allowance for some redistribution of moments, meaning some available ductility, Eurocode 4 prescribes that only those bars coming in addition to the welded mesh should be considered in the plastic resistance. The reason for this option is the ability of normal re-bars to yield, to be opposed to the low elongation at failure characterising welded bars of mesh. In the context of seismic design, the situation is more complex because it is not enough to define a reliable lower bound of the plastic moment : the capacity design of zones of the structure neighbour to the intended dissipative zones requires the neighbour zones to be more resistant than the real plastic resistance of the dissipative zones. This real resistance may mobilise all re-bars, welded mesh included, even if these fail when large displacements are applied to the structure. We can conclude that, for seismic checks of a structure, two plastic resistances of composite sections submitted negative moments should be considered :

$M_{p\text{max}}^-$, including all re-bars presents, to be used for capacity design checks (local checks)

M_p^- , including ductile re-bars present, to check the global resistance of the structure.

In the following, comparison between experimental and theoretical values are presented ; the theoretical values are computed considering all the re-bars present in the effective width considered, welded mesh included ; they correspond to $M_{p\text{max}}^-$ defined above (the symbol used hereafter is $M_{p\text{comp}}^-$).

Influence of the local design on experimental moments in the beams

The experimental results obtained in lines 2 and 3 of the test frame allow the following direct observations :

At floor 1, two densities of additional reinforcements are realised ; no significant difference in M_p^+ or M_p^- between lines 2 and 3 are set forward. Two reasons can justify this observations :

- yielding is essentially taking place in the bottom flange of the steel section, because of the higher f_y of the re-bars in comparison to the steel sections ;
- the two densities differ only by 15 % if the basic mesh is included in the evaluation.

At floor 2, in line 3, no contact exists between the concrete of the slab and the column, no studs are present in a circle of 1 m diameter around the columns and no "seismic" re-bars are present. In exterior columns, M_p^+ is 84 % of the reference line 2 when transverse rigid beams connected by end plates going into the concrete are used and 70 % of the reference with transverse hinged beams. M_p^- is around 95 % of the reference values. The greater influence on M_p^+ expresses that the reduction in the connection between steel and concrete in line 3 is greater than the reduction in effective re-bars density, once the welded mesh is considered. This is confirmed by the comparison to theoretical values below. At interior columns, the differences in M_p^+ and M_p^- are averaged. The most striking difference is between 2 C and 3 C (20 %).

At floor 3, in line 3, no studs are present in a circle of 1 m diameter around the columns. This, quite surprisingly, generates no significant difference in plastic or maximum moments between lines 2 and 3.

Comparison between experimental and computed moments with the steel section as reference.

At Table 3.3.2. are given the ratio of experimental plastic moments to computed plastic moments of the steel sections. Several conclusions can be drawn :

- the composite character of the section brings a significant increase in resistance, of the order of 2 ; it is clear that disregarding the composite character of sections in the evaluation of the seismic resistance of a composite frame and in the capacity design of its columns is certainly wrong ;
- the increase in resistance is high and does exist even when the connection between steel and concrete is weak or non existing near the connection of beams to columns ;
- the previous conclusion has an important practical impact, since it demonstrates that disconnecting the slab from the beams and the columns does not allow to consider that the resistant structure in dissipative zones is only made of the steel section ; a design based on the resistance brought purely by the steel components is also disqualified, in that case ;
- the increase in resistance brought by the composite character of sections is particularly high for positive bending moments M^+ (over 2.2 in the reference design).
- the increase is quite logically lower (1.60) for negative bending moments, where only the re-bars of the slab contribute to the plastic moment ;
- at interior columns, an average of the two increases observed for M^+ and M^- is obtained.

Table 3.3.2. Average M_p experimental/ M_p steel

	Exterior columns M^+			Exterior columns M^-			Interior columns M^+		
	Floor 1	Floor 2	Floor 3	Floor 1	Floor 2	Floor 3	Floor 1	Floor 2	Floor 1
line 2	2.20	2.78	2.85	1.60	1.88	2.20	1.78	2.04	2.26
line 3	2.28	2.13	3.05	1.53	1.42	2.22	1.75	1.75	2.40
Average									
line 2		2.61			1.89			2.02	

Comparison between experimental and computed plastics moments of composite sections.

At Table 3.3.3. are given the ratio of experimental plastic moments to plastic moments computed with reference to the effective width deduced from Eurocode 4. Several conclusions can be drawn :

- globally, the experimental values fit with the computed ones; looking at the reference design of line 2 ; the average ratios for the three floors are 1.08 for M^+ , 1.20 for M^- and 1.04 for M^+ , sum of the moments at interior columns ;
- the ratios are better with steel sections of higher slenderness.

Table 3.3.3. M_p experimental/ M_p ref comp EC4

Line	Exterior columns						Interior column		
	M^+			M^-			$M^+ + M^-$		
	A	D	AD	A	D	AD	B	C	BC
FLOOR 1									
Line 2	0.92	1.02	0.97	1.11	1.06	1.09	0.95	1.02	0.98
Line 3	1.01	1.00	1.01	1.06	1.02	1.04	0.94	0.99	0.96
FLOOR 2									
Line 2	1.09	1.19	1.14	1.14	1.25	1.20	1.06	1.05	1.05
Line 3	0.92	0.83	0.88	1.30	0.85	1.07	1.05	0.83	0.94
FLOOR 3									
Line 2	1.18	1.06	1.12	1.29	1.32	1.31	1.13	1.05	1.09
Line 3	1.17	1.15	1.16	1.29	1.34	1.31	1.12	1.19	1.16
Average									
Line 2	1.06	1.09	1.08	1.18	1.21	1.20	1.04	1.04	1.04

- the effective width proposed by PAULAY for negative bending moment M^- provides better fittings than Eurocode 4. The average of line 2 for M^- is 1.07 instead of 1.20. For M^+ , it becomes 0.98 instead of 1.04.
- it must be stressed that all the results at exterior columns are obtained in a structure where stiff edge beams are present ; these beams contribute to the existence of a maximum effective width, both for M^+ and M^- . For M^- , this can correspond to the 1.75 m effective width coming from Paulay's proposal. In a structure where edge beams would be less stiff, effective width would be smaller and the values deduced from EC 4 (1 m for M^-) could fit better than Paulay's one ; however it must be stressed again that the differences in fitting of computed values to experimental results between the two definitions of effective width are minor ; this is due to the shape of the (M_p, b_{eff}) curves, which are flat in the range of EC4 and Paulay's values of effective width.
- the positive effective width including only the direct compression and the inclined struts provides worst fitting than EC4. The average in line 2 for M^+ is 1.20 instead of 1.08. At this stage, the fitting is only based on one parameter : the effective width. Another approach could be done, based on the fact that the concrete facing the column is confined by additional transverse re-bars and that it leads to an increase of resistance of the concrete in compression, and consequently a greater positive plastic moment. This approach would minimise the role of the transverse beam, but is not convenient to use in a code.

3.3.6. Conclusions

The main practical conclusions from the test of the full scale 3 D composite steel concrete frame, are the following :

- the design relations concerning the reinforcement of the slab of composite beams, which are presented in the present paper, gave a layout which kept the intended integrity of the concrete during the cyclic testing.
- the effective widths of slab deduced from Eurocode 4 provide correct estimates of the real plastic moments of composite beams. Paulay's definition of effective width gives slightly better results.
- for capacity design purposes, the plastic moments must be computed taking into account all the re-bars present, welded mesh and simple re-bars.
- considering the steel sections only in the design of composite frames is totally inaccurate, it is also unsafe for what concerns the capacity design of columns.
- disconnecting the slab from the beams ends and from the columns does not prevent bending moments much higher than those of the steel sections to be realised in the plastic hinges.

3.4. DARMSTADT TESTS: A study on composite sub-assemblages

C. Doneux

Department of Civil Engineering, University of Liege, Belgium

H. Parung

Institute of Steel Construction, Darmstadt University of Technology, Germany

3.4.1. Introduction

The test program performed on joint sub-assemblages at Technical University of Darmstadt was part of a European global research project. Within this scope, the three sub-assemblages were replicas of parts of a three-dimensional structure tested at the ELSA research laboratory of ISPRA and described in two companion papers presented in this EAEE Conference (Bouwkamp et al. 1998, Plumier et al. 1998). The main goal of the research project was to study the role of the slab on moment transfer in earthquake resistant composite frames.

The purpose of the companion tests of Darmstadt was double: on one hand, we wanted to obtain the global behaviour of the particular joints to allow for the calibration of a non-linear beam-column computer model in order to model the whole 3-D frame and consequently to permit a better pre-test prediction of its load-displacement characteristics and of the test plan. On the other hand, we wanted detailed experimental data on the behaviour of the slab in the moment transfer mechanisms between beam and columns. It was not feasible in the test of the 3-D structure to introduce extensive instrumentation to study the local behaviour in certain regions; the sub-assemblages studies were therefore designed to provide this information and allow calibrating a detailed numerical model to be developed. The final aim of the whole research results would lead to improved model formulations for design of the slab in the beam-column region. In this paper, a detailed description of the Darmstadt tests and their main results are presented.

3.4.2. Description of the specimens

The structural characteristics of the three sub-assemblages, which are shown in Figure 3.4.1, are defined in the following :

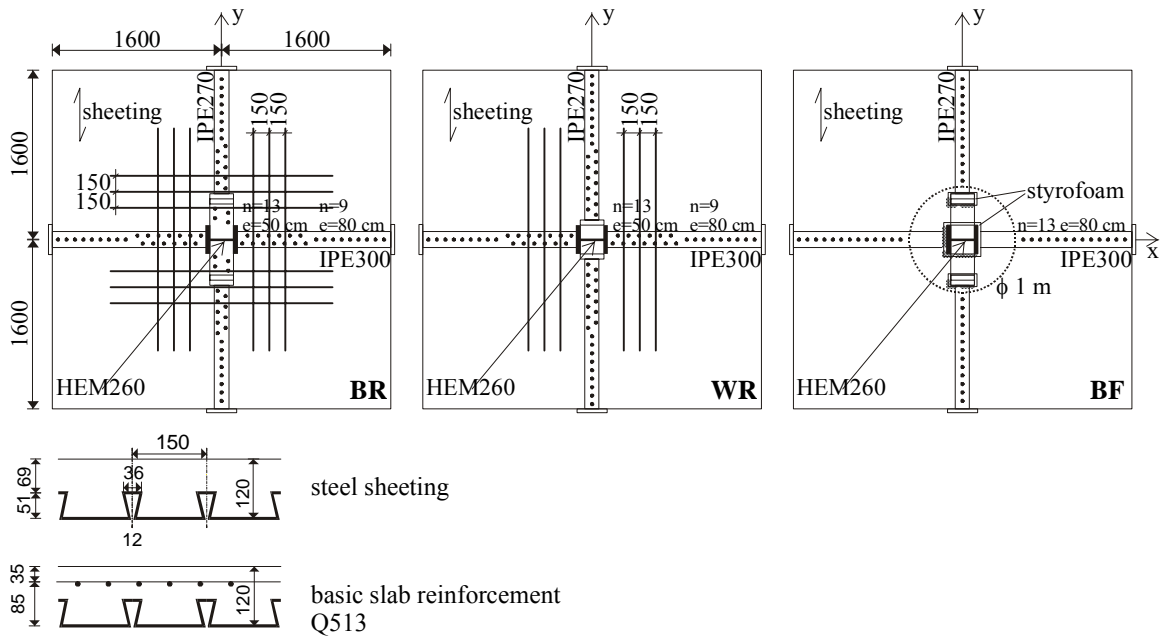
Specimen BR-X (Bolted Rigid - testing in X direction) has rigid, fully bolted bi-axial beam-column connections. The column is a HEM 260 steel section, the beams are IPE 300 in one direction and IPE 270 in the other direction respectively. The slab is cast on a steel sheeting parallel to beam IPE 270. It is 120 mm thick and the basic reinforcement is a Q513 welded mesh ($A = 5.13 \text{ cm}^2/\text{m}$). The composite section is a full shear connection composite section. The headed studs are $\phi 16$ mm diameter and 100 mm high. Three particular measures are taken to ensure the mobilisation of the maximal effective width of the slab:

- the slab is in full contact with the column.
- additional reinforcement is present to permit the development of additional strut and tie mechanisms in the slab. Three additional bars $\phi 10$ are placed on all 4 sides of the column.
- additional studs on the beams around the connection are placed to maximise the participation of the transverse beam in the transfer of the moment.

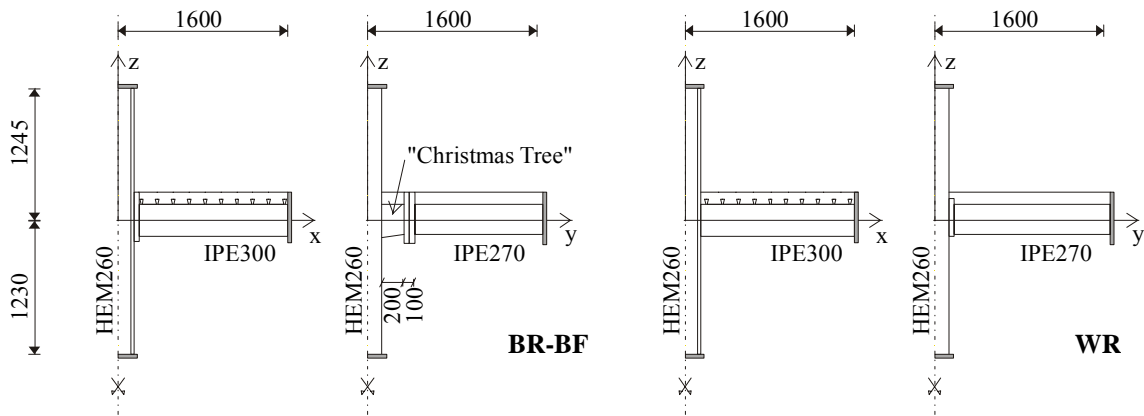
The basis of the design is described in Plumier et al. (1998).

Specimen WR-X (Welded Rigid - testing in X direction) also has rigid bi-axial beam-column connections, but instead of being fully bolted, they are all welded. Another difference with specimen BR-X is the particular layout of the additional reinforcement made of $\phi 10$ bars placed only on 2 sides of the column. This specimen should set forward the influence of the bolted connection on the global behaviour of the node and the effectiveness of a particular reinforcement design.

Specimen BF-X (Bolted Flexible - testing in X direction) has fully bolted connections as the first specimen, with exactly the same basic dimensions, steel sections and concrete slab. Particular measures are here taken to minimise the effect of the slab in the beam-column moment transfer. Additional slab reinforcement and concentrated shear studs around the column have both been omitted. Also, to eliminate any direct contact between the slab and the column section and end plates, 2 cm thick styrofoam strips have been placed around the steel section and plates.



(a) reinforcement and shear connectors layout of specimens BR, WR, BF



(b) configuration of the longitudinal and transverse beams

Figure 3.4.1. Description of the specimens

3.4.3. Test Setup

As in a moment resistant frame under lateral loads, the inflection points in the beams and columns are located at mid-length, the sub-assemblages were designed with hinges at those inflection points. No vertical dead loads were applied to the specimen. The beam-column moment transfer is realised by applying a double-acting actuator load at the top of the column and providing the necessary hinged support conditions at the other inflection points, as shown in Figure 3.4.2. The actuator is programmed to introduce displacement-controlled loads. Out-of-plane motion of the test specimen under load was prevented by parallel guide beams and a set of rollers.

3.4.4. Instrumentation

As the specimens were to be tested under displacement-controlled cyclic loads, a potentiometer with a range of + and -200 mm was installed to control the top displacement of the column versus a reference column located on the far side of the reaction frame. For measuring the applied cyclic loads, a load cell was attached to the 100 ton actuator. In order to measure the reaction forces in the pin-ended struts, one or both struts were instrumented with strain gages.

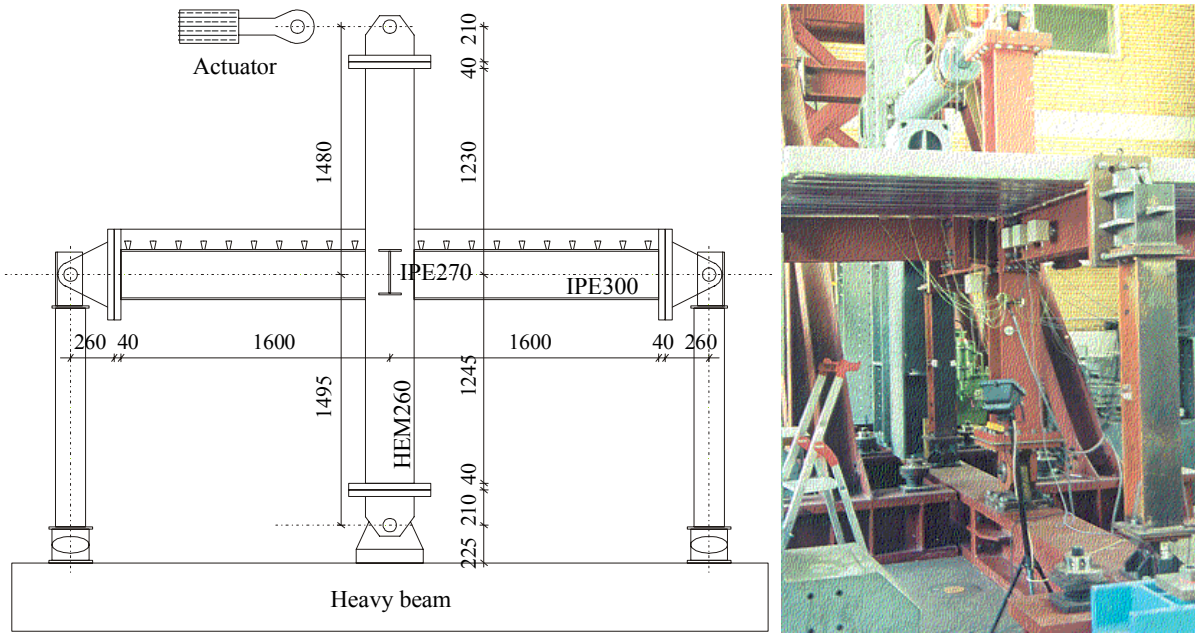


Figure 3.4.2. Test setup

Strain gages were placed at both sides of the top flange and in the middle of the bottom flange at different sections along the loaded beams. In order to measure in-plane transverse bending effects, strain gages were placed at both sides of the upper flange of one of the transverse beams. Strain gages were also placed on the reinforcing bars. LVDT's were installed on the concrete slab to measure the concrete strains at various locations. In order to measure the angular change between the beams and the column in the connection zone under loading, LVDT's were placed on each side of the column. Inclinometers were installed to measure the rotation of the column and beams. Detailed layouts of the instrumentation and notations of the measurements are not presented for each specimen, because they are not basically different.

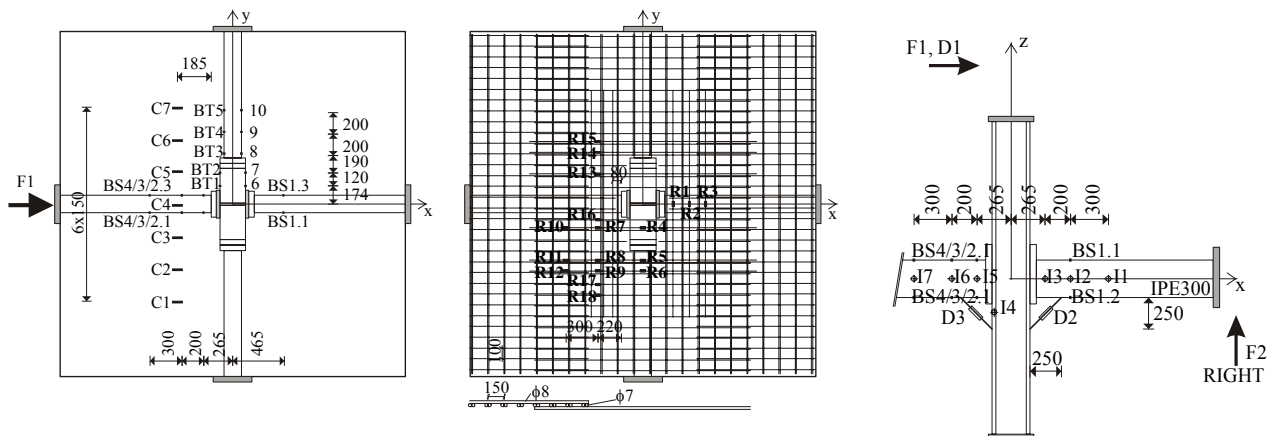


Figure 3.4.3. Instrumentation of specimen BR-X

Figure 3.4.3 presents the instrumentation of specimen BR-X, with: forces F_1 - F_2 , displacement transducers D_1 thr. D_3 , strain gages at sections BS_1 thr. BS_4 on IPE 300 and gages BT_1 thr. BT_{10} on transverse beam (IPE 270), inclinometers I_1 thr. I_7 on IPE 300, LVDT's C_1 thr. C_7 on slab and strain gages R_1 thr. R_{18} on reinforcing bars.

3.4.5. Test Procedure

The specimens were subjected to cyclic, displacement-controlled forces (F1). The cyclic displacement (D1) history was defined by the immediate test objective and aimed at establishing the performance of the joints up to a test displacement limit of $D1 = \pm 200$ mm (story drift = 6.67%). Specimen BR was first tested under cyclic, increasing, top-column displacements in the x-direction (to study the IPE300 moment transfer) up to maximum displacements of ± 48 mm. The specimen was then turned 90° and subjected to the same displacement history. Finally, the specimen was turned back to its original position and loaded up to maximum top displacements of ± 200 mm. It was showed that the x-direction test results were not affected by the intermediate y-direction testing. Consequently, specimen BF was directly tested in the y-direction up to maximum top-column displacements of ± 50 mm. Subsequently, the specimen was turned 90° and tested in the x-direction cyclically to maximum top displacements of ± 200 mm. Specimen WR was tested only in the x-direction up to the maximum top displacement of ± 200 mm, because the reinforcing bars layout was specifically designed to calibrate formulas under a one directional earthquake.

3.4.6. Experimental results

Cyclic Behaviour - General Characteristics

The global behaviour of the different specimens will be discussed on the basis of the behaviour of the left beam of each specimen tested in the x direction (i. e. bending of the IPE300). This choice was made necessary because of early failures in the right beam-to-column connection due to a missing fillet weld connecting the web of the IPE 300 web to the beam end-plate for specimen BR and a lack of penetration of the bottom flange weld for specimen WR.

Figure 3.4.4. presents the left moment versus global rotation curves for each specimen. The global rotation is the ratio of the controlled top column displacement by the height of the column. It has been considered as a good estimation of the global rotation of the beam because the joints have been designed to dissipate energy in the beams (column and panel zone remain elastic).

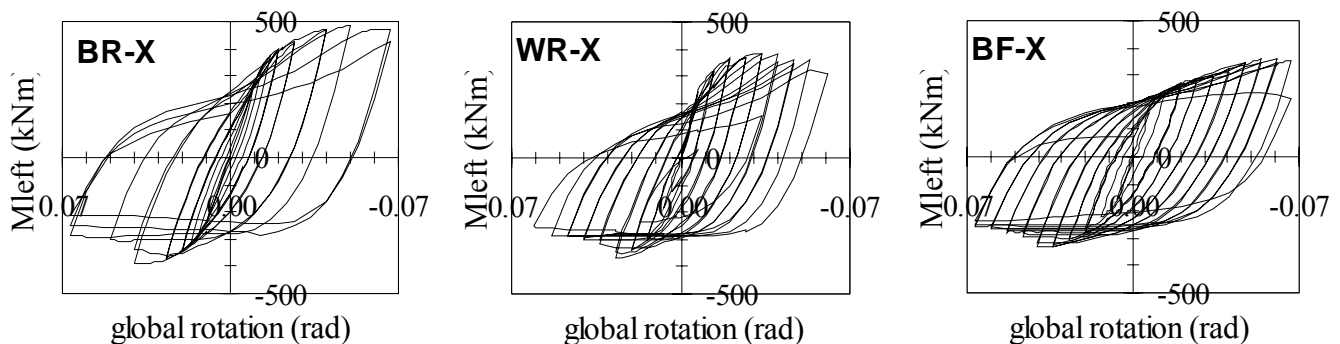
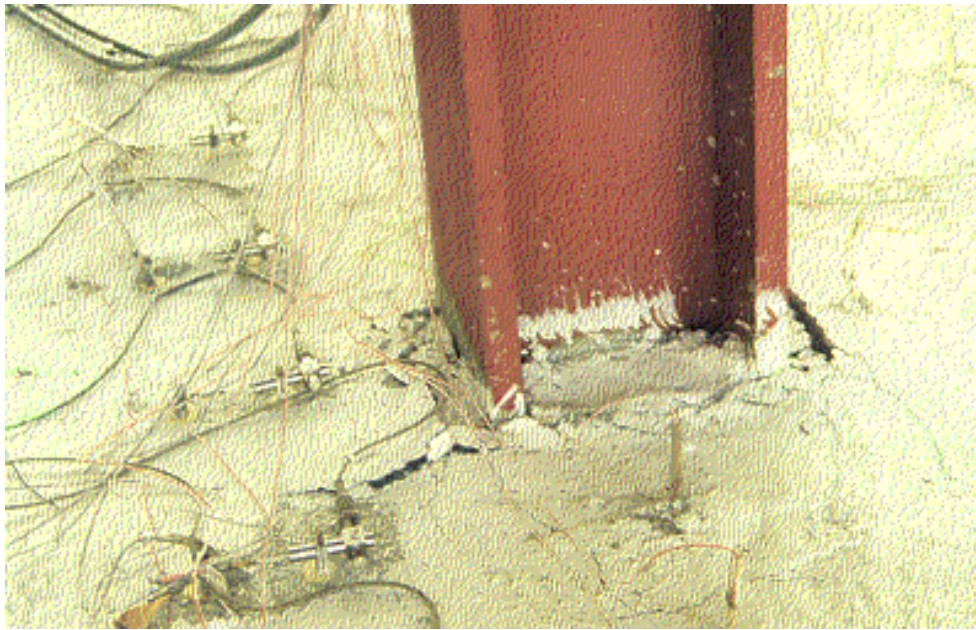


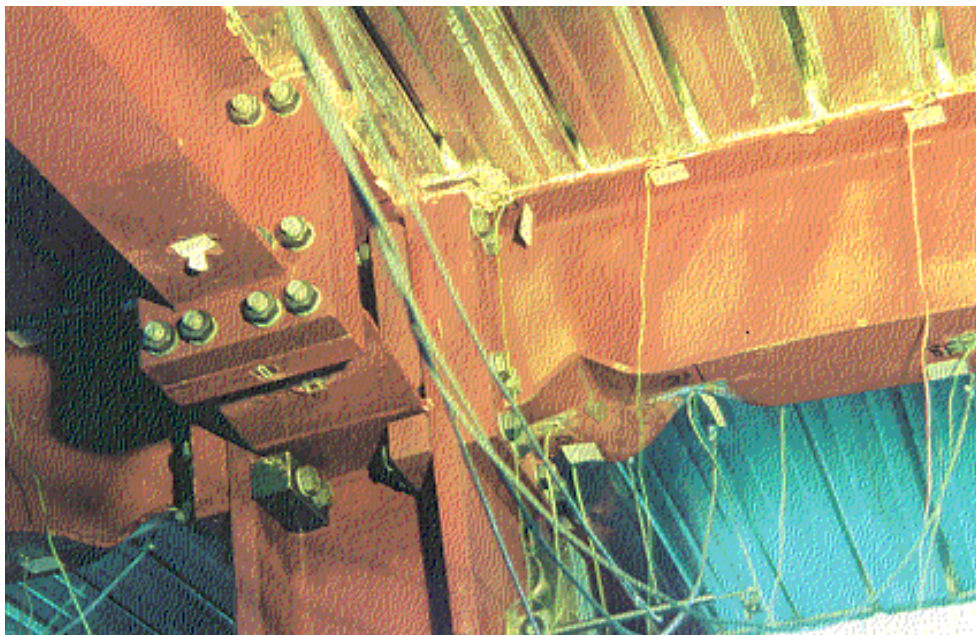
Figure 3.4.4. Moment at the end of the left beam versus global rotation of the node

An excellent ductile behaviour can be observed in general with stable cyclic hysteretic loops for all the three specimens. Under positive bending, specimen BR-X with the most rigid slab and the presence in the transverse direction of big plates (Christmas tree) shows the highest positive moment capacities. Specimen WR-X shows lower but also good moment capacities, bringing to the fore the good influence of the big plates in specimen BR-X. In specimen BF-X, no additional reinforcing bars, no studs around the column are present and styrofoam has been placed around the column section and end plates, included those of the Christmas tree to which the IPE 270 beams were connected. The positive resisting moments are logically lower than for the first two specimens. Under negative bending, the three specimens experienced flange buckling as illustrated by the flattening of the curves after several cycles. The low cycle fatigue of the lower flange, between compressive buckling and high tension, finally lead all the specimens to tension cracks in the lower flange of the steel beam. Crushing of the concrete slab in direct contact with the column is visible on the rigid specimens only. Specimen BF-X

showed also a light buckling of the upper flange - which was not connected to the slab in this case.



Picture 3.4.1. Specimen BR-X cracking and crushing of the concrete slab



Picture 3.4.2. Specimen BR-X buckling of the lower flange of the steel section

For the moment-rotation diagrams of each of the tested beam-to-column joint, a series of experimental quantities have been computed: the conventional positive and negative plastic moments M_p , which are deduced in accordance with the ECCS procedure (M_p corresponds to the intersection between the line of elastic behaviour and the “plastic” line, tangent to the monotonic envelope of the cyclic diagram and having a slope of 1/10 of the elastic one.), the corresponding elastic rotations θ_p , the elastic conventional joint stiffness $K_c = M_p / \theta_p$ and the ductility defined as θ_u / θ_p .

Besides these experimental values, theoretical resistant bending moments have been computed, with actual yield or failure stresses.

$M_{ref.steel}$ is the plastic moment of the steel section.

$M_{ref.comp+}$ is the positive plastic moment of the composite beam with an effective width obtained

using the concepts of Eurocode 4. The distance between the zero moment points l_0 is taken equal to 1.6 m and $b_{eff} = 0.4$ m. It has to be said that the mechanisms of transfer by direct compression and inclined struts of the compression in the slab to the column give the same order of magnitude of effective width $b_{eff} = b_c + 0.6 h_c = 0.442$ m without any transverse beam, but with the seismic transverse re-bars.

$M_{ref.comp-}$ is the negative plastic moment of the composite beam. Two different effective width are considered; the Eurocode 4 effective width $b_{eff} = 0.6$ m calculated on the basis of $l_0 = 1.5L = 2.4$ m; and the total width of the specimen [the l_0 corresponds to the old version of EC4; the new edition(2000) recommends $l_0 = 2L = 3.2$ m = the total width of the specimen]. Because of ductility requirements, Eurocode 4 disregards the contribution of welded mesh in the calculation of resistant moments. Within the scope of capacity design, all the reinforcing bars present in the effective width (including the mesh) are taken into account.

The material properties and the computed plastic moments of beams are presented in tables 3.4.1 and 3.4.2. The results of the test data reduction described above are summarised in tables 3.4.3 to 5.

Table 3.4.1. Material properties

Concrete	f_c cylinder	24.5	N/mm ²
Structural steel	f_y	287	N/mm ²
Reinforcing bars	f_s	570	N/mm ²

Table 3.4.2. Resistance

	$M_{ref.steel}$ kNm	$M_{ref.comp+}$ kNm (EC4)	$M_{ref.comp-}$ kNm (EC4)	$M_{ref.comp-}$ kNm (max)
Spec BR-X	180	275	-193	-322
Spec WR-X	180	275	-193	-297
Spec BF-X	180	275	-193	-297

Table 3.4.3. Plastic moments and rotations

	M_{p+} kNm	M_{p-} kNm	M_{p+} ref.steel	M_{p-} ref.steel	M_{p+} ref.comp	M_{p-} ref.comp	M_{p-} ref.comp(max)	θ_{p+} rad	θ_{p-} rad
Spec BR-X	310	-277	1.72	1.54	1.13	1.44	0.86	0.0108	0.0130
Spec WR-X	275	-287	1.53	1.60	1.00	1.49	0.89	0.0088	0.0127
Spec BF-X	208	-233	1.16	1.29	0.76	1.20	0.78	0.0107	0.0127

Table 3.4.4. Global rigidities and ductilities

	K_{c+} KNm/rad	K_{c-} kNm/rad	μ_{u+}	μ_{u-}
Spec BR-X	28704	-21336	4.54	2.92
Spec WR-X	31294	-22615	3.98	2.10
Spec BF-X	19442	-18307	5.70	3.15

Table 3.4.5. Intercomparison

	M_{p+}	M_{p-}	μ_{u+}	μ_{u-}	K_{c+}	K_{c-}
BR/BF	1.49	1.19	0.80	0.93	1.48	1.17
BR/WR	1.13	0.97	1.14	1.39	1.48	1.17

The comparison of the negative plastic moment with the reference composite moment (Table 3.4.3) clearly shows that the reference value is underestimated and that the real effective width is higher than the EC4 one. However, it is seen that all the bars of the specimen are not included in the plastic moment. For specimen BR and WR, the plastic resistance under positive bending is well evaluated by the EC4 approach. This is not the case for the third specimen where the resistance is overestimated. The reason is that the reference values are considering the composite section as a section with full

shear connection, which is questionable for the specimen BF without studs around the column and with a lack of transverse reinforcing steel causing splitting of the slab.

In the particular case of specimen BF, special measures were taken to minimise the participation of the slab in the connection zone. We could expect that the resistance of the beam would approach the resistance of the steel section only. Table 3.4.3 shows that we have an additional resistance of 16% for the positive moment and 29% for the negative one. This result is of high interest and demonstrates that it can be unsafe to design a composite structure by taking only the steel sections as resisting members. The effect of the Christmas tree can be estimated by comparing specimens BR and WR. The contribution of these plates to the positive plastic moment is +13% because of the role of support for the compressed concrete, bringing an increase of the effective width.

Slab behaviour

Crack patterns

The different crack patterns on the concrete slabs are given at Figure 3.4.5.

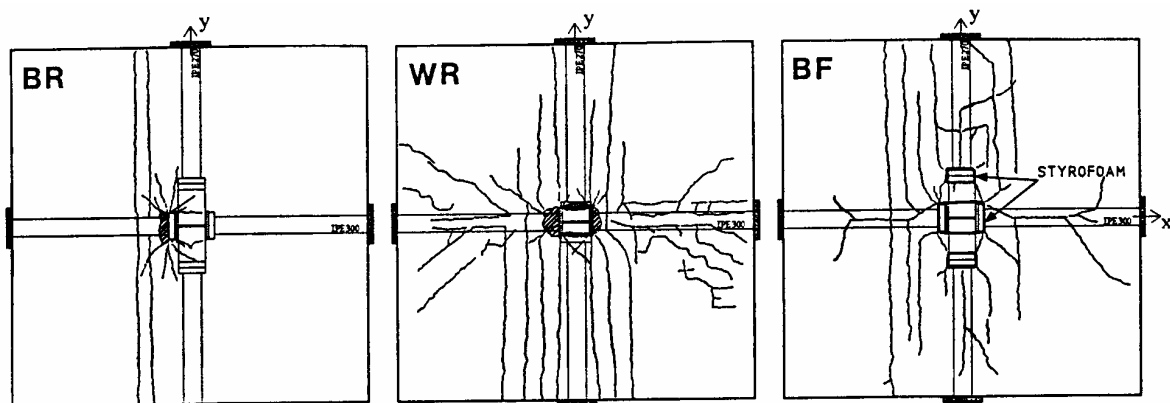


Figure 3.4.5. Crack patterns

The over-reinforced specimen BR shows very few cracks (given only for one half specimen): two main flexural cracks through the hole width of the specimen and perpendicular to the direction of loading and secondary cracks at the corner of the big end plates of the beam. At the end of the test, the concrete against the beam end plate is crushed, due to the high positive moment reached. It can be considered that the design according to the concepts presented in Plumier et al. (1998) reached the objective which is behind the concepts: low damages in the slab, maximum bending resistance.

Specimen WR is only over-reinforced in the transverse direction y , near the column. It is clearly reflected by the observed cracks. Near the column, cracks perpendicular to the loading are present, more numerous than in specimen BR because there are less reinforcement. Further, the transverse re-bars are not sufficient to avoid splitting of the concrete. Concrete compressive struts and diagonal cracks are also visible on the hole length of the slab (more at the ends), defending the tension flange model. Around the column, the crushing of concrete in direct contact with the column is very important. The weakness of longitudinal reinforcement (x direction) is certainly the cause of the serious crack state observed in the slab.

In specimen BF without additional re-bars and studs, one crack parallel to the loading direction strongly appears, just along the stud line on the longitudinal beam. The transverse reinforcement does not withstand the transverse tension and splitting occurs, leading to a reduction of the composite character of the section. Cracks perpendicular to the direction of the loading appear also. At the ends of the specimen, some cracks at 45° are observed. Again the weakness of reinforcement is certainly the cause of the serious crack state observed in the slab.

Measurements on transverse reinforcing bars

By the instrumentation of the additional transverse re-bars, we wanted to bring to the fore the possible anchorage of additional compressive struts in the positive bending moment regions. Figure 3.4.6. illustrates the strains measured on the transverse re-bars versus the moment in the beam.

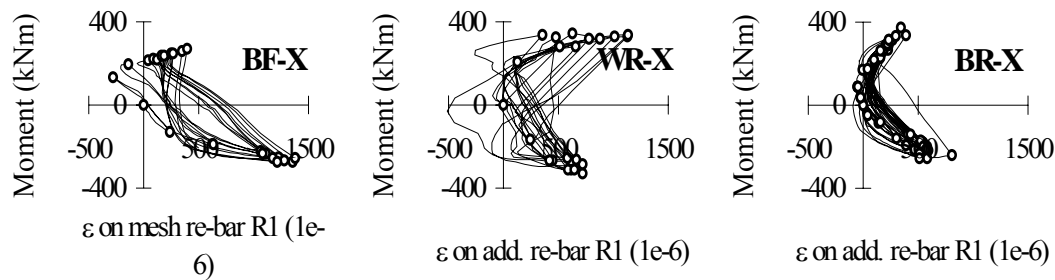


Figure 3.4.6. Measurements on transverse re-bars versus moment.

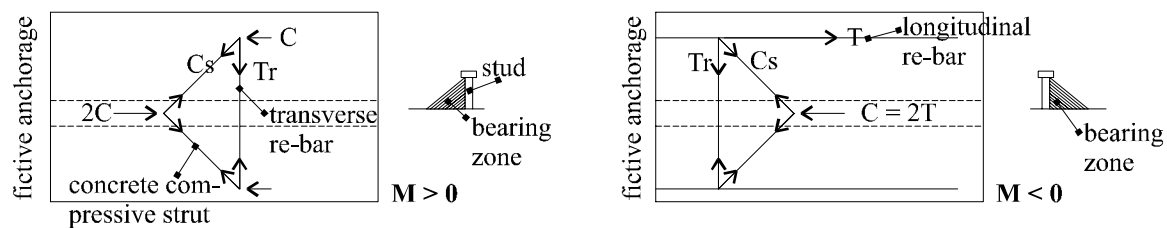


Figure 3.4.7. Spread of the forces in the slab of a composite section by shear mechanisms

Whatever the specimen is, the studied transverse re-bars are mainly in tension. In a composite element of the type studied here, it is the normal situation to have tension in the transverse re-bars under positive bending moment as well as under negative bending moment, as they allow for the spread of the force in the slab by shear transfer (Figure 3.4.7.).

In specimen WR, where additional re-bars are only put in the transverse direction, one may observe that the measured strains under positive bending moment are higher or equal to the strains obtained under negative moment. This could validate the idea of an additional anchorage of concrete struts on the sides of the column under positive bending.

In specimen BR where the re-bars are the same in both direction, the measured strains are smaller or equal to the strains under negative bending, showing no additional anchorage, certainly because the forces in the longitudinal re-bars are directly equilibrated by the same forces in the transverse re-bars and that there is no possibility of additional anchorage of concrete struts.

In specimen BF, no additional re-bars were placed. The measurements are made on the mesh. The re-bars are also the same in both directions. The tendency is the same as for specimen BR but the strains under negative bending are far greater than those under positive bending. This difference is not yet explained.

Measurements on longitudinal reinforcing bars

The types of measurements on the longitudinal re-bars in one particular section of the two fully connected specimens (BR – WR) are described at Figure 3.4.8.

One can observe that under positive bending, some bars are in compression and some are not. It seems to invalidate Paulay's tension flange postulate. However, its existence is possible if superposed with an important contribution of the compression flange in the surrounding of the column. This contribution seems to be more important in the case of this composite specimen than in the case of the concrete units tested by Paulay. The bars near the column are still in compression (effective width of the positive moment) while the bars near the edge of the specimen are in tension (anchorage of the bars in tension at the negative bending moment side – tension flange). Figure 3.4.9. is a sketch of the forces imagined on the transverse beam with the longitudinal strain measurements presented here. The distance between two points of zero strain could be imagined to derive effective width under positive moment at a certain level of loading in the studied section.

For the more flexible specimen BF, the strains under positive bending are always in compression, showing that no tension field develops in this specimen. In Figure 3.4.9., the tension T_x have to be

replaced by compression and the transverse beam is expected to be more loaded.

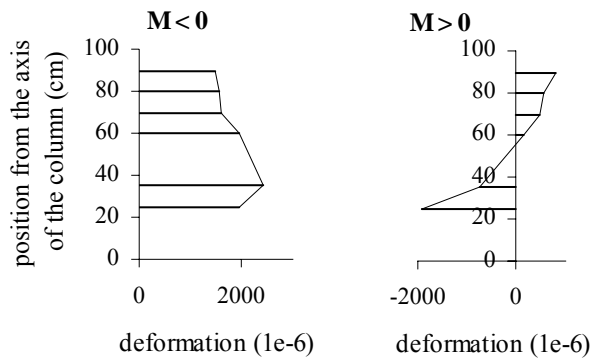


Figure 3.4.8. Measurements on the longitudinal reinforcing bars in one section of specimen BR-X at a top displacement $D1 = \pm 120$ mm.

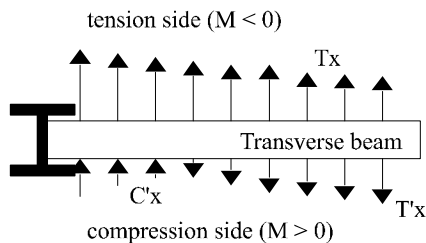


Figure 3.4.9. Presumed applied forces on the transverse beam for the rigid specimens

Stress field in the slab

The moment transfer mechanism is very dependent on the detailed design, which directly influences the magnitude of stresses in the reinforcing bars and in the slab.

In specimen BR, it is obvious that yielding is located in the steel part of the beams, and consequently no slab failure mechanisms are clearly observed.

In specimen WR, the smaller concentration of re-bars in the main direction make possible the formation of concrete struts at 45° . The strain measurements on longitudinal re-bars show tension and compression under positive bending moment, giving substance to a mechanism superposing the tension flange resistant scheme coming from the negative moment side and a compression of the slab in the surrounding of the column.

Specimen BF did not follow this resistant scheme. It is not illogical because around the column, everything is done to minimise the effect of the slab. However, it is now sure that the slab plays a role (see $M_p \text{ comp exp} / M_p \text{ steel} = 1.16$ or 1.29), maybe linked with the role of the transverse beam.

Transverse beam

The strain measurements on the transverse beam are aimed to quantify the participation of the transverse beam to the moment transfer from the beam to the column. The upper flange of the transverse beam is instrumented with couples of strain gages at 5 different sections. If the transverse beam is loaded by membrane forces in the slab, the induced torsion of the IPE profile will mainly introduce bending in its upper flange (Plumier et al. 1998). Under elastic loading, the measured couples of strains may be divided into normal and flexural strains. Assuming that the resistant steel section is the upper flange, an elastic bending moment and a normal force are computed.

The bending moments are presented in Figure 3.4.10. for the 3 specimens for a same load at the top of the column – $F1 = 165$ kN, corresponding to the top displacement $D1 = 30-25-60$ mm for specimen BR-WR-BF respectively.

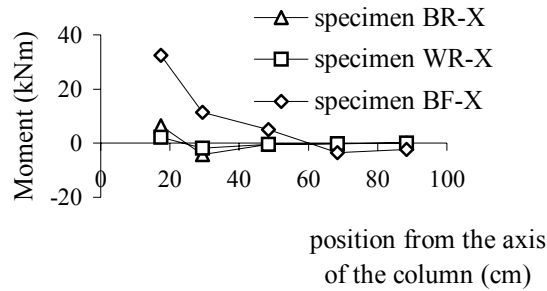


Figure 3.4.10. Moment in the upper flange of the transverse beam

The moment observed in the transverse beam of specimens BR-X and WR-X remains near zero. It means that the mechanism of struts and ties imagined with the transverse beam to contribute to increase the positive bending moment is not activated, or far less than in the specimen BF. This was well suggested by Figure 3.4.9. The presence of big plates on the transverse beam of specimen BR gives greater moments in the Christmas tree plate near the column than in the IPE270 beam of specimen WR (no Christmas tree). But the difference is not important enough to derive a quantitative conclusion at this stage.

In comparison, the transverse beam of specimen BF-X is strongly loaded and yield strains are even observed. The fact that there are no additional reinforcing bars and no additional studs leads to a greater flexibility of the specimen because the other ways to anchor struts and carry the load are not effective. The absence of additional devices makes the activation of the transverse beam mechanism possible. The greater stresses in the transverse beam of specimen BF-X may also be explained by the absence of studs 50 cm around the column. So, if compressed struts rest against the studs, the level of arm will be greater in this specimen than in the specimen BR-X and consequently, for a same load, the stresses will be greater.

These interesting observations remind that all the resistance mechanisms play a different role following their relative rigidity in the general resistant scheme and that one particular layout will promote one mechanism and weaken the other.

3.4.7. Conclusion

Tests on three composite beam-to-column sub-assemblages were realised: one bolted connection with detailed rules for rigid slab, one welded with rigid slab and one bolted with a more flexible slab. This description provides indications on the field of stresses existing in the slab for various layout of re-bars, studs and contact between concrete and column. The main results are:

- the measures taken to maximise the effective width are effective. the design relations presented in Plumier et al. (1998) gave a safe design, bringing the intended yielding scheme for a value of bending moment which can rather accurately be computed.
- design based on steel sections only is inaccurate and unsafe.
- the positive plastic moments are as well estimated on the basis of the EC4 definition of effective width as on the basis of the Plumier's mechanisms (direct compression and inclined struts) because in this particular case they give effective widths in the same order of magnitude.
- the negative plastic moments are underestimated on the basis of the "old EC4 definition" of effective width, but overestimated on the basis of the new EC4 definition of effective width.
- the transverse beam is not really activated in the case of a rigid slab, this third mechanism being too flexible to be activated in comparison with the high stiffness of the direct compression of the concrete on the column face and the inclined struts on the column sides.

3.5.MOMENT TRANSFER

A. Plumier, C. Doneux
Department of Civil Engineering, University of Liege, Belgium

Several presumed models exist to describe the behaviour of the slab in composite joints or reinforced concrete joints under vertical or horizontal loads. This section summarises the different approaches to which reference could be made during the research and analysis of the test results.

3.5.1. Eurocode 4

Eurocode 4 deals with composite structures under vertical loads. Section 8 deals in particular with the behaviour of composite joints. In case of unbalanced negative moments, the additional tension at one side is equilibrated by additional compression on the column at the other side of the joint through a strut and tie mechanism supported by the column. In this case, the longitudinal re-bars are designed to exclude failure in transverse reinforcement and to exclude brittle failure in concrete. Figure 3.5.1 illustrates this behaviour.

The condition on the longitudinal re-bars to exclude brittle failure of the concrete is:

$$A_{sL} \leq \frac{0.94 b_c t_{slab} f_{cd}}{\mu f_{sdL}} \quad \text{with } \mu = 1 - \frac{M_{left}}{M_{right}} \quad \text{and} \quad M_{left} < M_{right}$$

The condition on the transverse re-bars to exclude their yielding is:

$$A_{sT} \geq \frac{\mu}{2 \tan \delta} A_{sL} \frac{f_{sdL}}{f_{sdT}}$$

If the condition is applied to the case of maximal unbalanced forces allowed by the formula, which is in the case of exterior nodes under negative bending moment, $M_{left} = 0$, $\mu = 1$ and

$$A_{sL} \leq 0.94 b_c t_{slab} \frac{f_{cd}}{f_{sdL}}$$

With the assumption that the compression struts are at 45° , $\tan \delta = 1$ and

$$A_{sT} \geq 0.5 A_{sL} \frac{f_{sdL}}{f_{sdT}} \quad (1)$$

If the formula is applied to a structure submitted to horizontal loading, in which $M_{right,Sd}$ and $M_{left,Sd}$ can have opposite signs (< 0 and > 0 respectively), μ is greater than 1. In the case where $M_{left} = -M_{right}$, $\mu = 2$ and

$$A_{sL} \leq 0.47 b_c t_{slab} \frac{f_{cd}}{f_{sdL}}$$

$$A_{sT} \geq A_{sL} \frac{f_{sdL}}{f_{sdT}} \quad (2)$$

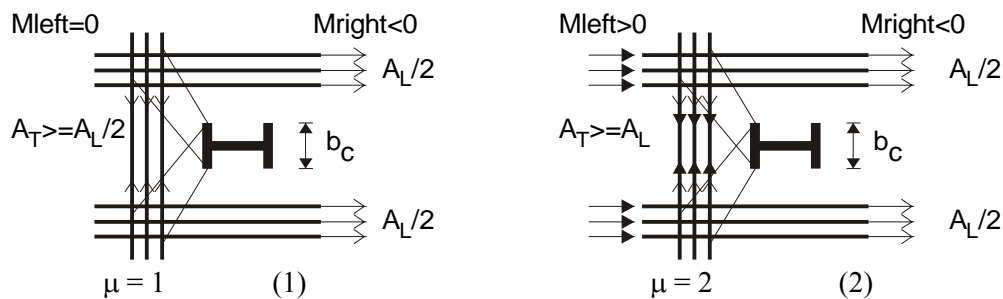


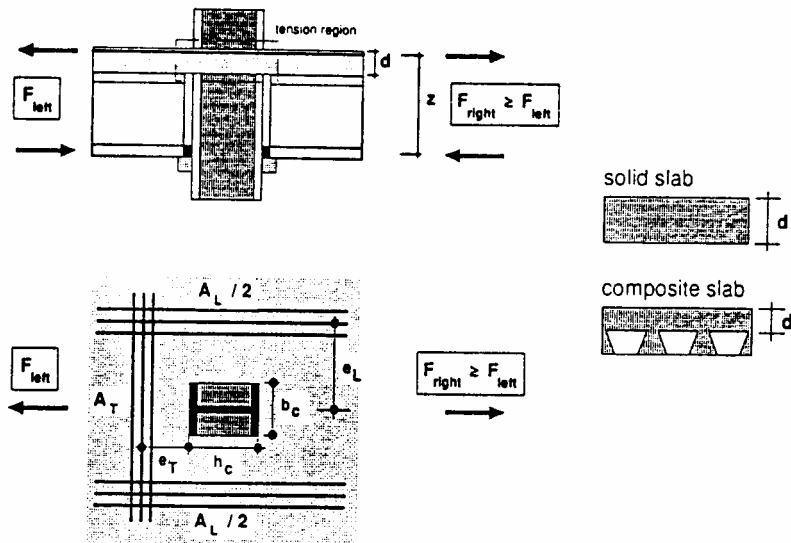
Figure 3.5.2. Limitation on re-bars following Eurocode 4

$$\mu = 1 - \frac{M_{left}}{M_{right}} \leq 1$$

$$\frac{e_L}{b_c} = 1 \div 1.5$$

$$\frac{e_T}{e_L} = 1 \div 1.5$$

$$\tan \delta = \frac{e_T - 0.3}{0.7}$$



M_{left}/M_{right} ... factor of unbalance	d ... thickness of slab
b_c ... width of column profile	A_L ... area of long.reinforcement
h_c ... height of column profile	A_T ... area of transverse reinforcement
	γ_s, γ_c ... safety factors
e_L ... distance of long.reinforcement	E_a ... modulus of elasticity (reinforcement \approx beam)
e_T ... distance of transverse reinf.	f_{yL}, f_{yT}, f_{ck} ... charact.strength long.,transv.reinf.,concrete
z ... lever arm of joint	$A_{L,beam}$... area of long.reinf. in beam beyond joint area
	b_b, t_b ... beam dimensions (width, flange thickness)

Initial Stiffness:

$$S_{j,ini,t} = E_a \cdot k_{10} \cdot z^2$$

equal forces (balanced loading):

$$k_{10,left} = k_{10,right} = \frac{2 \cdot A_L}{h_c \cdot (1 - K_{trans})}$$

unequal forces (unbalanced loading):

$$M_{right} > M_{left}$$

$$k_{10,left} = \frac{A_L}{h_c \cdot (-0.5 \cdot K_{trans})}$$

$$k_{10,right} = \frac{A_L}{h_c \cdot (1 + K_{\mu} - 0.5 \cdot K_{trans})}$$

transformation factor

$$K_{trans} = \frac{A_L}{A_{L,beam} + 0.64 \cdot t_b \cdot b_b}$$

redirection factor

$$K_{\mu} = v \cdot \mu \cdot (7.7 \cdot \mu^2 - 13.8 \cdot \mu + 8.9)$$

composite slab: $v = 1.0$

solid slab: $v = 1.4$

Design Resistance:

$$M_{j,Rd,T} = \frac{f_{yL} \cdot A_L \cdot z}{\gamma_s}$$

$$A_L \leq \frac{2 \cdot A_T \cdot \tan \delta \cdot f_{yT}}{\mu \cdot f_{yL}} \quad \text{to exclude failure in transverse reinf.}$$

$$A_L \leq \frac{0.94 \cdot b_c \cdot d \cdot \gamma_s \cdot f_{ck}}{\mu \cdot \gamma_c \cdot f_{yL}} \quad \text{to exclude BRITTLE failure in concrete}$$

Figure 3.5.1 EC4 approach under unbalanced negative moments (Cost C1 1997)

The concrete involved in the struts of the resistant mechanism is used to equilibrate the longitudinal force, whatever the origin of the longitudinal force is. In case of $\mu = 1$, the longitudinal force comes only from the tension of the longitudinal re-bars. In case of $\mu = 2$, the longitudinal force is for one half coming from the tension of the longitudinal re-bars (negative moment) and for the other half from the compression of the concrete (positive moment). If the longitudinal force is the same in both cases, the longitudinal re-bars section allowed by the proposed ductile mechanism in case of positive and negative moments can logically be no more than one half of the section allowed in case of negative moment only.

The above formulas were typically written to ensure a ductile mechanism to transfer the unbalanced negative moment through the compression of the concrete on the column.

The problem, in the case of the effect of seismic action, which generates a significant positive bending moment, is that it is not certain that the EC4 proposed mechanism provides enough resistance to achieve at one side a ductile negative moment and at the same time at the other side a ductile positive moment without crushing of concrete.

To study further this problem, we first present hereunder an approach proposed by Plumier et al. [2] to estimate reasonable resistant schemes necessary to transfer a full positive composite plastic moment with sufficient ductility.

3.5.2. Slab to column force transfer. Plumier approach: Slab design at the positive moment side of a beam to column joint under horizontal load without interaction with the negative moment side

General.

The proposed concepts aim at having minor damages in the slab, yielding being essentially taking place in the bottom flange of the steel section.

Under positive bending moments, composite T sections can be ductile if the crushing of the concrete is avoided. The buckling failure of the steel walls normally does not control the ultimate limit state of composite beams under positive bending moments, because of the connections between the upper flange and the concrete. To avoid concrete failure under positive bending moment, the proportions of a composite steel concrete section must be such that the steel on the bottom side yields before the concrete strains ε_c at the top of the section are too high; for reinforced concrete elements, submitted to cyclic loading, this is deemed to be satisfied when $\varepsilon_c \leq 2.10^{-3}$, when the strains ε_s in steel are high enough to obtain the required local ductility μ .

To have a chance to avoid crushing of concrete, the activated effective width has to be maximised in order to raise the neutral axis to realise the objective defined above. In the following development, the full positive composite plastic moment that we want to transfer is defined with an effective width deduced from the Eurocode 4 concept. Under seismic action, $\ell_0^+ = 0.6 \ell$ and $\ell_0^- = 0.4 \ell$ are reasonable estimates for the lengths ℓ_0 of the beam between 2 points of moment reversal. Then according to Eurocode 4, the positive effective width is: $b_{\text{eff}}^+ = 2b_e \cong (2 \times 0.6 \times \ell) / 8 = 0.15\ell$. The following resistant schemes are aimed to transfer this full positive composite plastic moment.

Transfer of the slab forces without transverse beam.

Without transverse beam, the transfer of the compression force F_{sc} corresponding to $b_{\text{eff}}^+ = 0.15\ell$ from the slab to the column can be realised through two mechanisms - Figure 3.5.3.

Mechanism 1 is a truss with 2 compressed concrete struts and one steel tie in tension. This mechanism can be developed only when the column cross section has some concave zones or special connecting devices on the sides – Mechanism 2 is the direct compression of concrete on the flange of the column. The design resistance of these two mechanisms can be estimated in a way similar to the one used in the design of reinforced concrete structure.

One important assumption made in the assessment of the following design resistance is that the gradient of stresses on the thickness of the slab is neglected. This assumption has usually no great implication when the ultimate limit state of the section is reached.

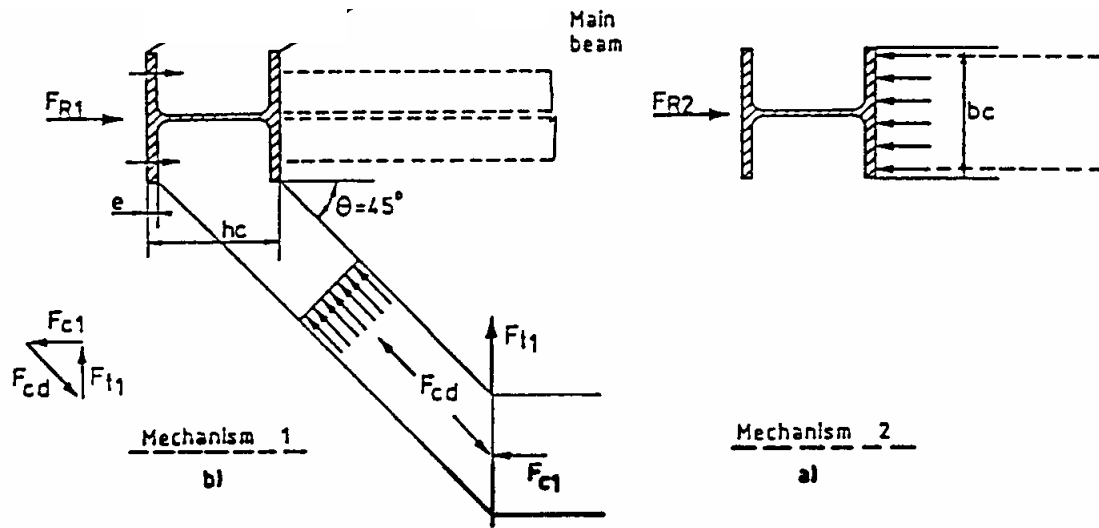


Figure 3.5.3. Two basic mechanisms of force transfer from the slab to the column

For mechanism 1, assuming an inclination $\theta = 45^\circ$ of the concrete struts:

$$b_o = (h_c - e) / \sqrt{2} \approx h_c / \sqrt{2}$$

$$f_{\text{strut}} = v f_{cd}$$

in EC2, 2 values of v may be found:

$v = 0.7 - f_{ck} / 200 \geq 0.5$ (f_{ck} in N/mm^2) for the shear strength of compressive struts in the transfer of shear in beams

$v = 0.4$ for the shear strength of the struts in the transfer of shear between web and flanges in T beams.

If $v = 0.6$ is chosen:

$$F_{cd} = 0.6 f_{cd} \cdot t_{\text{slab}} \cdot h_c / \sqrt{2}$$

$$F_{cl} = F_{cd} / \sqrt{2} = 0.3 f_{cd} \cdot t_{\text{slab}} \cdot h_c$$

$$F_{R1} = 2 F_{cl} = 0.6 f_{cd} \cdot t_{\text{slab}} \cdot h_c$$

$$F_{t1} = A_{s1} f_{sd}$$

By equilibrium, we have :

$$F_{t1} = F_{cl},$$

so that the section A_{s1} of re-bars transverse to the main beam should comply with :

$$A_{s1} \geq 0.3 \cdot t_{\text{slab}} \cdot h_c \frac{f_{cd}}{f_{sd}}$$

This section is distributed over a width equal to h_c . The minimal steel percentage is:

$$\rho_{sl} = \frac{A_{sl}}{t_{slab} h_c} \geq 0.3 \frac{f_{cd}}{f_{sd}}$$

For a C25/30 concrete and S500 steel,

$$f_{cd} = f_{ck}/\gamma = 25/1.5 = 16.7 \text{ Mpa and } f_{sd} = f_{sk}/\gamma = 500/1.15 = 440 \text{ Mpa.}$$

$$\rho_{sl} \geq 0.011$$

With material reduction factors γ taken equal to 1, the condition on the steel percentage becomes:

$$\rho_{sl} \geq 0.015$$

The proposed "seismic" reinforcement section A_{s1} is a transverse reinforcement ensuring the transfer of compression by strut and tie mechanism. In case of a real building resisting by moment frames in the 2 directions, it is easier to handle with identical sections in both directions. So, it has been decided that it would be better if the beam-to-column joints of the frames were designed with the same reinforcement around the column, longitudinal and transverse. And the proposed section is applied for longitudinal and transverse reinforcement. The corresponding layout of seismic re-bars is given at Figure 3.5.4.

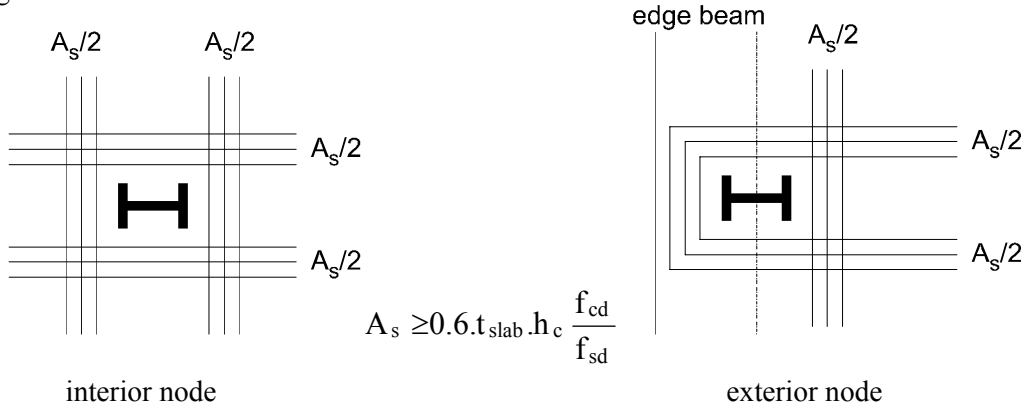


Figure 3.5.4. Layout of the Seismic re-bars

An additional comment can be made. Earthquake is an accidental action and a load factor $\gamma = 1$ for the actions at the time of the earthquake, including service load, is used, so that considering the reduced live load in earthquake condition, the steel computed for normal live loads may prove adequate to handle this earthquake requirement.

The design resistance F_{R2} of mechanism 2 simply is :

$$F_{R2} = \alpha f_{cd} \cdot t_{slab} \cdot b_c$$

F_{R2} is a rather concentrated force, which is spread through the width of the slab and induces a transverse tension force F_{t2} , which requires transverse anti bursting reinforcements. The spreading of force F_{R2} approximately takes place on a distance equal to half the effective width b_{eff} of the slab in current sections - Figure 3.5.5- and generate a transverse tension force F_{t2} which can be computed explicitly if b_{eff} is defined.

$$F_{t2} = \frac{F_{R2} b_{eff} - b_c}{4 b_{eff}} = 0.21 f_{cd} \cdot b_c \cdot t_{slab} \cdot \frac{0.15\ell - b_c}{0.15\ell} = A_{s2} f_{sd}$$

$$A_{s2} \geq 0.21 t_{slab} b_c \frac{0.15\ell - b_c}{0.15\ell} \frac{f_{cd}}{f_{sd}}$$

Assuming $b_c \cong 0.05 \ell$,

$$A_{s2} \geq 0.14 t_{\text{slab}} b_c \frac{f_{cd}}{f_{sd}}$$

The section of steel needed for F_{R2} should be realised with several re-bars spread in a zone width $0.6 b_{\text{eff}} = 0.09 \ell$, starting at a distance h_c of the column flange (Figure 3.5.6.). The steel percentage can be estimated:

$$\rho_{s2} = \frac{A_{s2}}{t_{\text{slab}} 0.09 \ell} \geq 0.08 \frac{f_{cd}}{f_{sd}}$$

For a C25/30 concrete and S500 steel,

$$\rho_{s2} \geq 0.003$$

With material reduction factors γ taken equal to 1, the condition on the steel percentage becomes: $\rho_{s2} \geq 0.004$

This percentage is low and effectively already covered by the reinforcements needed for the gravity and live load resistance.

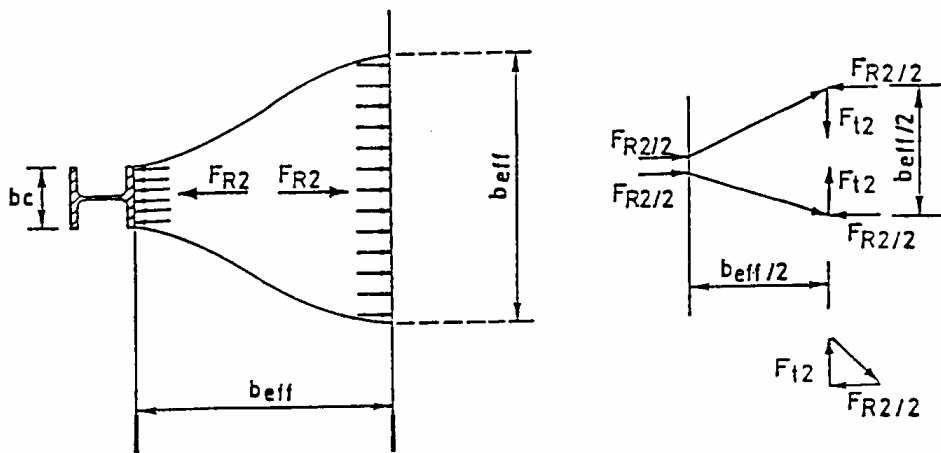


Figure 3.5.5. The spreading of F_{R2}

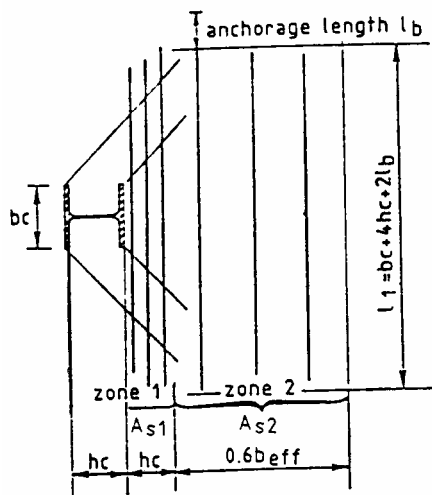


Figure 3.5.6. Re-bars A_{s1} and A_{s2} required by mechanisms 1 and 2

Without the presence of a transverse beam, the transfer of the compression force from the slab on the positive moment side can only take place through the two mechanisms described above. The highest resistance F_{Rd} offered at a beam-column connection can be estimated as the sum of F_{R1} and F_{R2} :

$$F_{Rd} = F_{R1} + F_{R2} = (0.7 h_c + b_c) \cdot t_{\text{slab}} \cdot 0.85 f_{cd}$$

Then, the effective width of concrete in the connection zone is, at the most :

$$b_{\text{eff,connec}} \cong (0.7 h_c + b_c) \cong 1.7 b_c \cong 0.085 \ell < b_{\text{eff}} \cong 0.15 \ell$$

$$b_{\text{eff,connec}} \cong 0.5 b_{\text{eff}} \quad (\text{with } b_c \cong h_c \text{ and } b_c \cong 0.05 \ell)$$

As the highest positive bending moment in the beam under earthquake action is precisely developed in the connection zone, this result means that :

- the connection section is the critical zone in which the highest strains are developed in both the concrete and the steel of the composite section ;
- the plastic moment of the composite beam in that section should be computed considering an effective width of concrete which is only $b_{\text{eff,connec}} = 0.085 \ell$

The plastic neutral axis of the composite section is thus lower in the beam end sections than in the mid-span sections and it is practically impossible that the ratio between the steel and concrete strains be such that the ductility criteria for the composite section could be satisfied ;

Considering the above evaluation, it can be concluded that, without the presence of transverse beams, it is not possible to develop a reliable composite plastic hinge at the end of the beams for positive bending moments. Without other force transfer than F_{R1} and F_{R2} the concrete in the beam-column connection zone will necessarily be crushed around the column after relatively low plastic rotations.

Transfer of the slab forces when a transverse beam is present

The transfer of the horizontal force from the slab into shear and bending of the column can be achieved in part by the resistance F_{R3} provided by transverse beams – Figures 3.5.7. and 3.5.8.

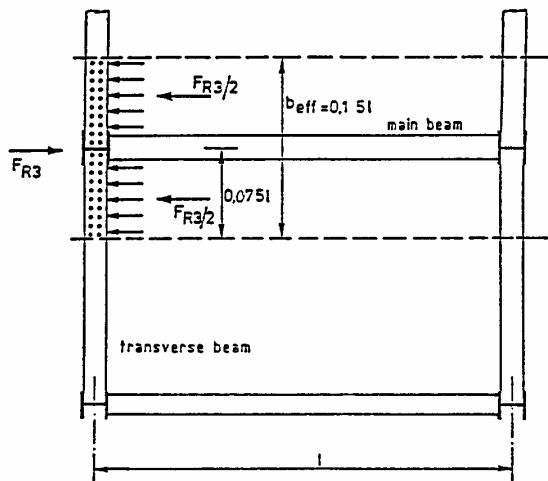


Figure 3.5.7. Transfer of Force F_{R3} from the slab to a transverse beam.

The horizontal force from the part of the slab facing the transverse beams can :

- mobilise a shear transfer between the slab and shear connectors placed on the transverse beam ; these connectors are then submitted to forces transverse to the transverse beam ;
- transmit these forces to the column, by means of shear, bending and torsion of the transverse beam.

An accurate calculation of these force transfers as well as the plastic resistance of the transverse beam is difficult because the stress state in the transverse beam is complex. However, for H or I section, because of their low torsion rigidity, we can estimate the stresses and F_{R3} if we ignore the web and consider that the torque is resisted only by non-uniform torsion. Then the only part of the section to be checked is the top flange, which is horizontally sheared and bent.

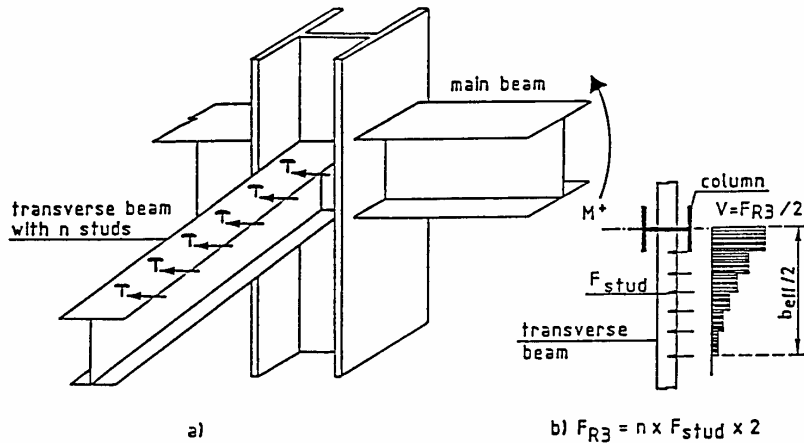


Figure 3.5.8. Transfer of slab compression to the transverse beam
a. general overview b. shear design

Synthesis on the transfer of slab forces under earthquake loading - positive and negative moments taken into account

Under earthquake loading at the connection of beams to column, there is not only a positive moment. At the same time, a positive bending moment, on one side, and a negative bending moment, on the other side, are transmitted to the column. This implies one transfer of forces from the steel part of the composite section, which take place through steel connecting elements and for which a design practice does exist, and another transfer of two forces F_{St} and F_{Sc} from the slab. F_{Sc} is the resulting compression force of the slab, on the positive moment side, while F_{St} is the resulting tension force of the re-bars, on the negative moment side.

To resist the F_{St} and F_{Sc} , two contributions F_{R1} and F_{R2} are always available and one, F_{R3} , depends on the presence of transverse beams and on their efficiency.

In a design option aiming at little degradation of the slab and yielding located essentially in the bottom flange of the steel section, the general design condition to fulfil is :

$$1.2 (F_{Sc} + F_{St}) \leq F_{R1} + F_{R2} + F_{R3} \quad \text{with } F_{R1}, F_{R2} \text{ and } F_{R3} \text{ given above.}$$

On the basis of practical design examples, the following conclusions have been established :

- it is possible to transmit most of the force from the part of the slab outside the column (compression on M^+ side and tension from the re-bars on M^- side) through the transverse beams ;
- if welded studs are used on transverse beams they may be one critical aspect of the design, because the required number of studs is high ;
- welded studs can be a satisfactory solution, if the tension force $F_S \ell$ from the longitudinal re-bars and the compression force from the slab are relatively low.

The simple addition of the resistances F_{R1} , F_{R2} and F_{R3} is rather coarse and may be incorrect; this static equilibrium solution only holds if the most rigid force transfer mechanisms are ductile enough ; it would not be the case if the concrete would crush on the flange of the column and bring resistance F_{R2} down to zero before a real force transmission takes place through the transverse beam.

However, the effectiveness of the force transfer through the 3 proposed mechanisms and especially through transverse beams has been observed in the Darmstadt and Ispra tests. These tests show that, within the limits of the dimensions of the test specimens, a force transfer corresponding to an effective width of $b_{eff}^+ = (0.6 \ell) / 4 = 0.15 \ell$ for the positive plastic bending moment and of $b_{eff}^- = (2 \times 0.4 \ell) / 4 = 0.2 \ell$ for the negative plastic bending moment, was effective. The weak points of this research is that no beam-to-column joints without transverse beam were included in the tests and that the design was such that the reinforcement under negative bending moment did not yield.

3.5.3. The concept of tension flange in reinforced concrete joints.

On the basis of several tests on reinforced concrete units, Paulay & Priestley (1992) postulated a mechanism for in-plane shear transfer in a slab of reinforced concrete frames to enable flange action to develop. He demonstrates by global and local equilibrium considerations that the enhancement of the resistance of the beam is mainly coming from the reinforcing bars of the slab in tension, from which the so called “tension flange”. The corresponding resisting mechanism is drawn at figure 3.5.9. At the negative bending side of the joint, the tension in the re-bars are transferred through a strut and tie mechanism to the core of the beam and equilibrated by the compression of the bottom part of the beam. These forces do not act in the same horizontal plane, allowing an additional bending moment to be resisted at that beam section.

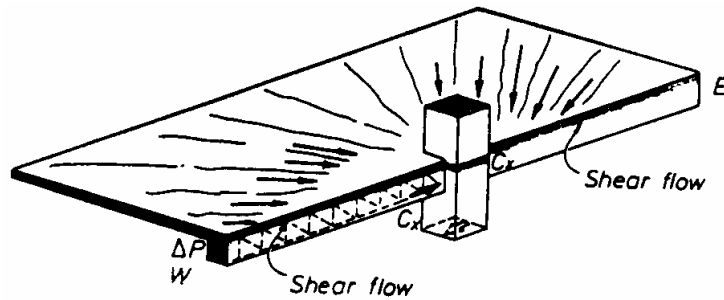


Figure 3.5.9. Behaviour of the slab as a tension flange

At the positive bending side, the anchored tension coming from the negative moment side is equilibrated by the same resisting scheme, but the compression is in the same horizontal plane and does not bring more bending resistance. The transverse beam is assumed to play a very small role in the transfer of forces and is even neglected. Paulay admit a small enhancement of the positive bending moment but not significant, because he assumes that the width of the compression flange is very limited around the column (Fig. 3.5.10). Another important consequence of the postulated mechanism is that the development of tensile forces in a (cracked) slab requires the simultaneous development of tensile transverse forces of comparable amplitudes. From which the idea that it is not possible to anchor additional forces coming from additional compression of concrete if the longitudinal and transverse reinforcement are of similar section.

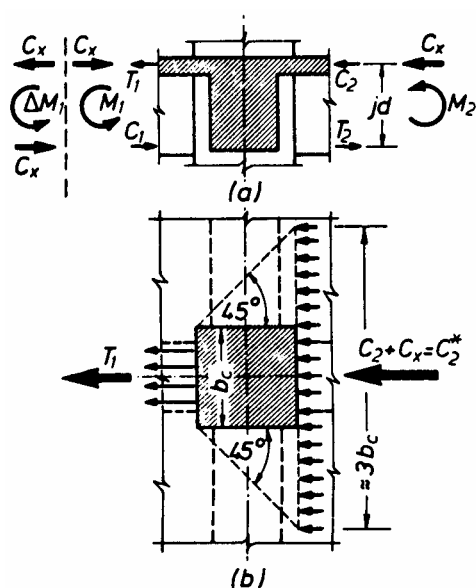


Figure 3.5.10. View of the loads transferred to the column

The detailed description of the model is given in Cheung et al. (1989).

3.6.MODELLING: Influence of a transverse beam in a typical composite steel concrete beam to column joint

C. Doneux

Department of Civil Engineering, University of Liege, Belgium

3.6.1.Description of the model

The finite element program, Castem 2000 developed at the "CEA-DRN/DMT/SEMT (Commissariat à l'Energie Atomique, France)", is used to perform the non-linear analysis of the composite structure.

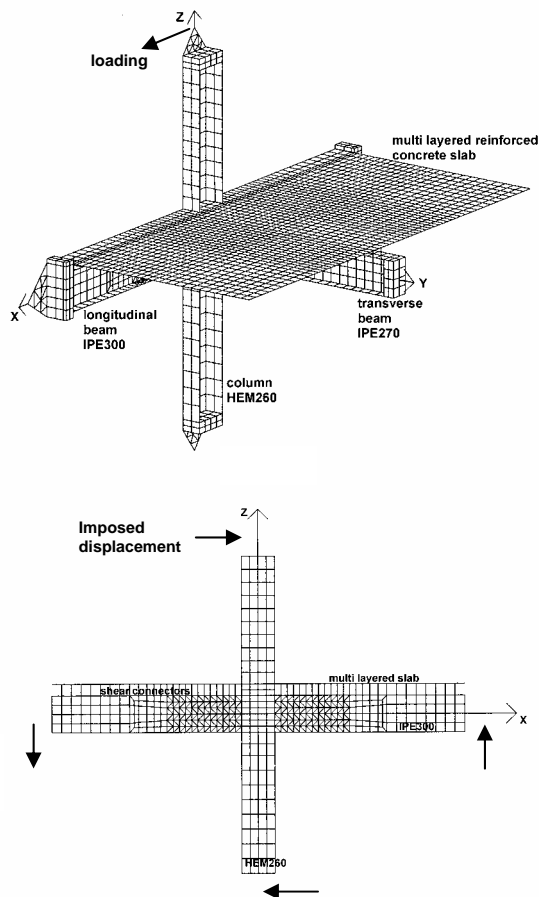


Figure 3.6.1. Mesh of the modelled beam-to-column node

The studied substructure is an interior beam-to-column joint, with or without transverse beam. Figure 3.6.1 gives a view of the mesh of the node. The node and its loading are symmetrical with respect to the axis of loading (Global axis X). So only one half of the node is modelled.

Most of the structural elements are modelled with 4 noded thin shells: column, longitudinal beam, transverse beam, stiffeners and reinforced concrete slab.

The contact between the slab and the column, characterised by the possibility of separation under negative moment and contact under positive moment, is modelled by using unilateral conditions of support.

The material laws of the steel elements are either elastic, or elasto-plastic according to whether they are likely to enter the non-linear field or not. The yield criterion is Von Mises with isotropic hardening. Certain typical plates of the test rig are coarsely modelled using elastic 8 noded bricks. The loading is carried out by a horizontal imposed displacement at the top of the column.

The slab is modelled with multi-layered thin shells, making it possible to take into account the flexural behaviour of the slab by the use of only one geometry with which is associated a set of layers in plane stress state, as shown in Figure 3.6.2.

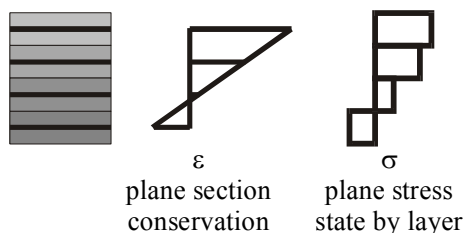


Figure 3.6.2. Multi layered slab assumptions

The layer of reinforcement is treated in the same shell as the concrete with plastic one-directional material laws.

The concrete model combines a Rankine fixed crack model for tension and an elasto-plastic law with Drucker-Präger criteria for compression. The failure criteria are drawn at Figure 3.6.3(a). In tension, there is cracking when one of the 2 principal stresses reaches the tension resistance of the concrete. The first crack in one integration point defines a cracking frame of reference and the only cracks then being able to appear form an angle of 90° with the first crack. Cracking involves a reduction in the shear strength taken into account by a reduction of the shear modulus. In compression, the theory of plasticity is used with associated flow rule and linear hardening rule. The damaged concrete (tension or crushing cracks) is regarded as a continuous medium with strain softening. The softening laws drawn at Figure 3.6.3(b) are linear and independent for the 2 directions of cracking. Compression is not possible as long as the tension cracks are open.

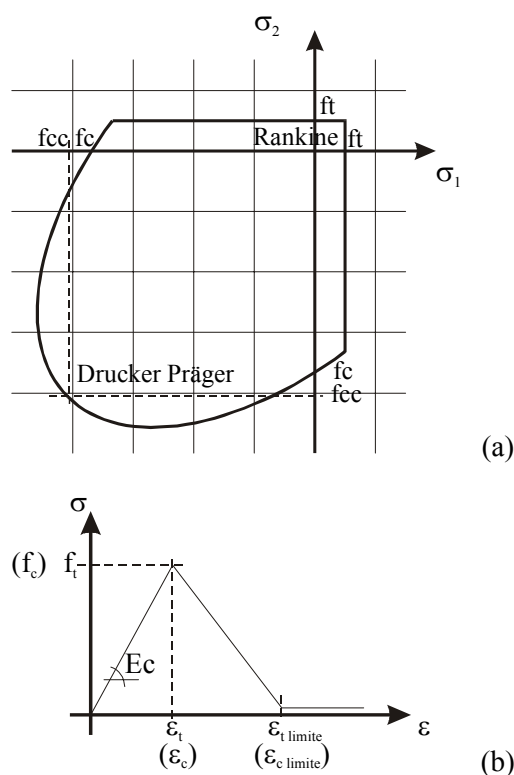


Figure 3.6.3. Concrete model
 (a) Failure criteria in the principal stress axes
 (b) Uniaxial behaviour – softening laws

This conceptually simple type of model presents some defects. The first one is that the use of a fixed crack model in tension coupled with a shear retention factor and a softening branch may lead to an overestimation of the true failure load. If the principal stress axes rotate after incipient cracking and

cease to coincide with the normal to the crack, the major principal stress may exceed the tensile strength in another direction. Neglecting this effect if straining of stress is important after the elastic loading may cause spurious stresses to occur and may result in overestimated collapse loads (Feenstra and de Borst (1995); Crisfield and Wills (1989)). The second defect concerns the localisation problem due to the softening branches. When the maximum resistance is reached and begins to decrease, the problem becomes ill posed from a mathematical point of view and does not have one single solution anymore. From a numerical point of view, that results in a loss of objectivity with respect to the mesh, i.e. a dependence of the results to the size of the finite elements called localisation. Our objective was to minimise the defects of the concrete model by the suitable choice of the parameters of the softening laws combined with a certain size of the finite elements.

Shear connectors are modelled by means of beam elements, connecting the higher flange of the beams and the neutral axis of the slab (its geometrical position). They are gauged on the basis of a shear force - slip law elastic perfectly plastic deduced from theoretical formulas. Equivalence is double: equivalent stiffness and equivalent resistance, given according to the number of modelled connectors compared to their real number. It is assumed that the strain profiles in the concrete and in the steel section are parallel, that means that there is no separation at steel/concrete interface and that the curvatures in each strain profile are the same. This assumption is translated in the model by equalising the rotations of the ends of the connectors.

The second order effects due to out of plane large displacements of shell elements to incorporate the possible buckling of the steel section under compression are neglected at this stage.

3.6.2. Calibration of the basic model.

The basic model is calibrated on a welded subassembly tested at Darmstadt (WR-X, see section 3.4.). The sensitive points of the model are the characteristics of the slab and the characteristics of the shear connectors. The influence of changing these parameters is presented hereafter.

Shear connectors – influence of initial stiffness

The influence of the stiffness of the connectors on the global response of the node is estimated by comparing the experimental behaviour of the composite beam with one modelling of the bare steel node and two modellings of the composite nodes in which the concrete remains elastic, one with flexible shear connectors and the other with rigid connectors.

Figure 3.6.4 shows the experimental curve and the 3 computed curves. The stiffness of the connectors is deduced from empirical formulas by Oehlers and Bradford (1995). In our case, it gives $K_{flex} = 35 \cdot 10^6$ N/m. The rigid studs have a Young's modulus 100 times greater than the steel modulus, which corresponds to a stiffness $K_{rig} = 1080 \cdot 10^6$ N/m $\cong 30 \cdot K_{flex}$. The upper part of the figure shows the behaviour of the composite beam under positive bending moment and the lower part of the figure is the behaviour of the composite beam under negative bending moment. M/L is the moment in the beam divided by the span, that is the reaction at the end of the beam. D_{top} is the imposed displacement at the top of the column.

It is observed that for the elastic part of the curve, the experimental curve corresponds better to a steel node than a composite one, whatever the sign of the loading is. The stiffening due to composite action begins afterwards, after some deformation has taken place in the connectors and in the concrete slab.

Under positive bending, no difference is observed between the modellings with rigid and flexible connectors. This is due to the configuration of the test specimen. At the ends of the beam, a plate goes through the thickness of the slab. Under the positive moment, this plate bears on the slab and plays the role of a big shear connector, which transmit a part of the shear from the steel beam to the slab by direct compression. The role of the connectors and the influence of their rigidity are here minimised. This first observation brings to the fore that it is important to be careful with the boundary conditions of the slab when testing composite sub-structures; a small detail like a plate, used in a short specimen, may change the response of the studied element.

Under negative bending moment, this extended end plate does not act on the slab and the stiffness given to the shear connectors influences the response of the node. After the initial loading, which follows the steel behaviour, the experimental stiffness is then similar to the initial stiffness obtained by

the modelling with flexible connectors. It confirms that the use of a very high rigidity for the connectors is not realistic and it is chosen to work with the empirical value proposed in Oelhers and Bradford (1995).

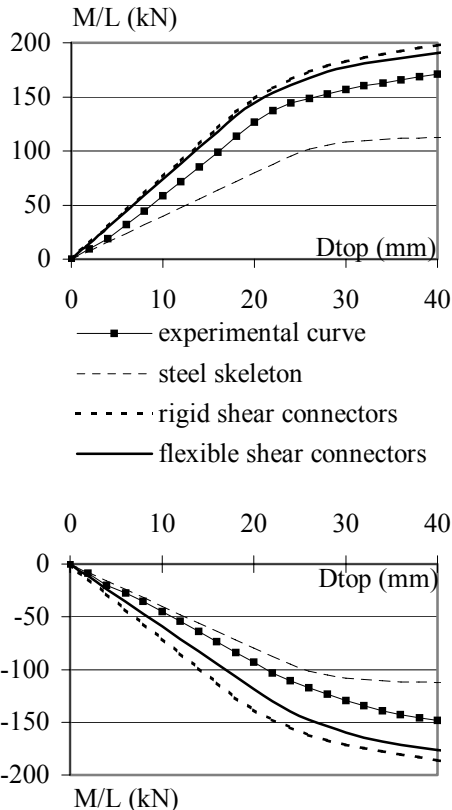


Figure 3.6.4. Global behaviour of the node – influence of the flexibility of the shear connectors

Localisation – concrete softening.

Figure 3.6.5 shows the softening curves in function of the ultimate strain for tension and compression superposed with the uniaxial compressive concrete law proposed in Eurocode 2.

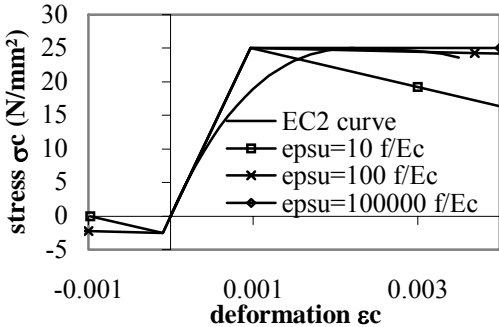


Figure 3.6.5. Softening curves for concrete compared with EC2

Different values of the ultimate strains have been tested, from very slow decreasing softening branches ($\epsilon_{ultimate} = 10^5$ resistance / E_c) to very sharp softening branches ($\epsilon_{ultimate} = 10$ resistance / E_c). The same concrete is used for the whole slab and a shear retention factor (β) of 0.1 is considered.

Table 3.6.1 gives an idea of the convergence problems met. “No convergence” means that no converged solution has been found with the used algorithm.

Table 3.6.1. Convergence in function of the ultimate strain of the concrete softening branches

Tension $\frac{\varepsilon_{tu}}{f_t / E_c}$	Compression $\frac{\varepsilon_{cu}}{f_c / E_c}$	Convergence until Dtop equal to.
10	10	22 mm
100	10	47 mm
50	50	58 mm
10	100	96 mm
100	100	94 mm
10^5	10^5	> 140 mm

The smaller the ultimate strain is, the bigger the convergence problems are. A small compressive ultimate strain gives more problems of convergence than a small tensile ultimate strain. This is due to the fact that when the concrete loses its tension resistance, reinforcements are present to continue to resist, which is not the case where the concrete is highly stressed in compression, because it is located in front of the column flange and is not reinforced in the direction of the largest compression stresses. When the softening begins in compression, the high non-linearity is difficult to be treated by the solver.

Localisation takes place where the concrete is highly stressed and the damage occurs in these zones without being able to spread. The distribution of damage in the slab is drawn at Figure 3.6.6 for two top displacements. One may see that there is a spreading of the damage at the tension side (left side), but under compression (right side), the spreading of damage is not so important.

This localisation in compression corresponds to some reality since the specimen experienced crushing of the concrete just in front of the column flange and on the bearing line of the inclined compressive struts.

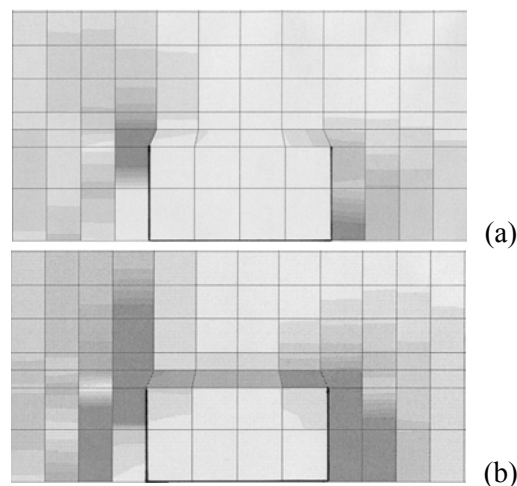


Figure 3.6.6. Distribution of damage in the concrete slab
(a) Dtop = 40 mm (b) Dtop = 80 mm – $\varepsilon_u = 100 f/E_c$

Because of the localisation, the dimension of the elements of the mesh influences the results. Larger elements are favourable for the global response in the sense that localisation takes place in a larger element, with a mean stress smaller than in a smaller element. The greater the ultimate strains are chosen and the greater the reinforcement percentage is, the lower is the influence of the mesh size. The calibration of the concrete ultimate strains is therefore directly linked with the dimensions of the mesh elements. One element of one size associated with a certain decreasing softening branch will be able to achieve full cracking for a certain fracture energy. The released energy by unit damage area is the important parameter. If we make the assumption that it has to be constant in the modelled medium, it

is clear that in one larger element, the ultimate strain has to be smaller to dissipate the same energy than in a smaller element. It has to be taken into account in the further parametrical studies. The final refinement of the mesh was finally also linked with the possible performance of the computer.

Figure 3.6.7 gives the numerical moment rotation curves obtained with different values of the ultimate strains compared with the experimental results. It is seen that the converged global behaviour is not drastically changed by the values of the ultimate strains. Greater values allow going further in the calculations and with a greater resistance but the greater resistance is some how artificial. The choice of high values of ϵ_u is practical to overcome the numerical problems, but it has an implicit signification: it artificially confines the concrete. The fitting of the numerical results with a high $\epsilon_{ultimate}$ ($= 10^5$ resistance / E_c) with the experimental curve is rather good in spite of a rather unrealistic choice of the concrete parameters. Two reasons for this:

- there is real confinement at some places.
- the slab is well reinforced, decreasing the influence of the properties given to the concrete. The reinforcement resists if the concrete is out.

The drawback of slow decreasing branches is that the real failure point is impossible to be found, because failure is never reached.

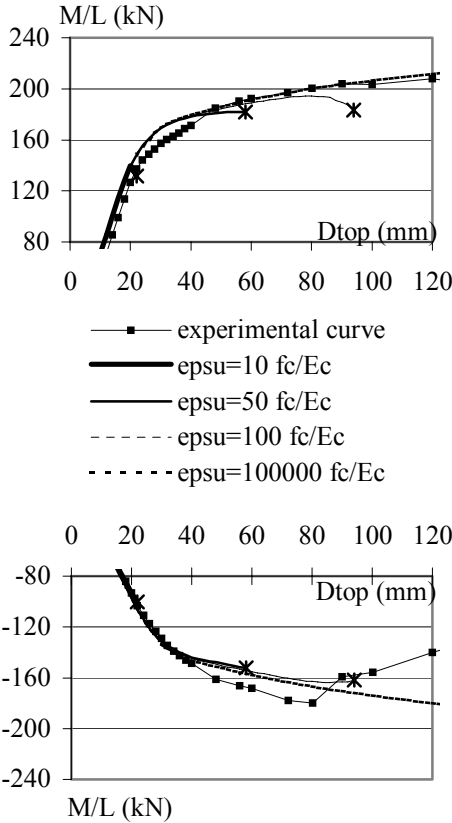


Figure 3.6.7. Global behaviour of the node – Influence of the ultimate strains – $\beta = 0.1$ – no confinement

So, a real confinement can be justified at some places, as for the concrete inside the column walls and for the concrete directly compressed on the column flange if adequate transverse re-bars are present. The degree of confinement is not clearly defined. The lateral restraint is quantifiable with the percentage of transverse re-bars in front of the column flange, but the vertical one is more subjective, depending on the transverse re-bars by a chain mechanism and also on possible friction on the column flange. Figure 3.6.8 gives an idea of how the confinement may take place in the studied structure.

Instead of taking the unrealistic high value of the ultimate strains in concrete, it is chosen to take a lower value of ϵ_u and to add confinement around the column. The confinement of concrete is not inherent in the concrete law because the law is bi-dimensional. Confinement has to be incorporated a

priori in the concrete elements around the column. The values of the basic ultimate strains are finally chosen equal to $100 f/E_c$.

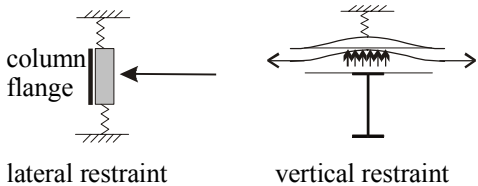


Figure 3.6.8. Confinement of the concrete bearing against the column flange

The addition of confinement with a resistance of 1.3 times the basic resistance of concrete and an ultimate strain 1.9 times greater than the ultimate strain of the unconfined concrete gives the best fitting between the numerical and the experimental results, especially under positive moment. Under negative moment, the influence of confinement is not so important, as it is seen in Figure 3.6.9. This choice gives a good compromise between reality and the constraints of the concrete model, and it allows finding a failure load.

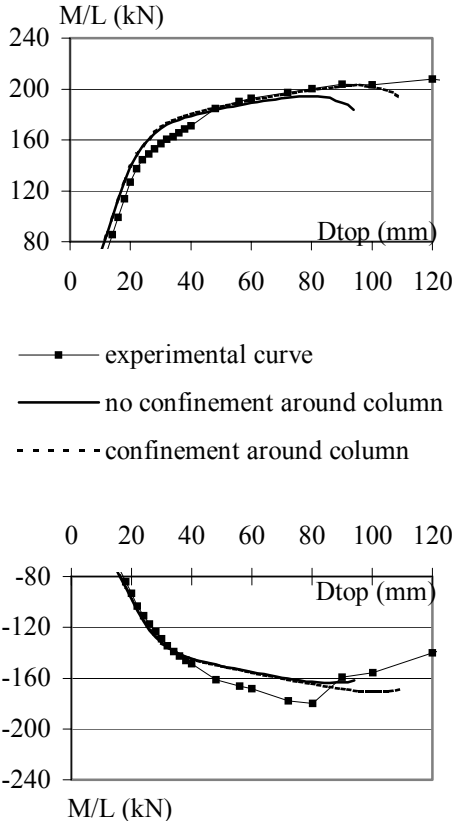


Figure 3.6.9. Global behaviour of the node – Influence of confinement around the column – $\beta = 0.1 - \epsilon_u = 100 f/E_c$

The shear retention factor has been taken equal to 0.1. This value is not a physically logical choice. A cracked reinforced concrete could still transfer by shear more than 0.1 times its initial shear capacity. Friction along the 2 sides of the crack and dowel action could give a capacity of $\beta = 0.4$ to 0.5 (Hand et al. (1999)). But here it is a way to diminish the possible spurious over resistance due to the fixed crack model. Figure 3.6.10 shows that under positive moment, the load capacity is unchanged when taking $\beta = 0.5$ instead of $\beta = 0.1$. Under negative moment, the greater stiffness due to the greater shear modulus is conserved until the maximal studied displacement. This can be explained by the following

facts. In zones of compression (as under $M > 0$), the tensile cracking is not so important than in zones of tension. As the plastic tensile stresses remain in the same direction as the elastic stresses, the influence of β is small and diminishes with loading. In tensile zones (under $M < 0$), the principal stress axes rotate during loading, the new principal stresses are not detected and the tensile resistance does not decrease.

The shear resistance difference remains during further loading.

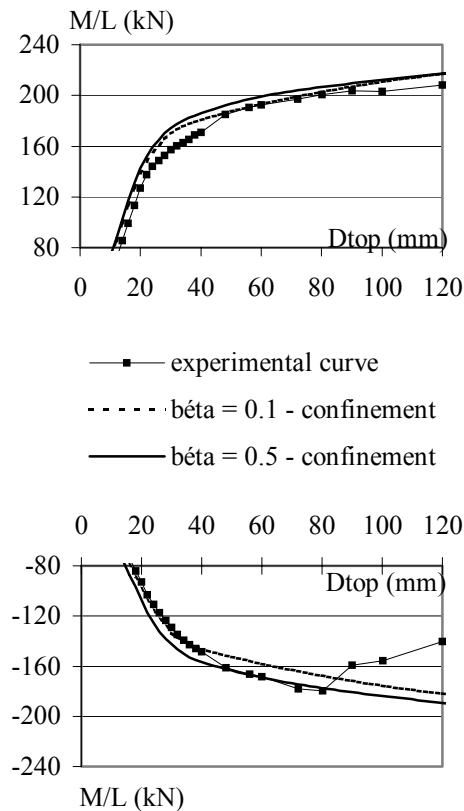


Figure 3.6.10. Global behaviour of the node – Influence of the retention shear factor $\beta - \epsilon_u = 10^5 f/E_c$

Finally, the calibration made to fit with the experimental global curve and to reduce spurious over strength and localisation due to the concrete model comes out with the following values of the parameters of the concrete law:

- a low shear retention factor $\beta = 0.1$
- slow decreasing softening branches with a zero resistance for an ultimate deformation greater than or equal to 100 times the elastic deformation (resistance/Young's modulus) combined with elements of 5 (to 10) by 5 (to 10) cm.
- confined concrete in and around the column.

3.6.3. Partial parametric study

A series of typical parameters of the composite beam has to be tested through the model. The most important are:

- the influence of the percentage of reinforcements
- the influence of the shear connectors
- the influence of the cross beam
- the influence of the ratio thickness of the slab to height of the steel beam.

Program of simulation

The first parametric investigation is made to set forward the involvement or non-involvement of the transverse beam in the transfer of moment at the node. To reach this goal, a series of numerical simulations has been performed, using different combinations of the material parameters. Only some results are presented because the trend is always the same.

The reference node is the Darmstadt node, but the configuration of the test set up is improved by taking a longer specimen without plates at the free edges of the slab.

At this stage, the concrete model is adequate in the case the slab has sufficient reinforcement to minimise the cracking. With a not or very little reinforced slab, the fixed crack model could overestimate the resistance. The slab is therefore unchanged (same thickness – same re-bars – same mesh) because of the uncertainty to use the concrete law in a predictive manner. Figure 3.6.11 presents four studied configurations.

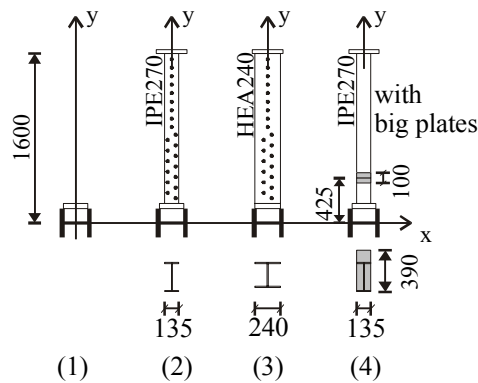


Figure 3.6.11. Configurations of the cross beams

- (1) no cross beam
- (2) cross beam IPE270 with studs
- (3) cross beam HEA240 with studs
- (4) cross beam IPE270 with big plates

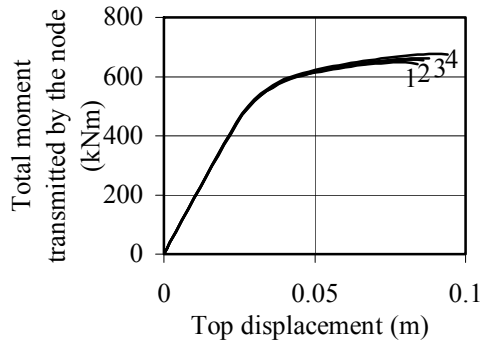
Discussion of the results

The comparison of the different results presented in Figure 3.6.12 does not show a big increase of the resisting moment of the main composite beam due to the addition of a transverse beam. Table 3.6.2 gives the increase of performance of the longitudinal beams in the different configurations in terms of maximal moments. The most rigid transverse system (simulation 4) gives a maximal increase of 4.4 %, which is very small. In terms of plastic moments, this increase would be smaller.

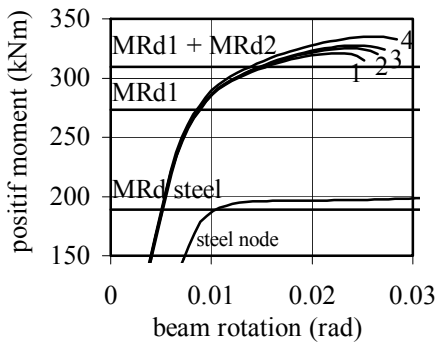
Table 3.6.2. Performance of the longitudinal beams.

	M^-_{max}	Increase	M^+_{max}	Increase
Simul 1	291		321	
Simul 2	294	+1.0 %	325	+1.2 %
Simul 3	297	+2.1 %	328	+2.2 %
Simul4	303	+3.1 %	335	+4.4 %

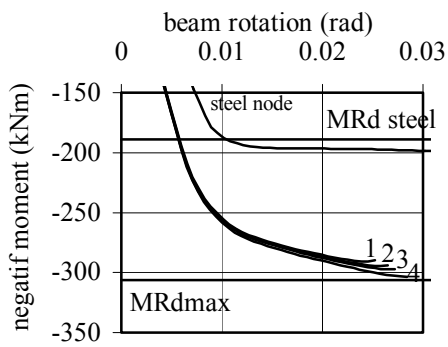
Mechanisms 1 and 2 are clearly present because the corresponding positive plastic moments are reached. Mechanism 3 exists but is not sufficient to increase the resistance capabilities of the composite beam.



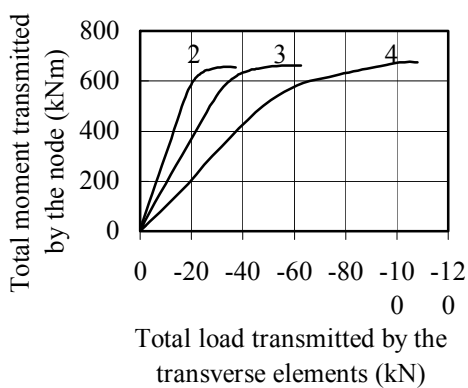
(a)



(b)



(c)



(d)

Figure 3.6.12 (a) Total moment versus top displacement
 (b) Positive moment versus beam rotation
 (c) Negative moment versus beam rotation
 (d) Total moment versus total load transmitted by the transverse elements (shear studs or big plates)

The transverse beam is supposed to resist the torque induced by the loads coming from the slab by

non-uniform torsion. Practically, it corresponds to the flexural bending of the upper flange of the transverse beam. The position of this upper flange, which is supposed to transfer the additional force to the column is located at the same level as the upper flange of the steel longitudinal beam. If the neutral axis of the main beam lies in the neighbourhood of this upper flange, the additional force will not contribute to increase significantly the plastic moment of the composite section. On the other hand, the order of magnitude of these additional forces is low. Under a positive bending moment of 310 kNm calculated with an effective width of $b_c + 0.7 h_c$ due to the resistance of mechanism 1 and 2, the neutral axis lies in the upper flange of the IPE300 and the resultant compression force in the concrete or tension force in steel is about 1200 kN. The maximal forces transmitted by the transverse beam are 40 kN for the IPE270, 75 kN for the HEA240 and 110 kN for the "big plates" (see Figure 3.6.12(d)), that is 30 to 11 times less than 1200 kN. So, even if these cross beam forces were placed at a greater distance of the neutral axis of the section, they would not increase much the resisting plastic moment. This situation is also linked with the fact that the dissipation of energy takes essentially place by extensive yielding of the bottom steel parts of the section. When the transverse beam could begin to play a role in the resisting scheme, the bottom steel fibre is yielded and its hardening is not sufficient to allow for a big increase in the transferred forces. The forces transmitted by the transverse beam increase but the total moment transmitted is constant – figure 3.6.12 (d).

Another limit to the maximal transferable load is the yielding of the upper flange of the transverse beam at its fixed end. No yielding was observed in the simulations with transfer of forces by studs (simul2 and 3). In simulation 4, the way to transfer the cross forces is slightly different. Because the plates stiffen the H profile on its whole height, the lower flange of the transverse beam is also involved in the transfer of load to the column. The force is concentrated at the plates and not distributed along the whole length of the transverse beam. The corresponding bending moment in the upper flange is consequently far higher for the same total transmitted load. Yielding of the upper flange occurred for a relatively low value of the transmitted force of 39 kN and a total moment at the node of 369 kNm. This problem of yielding is however more a secondary problem that can be bypassed by taking a section with larger upper flange and/or by increasing the yield resistance of the steel of the transverse beam.

For information, Figure 3.6.13 gives the distribution of the transverse forces transmitted by the shear studs in simulation 2 and 3 for a total moment at the node of 600 kNm. It shows clearly that the high densities of studs have to be placed (if needed) just near the column, not further than 50 cm of the column axis.

To maximise the efficiency of a transverse element and increase the moment transmitted to the column, the transfer of load should be at a level superior to the presumed neutral axis of the main beam and it should not be transferred by an element in torsion as a H beams. Only specific design, like horizontal cantilever beams covering the full depth of the slab and directly fixed to the column, would realise an effective mechanism 3.

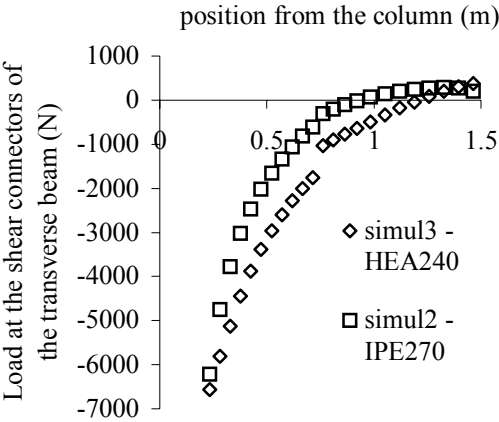


Figure 3.6.13. Distribution of the forces transmitted by the shear connectors on the transverse beam. $M_{tot} = 600$ kN

The work now under way considers the simulation of a node with transverse beam and without concrete around the column. The superposition of the 2 responses (with and without concrete around the column) would give the envelope of the total response of the node. The cross beam mechanism is clearly more flexible than the rigid mechanisms 1 and 2. It could demonstrate whether the transverse beam is necessary or not to ensure ductility of the beam, in the sense that when mechanism 1 and 2 are consumed and the resistance drops by crushing of concrete, mechanism 3 may be activated and supply some resistance. The simulation of exterior beam-to-column joints is also under way because in exterior node, where the compression of concrete on the column is not present, the influence of a transverse beam exists and has to be quantified.

3.6.4. Conclusions and future research

A first step has been made to model typical beam-to-column steel-concrete composite nodes and some results have been obtained.

The simple fixed crack model for the concrete in tension and the Drucker-Präger plasticity model for the concrete in compression have been used. A calibration of the parameters of these models has been made, so that relatively good agreement is obtained between calculation and experimental results. Until now, the applicability of the model is not certain for cases where strong degradation of concrete and yielding of steel would take place at the top of the section, since all the research work made and the experimental results obtained consider the design option in which the slab is not damaged and yielding takes place at the bottom part of the section. A certain confinement had to be taken into account in and around the column. Only this confinement and the accordingly increased ultimate strain can explain the plastic resistances observed. This is a first important result set forward by the numerical modelling presented here.

The role of the transverse beam has been studied. The conclusion is that its role is not as important as it was expected. This mechanism of resistance is far more flexible than the direct compression of the slab on the column flange and the inclined compressive struts at the sides of the column (mechanisms 1 and 2). The need of deformability to activate the third mechanism is so important that crushing of concrete takes place before on the column face. Also, the possibility of transferring a big force through a transverse beam working in non-uniform torsion without yielding the upper flange is small. The great plastic moment that is observed under positive bending moment is more due to confinement than to the presence of a transverse beam. Only specific design, like horizontal cantilever beams covering the full depth of the slab and directly fixed to the column, would realise an effective transverse beam mechanism. A further modelling isolating the cross beam mechanism in a beam-to-column joint without any direct compression of the slab on the column faces will be realised to study this detail.

A more complete study, considering different slab design, with different reinforcement ratio and different slab depth to beam depth ratio, is also foreseen. It will probably require a better model for concrete, especially concrete in tension; it is expected that a rotating crack model or even a plasticity model in tension would solve the over resistance problems and lead to more realistic ultimate loads.

3.7. BEHAVIOUR FACTORS. Particularities raised by the evaluation of load reduction factors for seismic design of composite steel-concrete structures

L. Sanchez

Department of Civil Engineering, University of Liege, Belgium

3.7.1. Introduction

Structures submitted to earthquakes can dissipate a substantial part of the input energy in plastic mechanisms. Structural reduction factors are used to characterise this ability of structures and to allow a static elastic analysis of the structures under earthquake forces reduced by these factors.

For composite structures there is a lack of estimation of reduction factor, especially in EC8, and the debate in Europe is open. In spite of the fact that the gaps in the knowledge of the seismic performance of composite structures are important, some attempts have been made to estimate values of reduction factors for the code.

The next paragraphs bring up the background of EC8 in order to remember that code behaviour factors are more related with simplified methods and with experience than with the non-linear analysis of MDOF systems.

Later on we are going to address some problems of definition when trying to estimate code behaviour factors by using non linear dynamic analysis of MDOF system, that have relevance when trying to estimate code behaviours factors for composite structures.

3.7.2. Force reduction in EC8.

We are going to use the notation $R_{\text{factor}} = \frac{S_{a,e}}{S_{a,d}}$, reduction factor, to represent the ratio between the elastic design response spectra, $S_{a,e}$, and the inelastic one, $S_{a,d}$. In EC8, this ratio depends on the period of the structure, the soil profile, damping and the behaviour factor.

$$R_{\text{factor}} (T, \text{soil profile, damping, behaviour factor} \equiv q(\text{structural typology})) = \frac{S_{a,e}}{S_{a,d}}$$

Behaviour factor, q , is a parameter used in EC8 related with the structure typology and, for moment resistant steel frames, its value depends on the plastic redistribution parameter of the structure. The behaviour factors given in the code have been established by engineering judgement and experience.

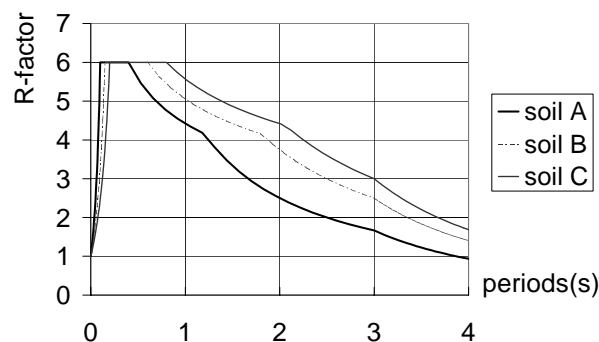


Figure 3.7.1. - Ratio between elastic and inelastic design spectra in EC8, for moment resistant steel frames.

The values of R-factor given in EC8 for steel structures are related with simplified methods based on the ductility factor theory, using the background of the non-linear dynamic analysis results of SDOF systems. The decreasing branch for $T > T_c$ has no connection with the computed R-factor for SDOF systems; it is related with a more conservative criteria than for low rise buildings, because in tall buildings non global mechanisms are more likely to appear, and second order effects are higher than in

low rise structures.

Although inelastic spectral techniques are not rigorously applicable to MDOF systems, the code practice that allows static elastic analysis instead of several non-linear dynamics ones, acquires sense throughout the code detailing rules. In EC8 specific rules for steel-concrete composite structures exist in an informative annex; they follow closely those given for steel structures because at the time they were written, there was a complete lack of more ductility based design rules.

R-factors in codes must account not only for the reduction in the maximum base shear due to the capacity of the structure to dissipate energy, but also for the load redistribution capacity of the structural system. For SDOF system the force reduction related with energy dissipation is increasing with the structure period –for short periods- and ductility, and depends strongly on the frequency content of the ground motion.

The over-strength of the code designed structures seems to be decreasing when increasing the period, for short periods, but the global ductility decreases when increasing the plastic redistribution parameter. In an indirect manner the codes account for these influences, but they are mixed and thus it is not easy to know what the code parameters physically represent.

3.7.3. Estimation of reduction factor using MDOF analysis.

Simplified methods based on ductility factor theory, methods based on energy approach, and methods based on the dynamic analysis of SDOF system or on the dynamic analysis of MDOF system are used to try to evaluate the reduction factor. The scatter of results from different methods can be important.

One way to check the reliability of a code is to design a set of structures according to the code, and compute reduction factors with methods based on the inelastic dynamic analysis of MDOF system, but the comparison with the code will always be difficult, not only because of the scatter of results for different methods, because of the use of different definitions of collapse, because of the difference in the designed structures and ground motions selection, but also because code reduction factors values include implicitly the safety level that has been adopted.

In order to establish reduction factors, there are methods based on the results of MDOF non-linear analysis that relate the acceleration multiplier at collapse, a_c , with the acceleration multiplier at first yield, a_y . The use of the earthquake acceleration multiplier at collapse and first yield instead of variables related with the internal force of the elastic system and the non-linear one at collapse comes from the Ballio and Setti method for SDOF system. It is assumed that the maximum internal load of the structure during the dynamic analysis remains constant for values of acceleration multipliers higher than the acceleration multiplier corresponding to first yield of the structure.

$$R_{\text{factor}} = \frac{a_c}{a_y} = \frac{S^{\text{elast}}(a_c)}{S^{\text{elas}}(a_y)} = \frac{S^{\text{elast}}(a_c)}{S_y^{\text{plas}}(a_y)} = \frac{S_c^{\text{plas}}(a_c)}{S_y^{\text{plas}}(a_y)} \frac{S^{\text{elast}}(a_c)}{S_c^{\text{plas}}(a_c)}$$

$\frac{S^{\text{elast}}(a_c)}{S_c^{\text{plas}}(a_c)}$ is related with the reduction of maximum shear due to energy dissipation.

$\frac{S_c^{\text{plas}}(a_c)}{S_y^{\text{plas}}(a_y)}$ is related with $\frac{\alpha_u}{\alpha_1}$; $\frac{S_c^{\text{plas}}(a_c)}{S_y^{\text{plas}}(a_y)}$ comes from the maximum shear in the dynamic analysis,

and $\frac{\alpha_u}{\alpha_1}$ from the static push-over. When $\frac{S_c^{\text{plas}}(a_c)}{S_y^{\text{plas}}(a_y)} \approx 1$, $R_{\text{factor}} = \frac{a_c}{a_y} \approx \frac{S^{\text{elast}}(a_c)}{S_c^{\text{plas}}(a_c)}$

In EC8, for steel moment resistant frames, for eccentric braced frames and for dual structures, $q = N \cdot \frac{\alpha_u}{\alpha_1}$ represents the behaviour factor of the structure, where N is a constant, and $\frac{\alpha_u}{\alpha_1}$ the

structure plastic redistribution parameter. It is the only expression of the code that in some manner distinguish a part of the behaviour factor related with the structural over-strength and another that

could be related with global ductility -the behaviour factor of the code are related with $R_{\text{factor}} = \frac{a_c}{a_y}$

only for the medium periods-. But it is difficult to understand the physical meaning of this expression. For example, the fact that for moment resistant steel frames higher plastic redistribution parameters lead to lower values of global ductility is not taken into account in this expression. It is also difficult to understand how $\frac{\alpha_u}{\alpha_1}$ and N , can be used later on together as a whole, in the expressions of the inelastic design spectra where q seems to be used as a global ductility of the structure.

3.7.4. Behaviour factor for composite structures.

An attempt is made in Europe to improve the code provisions in EC8 for steel-concrete composite structures. In this context, code behaviour factors for composite structures must be evaluated. Here two comments are made that could be relevant when evaluating behaviour factor for composite structures by using MDOF analysis.

Sensitivity of the reduction factor to the definition of structure first yield.

The definition of structure collapse is a problematic matter. Generally no attention is paid to the definition of first yield of the structure and it is usually difficult to find in the papers how the authors have defined the first yield of the structure.

Commonly it is considered first yielding of the structure the attainment of the first plastic hinge. In EC8, first yield of the structure is related with the attainment of the plastic moment in the most stressed section; this definition at the local level instead of a definition of first yield from the global behaviour of the structure, besides its drawbacks, has the advantage to allow an elastic linear analysis and to avoid a non-linear static one. When modelling the structure using concentrated plastic hinge with bilinear diagrams, the attainment of the first hinge and the attainment of the plastic moment become the same. When modelling composite structures using fibres in the section, or when modelling semi-rigid joints by a high non-linear empirical relationship, it is not so evident what the first yield of the structure is. It could be seen in the literature how the yield moment is used, or how other improvised definition of first yield of the structures are used when evaluating reduction factors (because is necessary to define something). The definition of first yield has a high influence in the computed reduction factor especially when the shape factor of the beam section is high. This is the case of composite structures using T beams made of a steel profile and a collaborating slab and thus, when trying to compare computed R_{factor} values with the code ones, or when comparing R_{factor} computed by different researchers, or when comparing steel and composite structure performances, attention must be paid to the definition of first yield used. This is shown with the simple next example.

Example

We run two non-linear dynamic analyses for two structures of three storeys and one bay, having the same columns and where the only difference between the structures is the shape factor of the beam sections. The first structure has IPE300 in the beams and in the second structure, the beams are computed T section having the same inertia and the same plastic moment, but a different shape factor; the masses are the same for the two structures. The periods of the two structures are the same with value $T=0.8$ s. The values of the shape factor of the beam section are $sf_1=1.12$ and $sf_2=1.79$.

The two structures have been modelled using fibre elements in the places where the plastic hinges are likely to appear, and using elements with concentrated plastic hinges for the rest.

In order to establish the first yield of the structure, four definitions of the moment curvature diagram of the sections have been used. The first one is considering first yield of the structure when the yield moment (M_y) is attained in one section. The second definition is considering the recommended definitions of the ECCS for testing, with two tangents to the curves, the first at the origin and the second one with a slope of ten percent of the slope of the first (MECSS). The third is to take two tangents to the curve, one at the origin and the second horizontal (M.bilinear). And the fourth definition is to consider an energy approach equating areas (M.energy).

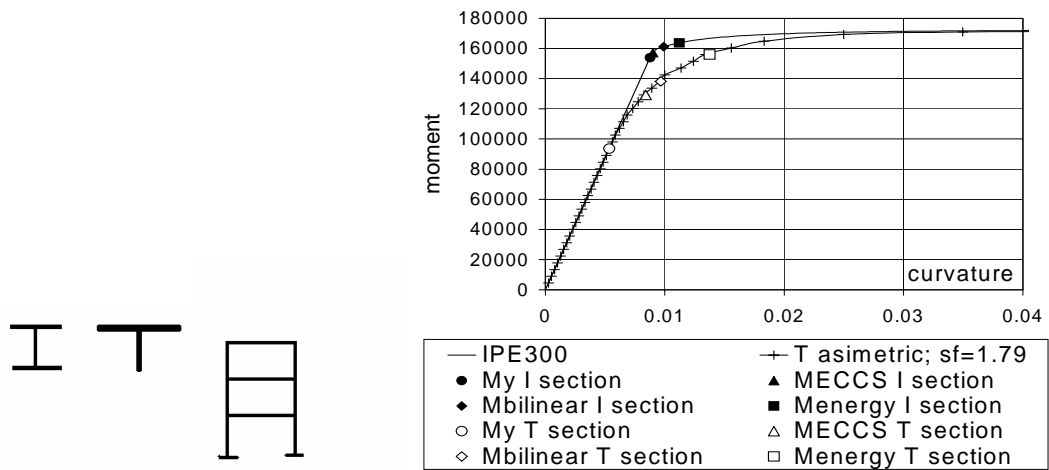


Figure 3.7.2-Moment-curvature for T sections and I.

The graphic of figure 3.7.3 represents the maximum curvature of the element that yields first for the two structures versus the acceleration multiplier of the earthquake as they are established by a set of non-linear dynamic analysis. The behaviour of the two structures is very similar, at global and local levels.

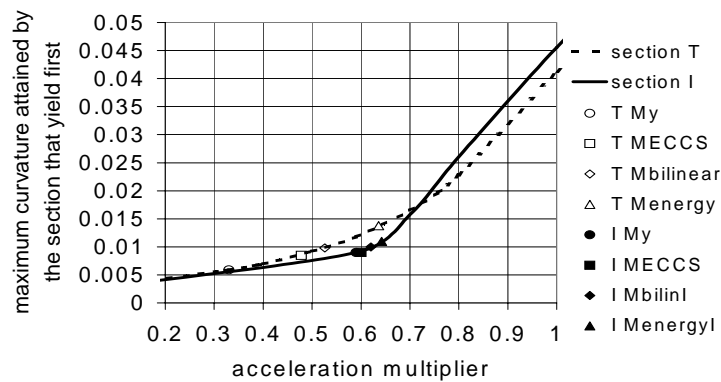


Figure 3.7.3- Yield acceleration multiplier corresponding to different definitions of first yield.

In the following table, we give the values of the yield acceleration multiplier, λ_e , ultimate acceleration multiplier, λ_u , and R_{factor} using the four definitions above: My, MECCS, Mbilinear and Menergy.

Table 3.7.1

	definition	λ_u	λ_e	R-factor	R(definition)/R(energy)	R T section/R I section
T section	My	4	0.33	11.45	1.93	1.78
	ECCS	4	0.48	7.91	1.33	1.25
	bilinear	4	0.53	7.19	1.21	1.18
	energy	4	0.64	5.94	1.00	1.01
I section	My	4	0.59	6.42	1.09	
	ECCS	4	0.60	6.32	1.07	
	bilinear	4	0.62	6.11	1.04	
	energy	4	0.64	5.90	1.00	

Computed R_{factor} values for symmetrical section vary from 4 % to 9 % depending on the definition of first yield, while for T sections the difference ranges from 21 % to 93%. The differences between

R_{factor} values, computed for the two structures (one with I sections, one with T sections), ranges from 0.7 %, if the fourth definition is used for both structures, to 78 %, if the first definition is used for both structures.

Using the first definition of yield and because up to first yield we are in the linear range, it can be shown that the next expression relates the values of R_{factor} of the two structures as a function of the shape factor of the beam sections ($sf1, sf2$), the ultimate acceleration multipliers ($\lambda u1, \lambda u2$), and the plastic moment and the moment under gravity load (Mp, Ms) of the beam section that yield first.

$$\frac{R_{factor1}}{R_{factor2}} = \frac{\lambda u2}{\lambda u1} \cdot \frac{sf2}{sf1} \cdot \frac{\frac{Mp}{Ms} - sf1}{\frac{Mp}{Ms} - sf2}$$

The graphic of figure 3.7.4 shows the ratio $\frac{R_{factor1}}{R_{factor2}}$, as a function of the ratio of shape factors ratio

($sf2/sf1$) and the ratio of moment under gravity load to plastic moment (Ms/Mp) -with the hypothesis that the two structures behave similar, meaning that the ultimate acceleration multiplier are very close-. It can be seen that high values of R_{factor} can be obtained depending on the definition of first yield used, that does not represent either a better performance of the structure (because these R_{factor} values are not related with higher global ductility of the structure), or an increase of the ultimate capacity of the structure with respect to design capacity (structural over-strength). In fact, these high values of R_{factor} correspond to a strong decrease of the yield acceleration multiplier due to the reduction of the difference between the yield moment to the moment under gravity load because of the definition used of structure first yield.

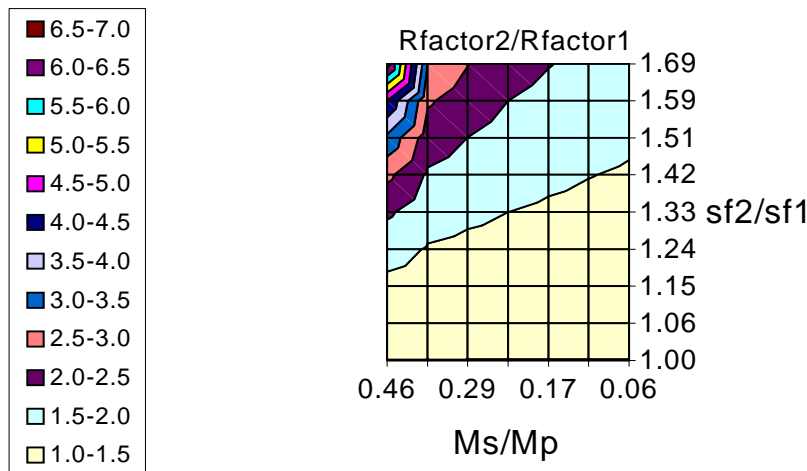


Figure 3.7.4

The formation of a plastic hinge requires the extension of yielding over a certain length of the beam, approximatively equal to the height of the section.

If we define a plastic hinge length, the rotation can be computed with the curvatures and lengths of all the finite elements along the hinge length. When we define first yield of the structure from the rotation in the hinge length, the values of R factor for the previous example are about 40 % lower than those obtained using Menergy attained in one particular element.

In the literature, different approaches to determine the structure first yield are found. One can mention developments made considering as first yield of the composite structure the M_y of the semi-rigid joints in Amadio et al. (1994); there are also developments where two different definitions are used to define the first yield of the composite structure (Broderick et al.(1996) and Elnashai et al. (1996)):

1- First instance of yield in a column to establish the plastic redistribution parameter for the static push-over analysis (this definition is used to avoid very high values of plastic redistribution

parameter, values of 20, when considering first yield of the structure the first instance of yield anywhere).

2- The yield of some monitored fibres of the finite beam element to define the first yield of the structure in the dynamic analysis. In this reference the evaluated reduction factors for composite structures with rigid connections, and full strength between the slab and the steel profile ranges from 9 to 21.

Plastic redistribution parameters.

Positive beam plastic moments are higher than negative plastic ones when the concrete slab collaborates with the steel profile. This asymmetry is amplified by the fact that moment under gravity load at the end of the beams are negative and it will play an influence in the global behaviour of the structure providing higher values of plastic redistribution parameter and lower values of global ductility than when the slab does not work.

Depending on the designed composite structure, values of reduction factor computed using MDOF analysis could be high due to structural over-strength. But designers, in order to take maximum profit of codes provisions, could design structures avoiding premature yielding of the hinges that become first in the static elastic push-over, reducing in this manner the structural over-strength without increasing significantly the ultimate capacity. When evaluating behaviour factor for composite structures, thinking on code provisions, it could be convenient to check the part of the reduction factor related with structural over-strength, and the part related with ductility, because composite structures will have higher values of structural over-strength and lower values of global ductility than steel structures.

This kind of problem exists because of the use of a definition at local level, first hinge, to characterise the global yielding of the structure. In the new generation of codes this problem will directly be avoided using the non-linear static push-over analysis to obtain an equivalent SDOF model to characterise the behaviour of the structure.

3.7.5. Conclusions.

From the previous comments we can draw the following conclusions:

- A correct reference to define first yield of the structure must allow the starting of internal force redistribution in the structure at global level. Thus structure first yield must be defined from rotation and not from material yielding or curvature that only allow redistribution of stress in the section or in the plastic hinge and not at structural level. Reduction factor could be overestimated if other definitions are used.
- Once this correct reference of first yield is used, it could be expected that reduction factors of composite steel-concrete structures are not too much different of those computed for steel structures. This would be our estimate at present.
- However some peculiarities of composite structures need to be considered before this conclusion is demonstrated. For instance, the difference in moment resistance between positive and negative bending might bring higher rotations demands in fewer plastic hinges than in the case of a structure made of symmetrical sections; this could result in lower reduction factors.
- On the contrary, the higher values of the plastic redistribution parameter $\frac{\alpha_u}{\alpha_1}$, characterising composite structures, would result in higher reduction factors.

A study is now ongoing in the University of Liège in order to evaluate reduction factor for composite steel-concrete structures using simplified methods and MDOF analysis, taking into account in a simplified manner the particularities of composite structures that could give higher influence in the reduction factor. Although method based on MDOF analysis are the most precise ones, to make a representative study for code provisions it could be a work more than cumbersome because of the variability of results for different structures and ground motions. The results obtained using simplified methods are less scattered and seem to be conservative.

3.8. Evaluation of behaviour factor for moment resisting composite frames on the basis of the Ispra Test

H. Parung

Institute of Steel Construction, Darmstadt University of Technology, Germany

The 3-D composite frame tested at the ELSA Reaction Wall, Joint Research Center of the European Communities, Ispra, Italy, was designed using a behaviour factor of 6.

The Drain-2dx Computer Program was used to perform the pretest analysis. The purpose of this pretest analysis was to determine the maximum expected actuator load necessary to deform the test structure + and -18 cm. The experimental results showed that the computer model could capture accurately the behaviour of the composite frame.

The computer model was also used to determine the behaviour factor of the composite frame tested in Ispra, Italy. For this calculation, only frame 2 in the x-direction was analysed. For this purpose, the earthquake record EI-Centro 1940 NS was used.

A ten story composite frame, designed assuming a behaviour factor of 6 was also modelled as the three-story composite frame. Behaviour factor of this frame was also calculated.

The results show that using a behaviour factor of 6, a properly designed composite frame can successfully resist a maximum EC8 design-specified earthquake.

3.8.1. General

Behaviour factor (q) is factor used for design purposes to reduce the forces obtained from a linear analysis, in order to account for the non-linear response of a structure, associated with the material and the structural system. This concept is based on the use of modal analysis in the linear range by assuming a design spectrum, which provides, as a function of period T , the normalised pseudo-acceleration, required for a specified level of inelastic response. These inelastic spectra are obtained in seismic codes by modifying the linear elastic design response spectrum with the behaviour factor, which takes into account the dissipative capacity of the structure up to failure.

In Eurocode 8, due to the lack of the more precise information, the same behaviour factors are used for composite structures as for steel structures of the corresponding structural type.

3.8.2. Evaluation of the behaviour factor

There are several methods available to evaluate the behaviour factor, namely:

1. method based on ductility factor theory: the theory of ductility factor is used to establish relations between the q -factor and some parameter characterising the post-elastic behaviour of steel frames.
2. method based on extension of the results concerning the dynamic inelastic response of simple degree of freedom systems: this method is strictly applicable to SDOF systems only, but has been extended to MDOFs systems.
3. method based on the energy approach: this method is the most general one, and does not require structural regularity and global mechanism hypotheses.

In this section, the Ballio and Setti method was used to evaluate q -factor. Their method is based on the use of ductility factor theory as a tool to interpret the results of dynamic elastic analysis. The theory of ductility factor states that the q -factor is coincident with the global ductility, provided that there are no limitations due to local ductility.

For a given structure and a given earthquake $a(t)$ a series of computations of dynamic non-linear response to calculate the behaviour factor is performed under an action defined $a(t)$ times a multiplier λ . By increasing the value of λ , following events are found (Figure 3.8.1):

1. λ multiplier such that all sections of the structure remain elastic. If the displacement D of one peculiar point of the structure is kept as parameter characterising the deformation of the structure, it can be seen that at first D 's increase proportionally to λ 's.

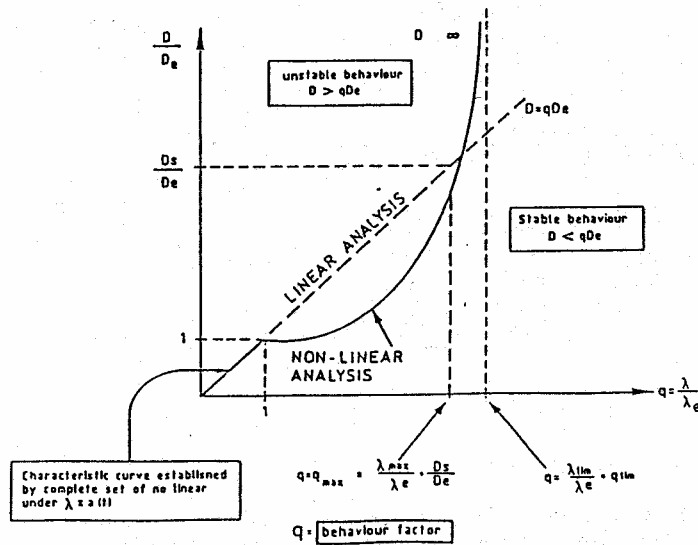


Figure 3.8.1. Definition of behaviour factor q

2. There is a peculiar λ value for which yield strength f_y is reached at the weakest point of the structure (λ_c). The displacement at the first yield is identified as D_e .
3. For certain λ multipliers, the D 's are smaller than the D 's that would be obtained in a structure remaining elastic as the result of energy dissipation by yielding.
4. Increasing λ finally gives a value of λ_{max} for which the computed non-linear displacement (D_{max}) is equal to the displacement found with the ever-elastic structure.
5. Increasing λ beyond the λ_{max} would result in the structure being unstable, and the ratio between D s and D_e would become infinite.

So, the behaviour factor q can be defined as:

$$q = \lambda_{max} / \lambda_e = D_{max} / D_e$$

3.8.3. Behaviour factor of composite frames

Dynamic analysis option of the Drain-2dx program has been used to determine behaviour factors of the three-story test structure and a ten-story composite frame. The frames were modelled by beam-column elements to model columns and the elastic section of beams, and fibre elements to model the inelastic section of beam (Figure 3.8.2).

In Drain-2dx Program, the viscous damping used is of *Rayleigh* type. The damping matrix of the structure is defined as the linear combination of the mass and the stiffness matrix, as formulated below:

$$C = \alpha [M] + \beta [K]$$

where C is the damping matrix, M is the mass matrix, K is the stiffness matrix, while α and β are the mass proportional damping factor and initial stiffness damping factor respectively. The α and β factors can be calculated by using the formula:

$$\begin{bmatrix} \alpha \\ \beta \end{bmatrix} = \frac{2 \xi}{\omega_1 + \omega_2} \begin{bmatrix} \omega_1 & \omega_2 \\ & 1 \end{bmatrix}$$

where ω_1 and ω_2 are the first and the second circular frequency of the test structure, and ξ is the damping ratio. Damping ratio was assumed 3% for the first and the second modes respectively.

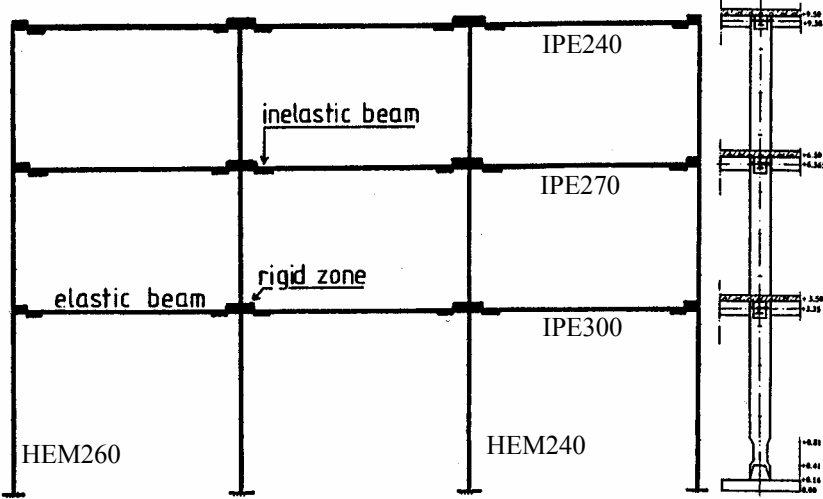
The EI-Centro earthquake was used in this study to calculate the behaviour factors of the composite frames. The intensity of the earthquake was increased step by step in order to determine the multipliers λ_e and λ_{max} , and the corresponding D_e and D_{max} .

a. Three-Story Composite Frame

The 3-D composite frame was designed to carry dead load (DL) and live load (LL), and earthquake load. For the design of the frame, behaviour factor of was assumed 6. The thickness of the slab was designed 12 cm, but in the reality, was increased to 15 cm.

Behaviour factors were calculated for both 12 cm and 15 cm slab, and also for different loading cases (DL and DL+LL). Also, to study the effect of styrofoam placed around beam-column connections, the composite frame was also analysed for two different conditions, namely without styrofoam and with styrofoam at all connections. For the analysis, real yield stress of steel sections were used (on the average 280 MPa for beams and 300 MPa for columns). Table 3.8.1 presents the behaviour factors of the 3-story test frame.

Although the three-story tested frame was designed for $q=6$, but increasing the earthquake load by 20% to take into account the accidental eccentricity, reduced the actual design q -factor to approximately 5. For the same condition (case 1), the q -factor was 5.1. If *dogbones* were not placed above the base plates, as shown in Figure 3.8.2, the q -factor should be larger than 5.1.



Frame 2/3

Figure 3.8.2. Three-story composite frame (frame 2)

Table 3.8.1. Behaviour Factor of 3-Story Composite Frame

No.	Slab cm	Loading	Styrofoam	Period, sec		Displ. cm		q factor
				1 st	2 nd	yield	max	
1	12	DL	no	0.44	0.13	4.8	21.1	4.4
2	12	DL+LL	no	0.52	0.16	4.8	24.5	5.1
3	12	DL + LL	yes	0.53	0.16	4.7	30.0	6.4
4	15	DL	no	0.47	0.15	4.4	18.0	4.1
5	15	DL+LL	no	0.54	0.17	4.8	21.6	4.5
6	15	DL+LL	yes	0.55	0.17	4.6	28.9	6.3

Table 3.8.1 also shows that the increase in the natural periods would also increase the behaviour factor. For case 1, where only the real mass was considered ($T = 0.44$ sec), the q - factor was 4.4. If additional mass due to the live load was also considered ($T = 0.52$ sec), the q -factor increased to 5.1. The slab thickness of the test frame was designed to be 12 cm, but in reality, was increased to 15 cm. Consequently, plastic moment capacities of the composite beams were also increased. As can be seen

from Table 3.8.1, for the cases without styrofoam, the behaviour factors of the frames with $t = 15$ cm were smaller than those with $t = 12$ cm as a direct result of the increase in the plastic moment capacities.

Frames with styrofoam placed around all beam-column connections, had larger behaviour factors than those without styrofoam. By placing styrofoam, the direct contact between slab and column was prevented. Consequently, the plastic moment capacities of composite beams with styrofoam would be smaller than those without styrofoam for the same sections. The reduction in the plastic moment capacities increased the q-factor.

Figure 3.8.3. shows the displacement-time histories of the three story composite frame for the case 4 (15 cm slab, DL only, and without styrofoam).

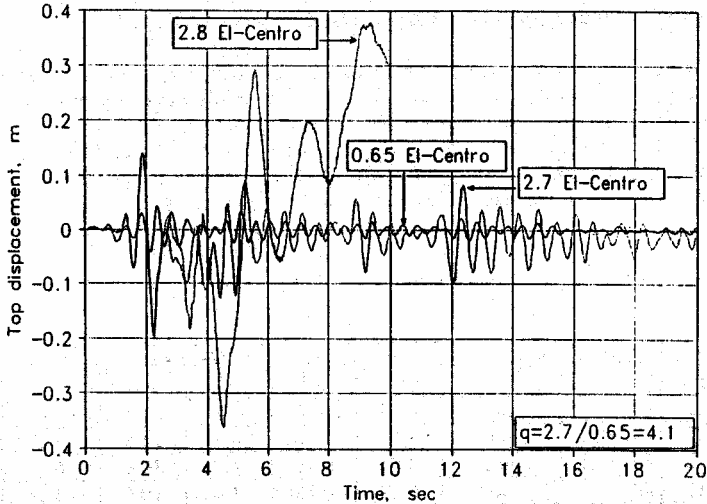


Figure 3.8.3. Top displacement time history of the three-story frame (case 4)

b. Ten-Story Composite Frame

A 10-story 3-bay by 3-bay composite frame was designed with a behaviour factor of 6. The natural first period of this frame was 1.13 sec. Sections of this frame are presented in the Table 3.8.2.

The behaviour factor of this 10-story composite frame was calculated for 2 different conditions, namely with and without styrofoam around beam-column connections. The yield displacement and the maximum displacement of the frame with rigid slab (without styrofoam) were 12.7 cm and 100 cm respectively, so the behaviour factor was 7.88. For the composite frame with styrofoam, the yield displacement and the maximum displacement were 13.4 and 117 cm respectively, so the behaviour factor was 8.71.

Table 3.8.2. Steel Sections of the 10-Story Composite Frame

Floor	Beam Section	Column Section
1-2	IPE450	HEB600
3-4	IPE400	HEB550
5-6	IPE400	HEB500
7-8	IPE330	HEB450
9-10	IPE330	HEB400

3.9. Analytical Investigation of the Behaviour of Composite Beams with Shear Connectors

M. Tsujii, A.S. Elnashai, R. Pinho

Engineering Seismology and Earthquake Engineering Section

Civil and Environmental Engineering Department, Imperial College, London SW7 2BU, UK

3.9.1. Significance of the Problem

The behaviour of conventional composite steel-concrete beams is influenced by the nature of shear connection and the effective width of the concrete slab. The partial shear connection between steel beam and concrete slab may provide considerable construction cost reduction. However, there are very few quantitative and comprehensive studies concerning the effect of partial shear connection on the global behaviour of composite beams. Analytical modelling is an effective way to undertake fundamental investigations of the behaviour, due to the prohibitive cost of large testing programmes. Several analytical studies using the finite element methods have been undertaken. Aribert (1992) proposed a finite element model representing the shear connectors as discrete diagonal trusses. However, the embedment behaviour is neglected in the adopted model. Ayoub and Fillipou (1997) adopted fibre representation for steel beam and concrete slab connected with non-linear spring elements. As the longitudinal shear force is applied linearly through the length of the beams, the flexural strength of composite beams and embedment force is not represented. Bursi and Caldara (1999) also conducted finite element analyses with spring elements for the shear connectors, comparing with experimental results of beam-column sub-assemblages. The model requires a detailed estimation of effective width of concrete slab and exact constitutive laws for the steel-concrete interface for stud connectors.

A simple model of the stud shear connector is needed for the study to investigate the fundamental flexural behaviour of composite beams and global frame behaviour in the earthquake loading. This is essential due to the wide parameter variation required, which leads to a very large number of analyses. Therefore, a simple mechanical model is proposed using joint elements that are capable of reflecting the three-directional behaviour for the stud connector. This model is constructed to be suitable for use in the advanced nonlinear analysis program 'ADAPTIC' (Izzudin and Elnashai, 1989) which has been developed at Imperial College. The proposed model is validated in comparison with the results of previous researchers on simple beam testing. A parametric study is then conducted to study the effect of the concrete slab width and the degree of shear connection in conventional composite beams. The rather promising application using partially encased composite member is also investigated as an alternative to beam members. Ductility of this partially encased composite member is investigated and contrasted with that of the conventional composite beams in the both case of simple beams and continuous beams.

3.9.2. Proposed Modelling of Composite Beams

3.9.2.1 Deformation Capacity of Stud Shear Connection

Many codes or standards for push tests use simple equation to evaluate strength of stud shear connectors, where the total load sustained is divided by the number of studs. In general, the deformational characteristics of the connectors are neglected and the non-uniform distribution of demand, both strength and deformation, are not accounted for. As such, these expressions do not provide insight into the resistance mechanisms.

Some parametric tests executed by Hawkins (1973) showed that the shear strength increases when the stud material is of high tensile strength. In their statistical analysis of the experimental data, Oehlers and Johnson (1987) focused attention on failure modes depending on tensile strength of the stud material f_u , and modified the usual expression given in equation (1) into that shown in equation (2) for the dowel strength P_u as,

$$P_u = 0.50 a (f_c E_c)^{0.5} \quad (3.9.1)$$

$$P_u = (5.3 - 1.3 / n^{0.5}) a f_u^{0.65} f_c^{0.35} (E_c / E_s)^{0.40} \quad (3.9.2)$$

where the units are in N and mm, and in which

- a : cross-sectional area of the shank of stud connector
- f_c : compressive cylinder strength of concrete
- E_c : Young's modulus of concrete
- E_s : Young's modulus for steel

Whereas equation (2) is one of the most used expressions for the dowel strength in push-out tests, it ignores the influence of the height of stud connectors that represents their resisting area. For example in support of this point of view, Yamamoto and Nakamura (1961) recommended the use of the resisting area 'dL' instead of 'a' in equation (1) for shanks shorter than $L/d = 6.0$, where d and L are the diameter and length of stud connector, respectively. Thus, more detailed research is needed to establish an accurate and verifiable expression for dowel strength.

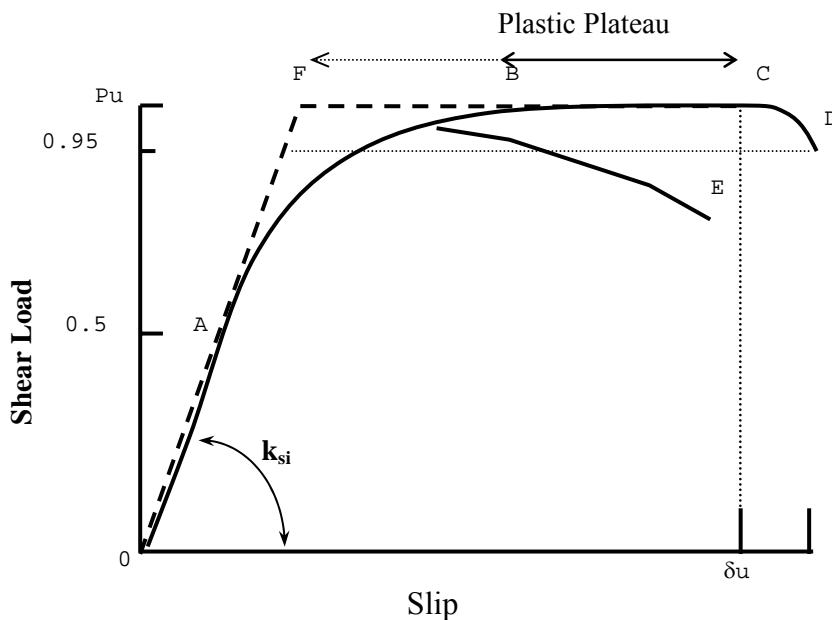


Figure 3.9.1 Load-Slip Curve of Stud Shear Connectors

Comparative experiments carried out by Ollgard *et al* (1971) showed that the results of push-out tests may often overestimate dowel strength over and above stud connectors in composite beams. Preceding this work, Chapman and Balakrishnan (1965) carried out a series of experiments on simply supported composite beams with various shear connectors. They recommended that shear connection should be designed to carry the horizontal shear force beyond the ultimate beam load. For this purpose, the ultimate capacity of shear connection in beams should possess more than 80 % of the ultimate capacity obtained from push-out test results. A limited number of experiments with controlled axial forces of the test similar to that of the real beam (Oehlers and Johnson, 1987) suggested that the dowel strength in the beam is decreased by approximately 19 % below push-out tests results. Therefore, equation (2) may be changed as shown,

$$P_u = (4.3 - 1.1 / n^{0.5}) a f_u^{0.65} f_c^{0.35} (E_c / E_s)^{0.40} \quad (3.9.3)$$

Figure 3.9.1 shows a typical load-slip curve of shear connectors in the case that the concrete slab is reinforced sufficiently. The dowel strength in bare concrete without reinforcement reduces in strength

after reaching the first ultimate strength P_u , similar to 0-A-E in Figure 3.9.1. However in the practical case of reinforced concrete, the dowel strength can sustain its maximum (ultimate) dowel strength P_u until the ultimate slip capacity. This property is shown as by 0-A-B-C-D in Figure 3.9.1. This curve is expressed by the proposal of Olgaard *et al* (1971) where the shear force F is expressed by two independent parameters λ and υ as,

$$F = P_u [1 - \exp(-\lambda\delta)]^\upsilon \quad (3.9.4)$$

The above expression is one of the most accurate for stud shear connectors. However in equation (4), the maximum shear resistance should be still determined from push-out tests. Notwithstanding, the expression is somewhat complex for implementation in large frame analysis where potentially thousands of connectors are modelled.

Oehlers and Johnson (1987) also investigated statistically the deformation capacity of stud shear connectors in reinforced concrete. They observed that a bilinear curve is capable of reflecting the elasto-plastic deformation of the stud shear connectors as shown by 0-A-F-B-C in Figure 3.9.1. In reinforced concrete slabs, the following expressions are derived in terms of the initial stiffness coefficient k_{si} and the ultimate slip capacity δ_u , giving

$$k_{si} = P_u / d (0.16 - 0.0017 f_c) \quad (3.9.5)$$

$$\delta_u = d (0.48 - 0.0042 d) \quad (3.9.6)$$

where d , f_u and f_c are the diameter of shear stud, the ultimate tensile strength of stud material and the compressive cylinder strength of concrete, respectively.

Modelling of the Structural Behaviour of Shear Connection

The two-dimensional modelling approach for conventional composite beams is proposed as in Figure 3.9.2. This model is recommended as a simple, yet accurate, representation of a composite members for large frame analysis. The element for concrete slab and steel beam employ a cubic elasto-plastic beam formulation, with fibre analysis in the sections. Shear connectors are modelled by an assembly of two rigid column elements and a joint element. The joint element can represent all structural characteristics of shear connectors for uncoupled axial, shear and moment actions. Independent curves may be given for each direction in the utilised computer code ADAPTIC (Izzuddin and Elnashai, 1989).

The most important effects modelled by joint elements are dowel strength and slip capacity of shear studs. The elasto-plastic model employs the equations by Oehlers and Johnson (1987) given in Equations (5) and (6). It is also needed to represent the behaviour in other directions and effects such as the embedment force and rotational resistance. There are very few studies on the embedment effect probably because of its rare occurrence in a real composite beams. The model assembled for this study employs the empirical equation recommended by McMackin *et al* (1973). They proposed an empirical equation for the embedment force X_{emb} by investigating several experimental data. This is expressed as,

$$X_{emb} = 1.88 f_c^{1/2} (h_{stud}/d - 0.5) (h_{stud}/d + 1) (0.3 + 0.7\rho) \quad (3.9.7)$$

where h_{stud} represents the height of stud shear connector. This failure mode is rarely observed and only when high concentrated forces exist. Moreover, the rotational resistance of shear connectors has not been researched because other failure mechanism would normally precede failure due to excessive rotation. Thus, the rotational stiffness may be set to a high value of stiffness and infinite strength.

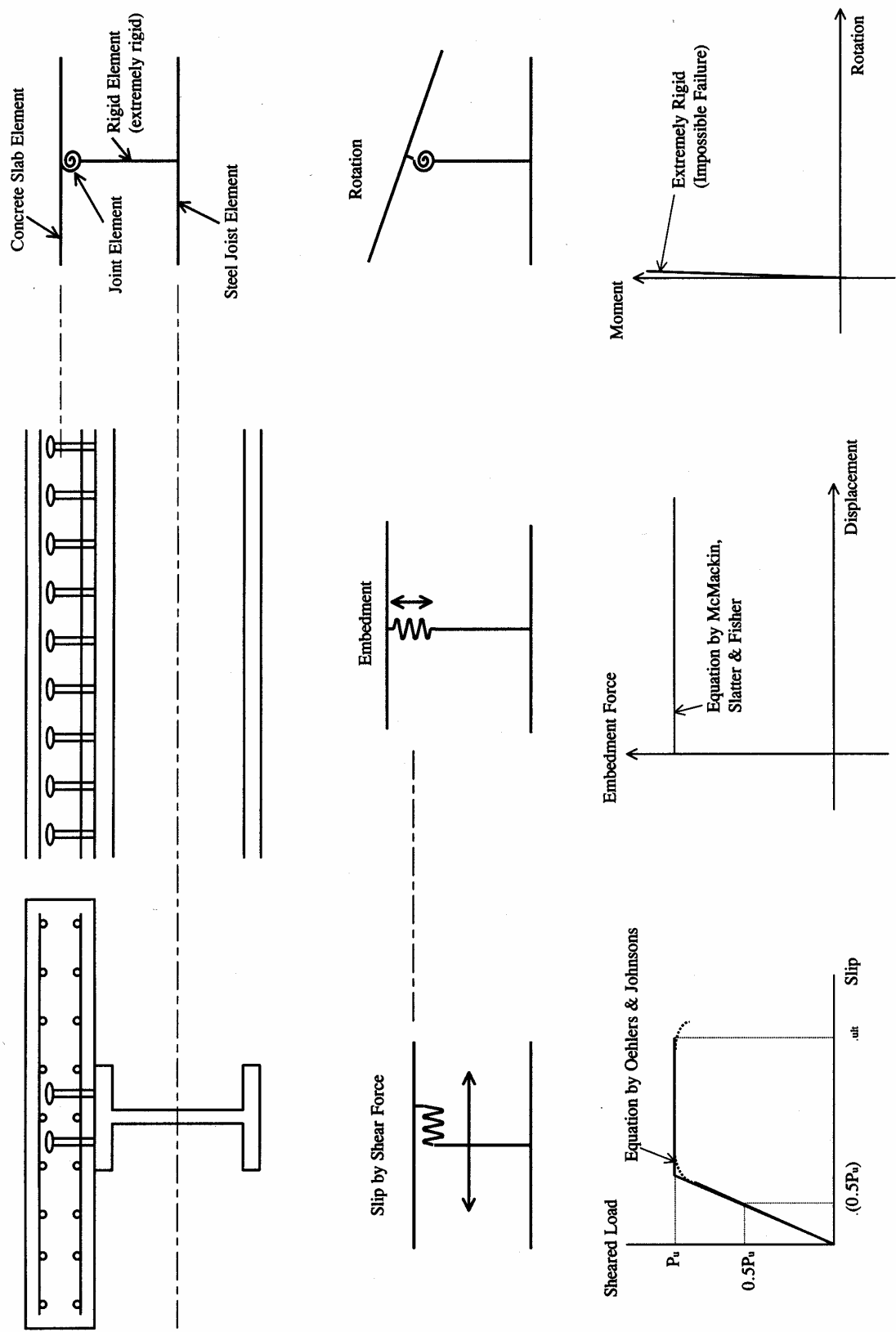


Figure 3.9.2 Proposed Analytical Model for Conventional Composite

3.9.2.3. Assumed Material Properties for Static Analysis

Widely used values of important material characteristics are chosen for static analysis to investigate the fundamental behaviour of composite beams. This is because the experimental investigations used hereafter for verification do not always give full material details. Several material stress-strain models are available in ADAPTIC, and these are not described here for brevity. The material properties used in this study are given below.

(a) Steel beam (multi-surface plasticity model; fe430, $E=2.0 \times 10^5$ N/mm²)

Yield strength ; $\sigma_{sy} = 270$ N/mm²
Ultimate tensile strength; $\sigma_{su} = 430$ N/mm²
Critical buckling strength; $\sigma_{cr} = 367$ N/mm²

The critical local buckling strength is calculated following the approach of Kato (1989). This criterion was used successfully in the previous research carried out by Broderick and Elnashai (1996) and Elnashai *et al* (1996).

(b) Reinforcing bars (Bilinear model)

Yield strength; $\sigma_{ry} = 400$ N/mm²
Ultimate tensile strength; $\sigma_{ru} = 430$ N/mm²

The bilinear model has been chosen in preference to the complex multi-surface formulation because the behaviour of reinforcing bars does not significantly affects the behaviour of composite beams, which are governed by the response of the beam and shear connection. The strain-hardening slope is set to be 2% in the bilinear stress-strain curve. In sagging bending, the ultimate criteria would be decided by the tensile strength of the beam or crushing of concrete. The strain hardening of reinforcing bars affects only in hogging bending response if the steel beam does not buckle in compression.

(c) Concrete Material (C40/50)

Cylinder strength; $f_c = 30$ N/mm², ($\epsilon_c = 0.2$ %)
Ultimate concrete strain; $\epsilon_{cu} = 0.4$ % (Unconfined concrete)

The ultimate strain for unconfined concrete is given as 0.35% in Eurocodes and varies between 0.30 and 0.39 in CEB-FIP (1970). These values lead to conservative design results though the loading speed affects the ultimate strain considerably. After investigation of detailed testing data and survey of collapsed structures in seismic regions, many researchers (Paulay & Priestley, 1992 & Wakabayashi, 1986 etc.) recommend a value over 0.4 % with regard to the evaluation of ductility. Therefore in this study, the ultimate value is set to 0.4 %. This is increased for the confined part, but only marginally because hoops are not normally extensively provided in composite beams.

3.9.2.4 Verification of Analytical Model

This analytical model can represent the interaction mechanisms between concrete slab and steel beam by calibrating the shear stud relationships to experimental results. For the investigation of the deformation of beams under sagging and hogging bendings, Ansourian (1981) conducted loading tests for continuous two span composite beams. The maximum deformation of sagging bending is at mid-span of the left beam whilst the maximum hogging deformation is at the opposite beam. For specimen CTB-1, comparison between experimental and analytical results is shown in Figures 3.9.3 to 5, which

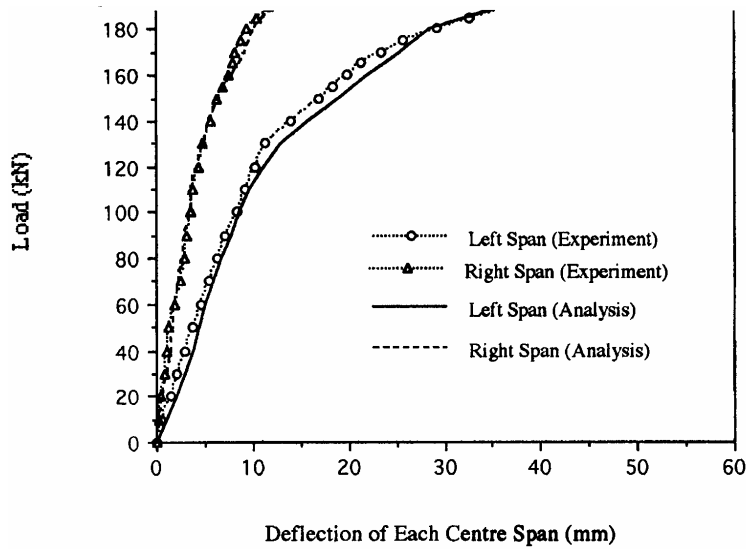


Figure 3.9.3. Comparison of Experiment (Ansourian - CTB-1) and Analysis

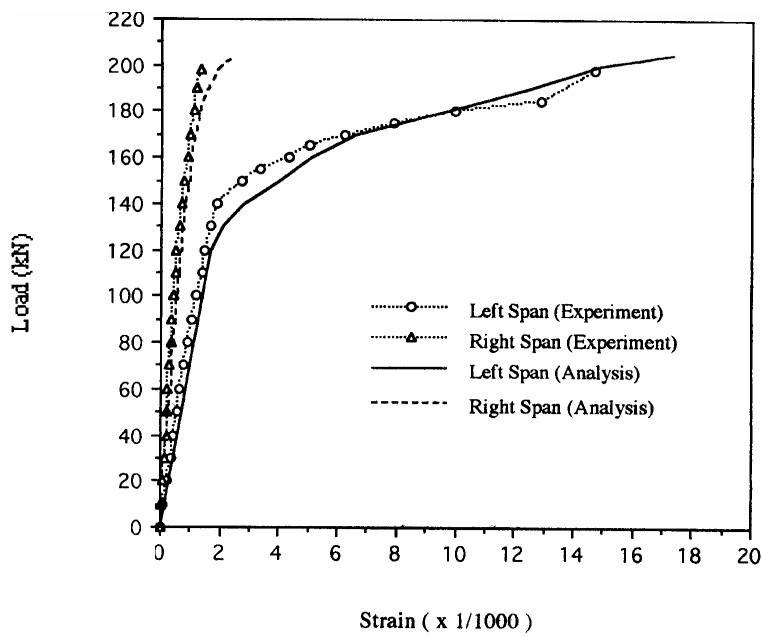


Figure 3.9.4. Comparison of Experiment (Ansourian - CTB-1) and Analysis

present the relationships between imposed loading and maximum deflection, maximum strain at the bottom of the steel beam and maximum curvature of steel beam, respectively. The analytical results concur well with the experimental results for the strength and deformation characteristics especially in the vicinity of initial loading and ultimate limit state. If detailed material characteristics for the tests were available, the discrepancies at mid-range may have reduced.

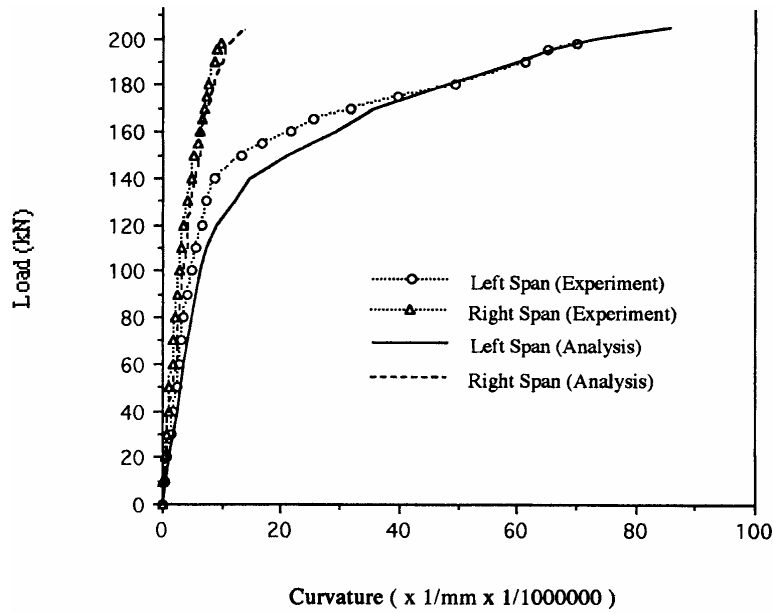


Figure 3.9.5 Comparison of Experiment (Ansourian - CTB-1) and Analysis

The published reference did not deal with detailed response quantities such as slip capacity of the shear stud. In this respect, Chapman and Balakrishnan (1964) executed series of loading tests on single span composite beams, focusing on the slip response between concrete slab and steel beam. They investigated the slip deformation for various shear connectors spacing in the simple beams. Comparison between these experimental results and the analytical model proposed in the current work is shown in Table 3.9.1. This average end slips at failure and maximum moment. The comparison confirms and verifies the analytical model proposed. The analysis reproduces the experimental results within 4-11%. It is noted that the analysis performs well in the cases of stud failure as well as slab crushing.

Table 3.9.1 Comparison of Experiment (Chapman and Balakrishnan, 1964) and Analysis

Beam	Average of End Slip			Max. Moment	Collapse Mode
	Exp. (E)	Anal. (A)	A/E	A/E	
A1	0.00mm	0.00mm	1.00	0.96	Slab Crushing
A2	0.04mm	0.04mm	1.00	0.98	Slab Crushing
A3	0.20mm	0.20mm	1.00	1.02	Slab Crushing
A4	0.35mm	0.36mm	1.03	0.96	Slab Crushing
A5	0.87mm	0.97mm	1.11	1.05	Slab Crushing
A6	1.18mm	1.23mm	1.04	0.96	Stud Failure
U1	1.12mm	1.10mm	0.98	1.05	Slab Crushing
U2	0.50mm	0.54mm	1.08	0.94	Slab Crushing
U3	0.86mm	0.91mm	1.06	0.96	Slab Crushing
U4	2.65mm	2.77mm	1.05	0.92	Stud Failure
U5	2.22mm	2.46mm	1.09	0.90	Stud Failure

Consequently, the analytical model proposed in current study is considered reasonably accurate, especially in the context of large frame analysis. This is indeed the main purpose for the development, since tests were planned within the ICONS framework, with support from ECOEST II on composite frames and steel frames with composite slabs.

3.9.3. Parametric Study on Composite Beams

3.9.3.1. Characteristics of Conventional Composite Beams for Parametric Study

Figure 3.9.6 shows the section and beam layout assembled for the parametric study. The composite beam is simply supported and has a span of 6 m. The material properties of steel beam, concrete slab and reinforcing bars are as assumed respectively in Section 2.3 above. The main parameters investigated in this study are the effective width of concrete slab and diameter of shear studs, as mentioned before. The effect of these parameters is investigated in terms of sagging and hogging loading.

3.9.3.2. Definition of Limit States

Since composite members consist of different elements (concrete slab, steel beam and stud connectors) and materials (steel and concrete), yield of an element or a fracture of a material cannot on its own determine the member deformation limit states. Therefore, an overall limit state (global, but on the member level) should be defined. In this parametric study, the yield and ultimate limit states are defined as follows:

(i) Definition in terms of Plastic Hinge Occurrence

Yield limit state; Plastic hinge occurrence

Sagging; Tensile yield at the bottom flange of the steel beam and compressive cylinder strength of concrete.

Hogging; Compressive yield of the bottom flange in the steel beam and tensile yield at the upper reinforcing bars.

Ultimate limit state; First fracture point (ultimate strength or ultimate slip)

Plastic hinge formation should be considered as the yield limit state because the deformation of the member changes after the plastic hinge formation. The starting point of plastic hinge formation is defined as the yield limit state occurrence at both top and bottom of the section (Elghazouli, 1992), each of which is defined above.

(ii) Definition in terms of Design Evaluation

Yield limit state; Elastic deformation corresponding to plastic bending moment capacity calculated by Eurocode 4 (1994) with all safety coefficient set to 1.0.

Ultimate limit state; First fracture point (ultimate strength or slip)

3.9.3.3. Effect of Slab Width

Variation of slab width

The range of variation of the slab is given by b or w_{eff} of 200, 400, 800, 1200, 1400, 1800 mm. All cases use the same stud connectors (2xD25@200) which have sufficient resisting capacity. Theoretically, in sagging moment, the neutral axis exists within concrete slab in all cases except $b = 200$. The neutral axis is located in the steel beam in all cases under hogging moment. If a 3-span continuous beam is considered with a transverse span of 6 m, the design effective width can be calculated following equations (3.6) and (3.7) of Eurocode 4 (1994) leading to:

For sagging region, w_{eff} (external span) = 1200mm and w_{eff} (internal span) = 1050mm

For hogging region, $w_{\text{eff}} = 750\text{mm}$

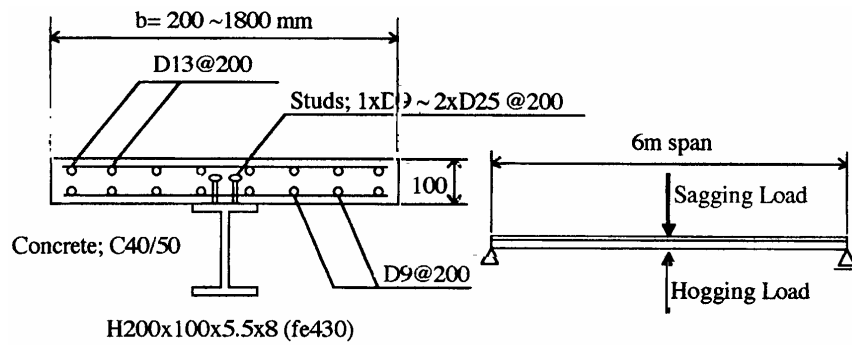
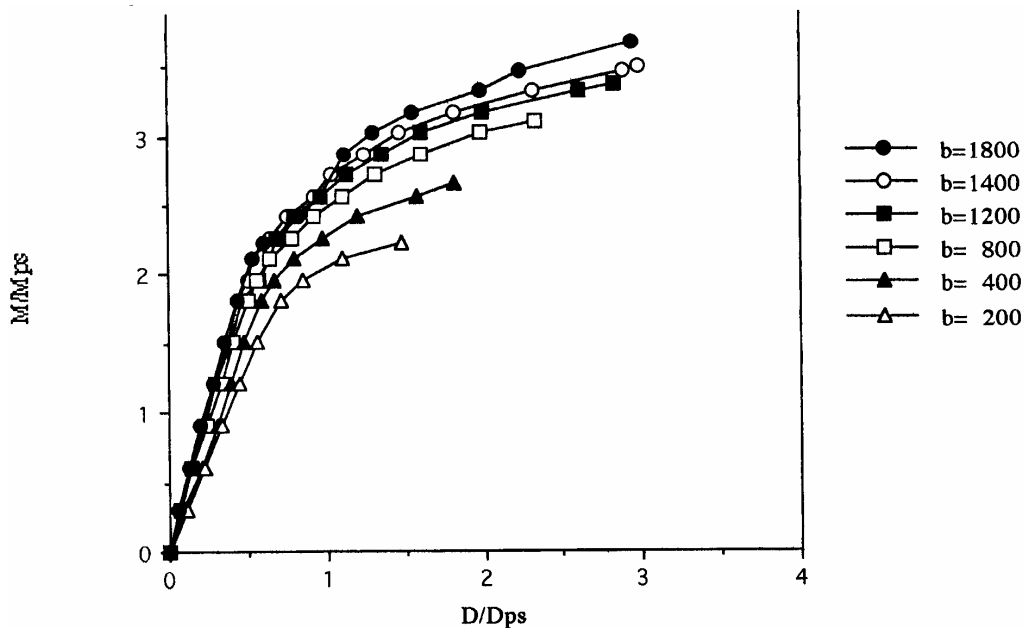


Figure 3.9.6 Section and Layout of Composite Beams for Analytical Study



M_p, D_{ps} ; Plastic moment and corresponding deflection for steel joist alone

Figure 3.9.7. Effect of Slab Width in Sagging Moment: Moment – Deflection

Thus, the selected variation of the slab width from 200 to 1800 mm brackets the range of widths sufficiently. In other words, the parametric range of variation represents 0.19 to 1.5 of the design effective width for sagging moment and 0.27 to 2.4 of the design width for hogging cases.

Effect of slab width

The results of parametric analyses for sagging moment are shown in Figures 3.9.7 to 9, whilst those for hogging moment are displayed in Figures 3.9.10 to 12. In those Figures, the notations have the following meaning:

- M ; Applied proportional moment
- M_{ps} ; Plastic moment capacity of steel beam alone (H200x100x5.5x8)
- M_p ; Plastic moment capacity of composite beam
- D ; Deflection of span centre point
- D_{ps} ; Deflection of steel beam alone at M_{ps}
- C ; Curvature
- C_{ps} ; Curvature of steel beam alone at M_{ps}
- $C_{mp,el}$; Elastic curvature of composite beam corresponding to M_p

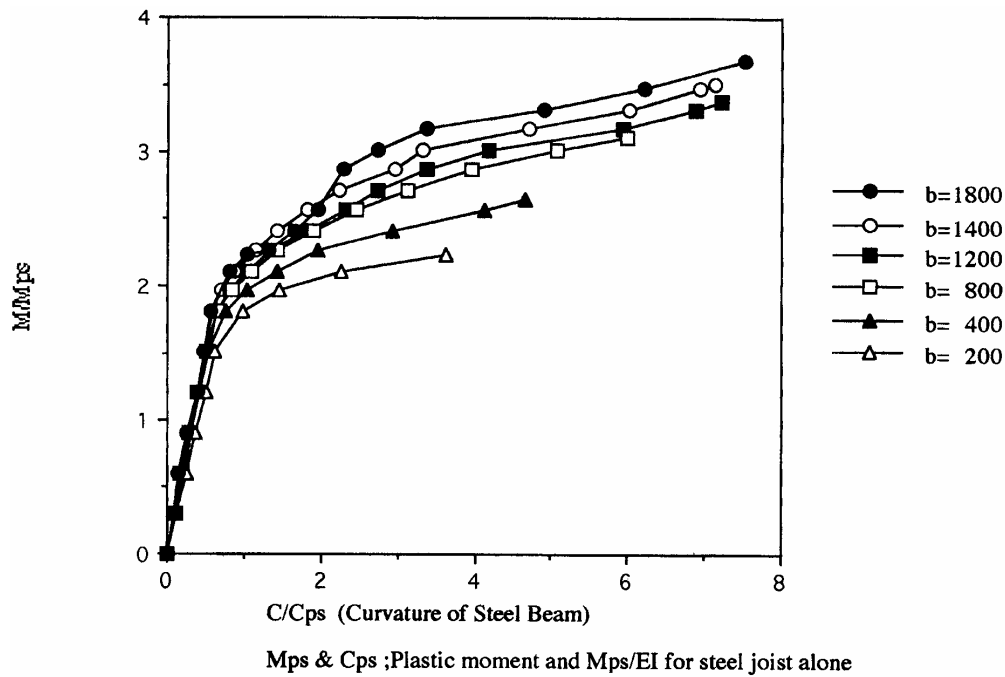


Figure 3.9.8. Effect of Slab Width in Sagging Moment : Moment – Curvature[1]

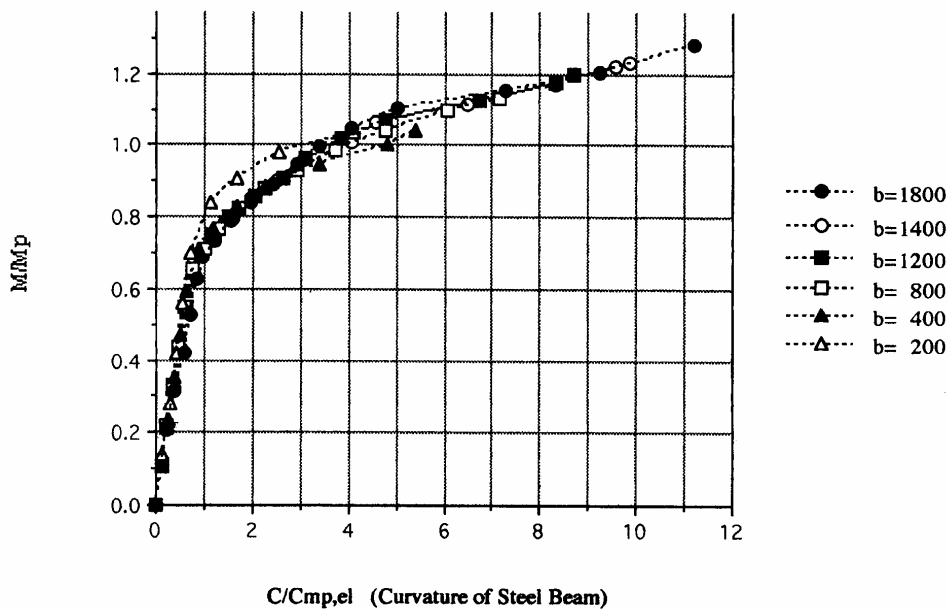


Figure 3.9.9. Effect of Slab Width in Sagging Moment : Moment – Curvature[2]

Failure in sagging moment is indicated by compressive concrete strain (0.4 %) at the top of the slab whilst failure in hogging moment corresponds to buckling of the bottom of the steel beam. In Figures 3.9.9 and 12, the most ductile case is $b = 1800$ mm exhibiting ductility of approximately 10 in sagging moments. On the other hand, the most ductile hogging moment case is $b = 200$ with ductility of more than 16.

In sagging moment, the ultimate curvatures of $b = 1200$ through 1800 are almost the same (Figure 3.9.8), but non-dimensional curvatures, Figure 3.9.9, are different. This indicates that beams with slab wider than the effective width of Eurocode 4 ($W_{eff} = 1050$ or 1200 mm in sagging bending) possess higher ductility capacity.

In hogging moment, the smaller the slab width is, the higher the ductility. This observation is totally the opposite of the cases of sagging moment. Accounting for slab widths larger than the Eurocode 4

value ($W_{eff} = 750\text{mm}$ in hogging bending) leads to a reduction in ductility. This result is physically convincing because a wider slab in compression allows the steel beam to develop its full ductile response prior to concrete crushing. Conversely, since the neutral axis travels downwards as the slab width is reduced in hogging moment, the extreme steel beam compressive strain reduces, thus delaying local buckling. Therefore, the decision in terms of effective width for design needs careful consideration, taking into account 'action capacity' as well as 'deformation capacity'. This issue is discussed further in subsequent sections.

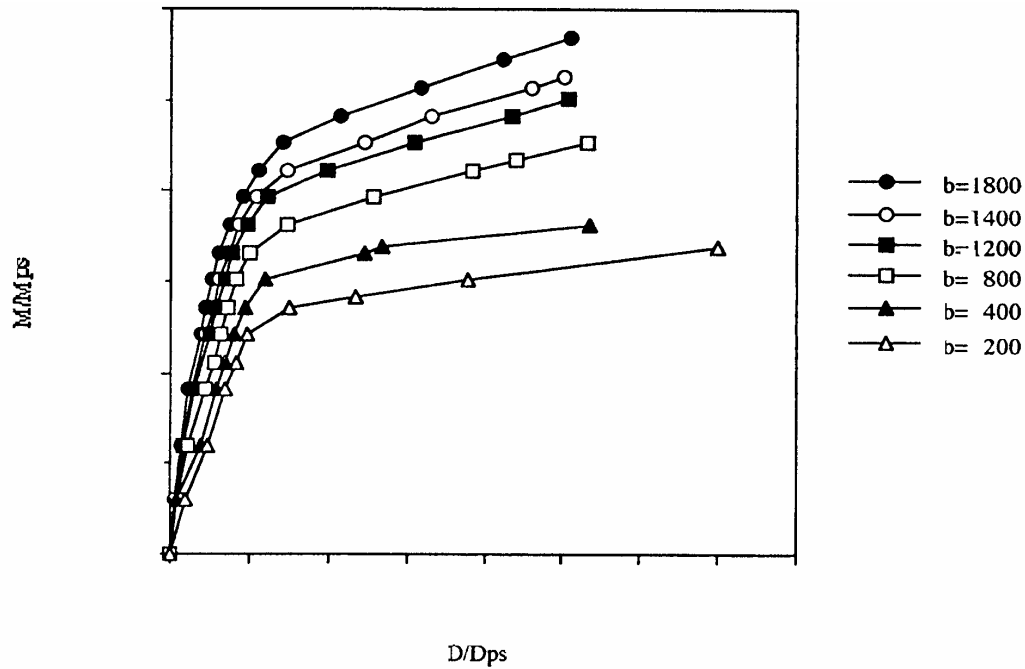


Figure 3.9.10. Effect of Slab Width in Hogging Moment : Moment – Deflection

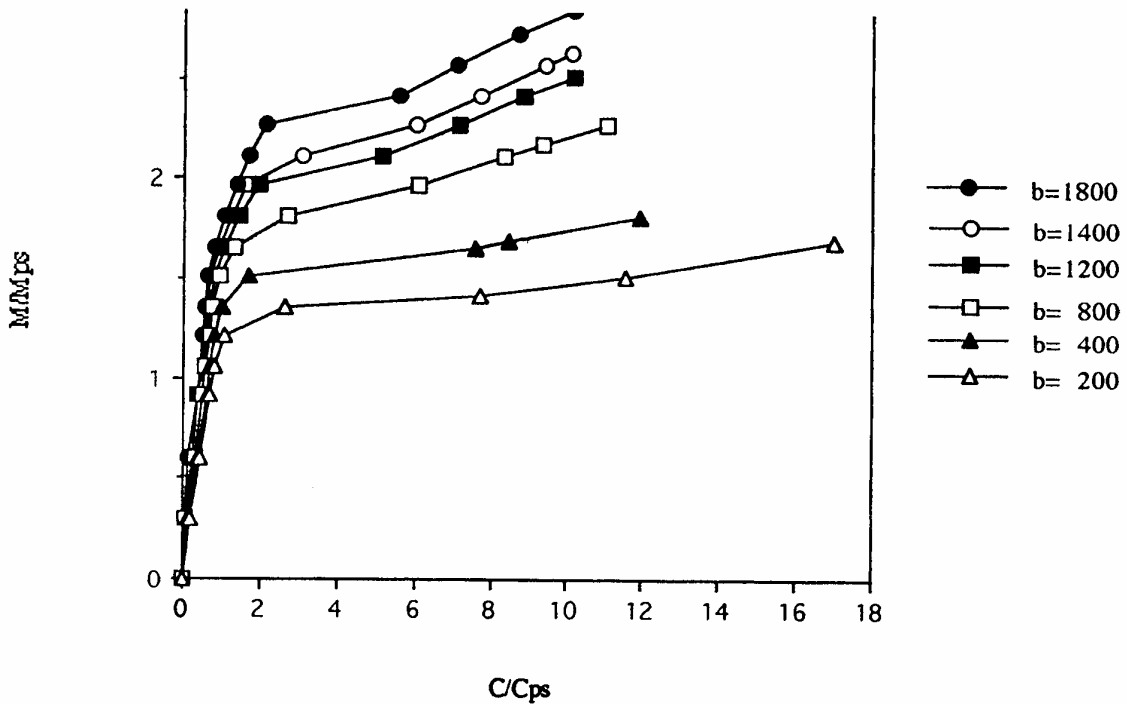


Figure 3.9.11 Effect of Slab Width in Hogging Moment : Moment – Curvature[1]

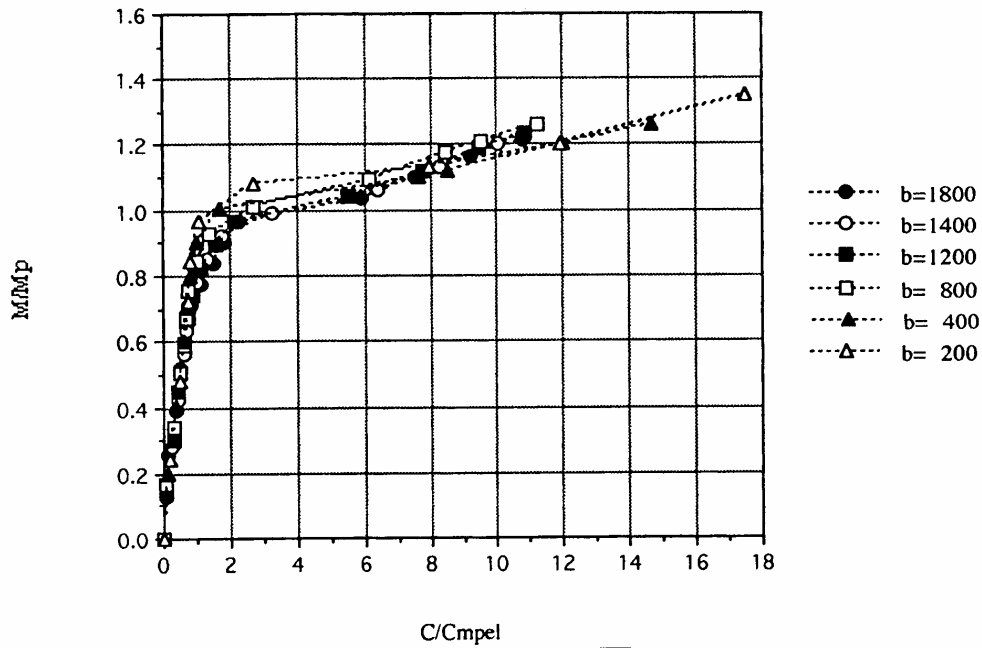


Figure 3.9.12 Effect of Slab Width in Hogging Moment : Moment – Curvature[2]

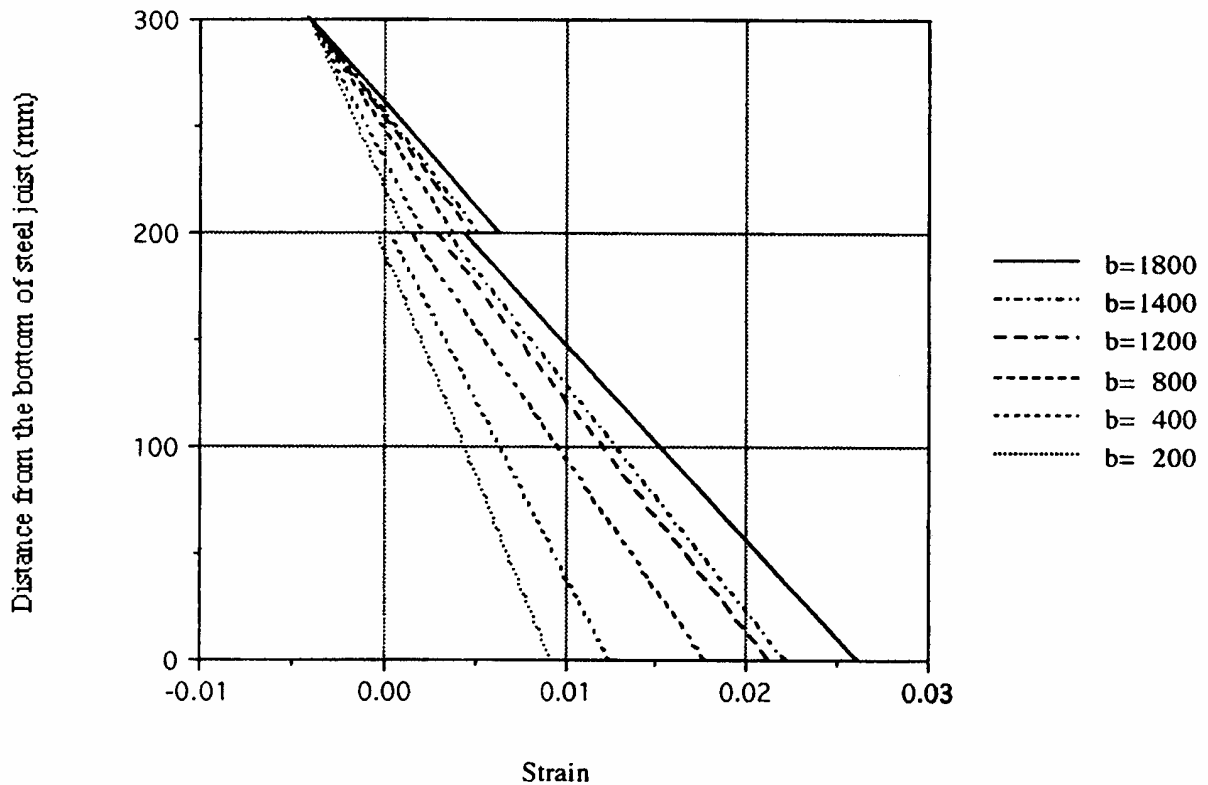


Figure 3.9.13 Strain diagram at the Ultimate Limit State in Sagging Moment with Various Slab Width

All cases of hogging moment deform into the strain hardening region ($\epsilon \geq \epsilon_{st} = 0.014$) of the steel beam at the ultimate limit state. In contrast, cases of $b = 200$ and 400 in sagging moment do not deform beyond yield. This is very important for the evaluation of moment redistribution of the composite beams since this depends on the strain hardening behaviour of the steel section. Rotter and Ansourian (1979) suggested that values of ductility parameter χ (given in Equation 8) in excess of 1.6 are needed for the achievement of sufficient sagging moment redistribution. The ductility parameter of $b = 400$

and 800 are 1.05 and 2.09, respectively, in this case. This result therefore supports their suggestion in sagging moment.

$$\text{Ductility parameter } \chi; = \frac{0.85 f_c b f_{cu} \tilde{A} (h_{conc} + h_{steel})}{A_{steel} f_{sy} (f_{cu} \tilde{A} + f_{st} \tilde{A}_s)} \quad (3.9.8)$$

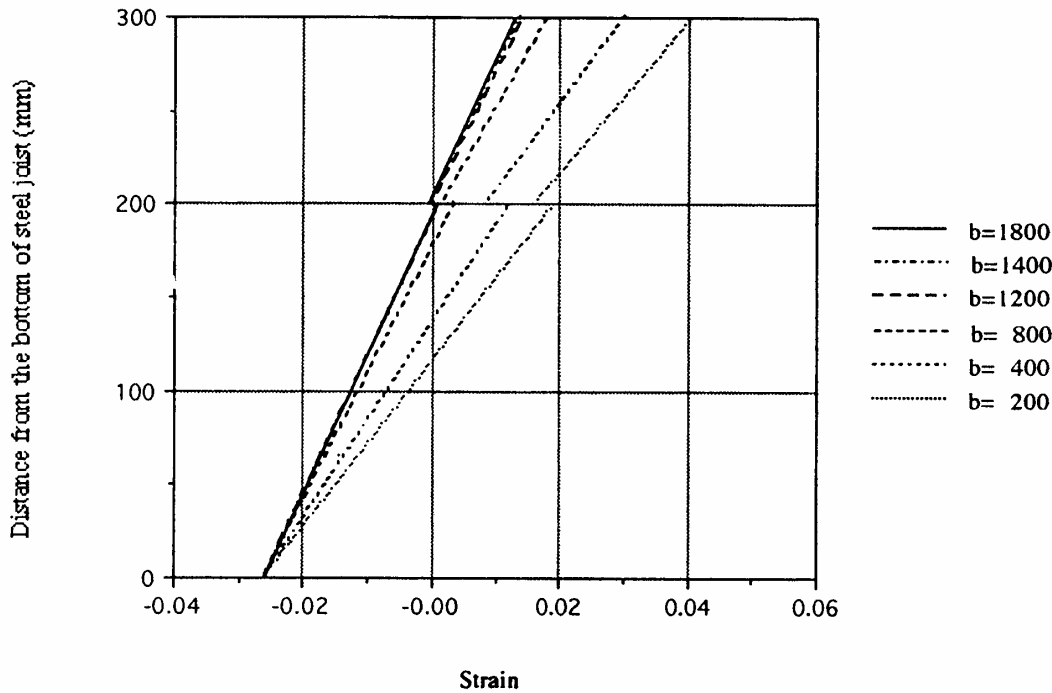


Figure 3.9.14 Strain diagram at the Ultimate Limit State in Hogging Moment with various Slab Width

The strain diagram at the limit state in sagging and hogging moments are shown in Figures 3.9.13 and 3.9.14, respectively. Although slip strain occurs between concrete and steel surfaces in sagging and hogging moments, the strain distribution in the concrete slab and the steel beam are parallel. This indicates that the same curvature can be maintained up to the ultimate limit state in both sagging and hogging moment.

Higher curvatures can be achieved for wider slabs in sagging moment, but the curvature decreases in hogging moment. This is discussed above and is clearly demonstrated in Figure 3.9.13 and 3.9.14.

3.9.3.4. Effect of Stud Shear Connectors

Parametric Variation of Degree of Shear Connection

The simple model employed in the current study provides an opportunity to study the effect of shear connector characteristics on the deformational quantities of composite beams. The range of parameter variation investigated is given below:

- (a) Continuous or perfect interaction (degree of shear connection; $\eta = \infty$)
- (b) Studs-2xD25@200 ($\eta = 400$ % in sagging, 430 % in hogging)
- (c) Studs-1xD19@200 ($\eta = 125$ % in sagging, 133 % in hogging)
- (d) Studs-1xD16@200 ($\eta = 90$ % in sagging, 95 % in hogging)
- (e) Studs-1xD13@200 ($\eta = 60$ % in sagging, 62 % in hogging)
- (f) Studs-1xD 9@200 ($\eta = 30$ % in sagging, 31 % in hogging)

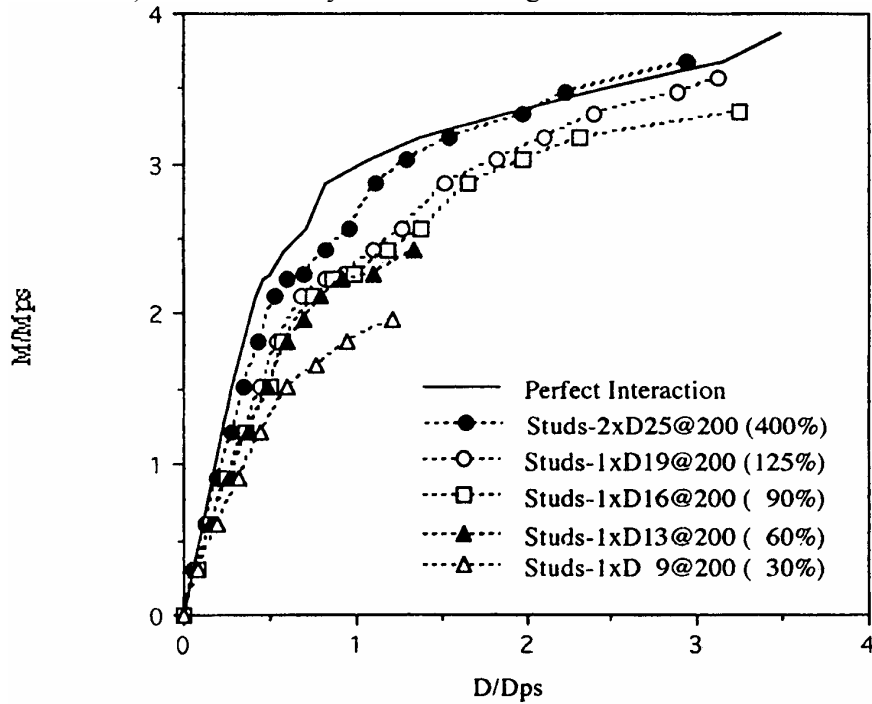
where degree of shear connection is defined as:

$$\eta = P_{shear} / \min.(P_{steel}, P_{conc}) \quad (3.9.9)$$

in which P_{shear} ; Total strength of shear connectors along the bending beam span
 P_{steel} ; Axial strength of steel beam section

P_{conc} ; Axial strength of concrete section

Full shear connection means $\eta=100\%$. The cases of $\eta<100\%$ means partial shear connection (partial interaction) which is usually avoided in design codes. All cases use the same slab width $b = 1800$ mm.



M_{ps}, D_{ps} ; Plastic moment and corresponding deflection for steel joist alone

Fig. 3.9.15. Effect of shear connectors in sagging moment: Moment–Deflection ($b=1800$, f_e430 , C40)

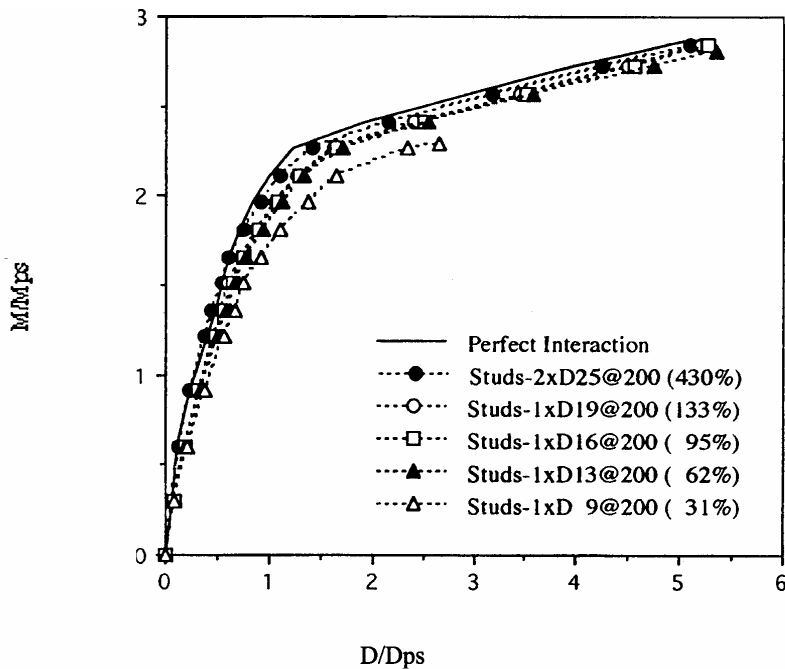


Fig. 3.9.16. Effect of shear connectors in sagg. moment: Moment–Curvature[1] ($b=1800$, f_e430 , C40)

Effect of Degree of Shear Connection

The results of the parametric study are shown in Figures 3.9.15 for sagging moment and Figure 3.9.16 for hogging moment. The cases of 1xD13 and 1xD9 in sagging moment failed due to slip while the remaining cases were controlled by compressive ultimate strain (0.4 %) at the top of concrete slab. In hogging moment, only 1xD9 failed by slip. All others cases were controlled by the buckling of the bottom of the steel beam.

The absolute values of maximum curvature are the same in the cases controlled by material failure (no slip failure) in sagging and hogging moments. Amongst the response curves depicted in Figures 3.9.15 and 3.9.16, the most ductile case is that of perfect interaction where ductility is approximately 13 in sagging and 11 in hogging moment. On the other hand, the least ductile case is 1xD9 with ductility is approximately 2 in sagging and 4 in hogging.

In sagging moment, the difference in non-dimensional ductility between perfect interaction and 1xD19 ($\eta = 125\%$) is a factor of more than 4. This difference is slightly less than 2 in hogging moment. These results suggest that the margin above 100 % shear connection (design value) should be considered in practical applications for increasing the ductility of composite beams. Contrary to cases of partial interaction, interaction parameters of higher than 100% have not been researched. They assume a higher degree of significance in the course of ductility-based and deformation-based seismic design.

Cases where to ultimate limit state was slip between steel beam and concrete slab (1xD13 and 1xD9 in sagging, 1xD9 in hogging moment) responded below the strain hardening region ($\epsilon \geq \epsilon_{\sigma\tau} = 0.014$) up to the attainment of the limit state of slip. All other parametric cases responded well into the strain hardening regime, indicating that even partial interaction may lead to moment redistribution of the beams. The region of interaction that leads to moment redistribution potential is between 60% and 90%. The effect of partial interaction on moment redistribution has rarely been investigated in previous research.

The strain diagrams corresponding to limit state attainment in sagging and hogging moments are shown in Figures 3.9.17 and 3.9.18, respectively. Those Figures confirm that the curvatures are almost the same where the behaviour is controlled by material response limit states (concrete and steel) without reaching slip limits, as discussed above. Only the cases of 1xD13 and 1xD9 in sagging and 1xD9 in hogging moments are conditioned by slip.

3.9.3.5. Proposal for Simplified Design Procedure

Figure 3.9.19 shows the relationship between degree of shear connection and slip strain at the ultimate limit state, whilst the relationship between degree of shear connection and M_{ult} / M_{ps} is shown in Figure 3.9.20. The slip strain (ds/dx) is the derivative of slip along the beam length and can be defined as follows:

$$ds/dx = (\text{Strain at bottom of concrete slab}) - (\text{Strain at top of steel beam}) \quad (3.9.10)$$

As shown by open circles and open triangles in Figure 3.9.19 and 3.9.20, it is clear that the material limit state attainment cases follow hyperbolic curves in sagging and hogging moment senses. The cases (solid circle and solid triangle cases) whose ultimate limit states are dependent on the stud failure (ultimate slip capacity) fail below these hyperbolic curves. If the relationship shown in Figure 3.9.19 is normalised by the strain at zero shear connection (no studs), referred to as 100% slip in the Figure, then the relationship between degree of shear connection η and ultimate slip strain ds/dx may be described by hyperbolic curves fitted to the response points of sagging and hogging moments. This is given as:

$$|ds/dx| = 1/(1+\eta^2) \quad (11)$$

For the verification of this equation, more parametric studies are needed. This equation is useful for

predicting the slip capacity because the ultimate slip strain for zero shear connection (no studs) is easily calculated from the response of steel beam and concrete slab acting independently.

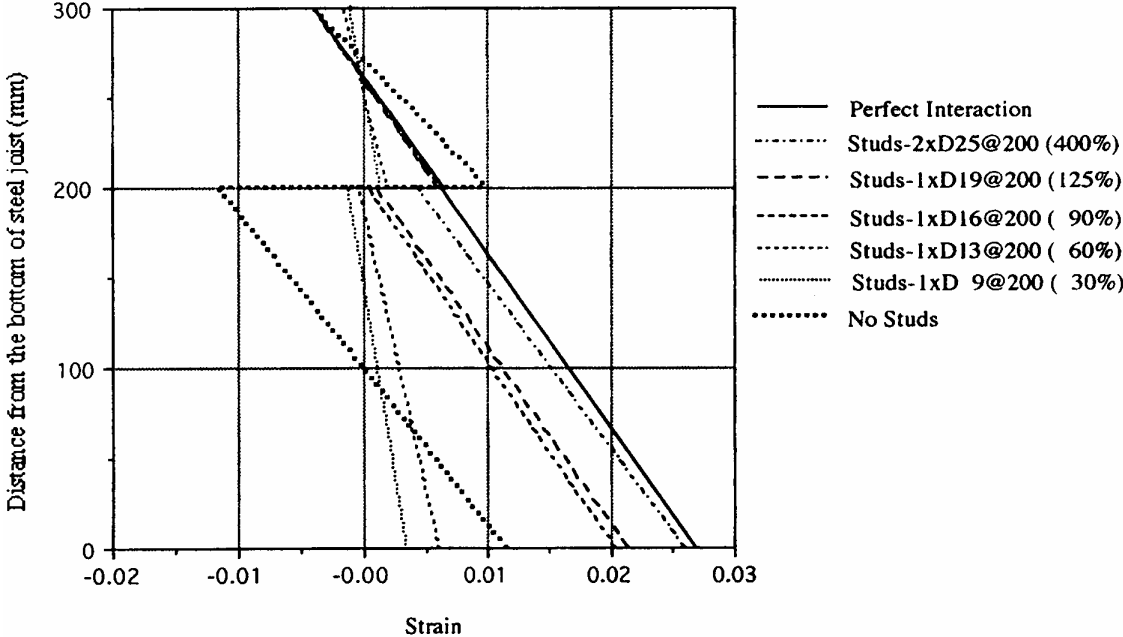


Figure 3.9.17. Strain Diagram at the Ultimate in Sagging Moment with Various Stud Connectors

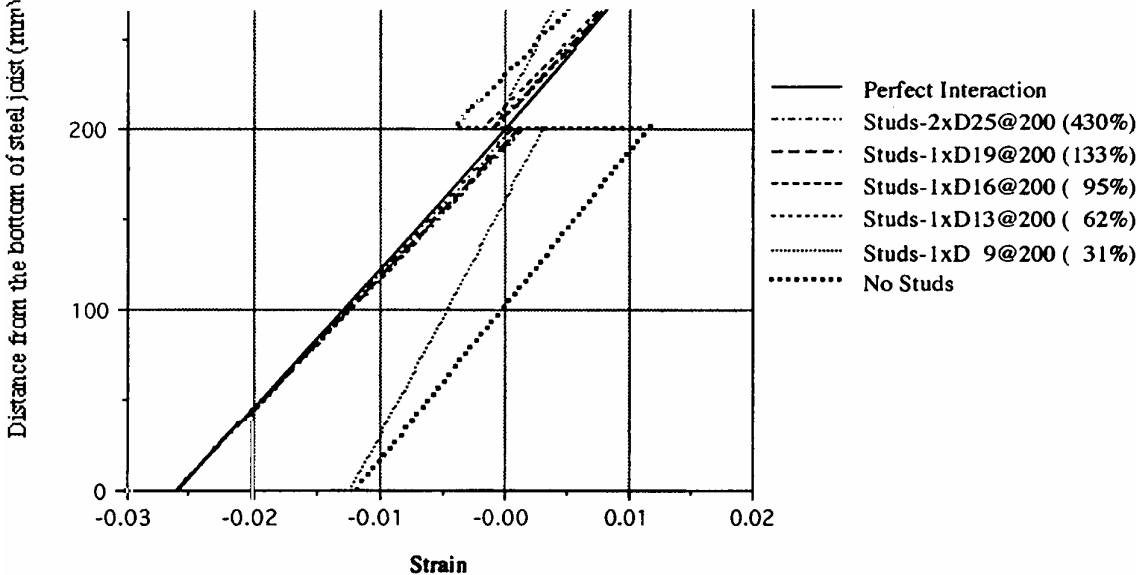


Figure 3.9.18. Strain Diagram at the Ultimate in Limit State in Hogging Moment with Various Stud Connectors

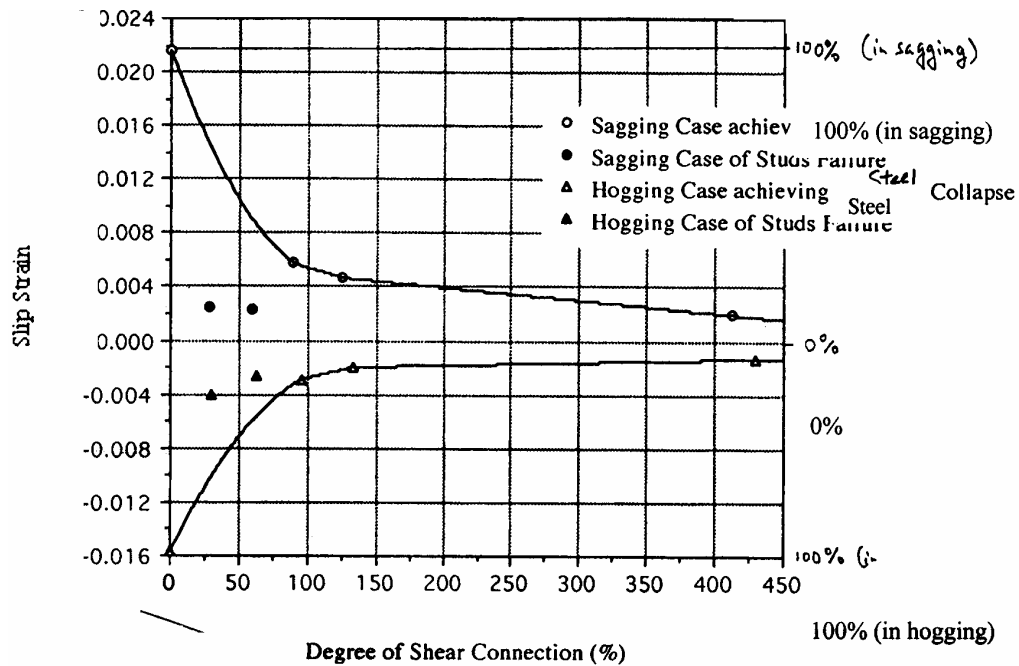


Figure 3.9.19. Relationship between Degree of Shear Connection and Slip Strain

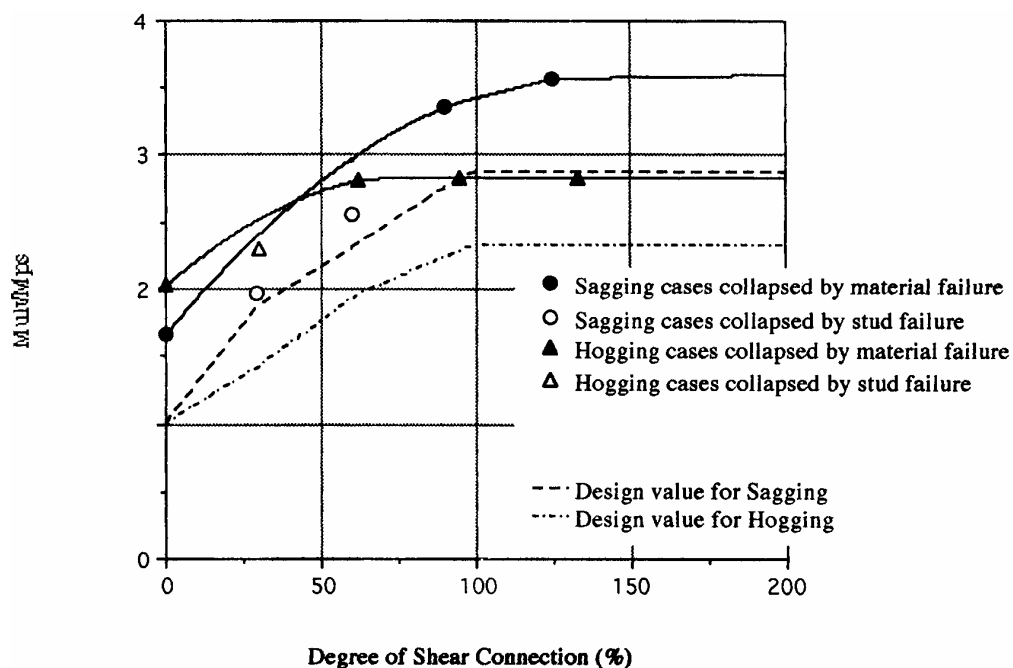


Figure 3.9.20 Relationship between Degree of Shear Connection and Ultimate Moment Capacity

3.9.4. Comparison of Conventional and Partially Encased Composite Beams

3.9.4.1. Equivalent Partially Encased Composite Beams

Due to the limitations of experimental work, mentioned above, analytical investigations are undertaken to compare conventional composite beam behaviour with that of partially encased beams. The equivalence criterion used is that the two beams should have the same plastic moment capacity. Other equivalence criteria may be envisaged, but the constant M_p case seems reasonable. The main motivation behind this study is that the partially encased composite configuration has exhibited exceptional deformation capacity as a column member (Elnashai and Elghazouli, 1993 and others). The same configuration is therefore investigated as beam members.

Partially encased section with approximately equivalent plastic moment to conventional composite beam with characteristics $b= 1800$ mm and Studs-2xD25@200 are compared in this Section of the report. The section of partially encased composite beam and of the bare steel equivalent are shown in Figure 3.9.21 . The analytical approach used is identical to that used above.

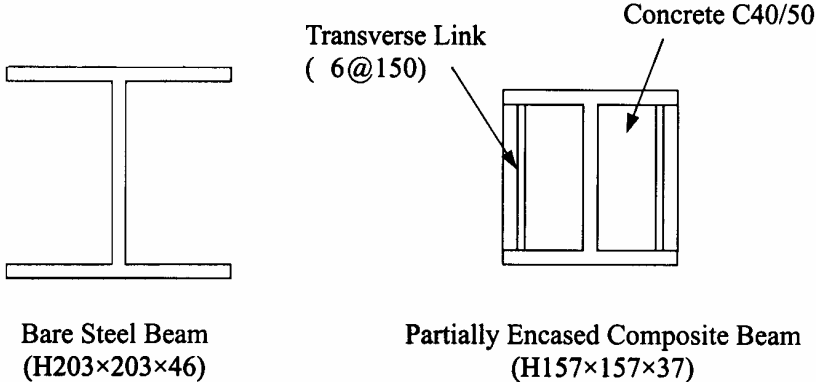


Figure 3.9.21. Equivalent Bare Steel Beam and Encased Composite Beam

The ultimate limit state of partially encased beam is defined as the local buckling. The critical buckling strain with transverse link spacing and flange slenderness is calculated according to Broderick and Elnashai (1996). In the current parametric study, the pitch of transverse links is assumed to be small enough (150 mm) to prevent local buckling up to and beyond the compressive (squash) capacity of the steel member.

3.9.4.2. Comparative Results for Simple Beams

The results of the comparison are shown in Figure 3.9.22 to 24. In the figures, M_{yall} represents the applied moment at the first plastic hinge formation, corresponding to yield at both top and bottom fibres. The symbols D_{yall} and C_{yall} denote the elastic deflection and elastic curvature, respectively, at mid-span when the plastic hinge occurs in any location along the beam.

The conventional composite beam reaches its ultimate limit state at the ultimate concrete slab compressive strain of the top (sagging moment) and at the steel beam buckling at the bottom (hogging). The corresponding limit states of bare steel beams is the critical buckling stress. Improved partially encased composite beams fail by the attainment of ultimate tensile strength of steel element because the encased concrete and transverse links prevent buckling of steel section if the links are sufficiently closely spaced.

From Figure 3.9.22, it is observed that the plastic moment of bare steel and partially encased composite beams lie between sagging and hogging plastic moments of conventional composite beam. High ultimate strength is observed for the cases of partially encased composite beams and sagging moment conventional composite beams. However, the mid-span deflection at which this ultimate strength is reached is much larger in the former case, which also exhibits superior ductility. In the relationship of normalised moment-deflection (Figure 3.9.23) and moment-curvature, conventional composite beams seem quite ductile. However, this is offset by the observation that they are less stiff, hence are difficult to use for the serviceability limit states, unless very high shear connection levels are achieved, since the loss of stiffness at about half the moment capacity is attributed to slip at the beam-slab interface.

Partially encased composite beams exhibit the highest curvature ductility, approximately 10% higher than the bare steel counterpart, and more than 80% higher than the conventional composite beams. Provided the spacing of links preventing local buckling is well-controlled, this structural form provides

an excellent earthquake design alternative to conventional configurations.

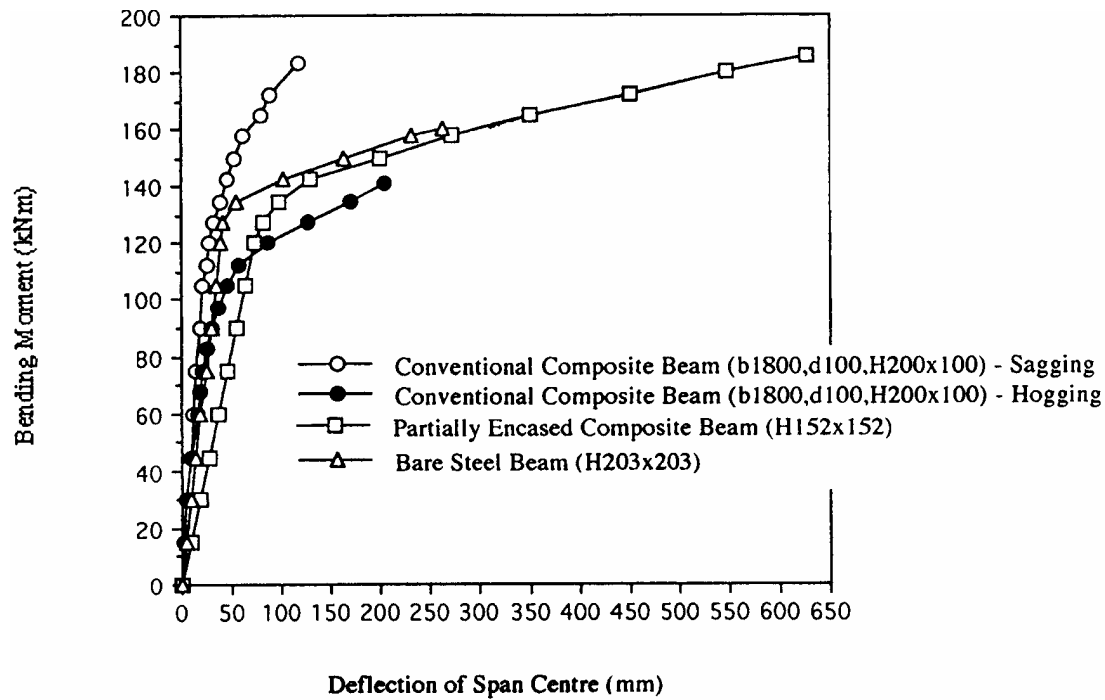


Figure 3.9.22. Comparison of Equivalent Beams ; Moment – Deflection[1]

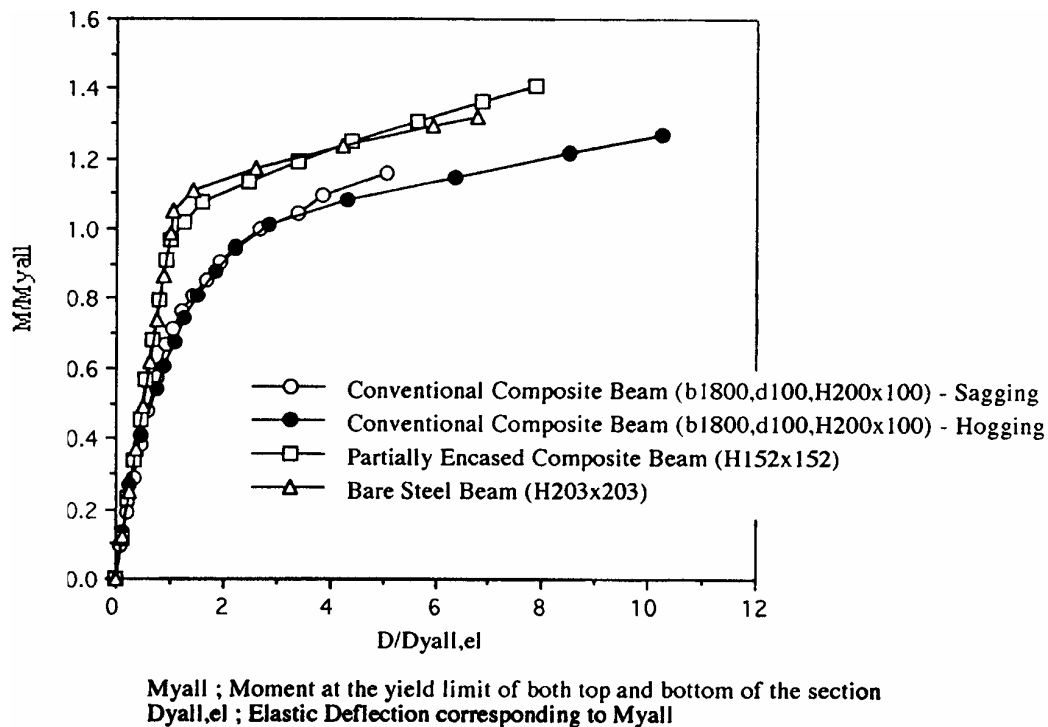


Figure 3.9.23. Comparison of Equivalent Beams ; Moment – Deflection[2]

Another important observation from Figure 3.9.23 is the ratio of maximum-to-yield moment, possibly termed member overstrength. It is clear that the overstrength of conventional composite beams are on the whole lower than those for partially encased beams. Noting that the overall structural overstrength is mainly influenced by member overstrength, redundancy and redistribution potential, if the latter two are the same, the structure with partially encased beams will exhibit higher overstrength than that with conventional composite beams. Consequently, the response modification factor (q or R) is likely

to also increase when encased beams are employed, thus reducing design forces, or increasing the safety of the structure when subjected to earthquake loads.

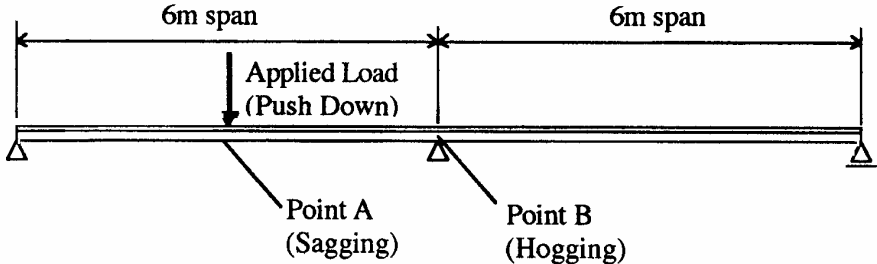
3.9.5. Analysis of Two Span Composite Beams

3.9.5.1. Moment Redistribution in Continuous Composite Beams

As mentioned above, the ability of a structure to resist seismic forces is affected by its ability to redistribute the applied actions from highly stressed locations to less stressed ones. In particular, beams are subjected to high moment gradients, and they behave differently in sagging and hogging moment sense, a characteristic not shared with columns. Therefore, investigating the ability of conventional and partially encased beams to redistribute moments along their spans is of significance to seismic design. The simplest form of structure where redistribution may be detected is a continuous beam, hence this section of the report deals with this structural form. The analyses are undertaken for a push-down and push-up loading configurations, as shown in Figure 3.9.24.

(Push Down Case)

- Case CCD Conventional Composite Beam (b=1800, Stud-2xD25)
- Case EC Partially Encased Composite Beam (H152x152x37)
- Case BS Bare Steel Beam (H203x203x46)



(Push Up Case)

- Case CCU Conventional Composite Beam (b=1800, Stud-2xD25)

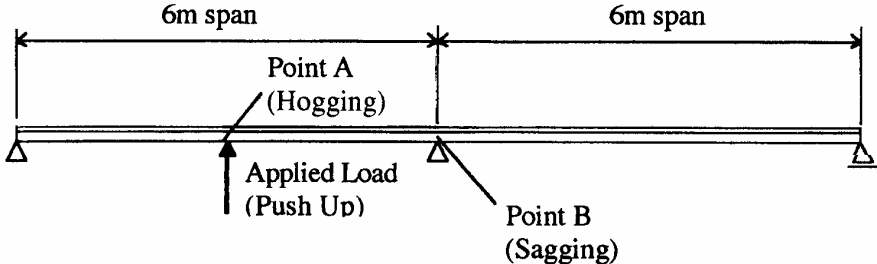


Figure 3.9.24. Push Up and Down Loading for Continuous Composite Beams

3.9.5.2. Results and Discussion

The results for the two-span continuous beams are shown in Figures 3.9.25 and 3.9.26, where redistribution potential is clearly depicted. In all cases, the analysis was terminated corresponding to the following limit state being achieved at point A, indicated in Figure 3.9.34 (the limit states were not achieved at point B):

- Case CCD: Concrete failure at P=157kN in sagging moment
- Case CCU: Local buckling of steel beam at P=147kN in hogging moment
- Case EC : Tensile strain of steel at P=174kN in sagging moment

Case BS : Tensile strain of steel at P=198kN in sagging moment

The behaviour of cases CCD and CCU are distinct from others due to the onset of slip. Figure 3.9.26 that all cases have $M/M_p > 1.0$ at point A. It is clear from the figure that the ability of the partially encased solution to redistribute actions hence to achieve higher values of normalised moment capacity is superior to conventional composite cases. Indeed, the former reaches values of normalised moment of more than 1.5.

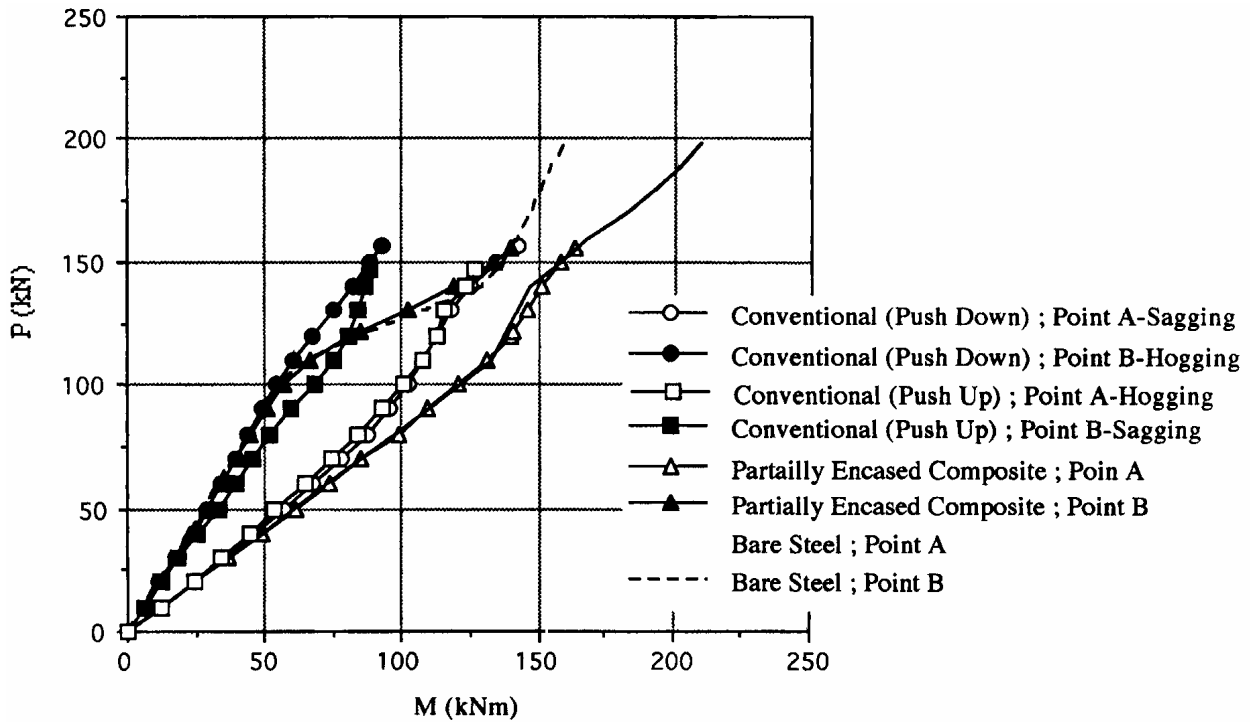


Figure 3.9.25. Moment Redistribution ; Load - Moment

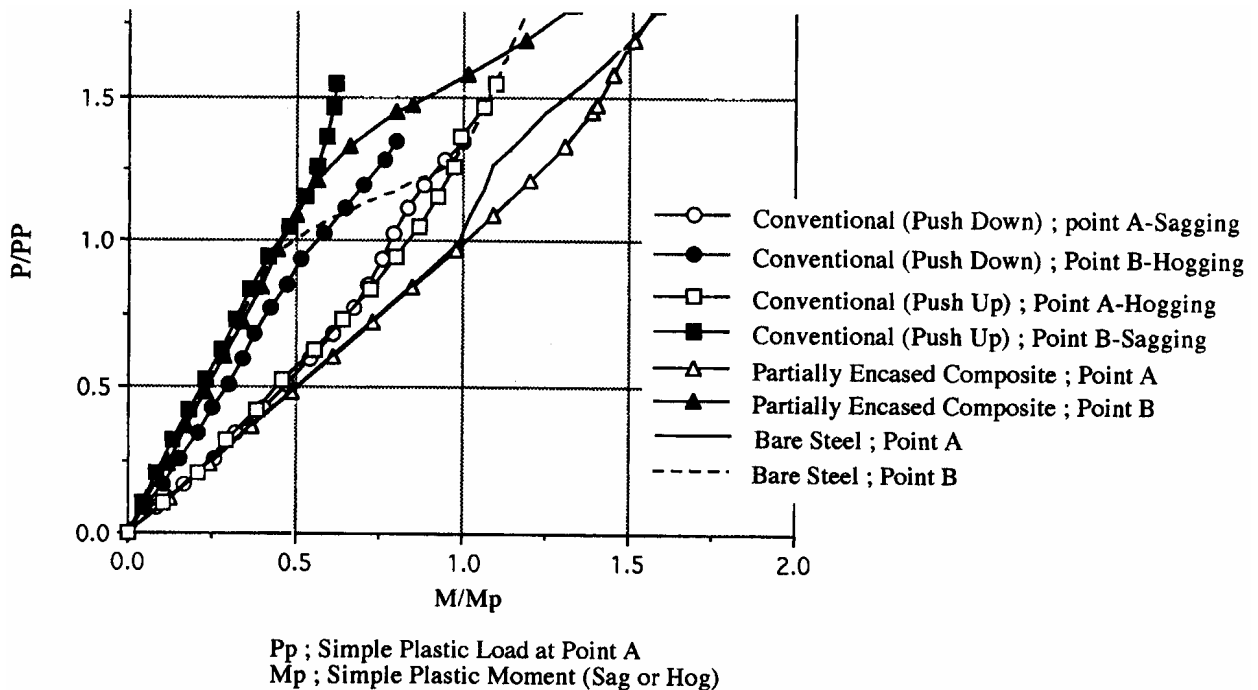


Figure 3.9.26. Moment Redistribution ; Load – Moment (non-dimensional)

It should be noted that the moment redistribution potential of CCD is higher than the CCU loading case,

where a drop is observed after loading of 120 kN ($P/P_p = 1.25$). This is because strain hardening has initiated at the bottom of steel beam of (point B) in hogging moment. It is concluded that balancing the various limit state attainment (i.e. material strain limits, deformation capacity and stiffness ratio) between sagging and hogging moments is critical to the seismic performance of conventional composite beams. This is due to their asymmetry about the horizontal beam axis, as well as the distinct behaviour of beam and slab under the two moment senses.

3.9.6. Summary of Analytical Observations

An analytical model has been proposed to represent the most salient features of the behaviour of composite beams (steel member, concrete slab and shear stud connectors). The model is simple and efficient, therefore can be used effectively in large inelastic frame analyses. The model is verified by comparison with the experimental results from the literature. This is followed by undertaking extensive parametric studies using the model for simple and continuous beams, with the beam section being bare steel, conventional composite and partially encased.

Effective width of concrete slab was varied in the parametric study between 0.16 and 1.5 times of the design width of Eurocodes in the conventional composite beam. Simply supported beams were analysed under a point load applied at mid-span in sagging and hogging directions. It was observed that under sagging moment, the wider the concrete slab is, the higher ductility the composite beam achieves. Conversely, in hogging moment, wider slabs result in the lower ductility. This is because a wider concrete slab in sagging moment allows the steel beam to enter into the strain-hardening regime in tension. On the other hand, hogging moments apply compression on the steel member, with an increased tendency for buckling as the neutral axis shifts towards the wider concrete slab. This calls for careful consideration of the balance between sagging and hogging capacity and ductility to achieve optimum seismic response.

The degree of shear connection has also been investigated by varying it between 30% and about 400%. It is shown that the theoretical 100% degree of shear connection is not optimal for ductility capacity, which is enhanced for higher interaction values in both sagging and hogging cases. The minimum shear connection effectiveness for seismic applications should be about 60%, since this allows a degree of yield penetration in the steel beam, thus enhancing energy absorption. It was also observed that the strain distribution in steel beam and concrete slab is independent of the degree of shear connection, which only affects the interfacial slip. An expression relating slip strain and degree of shear connection, suitable for design application, was given, based on the analytical parametric study results.

Partially encased composite beam and bare steel beam were compared with conventional composite beams of sufficient stud connection. The equivalence criterion used in the comparison was the plastic moment capacity. It was observed that partially encased composite beams achieve about 10% and 70% higher ductility capacity compared to bare steel and conventional composite solutions. Moreover, their initial and secant stiffness values are sufficiently high to enable deformation control at low limit states. The overstrength of the various members was studied, defined at the ratio between maximum and yield moments. It is clear that partially encased beams exhibit higher overstrength, therefore are potentially more effective in seismic design, where response modification factors are influenced appreciably by overstrength.

Analytical results from continuous beam studies have indicated that the partially encased solution is superior to the conventional composite beam. However, the latter's ability to redistribute moments along the span is adequate.

3.10. BRISTOL TESTS. Experimental evaluation of behaviour factors

A.S. Elnashai, M. Tsujii

Engineering Seismology and Earthquake Engineering Section Imperial College, London, UK

3.10.1. Testing objectives

The main purpose of the shaking table tests is comparison of seismic response for steel-concrete composite and bare steel frames mainly in terms of force reduction (behaviour) factors. The test programme is part of a larger research project concerned with the response of composite (steel-concrete) frames with a new type of member; this is a steel profile partially encased in concrete with shear links (Elnashai et al, 1991). In addition to the evaluation of behaviour factors for the tested frames, the results obtained would be used as a benchmark for calibration and validation of analytical models. These can then used to calculate behaviour factors for a much wider range of frame configurations.

3.10.2. The Bristol shaking table

These test were carried out on the shaking table of the University of Bristol. This shaking table, which was constructed in 1986 as an SERC (Science and Engineering Research Council, UK) facility, has been used to support nationally co-ordinated research programmes as well as European Collaborative. The table consists of a 3x3 m cast aluminium platform capable of carrying a 15 t payload. All six degrees of freedom are controllable by hydraulic actuators (Blakeborough et al, 1986). The characteristics of the earthquake simulator are shown Table 3.10.1.

Table 3.10.1 Characteristics of Shaking Table (University of Bristol)

Platform size (Practically used model size with overhang)	3 m×3 m (3 m×4.5 m)
Head room (Practically used model size)	4.5 m (3.7 m)
Platform motion	6 axes
Maximum payload	15 t
Maximum velocity X, Y, Z axes	0.5 m/sec
Maximum acceleration 5 t payload	1 g
Maximum payload at maximum acceleration in all axes	5 t
Maximum height of centre of gravity	1 m
Maximum displacement of X, Y and Z axes	+/- 150 mm

3.10.3. Model Characteristics and Dynamic Similitude

Table 3.10.2. shows the necessary scaling relationships for the test specimens. Geometrical scaling factor (ratio) l_r and scaling factor for Young's modulus E_r are 1/2 and 1. The similitude law is based on the artificial mass simulation approach, selected according to the following reasoning:

- True replica modelling in earthquake engineering is not usually attainable due to the constraints of the shaking table capacity and the difficulty of ideal material simulation. It is particularly difficult in terms of materials to satisfy the scaling requirements of both Young's modulus E and material density ρ (Moncarz and Krawinkler, 1991, Menu and Elnashai, 1988). Partial similitude modelling

is therefore the usual choice, the practicality and validity of which are proved by previous researches (Blakeborough et al, 1991 & Taskov et al,1992).

- For direct comparison of steel–concrete composite frames and bare steel frames on the shaking table, it is preferable to use prototype materials and standard sections.
- Artificial mass simulation is suitable for gravity loads, which is one of the important factors affecting the response of structural systems (Jurukovski et al, 1985).

Partial similitude was therefore applied in deriving the characteristics of the models and scaling of the input ground motion.

Table 3.10.2 Scaling Relationships for Dynamic Models

Physical Quantity (Similitude Parameters)	Artificial Mass Simulation
Length	l_r
Time	$l_r^{1/2}$
Frequency	$l_r^{-1/2}$
Displacement	l_r
Velocity	$l_r^{1/2}$
Acceleration	1
Gravitational Acceleration	1
Modules of Elasticity	1
Mass Density	Lumped masses, $E_r l_r^2$
Specific Stiffness	-
Force	l_r^2
Strain	1
Stress	1

$$l_r = (\text{model characteristic length}) / (\text{prototype characteristic length})$$

$$E_r = (\text{model material modulus of elasticity}) / (\text{prototype material modulus of elasticity})$$

3.10.4. Design of frame models

3.10.4.1. Moment Resisting Frames

Moment resisting frames are used extensively in static and seismic design. By virtue of their high ductility capacity, MRFs are allocated the highest force reduction factors in seismic codes. It is noted that only eccentrically-braced frames (EBFs) are regarded as possessing the same level of behaviour factors as moment resisting frames. However, energy dissipation is restricted in EBF to the link beam. It is therefore less likely that such a configuration as EBFs would benefit greatly from new column or beam member concepts. A moment resisting frame configuration is therefore selected for this investigation.

3.10.4.2. Frame Model Characteristics

The prototype building is designed to Eurocode 3 (1991), 4 (1994) and 8 (1994) as a 2 storey-2 bay building of 7.4 m total height and 9 m total width. It is designed for imposed load of 3.5 kN/m², and to a design earthquake of 0.15g to 0.40g ground acceleration, depending on the geometry, as described below. The high (highest in UBC) ground acceleration is selected to insure that the design is governed by seismic considerations.

Taking into account the capacity and space limitations of the shaking table facility, a scale model of 2:1 was selected. After a number of analytical investigations to determine the optimum number and layout of model, it was decided to build four frame models, subdivided into two series (referred to as Series A and Series B). The characteristics of Series A (Frame SA 1 & CA 1) are depicted in Figure

3.10.1. All members of Series A are scaled exactly in geometry by the similitude ratios of Table 3.10.2 to investigate the behaviour around the yield limit state, which is inherently sensitive to the dimension, and more so than the ultimate limit state. On the other hand, Series B (Frame SB 1 & CB 1) consisted of intentionally smaller beams. The design ground acceleration for Series was 0.15g. These frames are necessary for the testing programme, since it is more certain that they are tested up to their ultimate limit state. All frames are tested as two-dimensional (2D) models orientated in the long axis direction of the shaking table.

3.10.4.3. Selection of Member Sizes

Comparison of the characteristics of partially-encased composite columns with the same size bare steel columns was undertaken by analysis. The steel members were designed according to Eurocode 3 (1991), whilst the composite columns were designed using the procedure described in Tsujii (2001). The ensuing member sizes are shown in Table 3.10.3 and Table 3.10.4.

Table 3.10.3 Members for Series A Frames

Structural type	Columns	Beams
Composite Frame (Frame CA1)	H100×100×6×8 (composite column)	H125×40×6×8 (fabricated from H125×60×6×8)
Bare Steel Frame (Frame SA0 & SA1)	H100×100×6×8 (bare steel column)	H125×40×6×8 (fabricated from H125×60×6×8)

(Material; Steel - ss400, Concrete - C30/37)

Table 3.10.4 Members for Series B Frames

Structural type	Columns	Beams
Composite Frame (Frame CB1)	H100×100×6×8 (composite column)	H100×30×4.1×5.7 (fabricated from H100×55×4.1×5.7)
Bare Steel Frame (Frame SB1)	H100×100×6×8 (bare steel column)	H100×30×4.1×5.7 (fabricated from H100×55×4.1×5.7)

(Material; Steel - ss400 for columns, Steel - fe360 for beams, Concrete - C30/37)

All columns for composite and bare steel frames are made of the same sized H shape (wide flange H100x100x6x8) which is the smallest size of ready-made universal columns. The column of composite frames are partially-encased and are reinforced by transverse links (Φ 6mm) to enhance the section curvature ductility. The transverse links are threaded between the flanges during prefabrication. Series of pseudo-dynamic tests and analytical investigations were undertaken by Elnashai et al (1991) and Elnashai and Broderick (1994). The results demonstrated that this partially-encased composite section possesses higher energy dissipation capacity than the sections previously used in practice.

The same members were used for beam members of both composite and steel frame configurations in Series A. The beams were prefabricated from ready-made H shape (H125x60x6x8) sections. The flange is cut 10 mm off along the whole beam length as shown in Figure 3.10.1. This is necessary in order that capacity design regulations are followed (beam and not column hinging). Dynamic analyses were carried out beforehand to investigate the order of yield attainment with regard to various flange widths, leading to the sections selected and the fabrication undertaken.

Similarly for Series B, the flanges were reduced by 12.5 mm along the whole beam length from the original ready-made H shape of dimensions H100x55x4.1x5.7. This was necessary to ensure that the ultimate limit state is attained within the shaking table limitations. The section modulus of steel beams was 47,560 mm² for Series A and 20,890 mm² for Series B. The section modulus of the bare steel columns was 76,500 mm² for all series. The intentionally small beam capacity of Series B frames is reiterated.

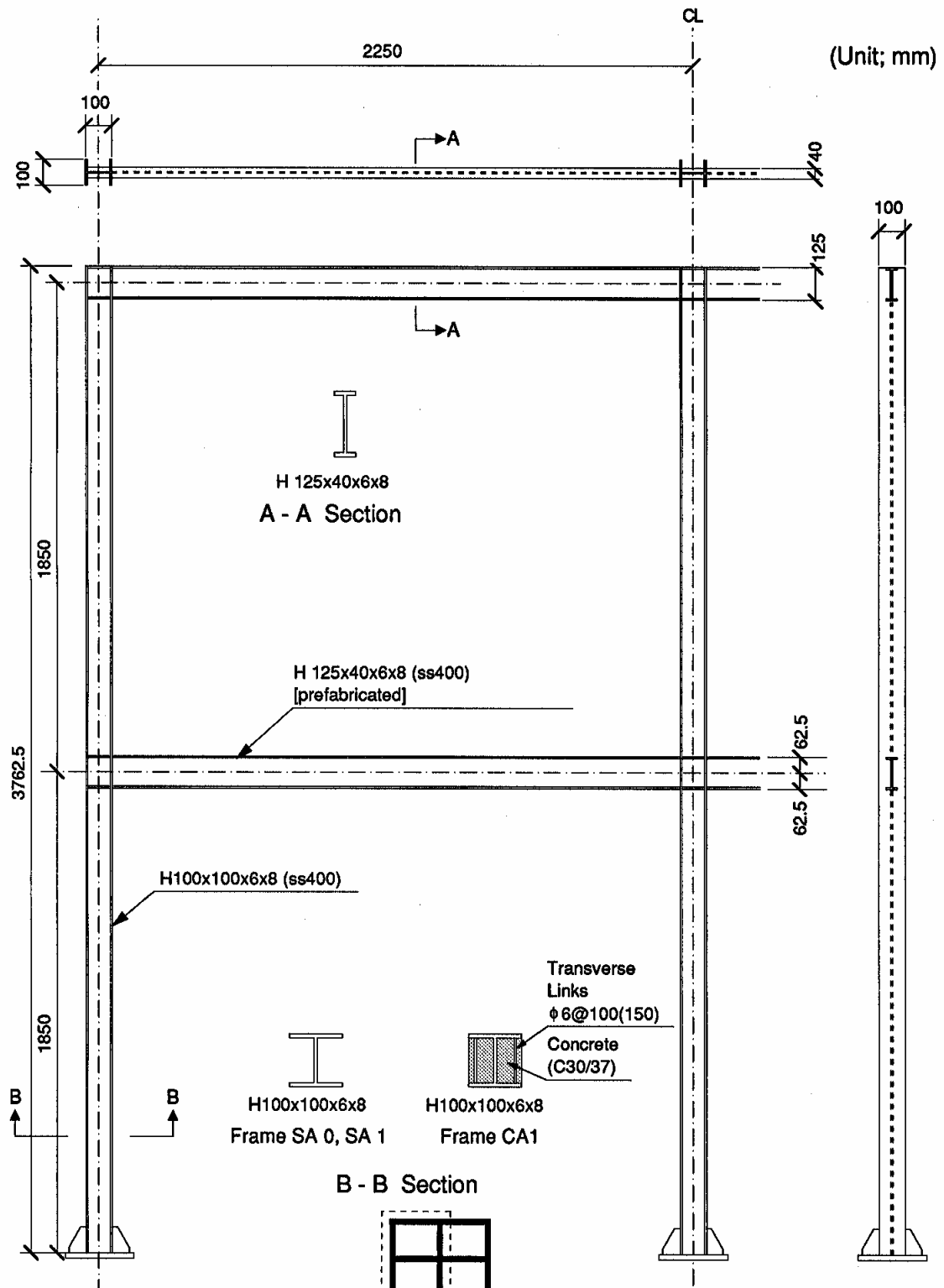


Figure 3.10.1 Test Frames for Series A (Frame SA0, SA1 & CA1)

The concrete slab was ignored in all four models. This approximation is justified by four considerations. Firstly, analytical procedures employed to evaluate behaviour factors in the ENV version of Eurocode 8 (1994) did not include the concrete slab explicitly. Secondly, there are serious difficulties in scale-modelling of the slab with reduced aggregate size and reinforcing bars. Thirdly, the contribution of the slab to the beam capacity would have lead to either lack of attainment of the ultimate limit state or further reduction in the already very slender beam members. Finally, the stability of the slab loaded by the inertia mass during testing is questionable at this small scale.

3.10.4.4. Materials for Frames

The results of the steel material tensile tests are shown in Table 3.10.5. Concrete compression tests gave an average characteristic strength of 34.5 N/mm².

Table 3.10.5 Results of Steel Material Tests

Specification	Code	Use	Yield Stress f_y (N/mm ²)	Tensile Strength f_u (N/mm ²)	Stress Ratio f_u / f_y	Elongation ϵ
H100×100×6×8	ss400	Columns	287	434	1.51	29 %
H125×60×6×8	ss400	Beams (Series A)	370	475	1.28	25 %
H100×55×4.1×5.7	Fe360	Beams (Series B)	305	411	1.35	36 %

3.10.4.5. Beam-column Connections

Beam-column connections of the frame models are illustrated in Figure 3.10.2.

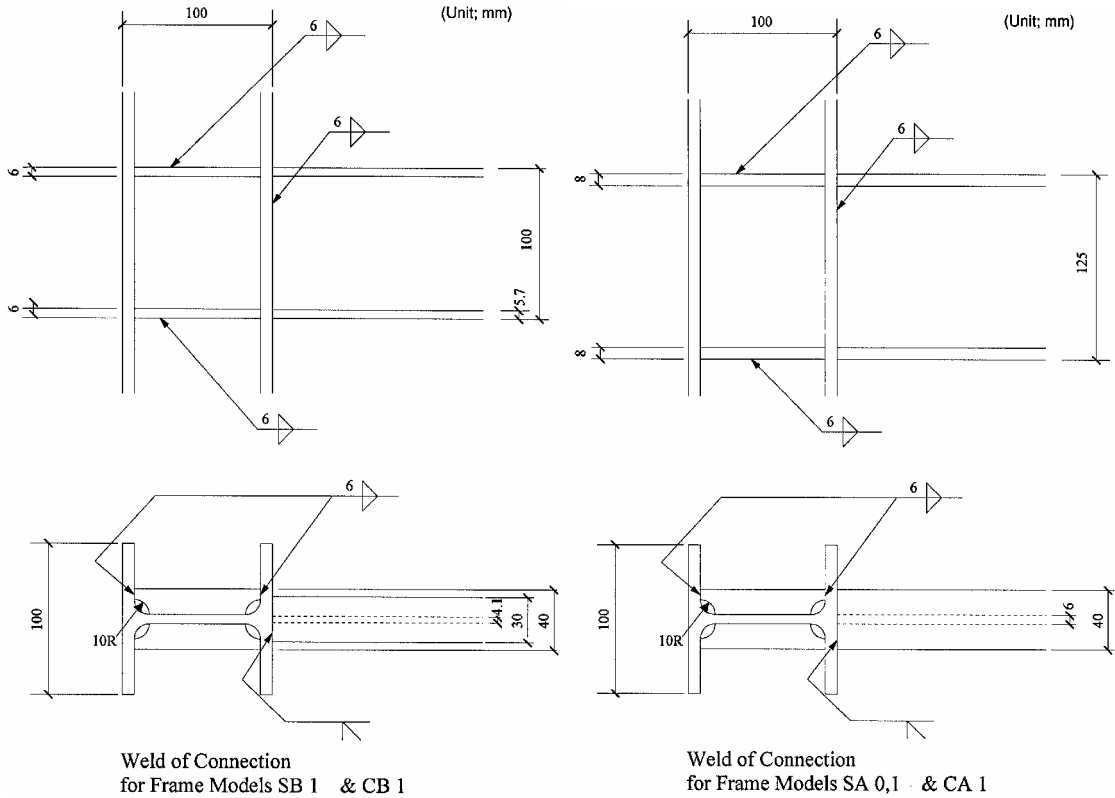


Figure 3.10.2. Rigid Beam-Column Connections

These connections and the base connection were designed to be fully welded rigid assemblages. Recent earthquakes (e.g. Hyogoken-Nanbu, 17 January 1995) highlighted the vulnerability of column base connections.

Action was taken to ensure that the welds possessed sufficient strength to allow the members of deform well into the elastic range. The weld strength was calculated to satisfy the design rules of IIW 15 (1976).

3.10.4.6. Frame Installation and Inertia Mass Arrangement

Out-of-plane motion, that would absorb energy and thus affect unrealistically the in-plane response, should be suppressed. Towards this end, two high-stiffness steel support frames were constructed. The test frame is then installed in between the two support frames. The test frame is kept aligned by means of ball bearings welded onto the support frames. An inertia mass of 7.2 t is attached to all composite and steel frames, thus represented similitude requirements. Four mass units are tied and connected by bolts and nuts. The total mass of the test frame and steel blocks was 8.1 t, which is very close to the capacity of the Bristol shaking table.

3.10.5. Limit State Criteria

The limit states defined for the testing programme are: yield limit state; occurrence of first plastic hinge; plastic hinge is detected when both extreme fibres of the section reach yield (Elghazouli, 1990); ultimate limit state. Four criteria are considered herein. These are (i) steel fracture stress in tension, (ii) steel buckling strain in compression, (iii) concrete crushing strain and (iv) global drift.

3.10.6. Execution of the shaking table tests

3.10.6.1. Instrumentation

The instrumentation is summarised in Table 3.10.6 These are intended to measure displacements, accelerations and strains at critical locations. The testing direction is defined as X.

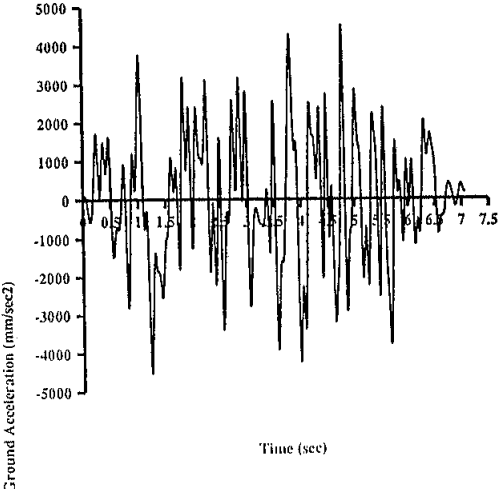
Table 3.10.6 Instrumentation Configuration

Channel No.	Instrumentation
1 – 3	Table accelerations (direction X, Y and Z)
4 – 7	Acceleration at 2 levels of the frame in X and Y direction
8 – 10	Absolute displacement at 2 levels and bottom of frame in X direction
11 – 22	Column element strain (12 points ; A1 – A4, B1 – B4, C1 – C4)
21 – 30	Beam element strain (10 points ; D1 – D6, E1 – E6)

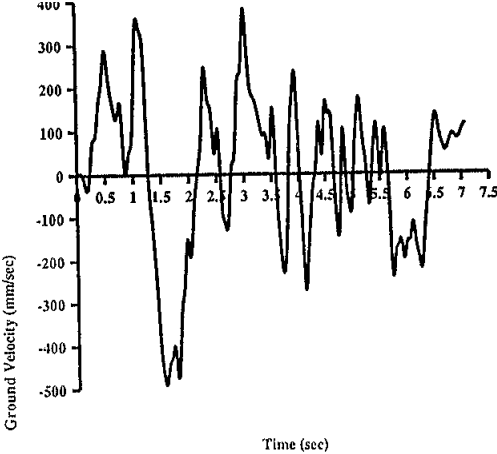
3.10.6.2. Input Earthquake Motion

After considerable analysis using four records generated to fit the elastic design spectrum soil sub-soil class B of Eurocode 8 (1994), the record referred to as EC8-4 was selected. The record imposes the highest demand on the test models, hence the possibility of achieving the ultimate limit state is maximised. The original time duration of this record is 10.0 sec. Since the duration of the input record should be compressed by the ratio of $1/2^{1/2}$ according to the similitude requirement in Table 3.10.2, the total duration of input motion is 7.0 sec. The acceleration, velocity and displacement of this record are shown in (a), (b) and (c) of Figure 3.10.3, respectively, in the case of the peak ground acceleration scaled to 0.46 g. This is estimated as the largest input motion that can be applied, as dictated by the

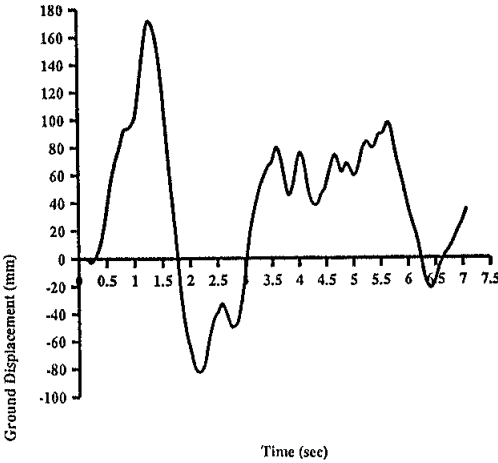
shaking table limitations. For the limit state satisfaction, the record is successively scaled in acceleration. There is no need for more sophisticated scaling, such as velocity spectrum intensity, since the record already represents the design code spectrum, hence scaling in acceleration is adequate.



(a) Ground Acceleration ($a_g = 0.46\text{ g}$)



(b) Ground Velocity of Input Record EC8-4



(c) Ground Displacement

Figure 3.10.3 Input Record EC8-4

3.10.6.3. Testing Procedure

The evaluation of response modification factors requires identifying the yield and collapse earthquakes. Towards this end, 5 testing steps for each frame were envisaged, as shown in Table 3.10.7. These comprehensively test the models up to the utilised limit state of 3% drift. After each run, analysis is undertaken using the program ADAPTIC (Izzuddin and Elnashai, 1989) to establish the next testing level without trial and error, often used in testing, and deemed here to have too significant an effect on the subsequent test run. In this manner, no trials were undertaken, but the target test limit state was achieved in one run.

Table 3.10.7. Testing Schedule for Composite and Steel Frames in Series A and B

Test No.	Scale (Peak a_g)	Purpose
1	a_{gyb} ¹⁾	Yield point of beams
2	a_{gyc} ²⁾	Yield point of columns
3	a_{gd} ³⁾	Design earthquake
4	a_{gu} ⁴⁾	Interstorey drift of 3.0 %
Addition	Harmonic input	Maximum amplification at minimum input

- 1) a_{gyb} is the peak ground acceleration (a_g) which achieves first yield in beams.
- 2) a_{gyc} is the a_g which achieves first yield in columns
- 3) a_{gd} is the design ground acceleration of the frames: 0.40g in Series A and 0.15g in Series B.
- 4) a_{gu} is the a_g at the attainment of the ultimate limit state (Interstorey drift of 3.0%).
This is adjusted based on updated ADAPTIC analysis results

For Tests CB1 and SB1 only, harmonic input motion was imposed to maximise the frame amplification within the shaking table limits and to draw smooth hysteretic loops for the response.

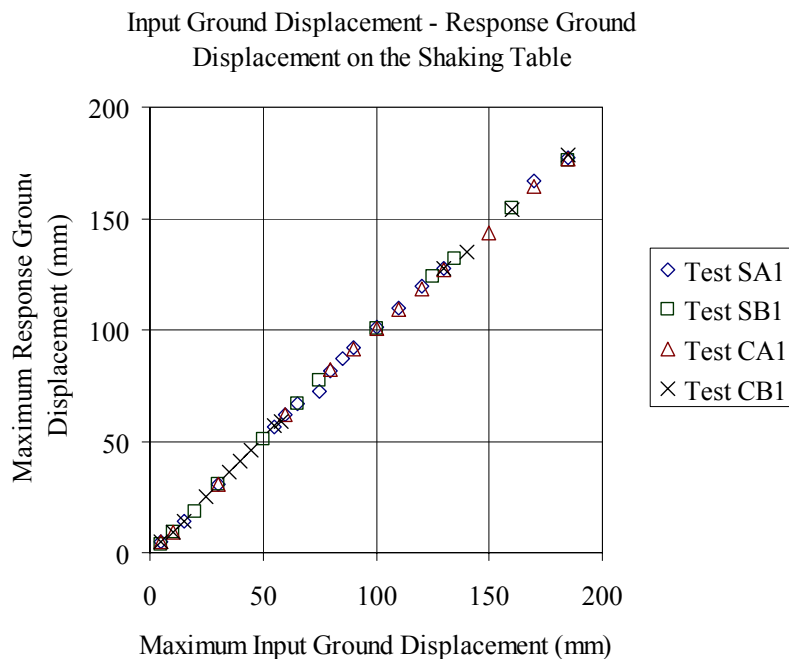


Figure 3.10.4. Ratio of input-to-measured displacement for shaking table

3.10.7. *Results of shaking table tests*

The results sampling rate was 1/240 seconds for all channels. The data was recorded and stored during the test run. The accelerations are measured as absolute values in the horizontal and vertical directions. The displacements are measured only horizontally and are relative to the table displacement.

3.10.7.1. Controllability of the Shaking Table

Shaking tables are controlled either by acceleration or displacements. It is noteworthy that recent developments of the software of the Bristol shaking table has rendered it more accurately controlled than when the above tests were undertaken. The shaking table used in this study is displacement-controlled. Therefore, the response table displacement should be compared with the input displacement signal. As mentioned above, the input motion for the shaking table tests is the generated acceleration record EC8-4. The input displacement time-history is obtained by double integration of the acceleration signal, whilst the table response is obtained from the displacement transducer of the platform.

Figure 3.10.4 shows the comparison between target and table displacements for test SA1, SB1, CA1 and CB1. The results are considered accurate and the table is well-controlled. The target displacement is indeed achieved on the table accurately, especially for maximum displacements not exceeding 150 mm. But, even beyond this level, the table displacement is still sufficiently accurate.

3.10.7.2. Detection of Limit States

Base shear and plastic hinges

All tests are executed successfully without any large problems. Three of four tests could achieve the global failure defined as more than 3.0 % of interstorey drift. The interstorey drift of Test CA1 only could not reach up to 3.0 % within the oscillation capacity of the shaking table. However, all testing cases gave the fruitful results as for the destruction phenomena with the earthquake ground motions.

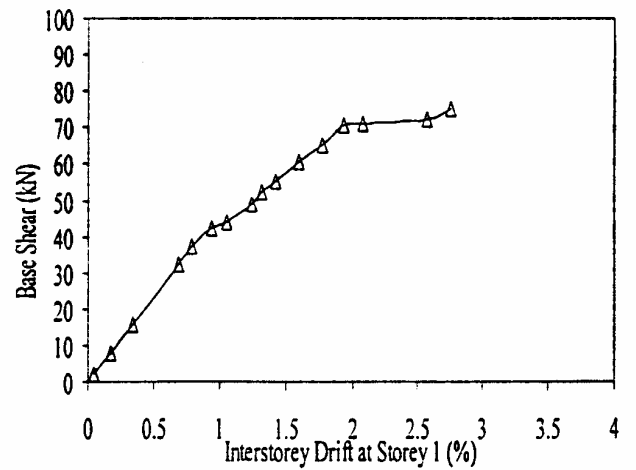
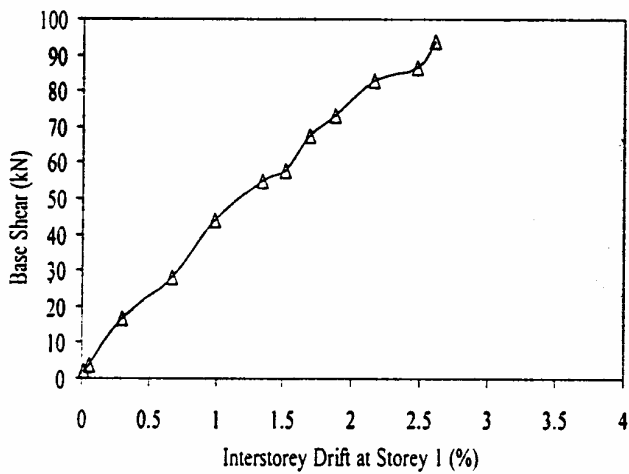
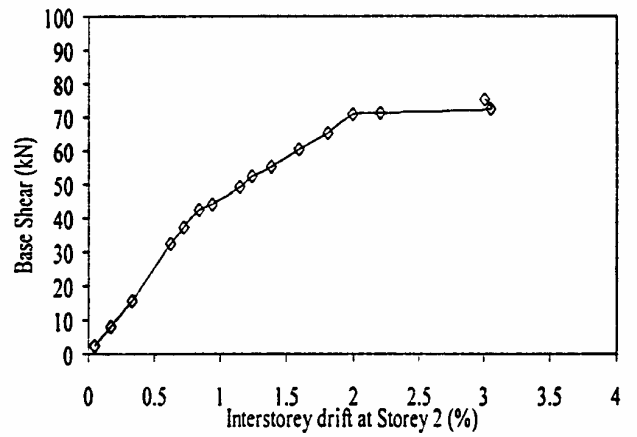
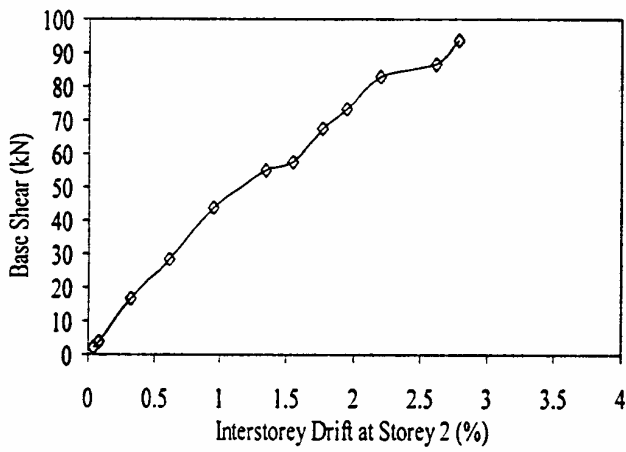
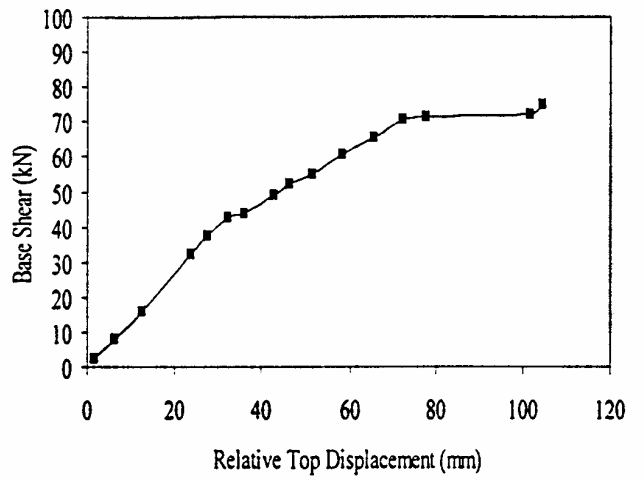
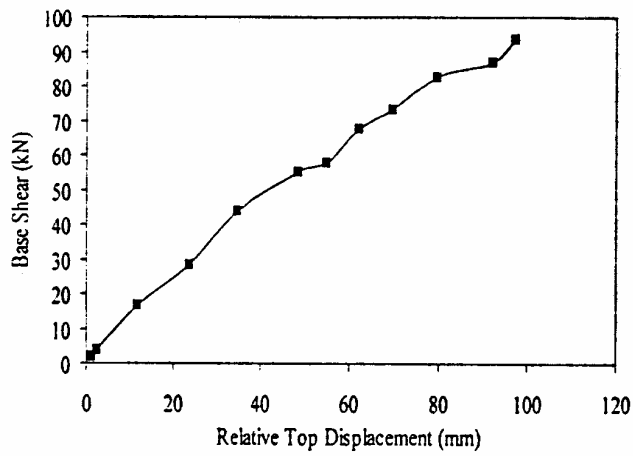
Base shear is useful indication for total input forces. To retrieve the value of base shear, the relative accelerations at each storey were used and a consistent mass formulation was employed to evaluate storey forces. These are then summed up in time to obtain the base shear versus time plots for the test models.

Figures 3.10.5 to 8 give plots of base shear versus time for the test models. Top, middle and bottom plots show the base shear versus relative top displacement, interstorey drift at storey 2 and interstorey drift at storey 1, respectively.

First plastic hinging occurred at the first storey beam end in all cases. The values of base shear corresponding to the first plastic hinge were 45.2 kN in test CA1, 44.2 kN in SA1, 23.4 kN in CB1 and 21.9 kN in SB1. The second plastic hinge was detected at the base of columns, when the base shear had the values 53.0 kN for CA1, 61.0k N for SA1, 57.4 kN and 48.0 kN for SB1.

Only models but CA1 reached the ultimate limit state of 3.0 % interstorey drift. The latter model had sustained the largest base shear of 93.9 kN, with the interstorey drift below 3%, reaching 2.8%. For the other models, base shear of 72.2 kN (SA1), 81.6 kN (CB1) and 56.7 kN (SB1) were recorded at the attainment of 3% interstorey drift.

Plastic hinges positions confirms that the capacity design approach adopted was realised in the tests. Only 4 plastic hinges are detected for model SA1. This is because this model has the smallest margin between beam and column capacities. The satisfaction of the weak-beam strong-column approach used in the design may indicate that it is the slab that causes levels of beam overstrength that undermines capacity design objectives at the beam-column sub-assembly level.

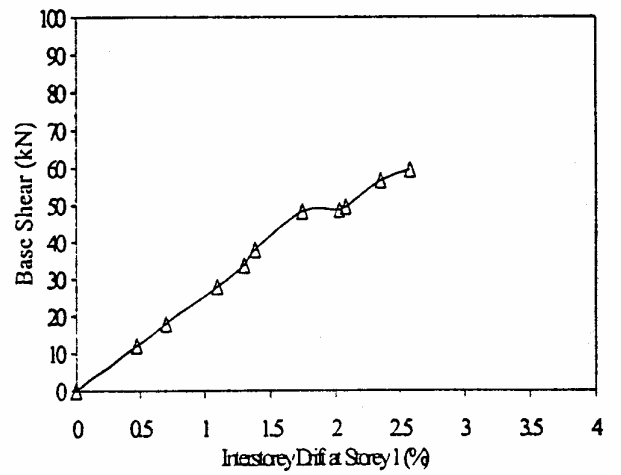
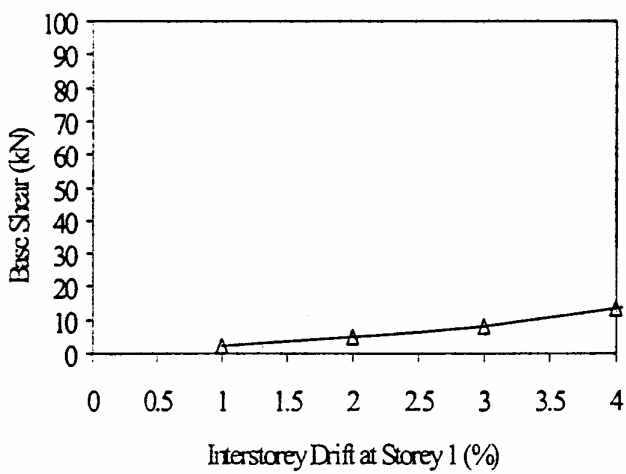
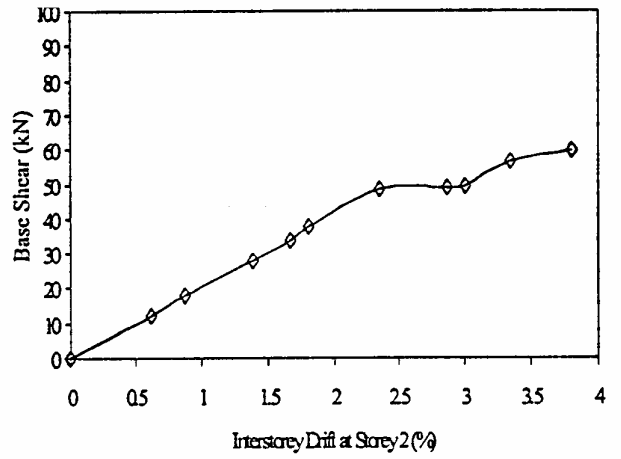
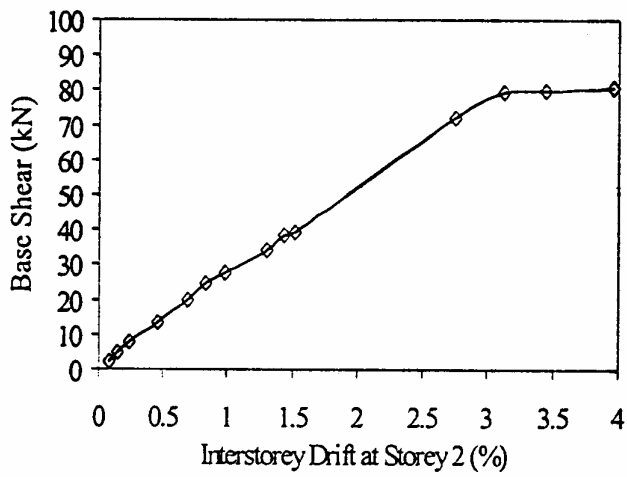
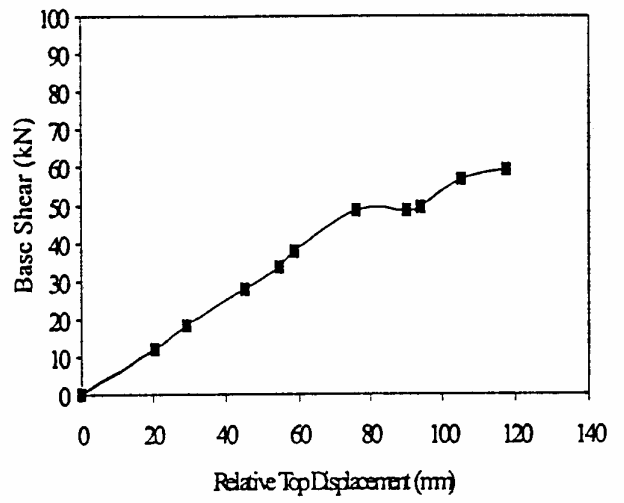
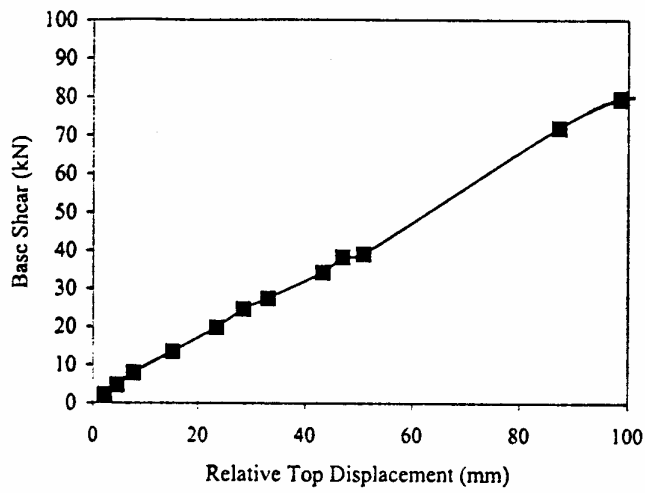


Deformation plots of model CA1

Deformation plots of model SA1

Figure 3.10.5.

Figure 3.10.6.



Deformation plots for model CB1

Figure 3.10.7.

Deformation plots for model SB1

Figure 3.10.8.

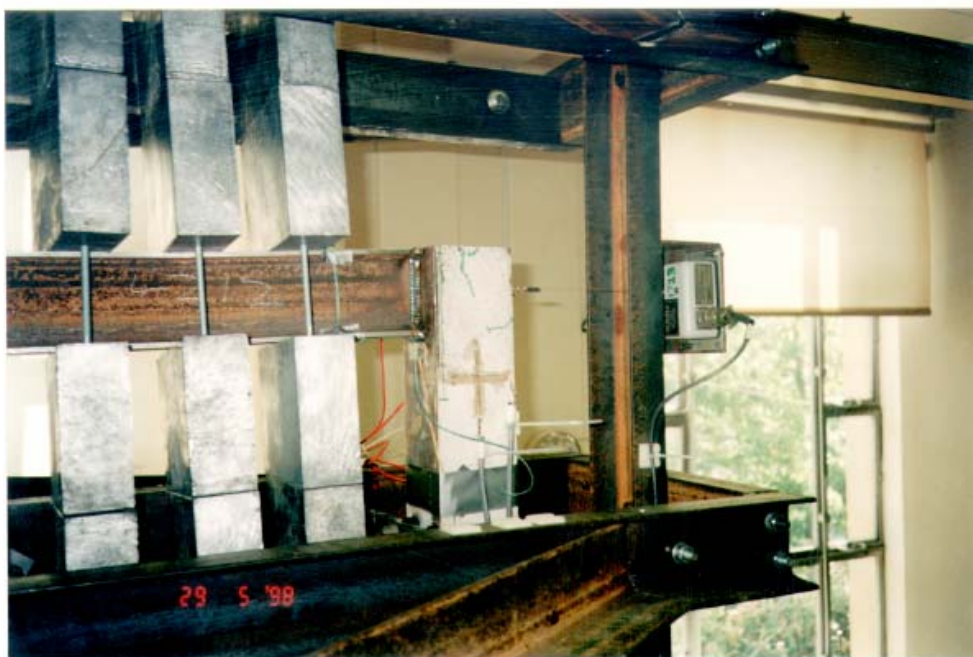


Plate 4.11 Damage at Top Corner after Testing (Test CB1)

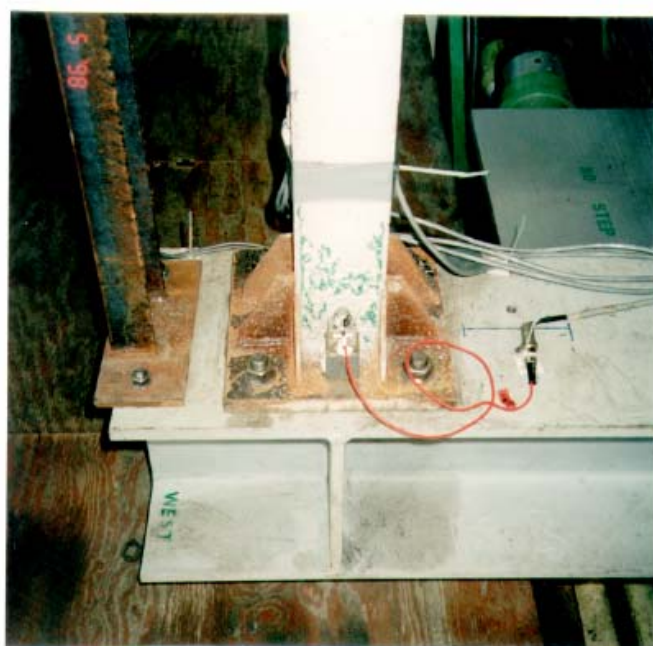


Plate 4.12 Damage at Column Bottom after Testing (Test CB1)

Figure 3.10.9. Specimen CB1 after testing.

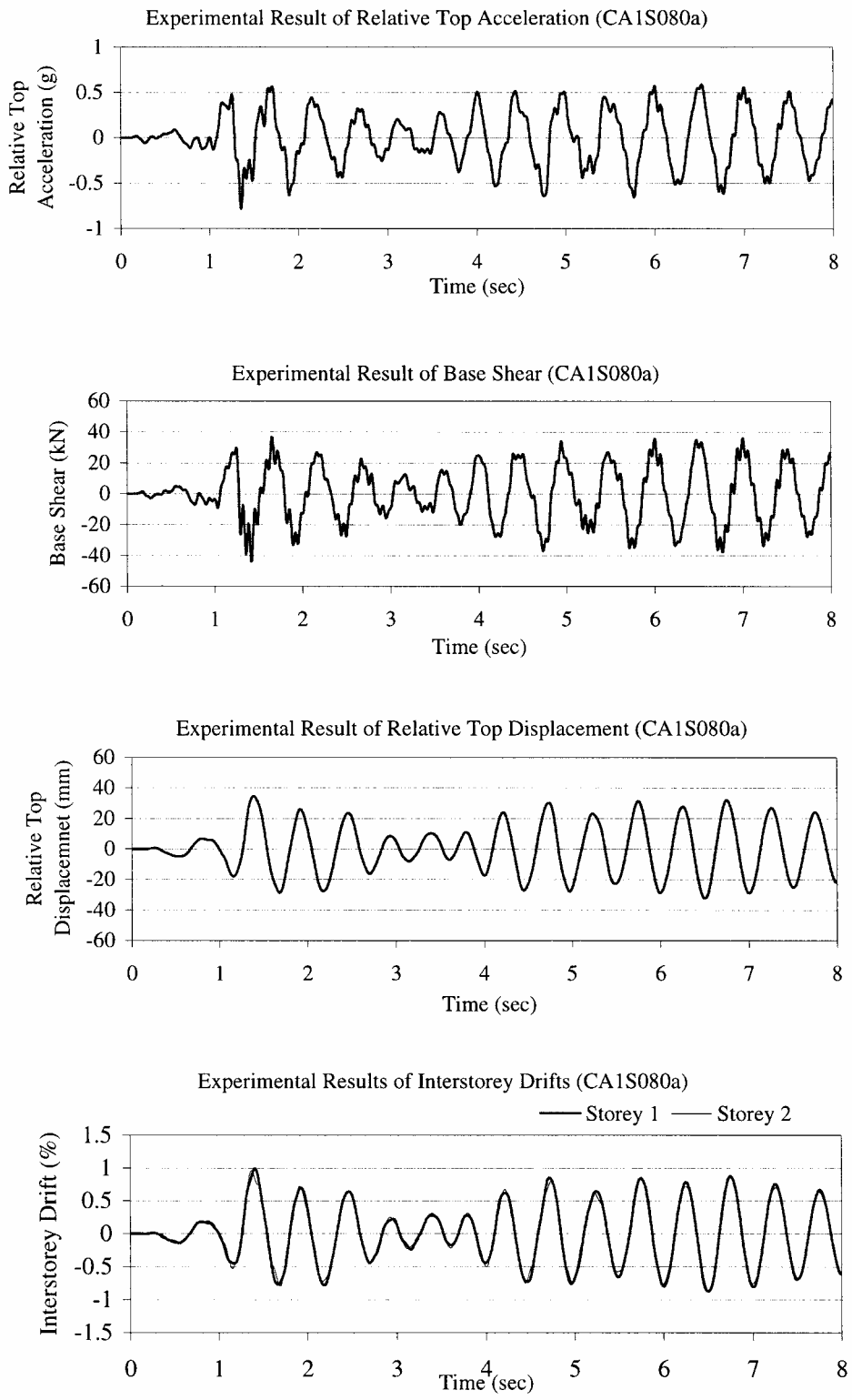


Figure 3.10.10. Experimental results at yield for model CA1

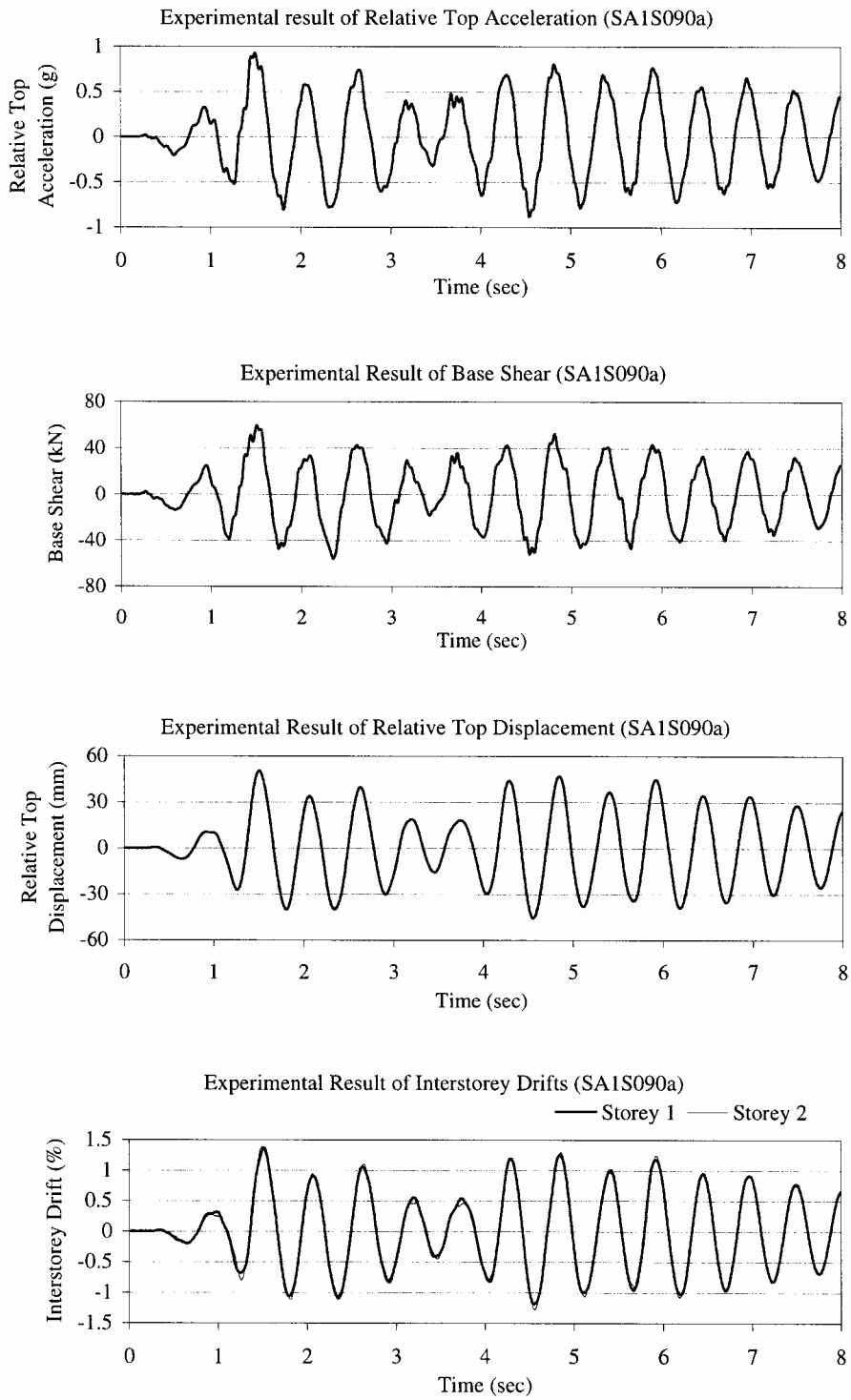


Figure 3.10.11. Experimental Results at yield for model SA1

Strains and state of beam-column connections

Measured strains in beams and columns at the first occurrence of plastic hinges for models CA1 and SA1, respectively confirm that when the beams reach yield, the columns are still in the elastic range. In specimen CB1, crack development in concrete is observed from the panel zone through to the interface between the steel flange and concrete. In panel section, diagonal cracks are visible. Figure 3.10.9 (Plate 12) also shows compounded cracking in concrete around the column base. Extensive cracking occurred at the connection corner between the yield limit state and ultimate limit state in all cases. It is interesting to note that cracking of concrete did not coincide with any indication of global deterioration of the frame. Therefore, the global response of the composite frames is not affected by local damage of concrete. Consequently, the latter role is mainly to protect the steel section from early buckling. The beams show sagging deformation. This is due to both the effect of intense transverse overstressing as well as the dead weight necessary to mobilise inertial effects.

Response of acceleration and deformation at limit states

The results are plotted at the attainment of each limit. See Figures 3.10.10 and 11 for specimen SA1. These give time-history plots of top acceleration, base shear and interstorey drift. It is noteworthy that whereas the displacement plots are smooth, acceleration plots show some erratic fluctuations. This is expected because very short period effects of snapping of masses and other sources of impact in the test may lead to such high frequency oscillations but these have no effect on displacements. The results for each pair of frames are quite similar. This holds for both yield and ultimate limit states, furnishing reassurance that the tests are repeatable and well-controlled. There is only a slight difference in forces where the composite frames respond at high frequencies upon concrete cracking. There is also some difference in inelastic response periods.

3.10.7.3. Observed Behaviour Factors

Experimental results of inherent behaviour factor

Table 3.10.8 displays the behaviour factors derived from the experimental results. Only Test CA1 did not achieve the target interstorey drift of 3.0%, with the quoted value of response modification factor corresponding the 2.7% drift. Therefore, strictly speaking, direct comparison of behaviour factors between composite and bare steel frame can only be made for series B. The behaviour factor of SA1 is 3.47, which is lower than the design value of 6 suggested for moment resisting frame in Eurocode 8 (1994). On the other hand, models CB1 and SB1 gave high behaviour factors of 9.06 and 8.93, respectively.

Table 3.10.8 Experimental Results of Response Modification Factors

Test Case	Peak a_g at Yield Limit State (g)	Peak a_g at Ultimate Limit State (g)	Behaviour Factor q
Test CA1	0.375	>1.295	>3.45
Test SA1	0.353	1.225	3.47
Test CB1	0.062	0.563	9.08
Test SB1	0.059	0.527	8.93

Notes: All yield limit states are first plastic hinge in beams

Only CA1 did not achieve the interstorey drift (Δ_i) of 3.0 % at maximum table capacity

Behaviour factor of CA1 derived at the peak acceleration corresponding to Δ_i of 2.8%.

Ultimate limit states of SA1, CB1 and SB1 at $\Delta_i = 3.0$ %.

The response modification factor of composite frame CB1 is only 1.7 % larger than that of bare steel frame SB1, a difference that is well below experimental errors. The ductility of the two systems

though are quite distinct with CB1 recording a displacement ductility of 3.77, 37% larger than the corresponding value for SB1. Whereas CA1 only reached 2.8% drift, it still exhibited higher ductility capacity than SA1 at 3% drift.

Experimental results of overstrength and true response modification factors

The ratio between design and actual strength is referred to as structural overstrength. There is not a unique definition of this parameter but its physical significance is clear regardless of its formal definition. It contributes to the safety of structures when the design forces are exceeded in earthquakes, an eventuality fully accepted by codes. Herein, overstrength is defined as the ratio between the design base shear and the base shear at actual yield. Other definitions may result in higher overstrength, hence this definition is conservative.

$$R_s = V_d / V_y$$

where V_d and V_y are the base shear at the design load and at first member yield, respectively.

Table 3.10.9 contains value of overstrength from the shaking table tests. The differences in overstrength are insignificant, and hence are equal for practical purposes. The values of overstrength in EC8 are similar for both type of structure, both set at 1.2. Although the experimentally evaluated factors are conservative (alternative definitions could be the ratio of design to maximum resistance, as opposed to yield force), they are still higher than the EC8 stipulations, indicating the possibility of increasing the code values.

The overstrength factors indicate that yielding occurs later than the design would have intended. Therefore, the behaviour factors given in Table 3.10.8 are conservative estimates of the true behaviour factors by which elastic forces should be scaled down. The overall behaviour factors are therefore the product of the inherent behaviour and the overstrength factors. These are given in Table 3.10.10.

Table 3.10.9 Experimental Results of Overstrength

Test Case	V_y (kN)	V_d (kN)	Overstrength α_i
Test CA1	45.2	60.8	1.35
Test SA1	44.2	60.2	1.36
Test CB1	23.4	34.2	1.46
Test SB1	21.9	30.8	1.41

Table 3.10.10 Inherent and True Response Modification Factors

Model ref.	Inherent R/q	Overstrength	True R/q
Test CA1	3.45	1.35	4.7
Test SA1	3.47	1.36	4.7
Test CB1	9.08	1.46	13.2
Test SB1	8.93	1.41	12.6

3.10.7.4. Inelastic Response Periods

Discrete Fourier amplitude spectra of the top acceleration response of the frames gives the actual response periods, including all sources of inelasticity. This has been undertaken, leading to the periods give in Table 3.10.11. The consistency of the results obtained from one test run to another is reassuring in so far as the test results are concerned. It is significant to note one of the sources of

overstrength in code design, which utilises rather conservative estimates of period, thus increasing design forces. An example of the response results used to calculate response periods for CB1 is shown in Figure 3.10.12.

Table 3.10.11 Measured response periods

Test Case	State	Test Run	Response Period (sec)	Ratio of Elongation ($T_{inelastic}/T_{elastic}$)
Test CA1	Elastic	CA1S030a	0.465	1.14
	Inelastic	CA1S130a	0.531	
Test SA1	Elastic	SA1S030a	0.539	1.12
	Inelastic	SA1S130a	0.598	
Test CB1	Elastic	CB1S035a	0.589	1.12
	Inelastic	CB1S130a	0.662	
Test SB1	Elastic	SB1S030a	0.652	1.11
	Inelastic	SB1S125a	0.724	

It is observed that the period elongation of composite frames (fourth column in Table 3.10.11) is marginally higher than bare steel frame values. This could be a consequence of concrete cracking. However, the differences are not of great significance.

3.10.7.5. Energy Dissipation by Members

As mentioned above, sine sweeps were imposed on frames CB1 and SB1, to investigate the hysteretic energy dissipation of the two frames. This is because transient earthquake signals are not amenable to producing regular hysteretic loops due to the mismatch between acceleration and displacement cycles and directions. Response plots from these test runs are given in Figures 3.10.13 and 14. These results do not carry the usual significance, since they have been obtained after the attainment of the ultimate limit state. They however show two important features. Firstly, composite frames are not inferior to steel frames in terms of energy dissipation capacity. Secondly it is clear that the beams are responsible for most of the energy dissipation capability, hence capacity design was successful.

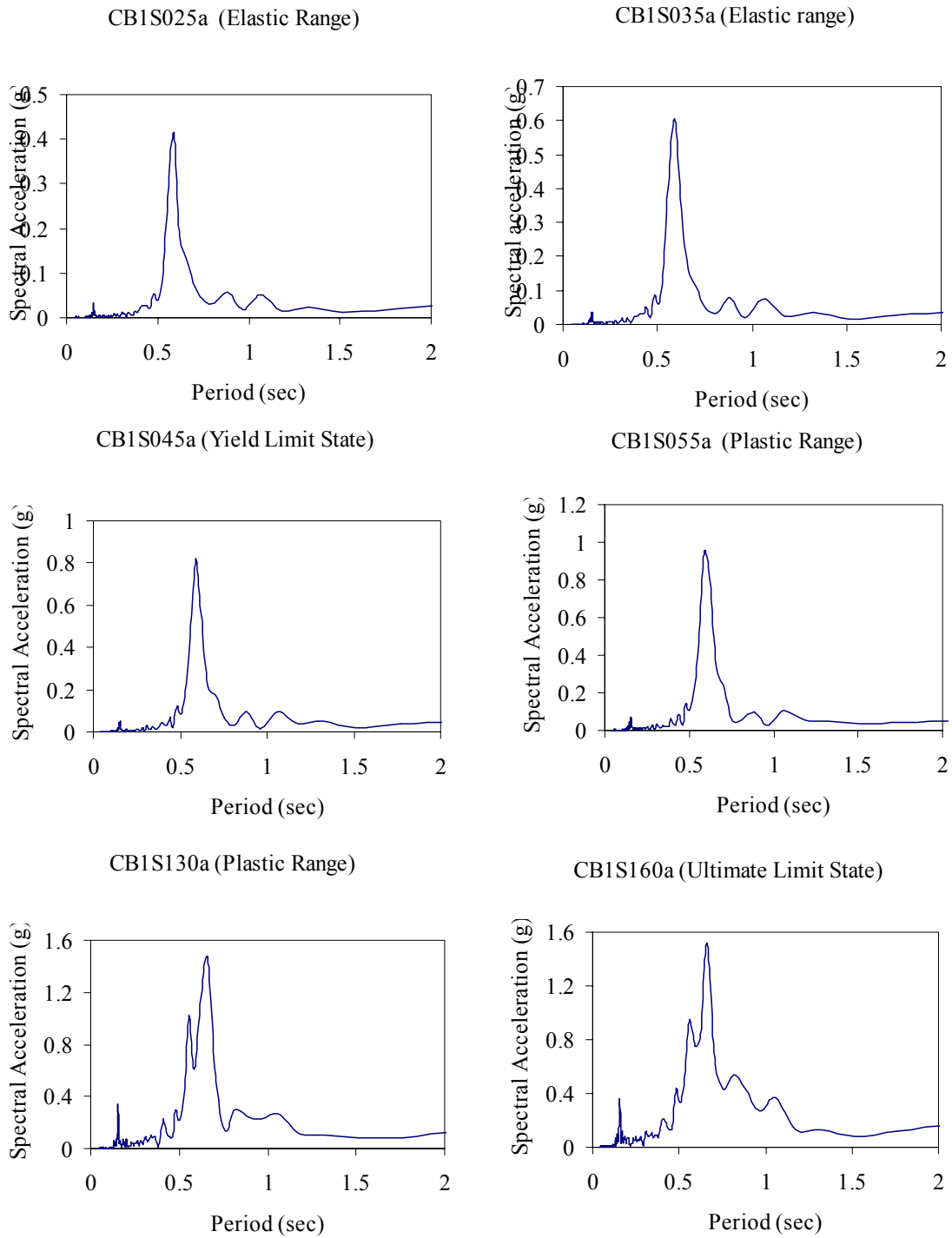
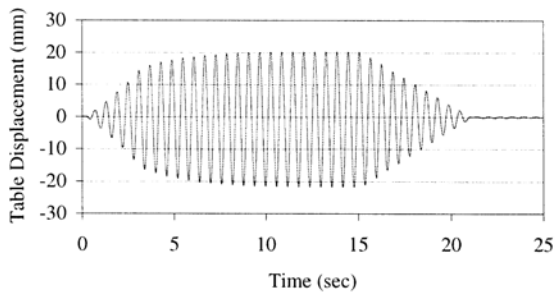


Figure 3.10.12. Discrete Fourier amplitudes spectra for response of CB1

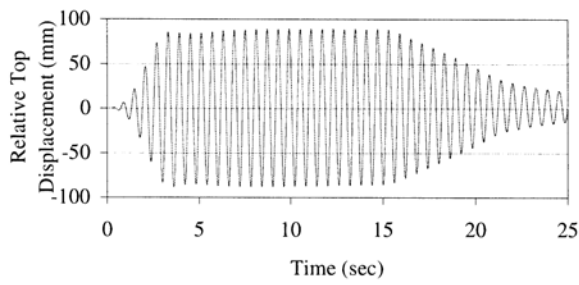
Table Displacement with Sine Cyclic Motion
(CB1D020a)



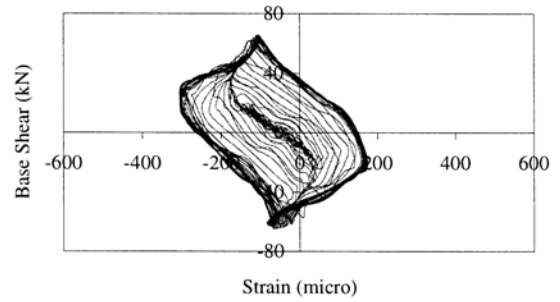
Point C1 in Storey 1 Column (CB1D020a)

(The strain gauge was broken.)

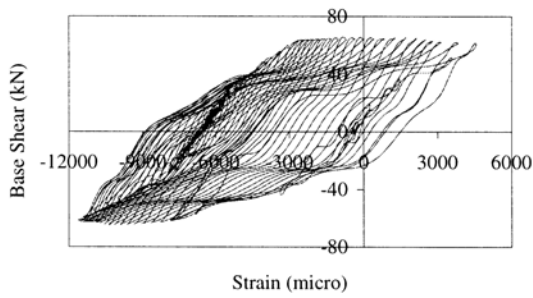
Relative Top Displacement with Sine Cyclic Motion
(CB1D020a)



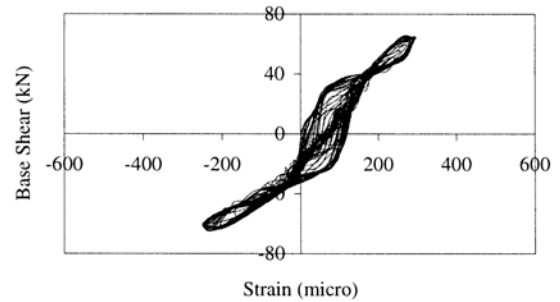
Point C2 in Storey 1 Column (CB1D020a)



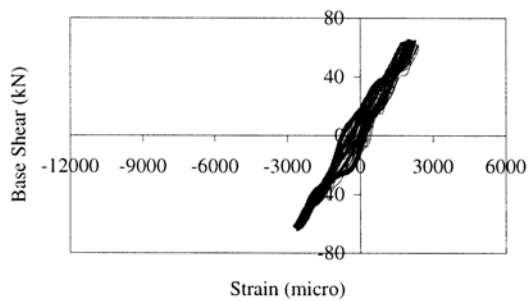
Point D6 in Storey 1 Beam (CB1D020a)



Point C3 in Storey 2 Column (CB1D020a)



Point E4 in Storey 2 Beam (CB1D020a)



Point C4 in Storey 2 Column (CB1D020a)

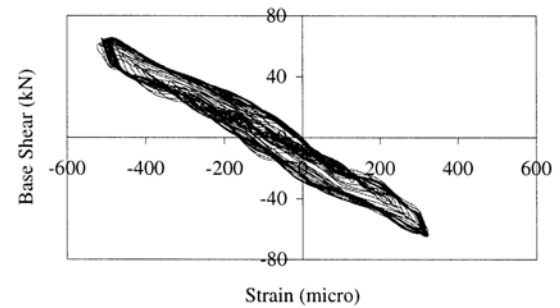
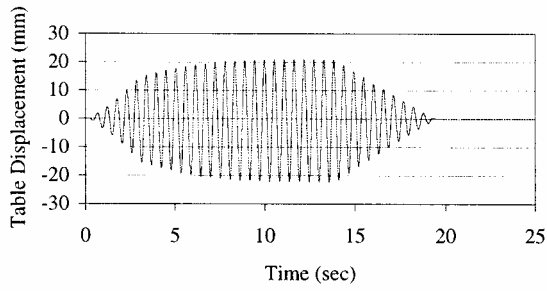


Figure 3.10.13 Hysteretic response under sine sweep (model CB1)

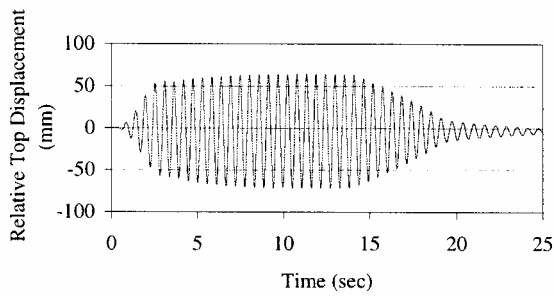
Table Displacement with Sine Cyclic motion
(SB1D020a)



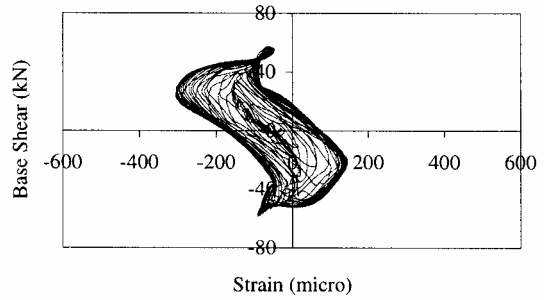
Point C1 in Storey 1 Column (SB1D020a)

(The strain gauge was broken.)

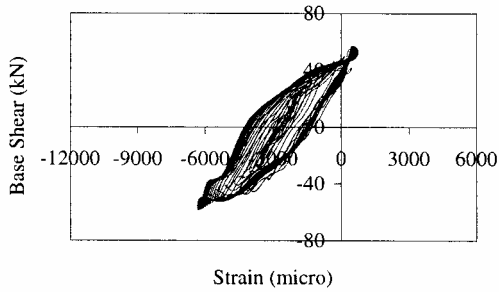
Relative Top Displacement with Sine Cyclic Motion
(SB1D020a)



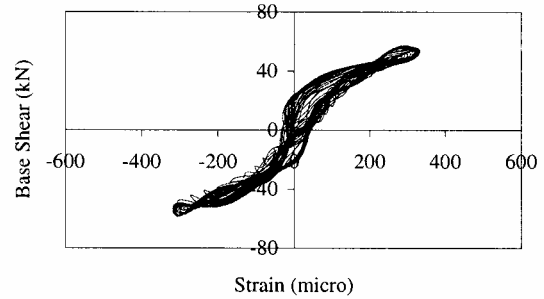
Point C2 in Storey 1 Column (SB1D020a)



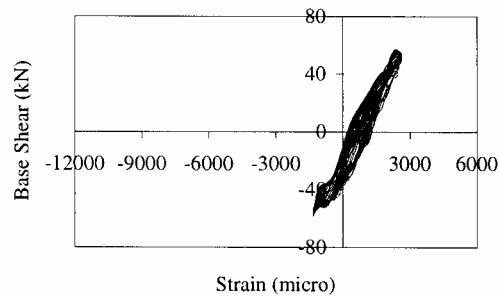
Point D6 in Storey 1 Beam (SB1D020a)



Point C3 in Storey 2 Column (SB1D020a)



Point E4 in Storey 2 Beam (SB1D020a)



Point C4 in Storey 2 Column (SB1D020a)

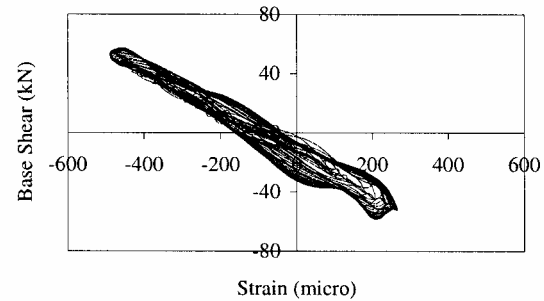


Figure 3.10.14. Hysteretic response under sine sweep (model SB1)

3.10.8. Summary and Conclusions

A series of shaking table tests was undertaken with the primary objective of evaluating response modification factors and overstrength parameters of composite steel-concrete partially-encased frames and bare steel frames. Towards this end, it was necessary not to repeat tests to achieve limit states but to have one well-controlled and determined a priori test run for a specific limit state. Use was made of partial dynamic similitude to scale down a 2x2 frame configuration into a half scale model. Two of the four frames had smaller beam sections to investigate the effect of column protection factors (capacity design) on seismic response. The salient observations from the test results are summarised below.

- The capacity design approach adopted was successful in ensuring beam hinging. All frames hit first yield by beam hinging, and were able to sustain the 3% drift limit without any of the local deformation limits being exceeded.
- The response modification factors (behaviour factors) of composite and bare steel frames are similar. They are both on the whole in excess of code values especially when taking into account the overstrength. These reassuring results should also be viewed in the light of the specific design of the test frames which was much more tuned by advanced analysis than design office practice would allow. It is therefore reasonable to recommend an increase in response modification factors in EC8.
- Whereas the behaviour factors of the two systems is similar, composite frames exhibited higher ductility during the shaking table tests.
- The overstrength parameters given in EC8 are realistic but somewhat conservative. An average value of ~ 1.4 was measured even for these test models that are controlled by seismic loading, and slimmed down to a bare frame with no slab. Practically designed buildings are bound to have higher overstrength factors, perhaps of up to 2.0 or more. There is therefore room for an increase in the EC8 overstrength factor of 1.2.
- Period elongation in the inelastic range was observed. This is about 11% higher than the elastic periods for steel and 15% for composite frames. The latter is affected by concrete cracking. These values explain in part the overstrength observed above.

In addition to the value of the tests in their own right, as an experimental confirmation of response modification factors and overstrength parameters, they have furnished a set of results of high quality, on simple-to-model frames, thus enabling the calibration and verification of analytical models. Therefore, the way is paved to extensive analysis for the evaluation of response modification factors for a much wider range of frames and input motion pairs.

3.11. ATHENS TESTS. Behaviour of a Moment Connection of a Beam with Slab under Dynamic Loading.

J.G. Bouwkamp, Institute of Steel Construction, Darmstadt University of Technology, Germany

A. Plakas, H.P. Mouzakis and P.G. Carydis, Department of Civil Engineering, National Technical University of Athens

3.11.1. Introduction

In order to evaluate the potential seismic response of structural elements, assemblages or entire structures through experimental tests, displacement-controlled quasi-static and pseudo-dynamic loading tests as well as dynamic shaking table studies are commonly used. Questions have been raised about the comparative validity of these different methods in as far as the test results - stiffness, load resistance and ductility - may be influenced by the loading-rate used in the different test procedures. Nevertheless, considering the fundamental frequencies of typical buildings and the test frequencies in general, this influence has been considered negligible under actual earthquake excitation.

On the other hand, considering the basically different characteristics of steel and concrete (being ductile and brittle, respectively, and having markedly different stress-strain relationships), the results of seismic tests on steel/concrete composite members and connections may possibly be affected by the different test methods used. Accordingly, several studies addressing this subject have been performed during the last decade. Ballio et al.(1990) focused on an assessment of the influence of the concrete on the seismic behaviour of composite connections under quasi-static load conditions. Constantinescu et al. (1992) presented the results of several pseudo-dynamic tests on composite steel/concrete joints with different levels of column-web ductility. Pradhan (1995) discussed the results of pseudodynamic tests considering the effects of various test parameters and the potential influence of experimental error propagation on the cyclic behaviour of composite beam-column joints. In order to allow a comparison of the pseudo-dynamic test results reported by Pradhan, several shaking table tests on identical composite beam-column joints were performed by Carydis et al. (1995). Detailed comparative studies of the results of the above noted pseudo-dynamic and shaking table tests were presented by Pradhan (1998).

Pradhan (1998) reports that the test specimens for both the pseudo-dynamic and shaking table tests were fabricated and concreted at Darmstadt and consisted of partially encased composite (in-filled concrete) beam (HEA260) and column (HEB300) sections with both bolted and welded joints. The specimens for the shaking table studies were subsequently transported to Athens for testing at the Laboratory for Earthquake Engineering of the National Technical University of Athens.

Using for the pseudo-dynamic tests (PDT) the same time-history input, lumped mass quantity and damping as for the shaking table tests (STT), the response time-histories of the PDT tests, carried out at the Darmstadt University of Technology, were compared with the corresponding STT results. Comparisons were made for a total of 8 specimens covering welded and bolted connections with shear-panel stiffnesses of 7, 11 and 15 mm, respectively. Considering the response force-histories for comparative tests, the results showed an excellent agreement, however, surprisingly, a comparison of the PDT and STT displacement histories for all tests showed a higher displacement response for the ST tests than for the PD tests. This would indicate that the test specimens exhibited a higher stiffness in the PD tests than under the real-time test conditions; a result basically contrary to the common phenomenon of increasing stiffness under increasing loading rates. Subsequent numerical simulations of both the ST and PD tests, considering different lumped masses and various filtered table-top accelerations did not reveal possible errors in the shaking-table test set-up or table input excitations. With the intent to clarify the earlier observations, it was decided to undertake a further study on the cyclic response of different composite steel/concrete beam-column assemblies, using both PDT and STT loading conditions. These studies were carried out at the Laboratory for Earthquake Engineering, National Technical University, Athens.

3.11.2. Test Specimens and Test Setup

The basic test specimen studied, was a welded steel beam-column assembly, consisting of a steel 200 cm long IPE 200 beam section, with a 60 cm wide and 10 cm thick concrete slab, and a HEB 220 column stub. The overall dimensions of the steel members and concrete slab, together with the layout of the reinforcing steel, are presented in figure 3.11.1.

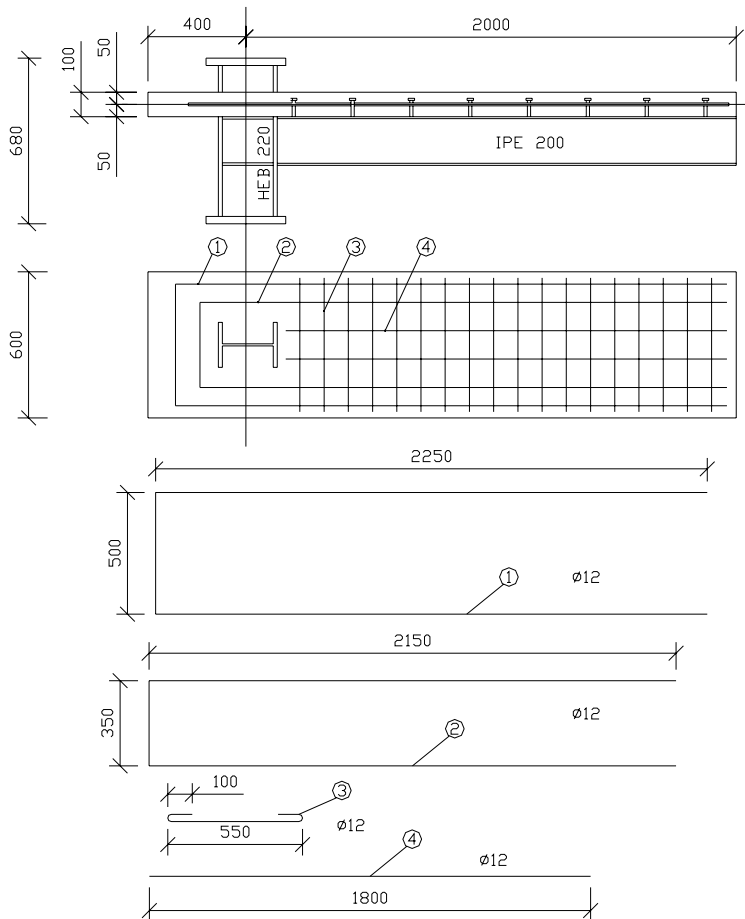


Figure 3.11.1 Test specimen and slab reinforcement

Typically, the headed shear studs had a diameter of 13mm and a length of 75mm. The slab reinforcement consisted of a single layered mesh of longitudinal and transverse bars positioned at mid-depth of the 10 cm thick concrete slab (see Fig. 3.11.2).

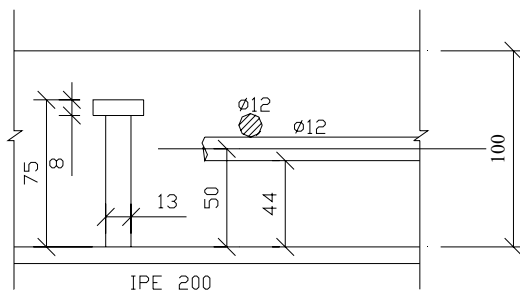
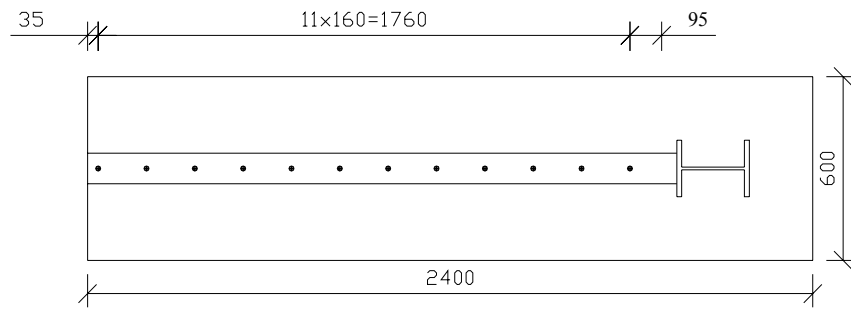


Figure 3.11.2 Detail of shear studs

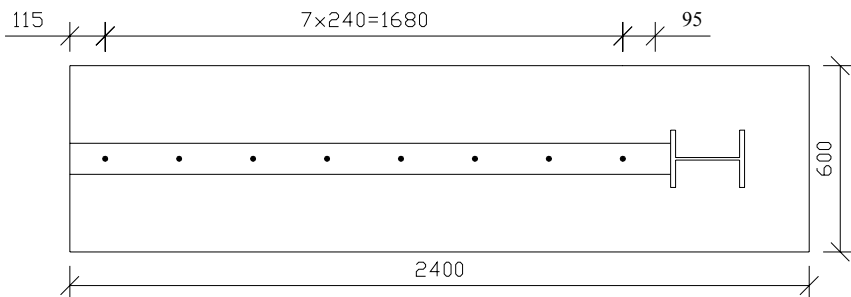
The specimens were designed to study the response of the composite concrete slab and steel beam section under cyclic cantilever beam moments and assess the possible influence of the loading rate by comparing the test results under both real-time (shaking table) and quasi-static test conditions. Two

studs densities are used corresponding to partial shear capacity of the shear connection. Two degree of shear connection were considered.

A first specimen, identified as C160, was designed with a degree of shear connection of 0.7 and a corresponding stud spacing of 160 mm (see Fig. 3.11.3).



(a) C160



(b) C240

Figure 3.11.3 Shear stud layout in specimens C160 and C240

A second specimen, identified as C240, was designed with a stud spacing of 240 mm (see Fig. 3.11.3) corresponding to a lower degree of shear connection of 0.45. In order to permit an evaluation of the influence of the slab under both positive and negative moment action, a third type of specimen with only a steel beam (without a slab) has been fabricated and tested. This specimen, identified as specimen S, would further allow an evaluation of the basic effect of real-time shaking versus pseudo-dynamic testing.

Considering the fact, that under bending the positive moment resistance of the composite cantilever section, with the concrete slab under compression, is larger than the negative moment resistance, and that yielding will occur first under a negative moment action, it was decided to use, for the shaking-table study, a symmetric test setup with two coupled test specimens (see Fig. 3.11.4). Under those conditions, the combined resistance of the coupled beams would be the same, independent of the dynamic forcing direction. Otherwise, in case of a single specimen, first yielding in either direction would initiate a potential progressive cyclic deterioration in that particular (first-yield) direction and lead to early failure. As shown in Fig. 3.11.4, the test specimens were mounted vertically on the table through 2 sets of short, 85 cm long, HEB 200 steel stubs. The specimens were connected to the stubs through 8 M16 10.9 HS bolts; the stubs in turn were mounted to the table by 4 M27 10.9 HS bolts.

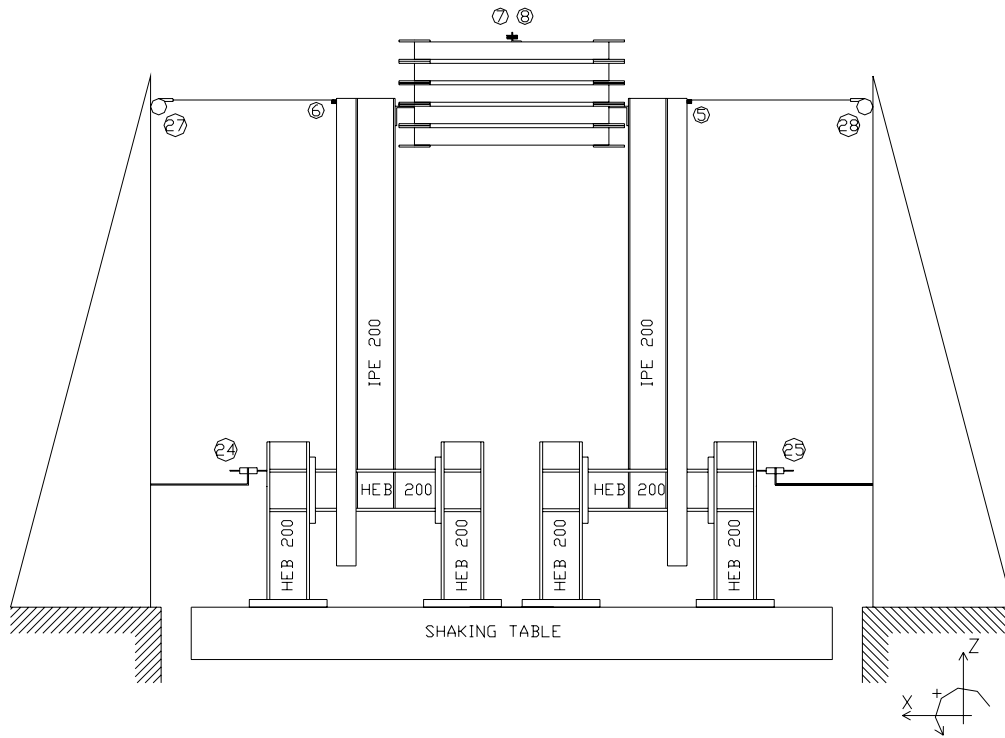


Figure 3.11.4 Experimental set-up and instrumentation in shaking table tests

The dynamic test mass consisted of five interconnected steel plates, placed on top of each other, with a total mass of 5 tons. The arrangement of the plates were such that the centre of mass was located

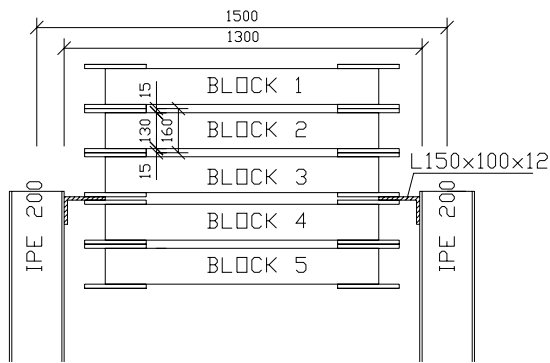


Figure 3.11.5. Mass between ends of beams

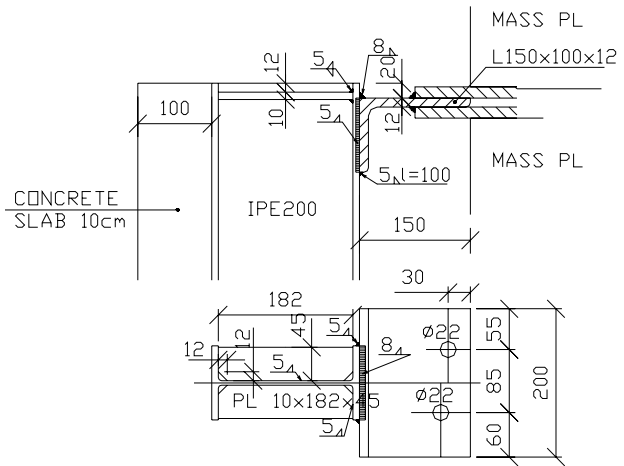


Figure 3.11.6. Detail of connection beam to mass

above the point of connection to the test beams. This was achieved by placing 3 steel plates above and 2 steel plates below the connection level. At that position, the mass was bolted through connection plates to angles (L 150x100x12) which were welded to the end of the bottom flanges of the test beams (see Fig. 3.11.5 and Fig. 3.11.6). In order to ascertain that the angle support would not fail prematurely, the type of support was pretested by subjecting the outstanding leg successfully to over 2000 cycles of +/- 40 mrad.

For the pseudo-dynamic tests, a single test specimen, as shown in Fig. 3.11.7, was mounted vertically in a reaction test frame in the same manner as on the shaking table. A double-acting, displacement-controlled, hydraulic load cylinder, connected to the tip of the test beam, was used to introduce the same displacement history at the beam end, as had been observed in the real-time shaking table tests.

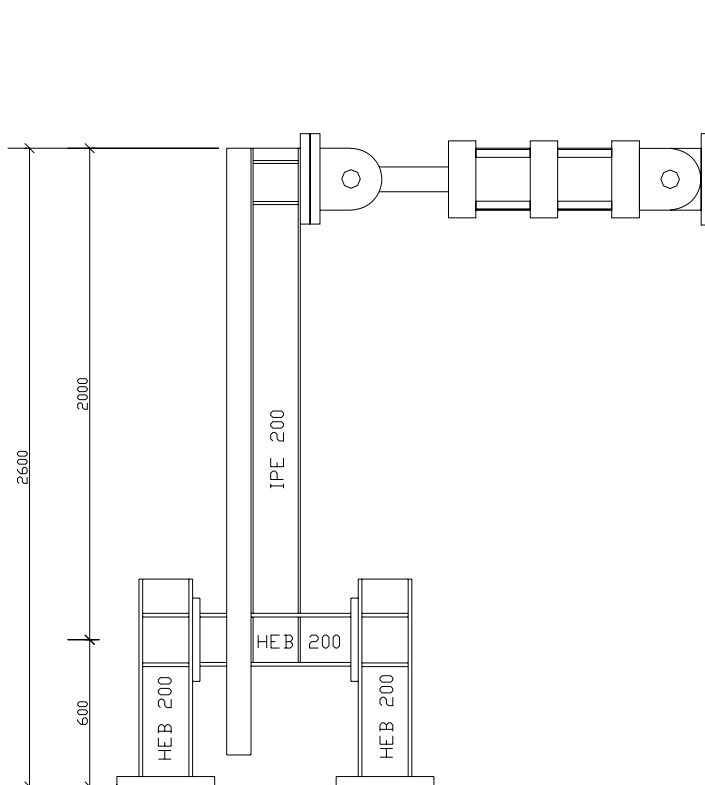


Figure 3.11.7 Test set-up for pseudo-static test

3.11.3. Test Program

In order to develop a dynamic non-linear response of the coupled test specimens, it was decided, to subject the table not to a particular seismic ground-displacement time-history but rather to a predefined cyclic displacement rampfunction with full displacement reversals. The cyclic test frequency was set constant at 80% of the natural frequency of the test setup. This procedure had been used successfully in previous studies, as the onset of yielding basically leads to a reduction of the natural frequency of the test setup and an increased dynamic amplification; thus resulting in an enhanced forcing efficiency of the table input. In these studies, the rampfunction selected had a uniformly increasing (10%) ascending branch of 10 full cycles, followed by 5 full cycles at the same maximum cyclic displacement level. After these 5 full cycles, the rampfunction called for 3 further, uniformly increasing (10%), displacement cycles, followed by 5 cycles of a constant magnitude. The test was concluded by an additional 5 cycles with linearly decreasing (20%) cyclic displacements, down to zero. The table displacement magnitudes were selected such that yielding of the test set up could be expected.

During the dynamic tests, the response of several accelerometers, placed on the test specimen both at the end of the cantilever beams (identified as numbers 5 and 6 in Fig. 3.11.4) and on top of the mass (numbers 7 and 8) were recorded. Also, the tip displacements of the cantilever beams (numbers 27 and 28) were recorded during the tests. In order to assess the efficiency (stiffness) of the column-stub mounting devices, additional displacements (numbers 24 and 25) were monitored and compared with other pertinent records.

For the pseudo-static cyclic tests, the specimens were subjected to displacement controlled forces using as input the corresponding dynamic displacement record measured at the tip of the cantilever beams under the above described table excitation. Considering that the displacements of the mounting devices relative to the table displacements were negligible, the observed displacement history recorded at the tip of the cantilever beam of the pertinent dynamic test specimen was used as the displacement-control input for the corresponding pseudo-static test.

3.11.4. Test Results

Considering the above test procedures, first, the coupled specimens under real-time dynamic test conditions were tested. Subsequently, after having obtained the displacement response at the tip of the cantilever beams, the displacement controlled pseudo-static tests on the single specimens were performed. The results of the dynamic tests of specimens C160, C240 and S, presented as the „effective“ beam moment at the face of the beam-column connection versus the induced tip displacement of the cantilever beam, are shown in Figures 3.11.8, 9 and 10, respectively. The „effective“ beam moment is in fact half of the total moment (of both beam cantilevers) or, the average of the positive and negative moments of the two cantilever beams, at any given instance.

Specifically, Fig. 3.11.8 shows the moment-displacement record of the second dynamic test run (test 2) performed on the coupled C160 specimens. In fact, a total of 7 test runs were performed on this test setup; while in test runs 1 and 6 the test specimen was subjected to only a few cycles of low-amplitude table displacements, in runs 2, 3, 4 and 5 complete table-displacement ram functions, as described earlier, were introduced with a table frequency of 3.89 Hz and maximum cyclic table accelerations of 12.5, 17.5, 20 and 20 m/sec², respectively. In the last test run (run 7), the coupled specimen was subjected to more than 70 full cycles of table motion at a reduced frequency of 2.89 Hz and a constant peak table acceleration of 10 m/sec². In order to illustrate the response of the coupled C160 specimen under these changing test conditions, not only results of test run 2 (Fig. 3.11.8), but also the results of test runs 4 and 7, as shown in Figures 3.11.11 and 12, respectively, are presented. These figures show the „effective“ cantilever beam-moment versus beam-tip displacement. In principle, the results of the several test runs allow evaluating the effectiveness of the closely spaced shear studs on the behaviour of the composite beam-slab cantilever under repeated cyclic loading.

The results of the pseudo-static tests for specimens C240 and S, showing the true cyclic beam moment

versus the corresponding cantilever tip displacement, are presented in Figures 3.11.13 and 14, respectively. Unfortunately, the test results for the pseudo-static test on specimen C160 were lost in the early data reduction process.

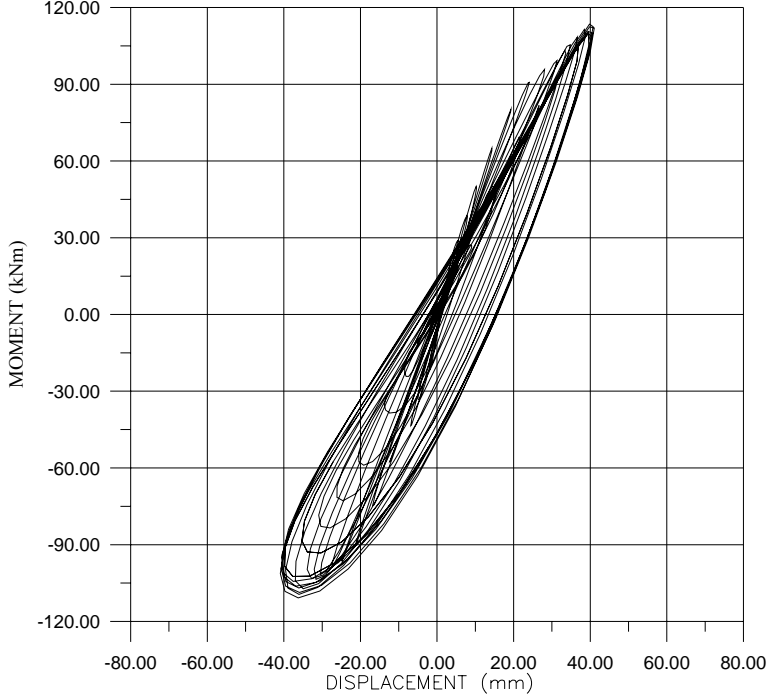


Figure 3.11.8. C 160 Dynamic (test 2).

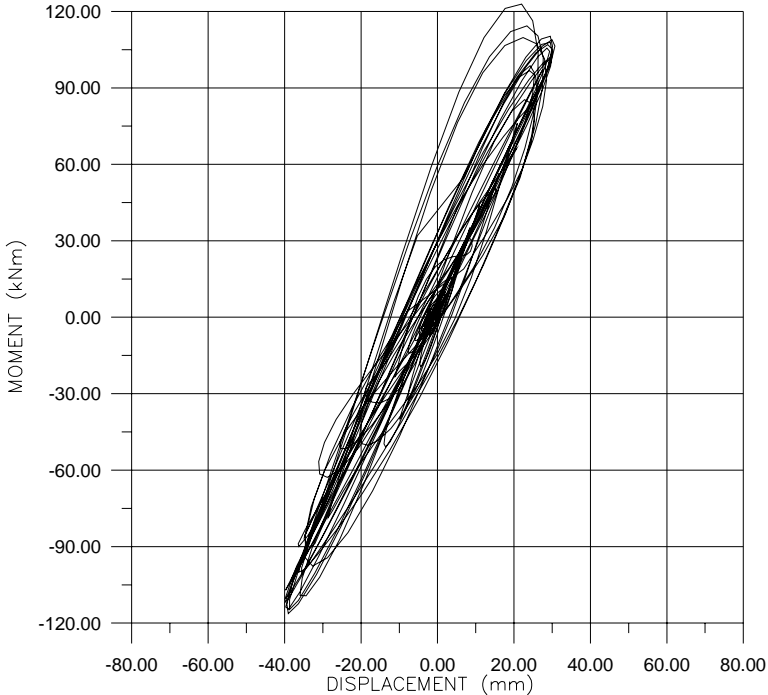


Figure 3.11.9. C 240 Dynamic

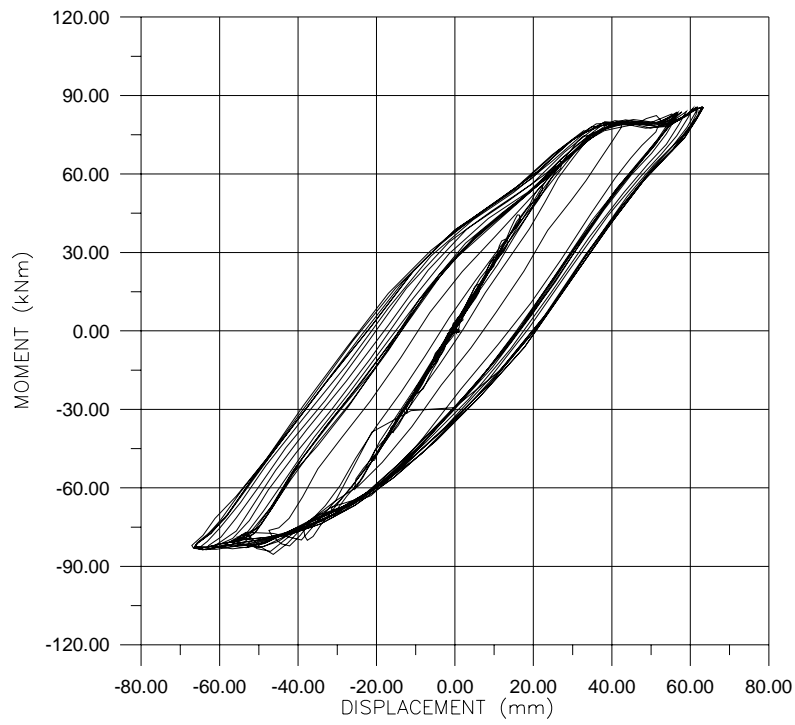


Figure 3.11.10. Steel Dynamic.

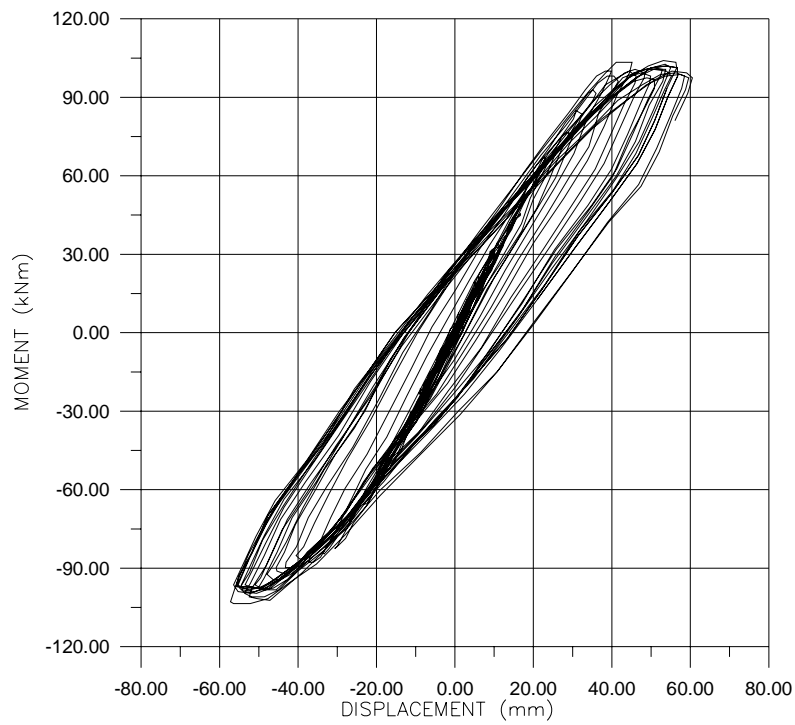


Figure 3.11.11. C 160 Dynamic (test 4).

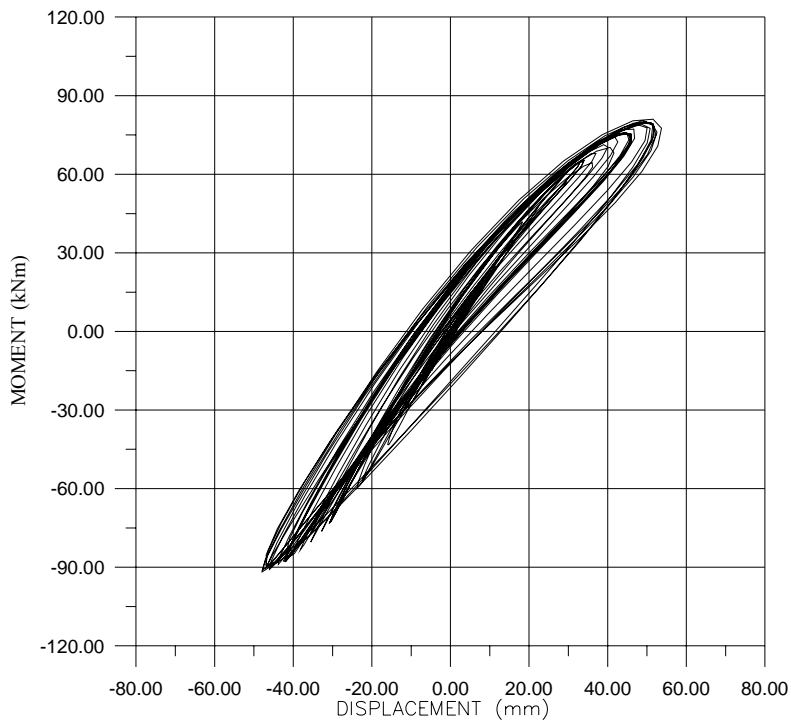


Figure 3.11.12. C 160 Dynamic (test 7).

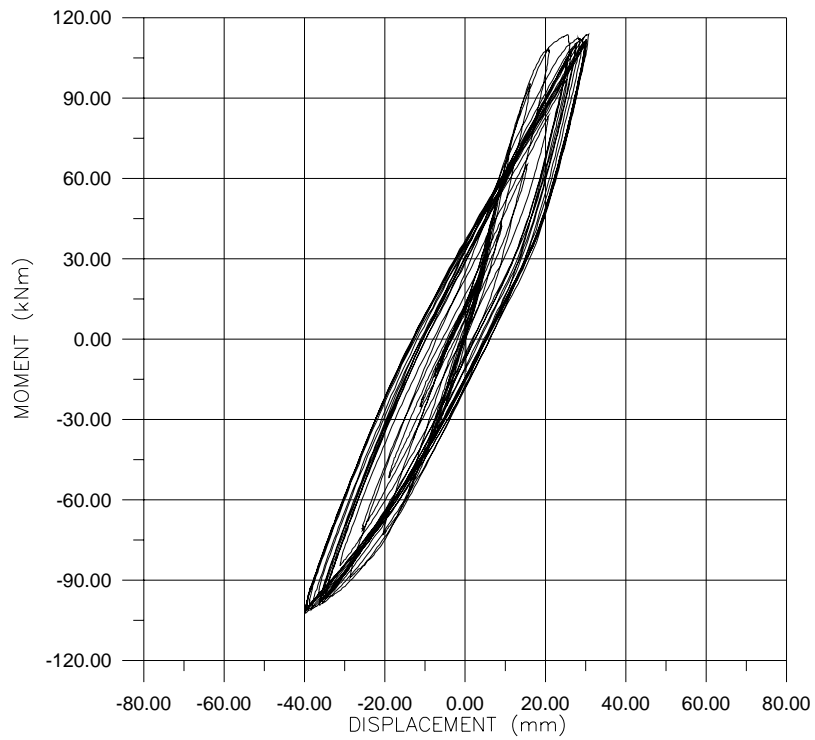


Figure 3.11.13. C 240 Pseudo static.

3.11.5. Test Interpretation

Pseudo-static Tests

In order to evaluate the basic characteristics of the composite test specimen in comparison with the single steel cantilever, the pseudo-static test results of specimens C240 and S (Figs. 3.11.13 and 14) are considered first. According to Fig. 3.11.14, the yield moment of the steel section was found to be 68 kNm, reflecting a yield stress f_{yd} of 310 N/mm². The moment-displacement curve clearly illustrates the flange buckling which occurred under negative-moment bending. A detailed observation of the first 7 test cycles showed an elastic moment „stiffness“, being the bending moment at the column face versus the cantilever-beam tip displacement, of 2.90 kNm/mm.

Considering similarly the first 7 cycles of the pseudo-static test results of the composite specimen C240, the moment „stiffness“ for the positive moment (slab under compression) - up to a tip displacement of + 10 mm - was found to be constant at a value of 6.7 kNm/mm. However, for the negative moment condition the „stiffness“ values, which were basically smaller than for the positive moment condition, varied depending on the magnitude of the displacement. Specifically, for displacements of -5 and -10 mm the „stiffness“ changed from 5.4 to 4.4 kNm, respectively. Comparing these values with the „stiffness“ of the steel beam only (specimen S), the composite section under a positive moment had an initial bending stiffness 2.31 times larger than the steel section. However, under a negative moment and tip displacements of -5 and -10 mm, respectively, the bending stiffness values for the composite specimen were only found to be between 1.86 and 1.52 times the bending stiffness of the steel cantilever beam specimen.

According to Fig. 3.11.13, the maximum positive and negative moments for the C240 specimen under pseudo-static loads were found to be + 114 and - 102 kNm, respectively. These values compare to calculated positive and negative resisting moment values (MRd) of + 110 and - 99 kNm, respectively. The positive moment resistance was based on values of $f_{yd} = 310$ N/mm² for the steel section and $\alpha f_{cd} = 0.85 \cdot 25/1 = 21.25$ N/mm² for the C25 concrete slab. The effective width (under compression) was assumed equal to the width of the HEB220 column flange ($b_{eff} = b_c = 220$ mm), which was about the maximal possible effective width reachable with the considered partial degree of shear connection. In calculating the negative resisting moment of - 99 kNm, the slab reinforcing steel was assumed to have a yield stress of $f_s = 600$ N/mm².

Dynamic Tests

Considering the moment-displacement curves for specimen C240 in Fig. 3.11.9, it is remarkable that the maximum displacements in the „effective“ positive and negative moment regions are significantly different, namely, about 30 mm in the positive moment range and close to 40 mm in the negative moment range. As both the test setup and the table-input rampfunction were symmetric, the noted response must be directly associated with a difference in the behaviour of the two coupled specimen. The symmetry of both the test setup and table forcing input was substantiated by the fact that a close observation of the first 7 to 8 cycles, with maximum tip displacements of up to + and - 10 mm, showed that the moment-displacement relationship was symmetric and linear. In fact, at the same tip displacement, the sum of the positive and negative cantilever moments, occurring simultaneously in the different beams, should be the same throughout the test. However, considering the noted differences in the maximum displacements, the test results seem to indicate a different shear-interface behaviour of the two beams with a progressive failure in one direction of motion. This behaviour is supported by the fact that observations after the test showed that several shear studs had failed (up to fracture).

The „effective“ maximum moments for a single cantilever beam, as presented in Fig. 3.11.9, should in fact have been the average of the possible maximum positive and negative moments of a (a single) C240 composite beam. With maximum values of +114 and - 102 kNm, as shown in Fig. 3.11.13, the „effective“ maximum moment should have been 108 kNm for both the positive and negative moment values. However, in comparison, Figure 3.11.9 shows maximum moment values of + 108 and - 115

kNm (despite subsequent failure of some of the shear studs towards the end of the test). However, considering the overall hysteretic response of the pseudo-static (Fig. 3.11.13) and dynamic tests (Fig. 3.11.9) of the C240 specimens, the shape of the hysteretic loops are quite similar.

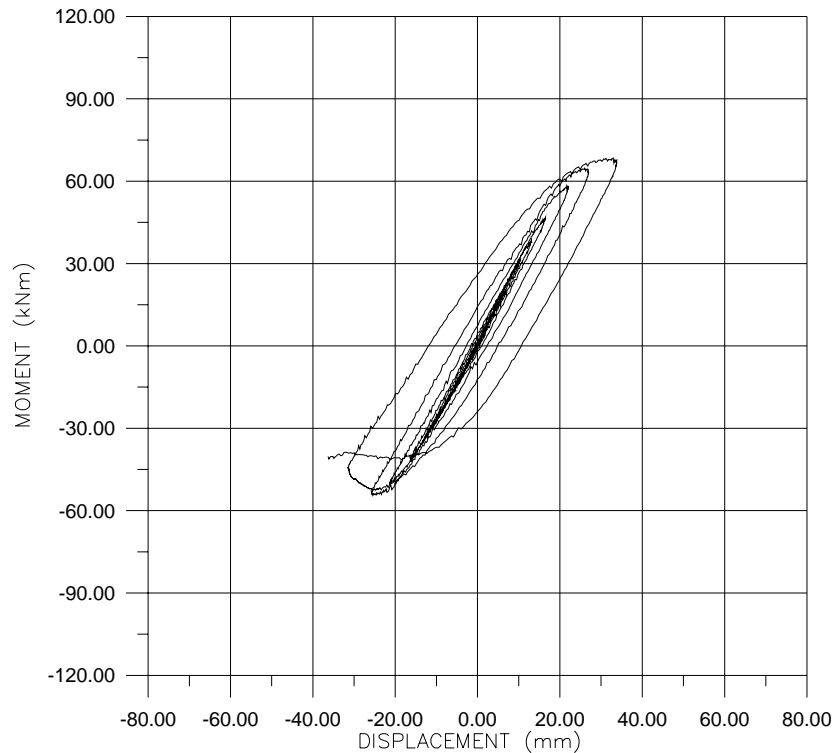


Figure 3.11.14. Steel pseudo static.

A comparison of the dynamic test results of the two coupled steel beam specimen S, presented in Fig. 3.11.10, and those of the pseudo-static test specimen (Fig. 3.11.14), shows a good agreement up to a cyclic displacement level of about 30 mm (at which premature flange buckling under a negative moment terminated the pseudo-static test). The first 7 cycles in both test cases indicate closely similar initial „stiffness“ values of 2.9 and 2.6 kNm/mm for the pseudo-static and dynamic tests, respectively. The almost 10% lower „stiffness“ for the dynamic test as compared with the pseudo-static test, is rather strange in consideration of the increased loading rate in the dynamic test case. However, because of possible test errors, the difference may not be significant. On the other hand, considering the unrealistically high plastic moment level of about 80 kNm of the steel sections in the dynamic test case (Fig. 3.11.10), reflecting a yield stress of 365 N/mm², in comparison with the maximum moment of 68 kNm observed under pseudo-static test conditions (Fig. 3.11.14), the dynamic test results may indicate that the actual dynamic mass may have been in fact smaller than the dynamic mass used in the data reduction process. In fact the acceleration data used in the data reduction process were measured at the top of the 5 ton mass and reflected not only translational motions of this mass-block, but also, to some degree, the amplified effect of the rotational motions of this mass. Correcting for such a discrepancy would basically reduce the dynamic test moments.

The natural frequencies of the dynamic test setups of the coupled specimens, C160 and C240, showed that the initial stiffness of both types of composite beams was identical. However, as signified by the difference in the maximum cyclic displacements noted before, C240 seemed to have experienced an early loss of the shear resistance at the slab-beam interface in one or both of the coupled beams.

Considering the results of test runs 2, 4 and 7 of the coupled C160-specimen test setup, as shown in

Figures 3.11.8, 11 and 12, respectively, a rapid deterioration at the shear stud interface does not seem to have occurred. Specifically, in test run 2 with maximum table accelerations of 12.5 m/sec^2 at a frequency of 3.89 Hz, the test results presented in Fig. 3.11.8, show maximum „effective“ moments of + 112 and – 110 kNm and maximum cyclic tip displacements of + and – 40 mm. During test run 3, with increased maximum table accelerations of 17.5 m/sec^2 at the same table operating frequency of 3.89 Hz, the test results showed exactly the same „effective“ maximum moments as in test run 2, but, because of the increased forcing level, increased maximum cyclic tip displacements of + 49 and – 51 mm. In principle, the results do not indicate any deterioration of the beam-slab interface.

In test run 4, during which the maximum table acceleration was increased further to 20 m/sec^2 at basically the same table frequency (3.88 Hz) as before in test run 3, the results shown in Fig. 3.11.11 indicate, as expected under the larger forcing input, a further increase of the maximum cyclic tip displacement to + 60 and – 55 mm. However, a reduction of the maximum „effective“ moments from about +/- 110 kNm to values of + 104 and – 103 kNm, seems to indicate the onset of a shear-interface deterioration. In test run 5, with the same maximum table acceleration of 20 m/sec^2 at a table frequency of 3.89 Hz, a reduction of the „effective“ maximum moments were observed with values of only + 90 and – 95 kNm. The associated maximum tip displacements also showed a significant reduction to only + 48 and – 51 mm. The later reduction is probably in part a result from a less effective table forcing input as the stiffness of the specimen had fallen by more than 30%, calling in fact for a table forcing frequency of about 3.2 Hz. The loss of moment resistance observed in test runs 4 and 5 are a clear indication of a distinctly non-symmetric loss of shear resistance at the beam-slab interface.

In the final test (test run 7), the table frequency had been adjusted to reflect the continuing loss of stiffness during the earlier test runs (which had reached, during a short exploratory run -- test run 6 – a value of 55% of the initial stiffness). Consequently, a table frequency of 2.89 Hz was selected and the coupled specimen subjected to over 70 cycles with a constant peak table acceleration of 10 m/sec^2 . Compared with the results of test run 5, the test results of test run 7, presented in Fig. 3.11.12, show a further reduction of the maximum „effective“ moments to + 81 and – 90 kNm. Because of the improved table forcing input, the maximum tip displacements did not further decrease significantly and reached values of + 52 and – 47 mm. In fact, the moment values approach the moment resistance of the bare steel sections and indicate an almost complete loss of beam-slab interface resistance.

3.11.6. Conclusions

Considering the basic objective of studying the influence of the loading rate effect on the composite interactive behaviour of a beam-slab cantilever section, the results show excellent agreement between the test results obtained under low-rate pseudo-static displacement controlled forcing conditions and high-frequency (3-4 Hz) real-time shaking table input conditions. In fact, it can be concluded that quasi-static or pseudo-dynamic test procedures are capable of capturing the real dynamic behaviour of composite structures.

Furthermore, despite identical initial stiffnesses, specimens with a code-designed stud spacing (160 mm in this case) corresponding to a partial degree of shear connection of 70 %, versus those with a 50% larger stud spacing (240 mm – degree of shear connection of 45%), showed a better than three-fold life expectancy under maximum, yield introducing, forcing conditions.

3.12. REFERENCES

- Amadio, C., Benussi, F., and Noe, S., 'Behaviour of Unbraced Semi-rigid Composite Frames Under Seismic Actions'. STESSA '94, 535-546.
- Ansourian, P. (1981). "Experiments on continuous composite beams", *Proceedings of Institution of Civil Engineers*, London, Vol. 73, Part 2, pp. 25-51.
- Arbed-Recherches. 1990. *Seismic Resistance of Composite Structures* - Project Final Report, C.E.C. Agreement No. 7210-SA/506
- Aribert, J.M. (1992). "Application and recent developments of a numerical model for composite beams with partial shear connections", *Composite Construction In Steel and*
- Aribert, J.-M., Grecea, D., A New Method to Evaluate the Q-Factor from Elastic-Plastic Dynamic Analysis and Its Application to Steel Frames. STESSA '97, 382-393.
- APK 1996. *Construction métallique et mixte acier-béton*. Paris: Eyrolles.
- Ayoub, A, and Filipou, F.C. (1997), "A model for composite steel-concrete girders under cyclic loading", *Build. To Last-Proceedings of Structural Congress. XV*, Portland, ASCE, Vol. 1, pp. 721-725.
- Ballio, G.1985. A Method to compute the behaviour factor for construction in seismic zones. *Costruzioni Metalliche*, No. 37/85.
- Ballio, G., Calado, L., Iori, I. and Mirabella Roberti, G. (1987), " I problemi delle grandi costruzioni in zon sismica", *Associazione Italiana Cemento Armato e Precompresso*, Roma, pp. 31-44.
- Ballio, G., Plumier, A. Thunus, B. (1990). Influence of concrete on the cyclic behaviour of composite connections. Report, IABSE Symposium, Brussels.
- Ballio, G. and Castiglioni, C.A. (1995), "A unified approach for the design of steel structures based under low and/or high cycle fatigue", *Journal of Constructural Steel Research*, Vol. 34, pp. 75-101.
- Barnard, P.R. and Johnson, R.P. (1965), "Plastic behaviour of continuous composite beams", *Proceedings of Institute of Civil Engineers*, London, Vol. 32, pp.180-197.
- Bertero, V.V. 1989. State-of-the-art report: Ductility based structural design, *Proceedings of 9th World Conference on Earthq. Engng.* (Tokyo-kyoto, Japan, Aug. 1988), VIII:673-686.
- Blakeborough, A., Severn, R.T. and Taylor, C.A. (1986), "The new UK national six-axis earthquake shaking table", *Proceedings of The 8th European Conference on Earthquake Engineering*, Lisbon Portugal, No. 7.1, pp. 97 - 100.
- Bouwkamp, J.G., Parung, H. & Plumier, A. 1998. Bi-directional cyclic study of a three-dimensional composite frame. In *proc. of the 11th European Conference on Earthquake Engineering*. Rotterdam: Balkema.
- Broderick, B.M. and Elnashai, A.S.(1994), "Seismic resistance of composite beam-columns in multi-storey structures. Part 2 : Analytical model and discussion of results," *Journal of Constructural Steel Research*, No. 30, pp. 231-258
- Broderick, B.M., and Elnashai, A.S. (1996), "Seismic response of composite frames Part I. Response criteria and input motion", *Engineering Structures*, Vol. 18, No. 9, pp. 696-706.
- Bursi, O. S. and Caldara, R. (1999), "A non-linear finite element study of steel-concrete composite substructures with partial shear connection", paper submitted to *Journal of Structural Engineering*.

- Carricilli, J. & Aloustaz, A. 1978. Influence de la précontrainte sur l'amortissement des vibrations transversales des poutres en béton précontraint. Bulletin 05/06-78 Laboratoire des Ponts & Charpentes.
- Carydis, P.G., Mouzakis, H.P., Taflambas, J.M. Vougioukas, E.A. (1995). Shaking table tests of composite steel-concrete, beam-column connections. Proc. 10 ECEE, Vienna.
- CEB 1997. Behaviour and modelling in serviceability limit states including repeated and sustained loads.
- Chapman, J.C. and Balakrishnan, S. (1964), "Experiments on composite beams", *The Structural Engineer*, No. 11, Vol. 42, November, pp. 369-383.
- Cheung, P.C., Paulay, T. & Park, R. 1989. *Interior and exterior reinforced concrete beam-column joints of prototype two-way frame with floor slab designed for earthquake resistance*. Research report 89-2. Department of Civil Engineering, University of Canterbury, ChristChurch, New Zealand.
- Constantinescu, D.R., van Kann, J., Pradhan, A.M., Ashadi, H.W. Bouwkamp, J.G. (1992). Pseudo-dynamic tests on composite steel/concrete joints. Proc. 10 WCEE, vol. 5, Madrid.
- Cost C1 1997. Composite steel-concrete joints in braced frames for buildings. *Semi-rigid behaviour of civil engineering structural connections*. Luxembourg: Office for Official Publications of the European Communities.
- Crisfield, M.A., Wills, J., "Analysis of R/C panels using different concrete models", ASCE, J. of the Eng. Mech., 115 (3), 1989.
- Doneux, C. 1996. Ductility of composite sections under positive bending (internal report), Department of Civil Engineering, University of Liege.
- Doneux, C., Parung, H., "A study on composite beam-column sub-assemblages", in Proceedings of the 11th European Conference on Earthquake Engineering, Balkema, Rotterdam, 1998.
- Elghazouli, A.Y. and Elnashai, A.S. (1993), "Performance of composite steel/concrete members under earthquake loading. Part II: Parametric studies and design considerations", *Earthquake Engineering and Structural Dynamics*, Vol. 22, pp. 347-368.
- Elnashai, A.S., Danesh Ashtiani, F.A. and Elghazouli, A.Y. (1996), Experimental and analytical investigation into the seismic behaviour of semi-rigid steel frames, Research report No. ESEE96-7, ESEE Section, Imperial College, London.
- Elnashai, A.S. and Broderick, B.M. (1994), "Seismic resistance of composite beam-columns in multi-storey structures. Part 1 : Experimental studies", *Journal of Constructional Steel Research*, No. 30, pp. 201-229.
- Elnashai, A.S. and Broderick, B.M. (1996), "Seismic response of composite frames - II. Calculation of behaviour factors", *Engineering Structures*, Vol. 18, No. 9, pp. 707-723.
- Elnashai, A.S. and Elghazouli, A.Y. (1993), "Performance of composite steel/concrete members under earthquake loading. Part I: Analytical model", *Earthquake Engineering and Structural Dynamics*, Vol. 22, pp. 315-345.
- Elnashai, A.S. and Izzudin, B. A. (1993), "Modelling of material non-linearities in steel structures subjected to transient dynamic loading", *Earthquake Engineering and Structural Dynamics*, Vol. 22, pp. 509-532.
- Elnashai, A.S., Takanashi, K., Elghazouli, A.Y. and Dowling, P.J. (1991), "Experimental behaviour of partially encased composite beam-columns under cyclic and dynamic loads", Proceedings of Institution of Civil Engineers, part 2, 91, pp. 259-272.

- Eurocode 3 (1991), Design of Steel Structures, ENV1992, CEN.
- Eurocode 4 (1994), Design of Composite Steel and Concrete Structures, ENV1994, CEN.
- Eurocode 8 (1994), Earthquake Resistant Design of Structures, ENV1998, CEN.
- European Convention for Constructional Steelworks 1986. Recommended Testing Procedures for Assessing the Behaviour of Structural Elements under Cyclic Loads, Technical Committee 1, TWG 1.3 – Seismic Design, *Publ. N° 45*.
- Fajfar, P., Vidic, T., and Fischinger, M., 'Seismic Demand in Medium- and Long-period Structures', *EARTHQUAKE ENGINEERING AND STRUCTURAL DYNAMICS*, **18**(8), 1133-1144, 1989.
- Fajfar, P., and Vidic, T., 'Consistent Inelastic Design Spectra: Hysteretic and Input Energy', *EARTHQUAKE ENGINEERING AND STRUCTURAL DYNAMICS*, **23**(5), 523-537, 1994.
- Fajfar, P. and Gaspersic, P., 'The N2 method for the seismic damage analysis of RC buildings', *EARTHQUAKE ENGINEERING AND STRUCTURAL DYNAMICS*, **25**(1), 31-46, 1996.
- Feenstra, P.H., de Borst, R., "Constitutive model for reinforced concrete", *ASCE, J. of the Eng. Mech.*, 121 (5), 1995.
- Hand, F. R., Pecknold, D. A., Schnobrich, W. C., "Nonlinear layered analysis of RC plates and shells", *ASCE, J. of the Structural Division*, 99 (7), 1491-1505, 1973.
- Hawkins, N.M. (1973), "The strength of stud shear connectors", *Civil Engineering Transactions*, Institute of Engineers, Australia, Vol. CE33, pp. 46-52.
- Izzuddin B.A. and Elnashai, A.S., 1989, ESEE report manual of Adaptive
- Johnson, R.P. (1970), "Research on steel-concrete composite beams", *Journal of Structural Engineering*, ASCE, Vol. 96, No. ST3, pp. 445-459, March.
- Johnson, R.P., "Composite structures of steel and concrete. Volume 1: beams, slabs, columns and frames for buildings", Blackwell, Oxford, 1994.
- Kanz, R. 1995. *Beitrag zur Berechnung von exzentrisch ausgesteiften Rahmen aus Verbundprofilen unter Erdbebenbelastung*. Dissertation, TH-Darmstadt, Germany.
- Kato, B. (1989), "Rotation capacity of H-section members as determined by local buckling", *Journal of Constructional Steel Research*, No. 13, pp. 95-109.
- Mazzolani, F. M., and Piluso, V. (1996). *Theory and Design of Seismic Resistant Steel Frames*. E & FN SPON.
- McMackin, P.J., Slutter, R.G. and Fisher J.W. (1973), "Headed steel anchor under combined loading", *Engineering Journal*, American Institute of Steel Construction, Second quarter, pp. 43-53.
- Mele, M. & Puhali, R. 1985. Experimental analysis of cold formed shear connectors in steel-concrete composite beams. In *Costruzioni Metalliche*, 5/6, *Rivista dei Tecnici dell'acciaio*.
- Menu, J.M.H and Elnashai, A.S. (1988), Earthquake time-history transformation for small scale dynamic testing., *Civil Engineering Dynamics Conference*, Bristol, 24-25, pp.155-172.
- Oehlers, D.J. and Johnson, R.P. (1987), "The strength of stud shear connections in composite beams", *The Structural Engineer*, 65B, June, 44-48.
- Oehlers, D. J., Bradford, M. A., "Composite steel and concrete structural members – Fundamental behaviour", Pergamon, Elsevier, Oxford, 1995.

Ollgaard, J.G., Slutter, R.G. and Fisher, J.W. (1971), "Shear strength of stud connectors in light-weight and normal-weight concrete, *Engineering Journal*, American Institute of Steel Construction, Vol. 8, pp. 55-64.

Paulay, T. & Priestley, J.M.N. 1992. *Seismic design of reinforced concrete and masonry buildings*. New York: John WILEY.

Plumier A. 1996. Problems and options in Seismic design of composite frames (internal report), Department of Civil Engineering, University of Liege.

Plumier, A., Doneux, C., Bouwkamp, J.G. & Plumier, C. 1998. Slab design in connection zone of composite frames. In *proc.. of the 11th European Conference on Earthquake Engineering*. Rotterdam:Balkema.

Plumier, A., Doneux, C., Bouwkamp, J.G., "Slab design in connection zone of composite frames", in Proceedings of the 1998 Annual Technical Session & Meeting of the Structural Stability Research Council, 1998.

Plumier, A., Doneux, C., "Design of composite structures in seismic regions", in Proceedings of the 6th International Colloquium on Stability and Ductility of Steel Structures SDSS'99, Dubina, D., and Ivanyi, M., (Editors), Elsevier ,27 – 34, 1999.

Pradhan, Amir M. Bouwkamp, Jack G. (1995). Pseudodynamic test effects: Interactive steel-concrete behaviour of beam-column joints. Proc. 10 ECEE, Vienna.

Pradhan, Amir Man (1998). Experimental and numerical studies on earthquake response of composite beam-column joints. Dissertation; Fachbereich Bauingenieurwesen, Technische Universitaet Darmstadt, Darmstadt.

Rea, D., Clough, R.W. & Bouwkamp, J.G. 1969. *Damping capacity of a model steel structure*. Report No. EERC.69-14. University of California, Berkeley, USA.

Rotter, J.M. and Ansourian, P. (1979), "Cross-section behaviour and ductility in composite beams", *Proceedings of Institute of Civil Engineers*, London, Vol. 67, Part 2, pp. 453-474.

Setti, P. (1985), Un Metodo per la Determinazione del Coefficiente di Struttura per le Construzioni Metalliche in Zona Sismica, *Construzioni Metalliche* n°3.

Tsujii, M. (2001), Seismic Response and Design of Composite Steel-Concrete Frames, PhD, thesis, University of London (to be submitted).

Ungureanu, A. 1993. *Ein Verfahren zur Bestimmung der Steifigkeitsparameter der rechnerische Tragwerksmodelle aus Versuchsergebnissen*. Dissertation, TH-Darmstadt, Germany.

Vidic, T., Fajfar, P., and Fischinger, M., 'Consistent Inelastic Design Spectra: Strength and Displacement', *EARTHQUAKE ENGINEERING AND STRUCTURAL DYNAMICS*, **23**(5), 507-521, 1994.

Wakabayashi, M. (1986), *Earthquake Resistance Design of Buildings*, McGraw Hill Inc.

Yamamoto, M. and Nakamura, S. (1961), "Experiments on stud shear connectors", *Report of Civil Engineering Research Centre*, Ministry of Construction, Japan, Vol. 109, pp. 1-24 (in Japanese).

IIW 15 (1976), "Design rules for arc-welded connections in steel submitted to static loads," *Welding in the World*, 14, International Institute of Weld, No. 5/6, pp 132.

4. DATA BANK OF LITERATURE REFERENCES ON COMPOSITE STRUCTURES.

A list of references has been developed by the ICONS Topic 4 group during the work. The development of this data base was based on the need to centralise all the papers and data concerning composite buildings – especially under earthquake loading.

The base for the list was an existing list already started at Université de LIEGE. It is organised in a simple way :

- An alphabetic list of authors is defined and the corresponding documents are classified in paper form in physical files M1, M2, ...M9.
- The list indicates the correspondence between

(Authors name and title of papers) \Leftrightarrow M_i

This procedure raises no problem of inserting a new document between 2 previous ones. Every new document is put in the last open physical file M_i and referred to it.

This list of references exists now and is available by simple request to c.doneux@ulg.ac.be. The total number of references was around 300 in May 2001.

Next table is an example of the list of references contained in the data bank.

ICONS-TOPIC4-COMPOSITE STEEL CONCRETE STRUCTURES. LIST OF REFERENCES					
Auteur	Année	Titre	Edition	Volume	Code
Aribert J.-M.	1998	State-of-the-art review on the experimental (and theoretical) behaviour of composite beam-to-column joints subjected to cyclic loading	Inco-Copernicus "recos" project - INSA-Rennes		M6
Aribert J.-M.	1992	Application and recent development of a numerical model for composite beams with partial shear connection	Composite Construction in Steel and Concrete II ed. by S. Easterling and W.M. K. Roddis (ASCE)	742-757	M2
ASCE Tasks Committee on Design Criteria	1998	Design Guide for partially restrained composite connections	Journal of Structural Engineering	1099-1114	M7
Astaneh A.	1994	Seismic design of composite structures in the united states	congres STESSA '94, Timisoara	448-457	M4
Azizinamini A., Prakash B., Prishtina B., Salmon D. C.	1992	New steel beam to composite column connection detail	Composite Construction in Steel and Concrete II ed. by S. Easterling and W.M. K. Roddis (ASCE)	854-868	M3
Balakrishnam S., Murray D.	1988	Prediction of R/C panel end deep beam behavior by NLFEA	ASCE, J. of the structural eng.	114(10)	M2
Ballerini M., Bursi O.S.	1995	Experimental analysis of steel-concrete composite beams with full and partial shear connection	C.T.A., Giornate italiane delle costruzione in acciaio		M3
Ballio G., Plumier A., Thunus B.	1990	Influence of concrete on the cyclic behaviour of comp. connections	IABSE Symp., Brussels		M2
Barzegar F., Maddupidi S.	1997	Three-dimensional modelling of concrete structures. II: reinforced concrete	J. of Structural Engineering	123 N°10	M6
Beguín Ph., Grimault J.P.	1996	Appl. de l'eurocode 4-Dimensionnement des poteaux mixtes	Revue Construction métallique		M4
Bernuzzi C., Leon R.T., Noè S.	1997	Influence of the joint modelling on the response of steel-concrete composite frames	Proc. of STESSA '97, Kyoto	546-553	M6

5. CONCLUSIONS AND RESEARCH NEEDS

A huge research effort, involving experimental activity, numerical modelling and the analysis of the existing background about composite steel concrete structures, has been made in the ICONS Project. At the end of this work, it can be stated that a number of problems have been addressed and, to a variable extent, solved.

The Section 2 of the present report, "Design rules for Eurocode 8 and their background" expresses with details the deliverables and limits of the work realised. For sure, the main success is that such a text does exist now, since it was missing before the ICONS project, and that this text provides design possibilities in a certain range of structures typologies and design options.

The main achievements of the ICONS project are to be found on the following issues :

- encased, partially encased and filled elements, for which design guidance and tables on limits of wall slenderness related to different structure ductility levels are provided;
- steel beams with slab in moment frames, with the developments of design effective width, ductility conditions, layout of re-bars, rules for connections of beams to columns and for shear connectors ;
- data for the elastic analysis and the assessment of the ultimate capacity of composite moment frames;
- original layout of slab connection to façade steel beams and its validation by tests;
- concepts for the design of dissipative concentrically and eccentrically braced frames
- design guidance for composite systems made of composite walls and steel or composite beams, based on the US and Japanese experience.

As normally at the end of a research activity, one knows better the remaining questions and problems, which require further research to provide safe design guidance and more economical.

Research needs have been identified on the following problems :

- evaluation of the composite resistance of encased and filled sections in dissipative zone, especially for what concern their resistance to shear;
- evaluation of the behaviour of components under a different objective than the one selected as a basis to all the developments in ICONS, that is the "no degradation of concrete" condition;
- evaluation of the resistance and ductility of partial strength connections in moment frames, including effective width and lay out of re-bars problems;
- relationship between the seismicity of a zone and the requirement on classes of sections; this is a also an open question for pure steel structures; behind that problem is the poorer low cycle fatigue behaviour of unsymmetrical sections in comparison to symmetrical ones partly addressed in 3.2.
- development of a design philosophy about the use of dissipative composite braces; these ones raise design problems associated to their buckling resistance and the capacity design of neighbour elements;
- development of a design philosophy about the use of composite seismic links; these ones raise the problem of a stable hysteretic behaviour in the large local deformations range.

ACKNOWLEDGEMENTS

The research activity presented has been developed with funding of DGIII and DGXII of the European Commission, through the ICONS project (a research network financed by the TMR program), the ECOEST1 and ECOEST2 projects (Large Installation Network projects) and the RECOS project (an INCO-COPERNICUS project).

May the contributors listed on the front page of this Report, as well as the European Commission Officials who approved and managed the financial support to the important research effort presented here, be thanked for their effective contribution.